

Tensor-based multivariate function approximation: methods benchmarking and comparison

A.C. Antoulas¹, I-V. Gosea², C. Poussot-Vassal^{*3}, and P. Vuillemin³

¹Department of Electrical and Computer Engineering, Rice University, Houston
(aca@rice.edu)

²Max Planck Institute, CSC Group, Magdeburg, Germany
(gosea@mpi-magdeburg.mpg.de)

³ONERA, DTIS, Université de Toulouse, France
(charles.poussot-vassal@onera.fr and pierre.vuillemin@onera.fr)

June 13, 2025

Abstract

In this note, we evaluate the performances, the features and the user-experience of some methods (and their implementations) designed for tensor- (or data-) based multivariate function construction and approximation. To this aim, a collection of multivariate functions extracted from contributive works coming from different communities, is suggested. First, these functions with varying complexity (e.g. number and degree of the variables) and nature (e.g. rational, irrational, differentiable or not, symmetric, etc.) are used to construct tensors, each of different dimension and size on the disk. Second, grounded on this tensor, we inspect performances of each considered method (e.g. the accuracy, the computational time, the parameters tuning impact, etc.). Finally, considering the "best" parameter tuning set, we compare each method using multiple evaluation criteria. The purpose of this note is not to rank the methods but rather to evaluate as fairly as possible the different available strategies, with the idea in mind to guide users to understand the process, the possibilities, the advantages and the limits brought by each tools. The contribution claimed is to suggest a complete benchmark collection of some available tools for tensor approximation by surrogate models (e.g. rational functions, networks, etc.). In addition, as contributors of the multivariate Loewner Framework (**mLF**) approach [3] (and its side implementation in **MDSPACK** [10]), attention and details of the latter are more explicitly given, in order to provide readers a digest of this contributive work and some details with simple examples.

Contents

1	Introduction	4
1.1	Starting point and motivations	4
1.2	Contribution and report structure	5
1.3	Overview of the methods tested	6
1.4	Examples assumptions	9
1.5	Examples evaluation procedure	9
1.6	Report description (score report)	10
1.7	Report description for M1 [3, Alg. 1]	10

*Corresponding author: charles.poussot-vassal@onera.fr

2	The multivariate Loewner Framework (mLF) at a glance	11
2.1	Forewords	11
2.2	n -D tensor data, Loewner matrix, and Lagrangian form	11
2.3	Decoupling and taming the curse of dimensionality	12
2.4	Simple detailed example with MATLAB code	15
2.5	Summary	18
3	Overview of the results	19
3.1	Approximation performances statistics	19
3.2	Preliminary remarks	25
4	Detailed examples exposition and results	26
4.1	Function #1 ($n = 2$ variables, tensor size: 12.5 KB)	27
4.2	Function #2 ($n = 2$ variables, tensor size: 12.5 KB)	30
4.3	Function #3 ($n = 2$ variables, tensor size: 12.5 KB)	33
4.4	Function #4 ($n = 3$ variables, tensor size: 500 KB)	37
4.5	Function #5 ($n = 4$ variables, tensor size: 19.5 MB)	40
4.6	Function #6 ($n = 2$ variables, tensor size: 12.5 KB)	43
4.7	Function #7 ($n = 2$ variables, tensor size: 12.5 KB)	46
4.8	Function #8 ($n = 2$ variables, tensor size: 42.8 KB)	49
4.9	Function #9 ($n = 2$ variables, tensor size: 12.5 KB)	52
4.10	Function #10 ($n = 2$ variables, tensor size: 52.5 KB)	56
4.11	Function #11 ($n = 2$ variables, tensor size: 12.5 KB)	60
4.12	Function #12 ($n = 2$ variables, tensor size: 12.5 KB)	64
4.13	Function #13 ($n = 2$ variables, tensor size: 12.5 KB)	68
4.14	Function #14 ($n = 4$ variables, tensor size: 1.22 MB)	71
4.15	Function #15 ($n = 2$ variables, tensor size: 12.5 KB)	74
4.16	Function #16 ($n = 2$ variables, tensor size: 12.5 KB)	79
4.17	Function #17 ($n = 2$ variables, tensor size: 12.5 KB)	84
4.18	Function #18 ($n = 2$ variables, tensor size: 12.5 KB)	87
4.19	Function #19 ($n = 2$ variables, tensor size: 12.5 KB)	92
4.20	Function #20 ($n = 3$ variables, tensor size: 500 KB)	95
4.21	Function #21 ($n = 4$ variables, tensor size: 1.22 MB)	98
4.22	Function #22 ($n = 4$ variables, tensor size: 1.22 MB)	101
4.23	Function #23 ($n = 4$ variables, tensor size: 1.79 MB)	104
4.24	Function #24 ($n = 2$ variables, tensor size: 13.8 KB)	107
4.25	Function #25 ($n = 2$ variables, tensor size: 12.5 KB)	110
4.26	Function #26 ($n = 3$ variables, tensor size: 1.65 MB)	114
4.27	Function #27 ($n = 5$ variables, tensor size: 90.6 MB)	117
4.28	Function #28 ($n = 2$ variables, tensor size: 30 KB)	120
4.29	Function #29 ($n = 2$ variables, tensor size: 12.5 KB)	123
4.30	Function #30 ($n = 8$ variables, tensor size: 128 MB)	126
4.31	Function #31 ($n = 6$ variables, tensor size: 128 MB)	129
4.32	Function #32 ($n = 2$ variables, tensor size: 12.5 KB)	132
4.33	Function #33 ($n = 2$ variables, tensor size: 28.1 KB)	135
4.34	Function #34 ($n = 2$ variables, tensor size: 1.22 MB)	138
4.35	Function #35 ($n = 2$ variables, tensor size: 1.22 MB)	141
4.36	Function #36 ($n = 3$ variables, tensor size: 62.5 KB)	144
4.37	Function #37 ($n = 4$ variables, tensor size: 1.22 MB)	149
4.38	Function #38 ($n = 3$ variables, tensor size: 1.65 MB)	152
4.39	Function #39 ($n = 3$ variables, tensor size: 500 KB)	155
4.40	Function #40 ($n = 4$ variables, tensor size: 19.5 MB)	158
4.41	Function #41 ($n = 5$ variables, tensor size: 781 KB)	161
4.42	Function #42 ($n = 6$ variables, tensor size: 7.63 MB)	164

4.43 Function #43 ($n = 7$ variables, tensor size: 76.3 MB)	167
4.44 Function #44 ($n = 8$ variables, tensor size: 763 MB)	170
4.45 Function #45 ($n = 9$ variables, tensor size: 76.9 MB)	173
4.46 Function #46 ($n = 10$ variables, tensor size: 461 MB)	176
5 Discussions and conclusions	179
5.1 Discussion and generic comments	179
5.2 General conclusion	179

1 Introduction

1.1 Starting point and motivations

1.1.1 Multivariate functions

A continuous n -variable function \mathbf{H} is defined as

$$\begin{aligned} (\mathcal{X}_1, \mathcal{X}_2, \dots, \mathcal{X}_n) &\longrightarrow \mathcal{Y} \\ (x_1, x_2, \dots, x_n) &\longmapsto y := \mathbf{H}(x_1, x_2, \dots, x_n), \end{aligned} \quad (1)$$

where $x_l \in \mathcal{X}_l$ ($l = 1, \dots, n$) is the l -th input variable of \mathbf{H} , and $y \in \mathcal{Y}$ is the output variable. In a general (continuous) setting, these sets either denote real \mathbb{R} or complex \mathbb{C} domains.

Remark 1 (Domains restriction) *In this note, we will restrict our evaluation to the real and bounded domains, thus to real-valued multivariate functions, i.e.*

$$\mathcal{X}_l := [\underline{x}_l, \bar{x}_l] \subseteq \mathbb{R} \quad \text{and} \quad \mathcal{Y} := [\underline{y}, \bar{y}] \subseteq \mathbb{R}. \quad (2)$$

These restrictions may be removed for some configurations and methods, but are necessary to compare as fairly as possible the approaches considered in this note.

1.1.2 From multivariate functions to tensors

Evaluating eq. (1), over a finite discretization grid along each variable, each with finite dimension $\{N_1, N_2, \dots, N_n\} \in \mathbb{N}$, leads to

$$\begin{aligned} (\mathcal{X}_1^{N_1}, \mathcal{X}_2^{N_1}, \dots, \mathcal{X}_n^{N_n}) &\longrightarrow \mathcal{Y}^{N_1 \times N_2 \times \dots \times N_n} \\ (\mathbf{x}_1, \mathbf{x}_2, \dots, \mathbf{x}_n) &\longmapsto \mathbf{tab}_n := \mathbf{H}(\mathbf{x}_1, \mathbf{x}_2, \dots, \mathbf{x}_n), \end{aligned} \quad (3)$$

where $\mathbf{x}_l \in \mathcal{X}_l^{N_l}$ ($l = 1, \dots, n$) is the discretized vector of the l -th variable, with dimension N_l (i.e. discrete set of variable x_l within the considered bounds). The resulting n -array tableau, denoted \mathbf{tab}_n , is a **n -dimensional tensor**, also illustrated in Figure 1, where $x_l(j_l)$ denotes the j_l -th element of the l -th variable ($j_l = 1, \dots, N_l$).

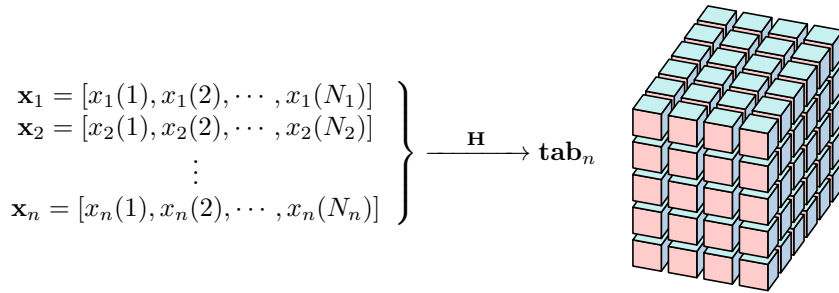


Figure 1: Data to tensor construction (via \mathbf{H}) illustration. Left hand side are the discrete data along each variables, while right hand side is the tensor (here, graphical representation limited to $n = 6$).

1.1.3 Tensor-based model approximation: context and motivations

Multivariate tensor approximation aims at constructing (exact, simplified or reduced-order) **model / surrogate** (i.e. function, network, realization, etc.) that accurately captures the behavior of a potentially **large-scale multi-dimensional tensor** data-set, constructed from simulations or experiments evaluated along the n variables. Eventually one may expect to **discover the true underlying function** and its complexity. In general settings, these data may result from any

measurements obtained from a parametrized experiment. In this report, **the simulator or the experiment is materialized by the function \mathbf{H}** , considered as unknown. The evaluations of \mathbf{H} generate the outputs (tensor) to be approximated, or function to be discovered. More specifically, being given eq. (3) (generated by \mathbf{H}), we seek for \mathbf{G} described as

$$\begin{aligned} (\mathcal{X}_1, \mathcal{X}_2, \dots, \mathcal{X}_n) &\longrightarrow \hat{\mathcal{Y}} \\ (x_1, x_2, \dots, x_n) &\longmapsto \hat{y} := \mathbf{G}(x_1, x_2, \dots, x_n) \end{aligned}, \quad (4)$$

where $\hat{y} \in \hat{\mathcal{Y}}$ is the approximated function output and space, respectively. Obviously, we seek \mathbf{G} such that $\hat{y} \approx y$ and eventually $\mathbf{G} \approx \mathbf{H}$, i.e. recovers or approximates the original model or system (either dynamic or static).

Remark 2 (The dynamical systems case) *In the special context of dynamical systems governed by differential and algebraic equations, the multivariate nature comes from the parametric dependency of the underlying dynamical system, which accompany the (first) variable being the dynamical s -variable (Laplace) or z -variable. This first variable accounts for the dynamical nature (frequency or time-dependency) while the rest of the parameters or variables account for physical characteristics such as mass, length, or material properties (in mechanical systems), flow velocity, temperature (in fluid cases), chemical properties (in biological systems), age, weight, pressure (in clinical systems), etc. In many applications, the parameters are embedded within the model as tuning variables for the output of interest. One specific aspect is the physical meaning of this first variable, often complex, which deserves a specific treatment. In [3], this point is also considered through the construction of a multivariate Lagrangian realization associated to \mathbf{G} . This setting is out of the scope of this note. Instead, here, we consider static multivariate functions, only.*

1.1.4 Tensors and the curse of dimensionality (C-o-D)

According to Richard E. Bellman, the "curse of dimensionality" (C-o-D) refers to the diverse phenomenon occurring when analyzing or ordering data in large dimensional spaces, that are not present in lower cases [6]¹. In this note, and following [3], we are using the C-o-D term to refer to both the **computational (floating point arithmetic, flop)** and to the **storage (size on the disk, Bytes)** limitations encountered when constructing multivariate model approximation from large multi-dimensional data sets as defined in eq. (3); as a side effect, we also claim that taming the C-o-D will also notably **improve the accuracy**.

Accordingly, one important element presented in this report is the impact of the dimension of the tensor in the ability of each method to succeed. In other terms, we evaluate the accuracy, the computational time and burden through very complex examples (i.e. tensor size and dimensions). Indeed, we believe the scalability is an important feature so that the method achieves its full potential in real-life and industrial applications.

1.2 Contribution and report structure

The purpose of this report is not to detail or claim new methods or material for tensor-based multivariate function approximation, but rather to evaluate some existing approaches in term of accuracy, scalability, user experience, etc. The report is organized as follows. First, this Section 1 introduces the big picture and main definitions, as well as the benchmarked methods and procedure. Then, Section 2 provides a quick description of one method proposed by the authors, namely the **multivariate Loewner Framework (mLF)** [3]; this brief summary is accompanied with MATLAB code examples². Then, Section 3 provides an overview of the results in term of accuracy, computational time, model complexity, etc. obtained with the 46 examples considered. Preliminary comments regarding potentiality and limitations of each methods are discussed. Then, the core contribution is given in Section 4: we list, for the 46 examples considered, the detailed

¹See also the Wikipedia dedicated page https://en.wikipedia.org/wiki/Curse_of_dimensionality.

²Based on the MATLAB +mLF package available at <https://github.com/cpoussot/mLF>

statistics for the different methods; in addition, when not too long, a detailed analysis is given for the method exposed in [3, Alg. 1]. We believe this exhaustive collection provides insightful details for researchers and practitioners, as well as a comprehensive view of the method presented in [3]. Conclusions and outlooks are discussed in Section 5.

Remark 3 (Report evolutions) *Authors insist that the present report is aimed at being updated along with time, with updated codes, methods and additional examples. In this philosophy, feedbacks from readers are welcome and will be carefully used for improvements of future versions.*

Remark 4 (Caution and acknowledgements) *In what follows, we investigate different methods aiming at constructing models on the basis of tensors. While the first three methods (later denoted M_1 , M_2 and M_3) have been implemented by the authors, the other ones (later denoted M_4 , M_5 , etc.) are constructed by third parties. First we want to give them credit in making the code available, second, we want to point out that as non-experts and not main authors, we may have badly parametrized them. Therefore, no conclusion regarding neither the nature nor the quality of these algorithms is intended. In addition, authors want to point out that using these codes was actually relatively easy.*

1.3 Overview of the methods tested

We compare different tensor-driven multivariate approximation methods (or software). Each method has its own tuning parameters. In what follows a subset of possible parametric configuration combinations are evaluated. These configurations are detailed in what follows.

1.3.1 M1 - Method 1 [3, Alg. 1]

MATLAB implementation of the **direct mLF** rational model approximation approach [3, Alg. 1]. This method has the following tunable parameters: `{tol_ord / null_method}`.

- **tol_ord:** $[1/2, 10^{-1}, 10^{-2}, 10^{-3}, 10^{-4}, 10^{-6}, 10^{-9}, 10^{-10}, 10^{-11}, 10^{-12}, 10^{-13}, 10^{-14}]$, being the normalized singular values tolerance threshold used in the univariate Loewner step for the order selection;
- **null_method:** is the null space computation method used, being either:
 1. is SVD decomposition (using last right singular vector);
 2. is QR decomposition (using the last right orthogonal factor vector);
 3. is linear resolution with \ of the Loewner matrix first $n - 1$ columns with the last one;

Additional details and preliminary version of the code are available here: <https://github.com/cpoussot/mLF>. We also refer to Section 2 for philosophy, proofs and notations.

1.3.2 M2 - Method 2 [3, Alg. 2]

MATLAB implementation of the **adaptive mLF** rational model approximation approach [3, Alg. 2]. This method has the following tunable parameters: `{tol / null_method}`.

- **tol:** $[10^{-15}]$, being the expected maximal mismatch error (weighted by the maximal value) tolerance;
- **null_method:** similar to M1.

Additional details and preliminary version of the code will be made available soon here: <https://github.com/cpoussot/mLF>. We also refer to Section 2 for philosophy, proofs and notations. This algorithm is still under improvement, to make it more reliable. Future versions will provide improved implementations.

1.3.3 M3 - Method 3 [10]

MDSPACK implementation of the **direct mLF** rational model approximation method. It is an adaptation of M1, [3, Algorithm 1]. More specifically, it is a preliminary version of a FORTRAN code interfaced with MATLAB, Python and Command Line interfaces, under development at **MOR Digital Systems**. This method has the following tunable parameters: `{tol_ord / tol_k}`.

- `tol_ord`: similar as in M1;
- `tol_k`: $[10^{-2}, 10^{-4}, 10^{-6}, 10^{-9}, 10^{-12}, -1]$, is the relative null space vector magnitude tolerance for each elements; if below, entry is removed (-1 means no deletion).

Additional details will be made soon available here: https://mordigitalsystems.fr/static/mdspack_html/MDSpack-guide.html (documentation) and <https://mordigitalsystems.fr/en/products.html> (software main page). We also refer to Section 2 for philosophy, proof and notations. As M2, this algorithm is still under development.

1.3.4 M4 - Method 4 [12] (downloaded on January 28th, 2025)

MATLAB implementation of a multivariate **Kolmogorov Arnold Network (KAN)**-based method. This method has the following tunable parameters: `{method / alpha / Nrun / lambda / n / q / p}`.

- `method`: $[1, 2, 3, 4]$, is used to define different basic functions in the KAN graph, being either:
 1. is cubic splines, identification method - Gauss-Newton;
 2. is cubic splines, identification method - Newton-Kaczmarz, standard;
 3. is cubic splines, identification method - Newton-Kaczmarz, accelerated;
 4. is piecewise-linear, identification method - Newton-Kaczmarz, standard;
- `alpha`: $[0.95, 1]$, is the damping factor (learning rate) for iterative parameter update;
- `Nrun`: $[50]$, is the number of iterations;
- `lambda`: $[0.01]$, is the Tikhonov regularization parameter for Gauss-Newton method;
- `n`: $[4, 6, 10]$, is the number of bottom nodes (input layer);
- `q`: $[4, 6, 12]$, is the number of top nodes (output layer);
- `p`: $[2n + 1]$, is the number of intermediate nodes (hidden layer); this choice is the optimal according to the Kolmogorov-Arnold theorem).

Additional details are available here: <https://github.com/andrewpolar>. We also refer to [12] for philosophy, proofs and notations.

1.3.5 M5 - Method 5 [5] (downloaded on April 11th, 2025)

MATLAB implementation of the **parametric Adaptive Anderson Antoulas (pAAA)** rational model approximation approach. This method has the following tunable parameters: `{tol}`.

- `tol`: $[10^{-3}, 10^{-6}, 10^{-9}]$, being the expected maximal mismatch error (weighted by the maximal value) tolerance.

Additional details are available here: <https://zenodo.org/records/14794468>. We also refer to [5] for philosophy, proofs and notations.

1.3.6 M6 - Method 6 [5] (downloaded on May 17th, 2025)

MATLAB implementation of the **Low Rank parametric Adaptive Anderson Antoulas (LR-pAAA)** rational model approximation approach. This method has the following tunable parameters: {`tol` / `rank`}.

- `tol`: $[10^{-3}, 10^{-6}, 10^{-9}]$, being the expected maximal mismatch error (weighted by the maximal value) tolerance.
- `rank`: $[3, 4, 5]$, being a constraint for number of terms included in the **CP** decomposition used to represent the barycentric coefficients.

Additional details are available here: <https://zenodo.org/records/14794468>. We also refer to [5] for philosophy, proofs and notations.

1.3.7 M7 - Method 7 [1] (downloaded May 20th, 2025)

Python implementation of the **Multi Layer Perceptron (MLP)** neural network approximation approach. This method has many tunable parameters. In this first version we fixed all of them. Moreover, we limit the application of this methods to tensors with dimension $n \leq 4$. Future versions will investigate different tuning and larger tensors.

- `layer`: one single neuron layer is used with dense connections, being the topology selected (according to the Universal Approximation Theorem, this should be enough for approximation).
- `neurons`: 64, being the number of neurons.
- `activation`: '`relu`', being the activation function.
- `optimizer`: '`adam`', begin the optimization strategy.
- `loss`: '`mse`', being the cost function.
- `epochs`: 500, being the number of allowed iterations.

Additional details are available here: <https://www.tensorflow.org/>³. Notice that examples #29, 34, 35 are not tested since implementation was not straightforward. Then, #9 failed but would benefit from more efforts in the future.

1.3.8 Comments on relevant similarities and differences of the methods

It is generally complicated to compare algorithms that are grounded on different mathematical background or designed for different objectives. This is why we should point out some important common points and differences between the evaluated approaches. Some of the most relevant, according to the authors, are listed in Table 1.

	M1	M2	M3	M4	M5	M6	M7
G model structure	rational	rational	rational	KAN	rational	rational	MLP
Deal with complete tensor?	yes	yes	yes	yes	yes	yes	yes
Deal with incomplete tensor?	no	no	no	yes	no	no	yes
Deal with real variables?	yes	yes	yes	yes	yes	yes	yes
Deal with complex variables?	yes	yes	yes	no	yes	yes	no

Table 1: Some properties and features for each methods.

³Acknowledgements to R. Vassal for discussions and initial code set up.

1.4 Examples assumptions

To conduct the benchmarking, let us consider the following assumptions, shared by all methods:

- A1 Each function \mathbf{H} is n -variable with one single measured output, of the form eq. (1);
- A2 The input variables and measured output are real-valued, as given in eq. (2);
- A3 The common input argument for each method is a n -dimensional tensor \mathbf{tab}_n (with the corresponding evaluation points), as given in eq. (3) and illustrated in Figure 1;
- A4 No noise is considered on the measured output. Regarding this matter, we refer reader to signal processing or system identification communities, where filtering or output averaging methods are deployed, together with statistical tools (see e.g. [11]). Obviously, this is definitely an axis for future investigations, possibly including other contributors.

1.5 Examples evaluation procedure

Let us now detail the evaluation process. The evaluation procedure is common to every methods, and is detailed step by step in what follows:

- S1 Consider the n -variable function, together with domain, as given in eq. (1) and eq. (2);
 - S2 Consider a discretisation of the input space and compute the tensor \mathbf{tab}_n as in eq. (3);
 - S3 For every methods $m = \{\text{M1}, \text{M2}, \dots\}$, enumerate all combinations of the tuning parameters configurations p and construct a surrogate model $\mathbf{G}_{m,p}$, see Section 1.3;
 - S4 For 500 random draw of $\{x_1, x_2, \dots, x_n\}$ within the considered domain bound \mathcal{X}_l , evaluate both \mathbf{H} (eq. (1)) and $\mathbf{G}_{m,p}$ (eq. (4)) and compute the root mean square error (RMSE) given as
- $$\text{RMSE}_{m,p} = \sqrt{\frac{1}{500} \sum_{j=1}^{500} (\mathbf{G}_{m,p}(x_1, x_2, \dots, x_n) - \mathbf{H}(x_1, x_2, \dots, x_n))^2}. \quad (5)$$
- S5 For each method m , keep the best model along the possible parameter set (i.e. the one achieving lowest RMSE), now denoted \mathbf{G}_m ;
 - S6 Report and plot of the best candidate \mathbf{G}_m , for each method (see Section 4).

Remark 5 (Computational setup) *The computations are carried out on Matlab 2023b, with a MacBook Air (with Apple M1 with 16 GB memory). Notice that result may vary with different architecture.*

Remark 6 (About RMSE) *We believe the RMSE is an interesting metric to monitor since it usually makes sense for most engineers, and none of the method actually are specifically targeted to minimize this metric. Notice also that worst case error is also used.*

1.6 Report description (score report)

The collection of 46 examples with additional detailed informations is reported in Section 4. For each case, the original function \mathbf{H} eq. (1) (used to generate the tensor), the reference where it has been used (if any), domain and bounds \mathcal{X}_l ($l = 1, \dots, n$) eq. (2), and the tensor \mathbf{tab}_n sizes, are first given. Then, for each evaluated method, the tuning parameter configuration set p leading to the lowest RMSE eq. (5) (evaluated over 500 random input variables draw) is reported in a tableau with the following entries (NaN, when no model has been found):

- #: the identification number of the function;
- Alg.: the algorithm (or method) name used;
- Parameters: method parameters configuration leading to the best model \mathbf{G}_m ;
- Dim.: best model dimension, i.e. number of elements needed to evaluate the surrogate model;
- CPU [s]: best model construction computational time;
- RMSE: best model root mean square error;
- min err.: best model minimal error;
- max err.: best model maximal error;

1.7 Report description for M1 [3, Alg. 1]

In addition to the above statistics, details of method M1 are also given. More specifically:

- $k_l \in \mathbb{N}$ denotes the number of right interpolation points along the l -th variable;
- ${}^l\lambda_{j_l} \in \mathcal{X}_l$ denotes the j_l -th interpolation point along the l -th variable;
- \mathbb{L} denotes the associated n -D Loewner matrix (not constructed with M1);
- \mathbf{c} denotes the barycentric weight of the n -D Lagrangian rational function, being also the null space of the \mathbb{L} matrix;
- \mathbf{w} denotes the evaluation of \mathbf{H} at the interpolation point ${}^l\lambda_{j_l}$;
- $\mathbf{Lag}(x_1, \dots, x_n)$ denotes the Lagrangian basis.

For some simple cases, we believe that it is interesting to provide even more details to improve user's experience. The purpose of these details is to provide a deep understanding of the steps and features of the rationale proposed in [3]. More specifically, this includes the numerical values of the **rational Lagrangian model** and the link with the **Kolmogorov Superposition Theorem (KST)** and **decoupling** feature of this method. In details and in addition to what is listed above the following are given (see also Section 2 for meaning of each variables):

- the right interpolation points ${}^l\lambda_{j_l}$ values (along each variables);
- the values of \mathbf{c} , \mathbf{w} , $\mathbf{c} \cdot \mathbf{w}$ and $\mathbf{Lag}(\cdot)$;
- the connection of the above result with the **KST**, applied first on the barycentric weight \mathbf{c} . More specifically, \mathbf{c}^{x_l} denotes the vectorized ($\text{vec}(\cdot)$) collection of 1-D sub-Loewner matrices null-spaces, which Kronecker multiplication leads to the barycentric weight along variable x_l . It follows the same decoupling for \mathbf{w} , the evaluation of \mathbf{H} along the right interpolation points. For the denominator only, the univariate vector-wise functions, solution to the **KST**, is given in \mathbf{D} , together with the denominator and numerator reconstruction formulae;
- and the equivalent **Neural Network (NN)** graph of the denominator \mathbf{D} is given as a KAN with basis functions defined by rational (Lagrangian) forms. We believe that this may also help in bridging the gap with the **NN** and the **rational approximation** communities.

2 The multivariate Loewner Framework (mLF) at a glance

2.1 Forewords

This method, celebrated as **multivariate Loewner Framework (mLF)**, has been first introduced in [3]. It relies on the **Loewner Framework (LF)** at its core. One important contribution in this work is to provide a solution to address the problem of **dimensionality**, occurring essentially when the number of variables and tensor size increase, thanks to a **variables decoupling**. More specifically, we present connections between the **LF** for rational interpolation of multivariate functions and **KST restricted to rational functions**. The result is the formulation of the **KST** for the special case of rational functions. As a byproduct taming the curse of dimensionality (C-o-D), in computational complexity, storage and numerical accuracy, is achieved. This framework encompasses the limitation of the real domain and thus **all variables may also belong to the complex domain**.

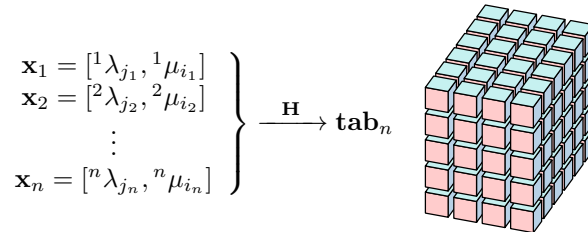
2.2 n -D tensor data, Loewner matrix, and Lagrangian form

2.2.1 Tensor data

The data-set is the primary ingredient of the n -variable **data-driven** rational interpolation and approximation. This set is obtained by evaluating the n -variable function $\mathbf{H}(x_1, x_2, \dots, x_n)$, either through a computer simulation or directly an experimental set-up along the discretized grid $\mathbf{x}_1, \dots, \mathbf{x}_n$. In the context of the **LF**, these points are split into columns and rows **interpolation, or support points**⁴.

The n -variable measurement set, called **tab_n** (eq. (3)), is schematically recalled in the right frame. Similarly to the classical 1-D and 2-D cases, evaluating the process $\mathbf{H}(x_1, x_2, \dots, x_n)$ along with the combinations of the support points $\{{}^1\lambda_{j_1}, {}^2\lambda_{j_2}, \dots, {}^n\lambda_{j_n}\} \in \mathbb{C}$ and $\{{}^1\mu_{i_1}, {}^2\mu_{i_2}, \dots, {}^n\mu_{i_n}\} \in \mathbb{C}$, thus forms a n -dimensional tensor, denoted **tab_n** ($j_l = 1, \dots, k_l$, $i_l = 1, \dots, q_l$ and $l = 1, \dots, n$).

Notice here that ${}^l\lambda_{j_l}$ and ${}^l\mu_{i_l}$ are a separation of x_l ; let us also assume for simplicity that $j_l + i_l = N_l$.



Following the Loewner philosophy detailed e.g. in [9, 2, 7] and [3], let us define $P_c^{(n)}$, the column data, and $P_r^{(n)}$, the row data, being two sub-sets of the original n -D tensor **tab_n**, leading to $\mathbf{w}_{j_1, j_2, \dots, j_n}$ and $\mathbf{v}_{i_1, i_2, \dots, i_n}$. More specifically these sub-sets are given as follows:

$$\left\{ \begin{array}{l} P_c^{(n)} := \{({}^1\lambda_{j_1}, {}^2\lambda_{j_2}, \dots, {}^n\lambda_{j_n}; \mathbf{w}_{j_1, j_2, \dots, j_n}), j_l = 1, \dots, k_l, l = 1, \dots, n\} \\ P_r^{(n)} := \{({}^1\mu_{i_1}, {}^2\mu_{i_2}, \dots, {}^n\mu_{i_n}; \mathbf{v}_{i_1, i_2, \dots, i_n}), i_l = 1, \dots, q_l, l = 1, \dots, n\} \end{array} \right. . \quad (6)$$

2.2.2 n -D Loewner matrix

The **tensor data** now may serve for the construction of the n -D Loewner matrix \mathbb{L}_n , which may be viewed as a linear operator mapping the interpolation points and n -D tensor onto a $Q \times K$ matrix, with $Q = q_1 q_2 \dots q_n$ (rows) and $K = k_1 k_2 \dots k_n$ (columns), i.e.

$$\begin{aligned} (\mathbb{C}^{k_1} \times \mathbb{C}^{q_1} \times \dots \times \mathbb{C}^{k_n} \times \mathbb{C}^{q_n} \times \mathbb{C}^{(k_1+q_1) \times \dots \times (k_n+q_n)}) &\longrightarrow \mathbb{C}^{Q \times K} \\ (\underbrace{{}^1\lambda_{j_1}, {}^1\mu_{i_1}, \dots, {}^n\lambda_{j_n}, {}^n\mu_{i_n}}_{\mathbf{x}_1}, \mathbf{tab}_n) &\longmapsto \mathbb{L}_n \end{aligned} , \quad (7)$$

⁴In what follows, ${}^l x_i$ denotes the l -th variable evaluated at the i -th element. We also denote $j_l = 1, \dots, k_l$ and $i_l = 1, \dots, q_l$ with $l = 1, \dots, n$. k_l and q_l are the available data along the l -th variable.

where each entry of the \mathbb{L}_n matrix reads

$$\ell_{j_1, j_2, \dots, j_n}^{i_1, i_2, \dots, i_n} = \frac{\mathbf{v}_{i_1, i_2, \dots, i_n} - \mathbf{w}_{j_1, j_2, \dots, j_n}}{({}^1\mu_{i_1} - {}^1\lambda_{j_1}) \cdots ({}^n\mu_{i_n} - {}^n\lambda_{j_n})}. \quad (8)$$

2.2.3 Lagrangian (barycentric) rational model

By considering appropriate number of (right) interpolation points k_l ($l = 1, \dots, n$), one can compute $\mathbb{L}_n \mathbf{c}_n = 0$, the right null space of \mathbb{L}_n , which contains the so-called **barycentric coefficients**,

$$\mathbf{c}_n^\top = [\ c_{1,\dots,1} \ \cdots \ c_{1,\dots,k_n} \ | \ \cdots \ | \ c_{k_1,\dots,1} \ \cdots \ c_{k_1,\dots,k_n}] \in \mathbb{C}^K. \quad (9)$$

Then, the multivariate Lagrangian (barycentric) form

$$\mathbf{G}(x_1, \dots, x_n) = \frac{\sum_{j_1=1}^{k_1} \cdots \sum_{j_n=1}^{k_n} \frac{c_{j_1, \dots, j_n} \mathbf{w}_{j_1, \dots, j_n}}{(x_1 - {}^1\lambda_{j_1}) \cdots (x_n - {}^n\lambda_{j_n})}}{\sum_{j_1=1}^{k_1} \cdots \sum_{j_n=1}^{k_n} \frac{c_{j_1, \dots, j_n}}{(x_1 - {}^1\lambda_{j_1}) \cdots (x_n - {}^n\lambda_{j_n})}}, \quad (10)$$

interpolates the n -D data tensor and eventually reveals the true underlying function \mathbf{H} (if rational). Reducing either k_l , or directly K (the null space entries), reduces the complexity of \mathbf{G} and leads to approximation of the tensor.

2.3 Decoupling and taming the curse of dimensionality

2.3.1 Variables decoupling

Following [3], Theorem 1 describes how the n -D Loewner null space \mathbf{c}_n can be expressed as a linear combination of a 1-D Loewner matrix null space and k_1 , $(n-1)$ -D Loewner null spaces. This result is recalled hereafter.

Theorem 1 *Being given the data $P_c^{(n)}$ and $P_r^{(n)}$ in response of the n -variable $\mathbf{H}(x_1, \dots, x_n)$ function, the null space of the corresponding n -D Loewner matrix \mathbb{L}_n , is spanned by*

$$\mathcal{N}(\mathbb{L}_n) = \text{vec} \left[\mathbf{c}_{n-1}^{{}^1\lambda_1} \cdot \left[\mathbf{c}_1^{({}^2\lambda_{k_2}, {}^3\lambda_{k_3}, \dots, {}^n\lambda_{k_n})} \right]_1, \dots, \mathbf{c}_{n-1}^{{}^1\lambda_{k_1}} \cdot \left[\mathbf{c}_1^{({}^2\lambda_{k_2}, {}^3\lambda_{k_3}, \dots, {}^n\lambda_{k_n})} \right]_{k_1} \right],$$

where

- $\mathbf{c}_1^{({}^2\lambda_{k_2}, {}^3\lambda_{k_3}, \dots, {}^n\lambda_{k_n})}$ spans $\mathcal{N}(\mathbb{L}_1^{({}^2\lambda_{k_2}, {}^3\lambda_{k_3}, \dots, {}^n\lambda_{k_n})})$, i.e. the null space of the 1-D Loewner matrix for frozen variables $\{{}^2\lambda_{k_2}, {}^3\lambda_{k_3}, \dots, {}^n\lambda_{k_n}\}$, and
- $\mathbf{c}_{n-1}^{{}^1\lambda_{j_1}}$ spans $\mathcal{N}(\mathbb{L}_{n-1}^{{}^1\lambda_{j_1}})$, i.e. the j_1 -th null space of the $(n-1)$ -D Loewner matrix for frozen ${}_1x_{j_1} = \{{}^1\lambda_1, \dots, {}^1\lambda_{k_1}\}$.

As a consequence, the following decoupling Theorem 2 holds.

Theorem 2 *Given the data $P_c^{(n)}$ and $P_r^{(n)}$ and Theorem 1, the latter achieves variables decoupling, and the null space can be equivalently written as:*

$$\mathbf{c}_n = \underbrace{\mathbf{c}_n^{x_n}}_{\text{Bary}(x_n)} \odot \underbrace{(\mathbf{c}^{x_{n-1}} \otimes \mathbf{1}_{k_n})}_{\text{Bary}(x_{n-1})} \odot \underbrace{(\mathbf{c}^{x_{n-2}} \otimes \mathbf{1}_{k_n k_{n-1}})}_{\text{Bary}(x_{n-2})} \odot \cdots \odot \underbrace{(\mathbf{c}^{x_1} \otimes \mathbf{1}_{k_n \dots k_2})}_{\text{Bary}(x_1)}. \quad (11)$$

where \mathbf{c}^{x_l} denotes the vectorized barycentric coefficients related to the l -th variable.

As an illustration, in Theorem 2,

- $\mathbf{c}^{x_1} = \mathbf{c}_1^{({}^2\lambda_{k_2}, {}^3\lambda_{k_3}, \dots, {}^n\lambda_{k_n})}$ while

- \mathbf{c}^{x_2} is the vectorized collection of k_1 vectors $\mathbf{c}_1^{(1\lambda_1, 3\lambda_{k_3}, \dots, n\lambda_{k_n})}, \dots, \mathbf{c}_1^{(1\lambda_{k_1}, 3\lambda_{k_3}, \dots, n\lambda_{k_n})}$ and so on.

Theorem 1 and Theorem 2 then suggest a recursive (or cascaded) scheme, where only a collection of single variable null space computation is needed, instead of a single very large-scale one.

Next, we assess how much this contributes to taming the **C-o-D**, both in terms of flop and memory savings. For details and examples, reader is invited to refer to [3, Sec. 5].

2.3.2 Computational effort

Obviously, computing the null space vector in eq. (9) for $\mathbb{L}_n \in \mathbb{C}^{Q \times K}$ may be practically performed by mean of an SVD. By noticing that $Q \times K$ matrix SVD flop estimation is QK^2 (if $Q > K$) or, in the most favorable case N^3 (if $Q = K = N$), the complexity curve of $\mathcal{O}(N^3)$ will limit the method utilization. By recursively applying the result in Theorem 1 (or equivalently Theorem 2), it appears that the null space corresponding to a n -D Loewner matrix can be obtained with only 1-D Loewner matrices null space computations. See [3] for details, proofs and didactic examples (refer also to Section 4 for many examples). The direct consequence in terms of flop complexity is stated as follows.

Theorem 3 *The flop number for the recursive approach given in Theorem 1, is:*

$$\text{flop}_1 = \sum_{l=1}^n \left(k_l^3 \prod_{j=1}^l k_{j-1} \right) \text{ where } k_0 = 1.$$

Corollary 1 *The most computationally demanding configuration occurs when each variable x_l is of the same order $d_l = k_l - 1 = k - 1$ ($l = 1, \dots, n$), thus requiring k interpolation points each. In this configuration, the worst case flop writes (note that $N = k^n$)*

$$\overline{\text{flop}_1} = \overbrace{k^3 + k^4 + \dots + k^{n+2}}^{n \text{ terms}} = k^3 \frac{1 - k^n}{1 - k} = k^3 \frac{1 - N}{1 - k}, \quad (12)$$

which is a (n finite) geometric series of ratio k .

Consequently, an upper bound of eq. (12) can be estimated by considering that $k > 1$ and for a different number of variables n . As an example, the complexity is upper bounded by $\mathcal{O}(N^3)$ for $n = 1$, $\mathcal{O}(N^{2.29})$ for $n = 2$, $\mathcal{O}(N^{1.94})$ for $n = 3$, $\mathcal{O}(N^{1.73})$ for $n = 4$ and already $\mathcal{O}(N^{1.5})$ for $n = 6$. One can clearly observe that when the number of variables $n > 1$, the flop complexity drops, and this decreases as n increases; e.g. for $n = 50$ one gets $\mathcal{O}(N^{1.06})$. This is illustrated in Figure 2 which shows the worst-case $\overline{\text{flop}_1}$ as a function of n , and compares it to classical complexity references (notice that standard Loewner approaches is $\mathcal{O}(N^3)$).

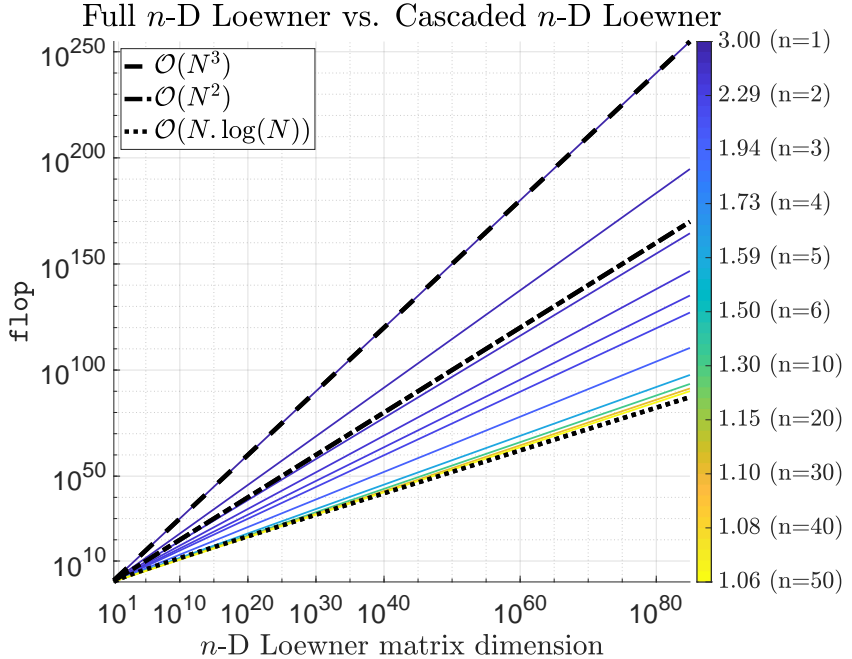


Figure 2: flop comparison: cascaded/recursive n -D Loewner worst-case upper bounds for varying number of variables n , while the full n -D Loewner is $\mathcal{O}(N^3)$ (black dashed); comparison with $\mathcal{O}(N^2)$ and $\mathcal{O}(N \log(N))$ references are shown in dash-dotted and dotted black lines.

2.3.3 Storage effort

Second, and equally important as the computational burden, the storage needed for the \mathbb{L}_n matrix of dimension $Q \times K$ is $\frac{8}{2^{20}} QK \text{ MB}$, or simply $\frac{8}{2^{20}} N^2 \text{ MB}$ (if equal number of columns and rows are considered). Then, the following holds.

Theorem 4 *Following Theorem 1 (and Theorem 2) process, one only needs to sequentially construct single 1-D Loewner matrices, each of dimension $\mathbb{L}_1 \in \mathbb{C}^{k_1 \times k_1}$. The largest stored matrix is $\mathbb{L}_1 \in \mathbb{C}^{\bar{k} \times \bar{k}}$, where $\bar{k} = \max_l k_l$ ($l = 1, \dots, n$). In complex and double precision, the maximum disk storage is $\frac{8}{2^{20}} \bar{k}^2 \text{ MB}$.*

2.3.4 Summary: full vs. cascaded (with an example)

The data storage for \mathbf{tab}_n is (in complex and double precision) is given by $\frac{8}{2^{20}} \prod_{l=1}^n (q_l + k_l)$ MB. For example $\mathbf{tab}_{n=6}$ of dimension $2 \cdot [20, 6, 4, 6, 8, 2] = 2 \cdot [k_1, k_2, k_3, k_4, k_5, k_6]$ needs 45 MB (we assume $q_l = k_l$). Then, according to the full or the cascaded null space computation version, the following figures hold.

Full n -D Loewner

- The construction of the $\mathbb{L}_n \in \mathbb{C}^{N \times N}$ matrix, where $N = K = Q$, needs

$$\frac{8}{2^{20}} N^2 = \frac{8}{2^{20}} 46,080^2 \text{ MB}$$

being 31.64 GB in our example.

- The required flop is N^3 , being $9.78 \cdot 10^{13}$ flop in our example.

Cascaded n -D Loewner

- The construction of the $\mathbb{L}_1 \in \mathbb{C}^{\bar{k} \times \bar{k}}$ matrix, where $\bar{k} = \max_l k_l$, needs

$$\frac{8}{2^{20}} \bar{k}^2 = \frac{8}{2^{20}} \bar{20}^2 \text{ MB}$$

being 6.25 KB in our example.

- The required flop is flop₁ as in Theorem 3, being $1.78 \cdot 10^6$ flop in our example^a.

^aNote also that flop may be decreased to $8.13 \cdot 10^5$ flop when variables optimally ordered, see [3].

In the next section, a MATLAB code is proposed to illustrate these features. In addition, the (very simple) example #3 from Section 4 is also detailed.

2.4 Simple detailed example with MATLAB code

Let us now practically detail with a very simple example how to deploy the recursive null space computation scheme presented in this section and detailed in [3]. This is exemplified with the MATLAB package +mLF, available as a [GitHub](#) repository at the following link:

<https://github.com/cpoussot/mLF>

Clone the repository. First, let clone the GitHub repository in the directory of your choice as follows (open a command line interface):

```
cd "directory_for_mLF"
git clone git@github.com:cpoussot/mLF.git
```

MATLAB interface. Now in MATLAB, add the path of the cloned repository as follows, and start using the available features:

```
%% Add the location of the +mlf package
addpath("directory_for_mLF")
```

We now start the illustration with a very simple rational example. Let us first start by defining a two-variable test function, i.e. $l = \{1, 2\}$ and $n = 2$,

$$\mathbf{H}(x_1, x_2) = x_1 x_2^2,$$

together with its bounds and discretization mesh $2N_l = 40$,

$$\mathcal{X}_l := [-1, 1].$$

```

%%% Define a multivariate handle function
n      = 2; % number of variables
H      = @(x1,x2) x1*x2^2; % multivariate function definition
Nip    = 20; % number of interpolation points for rows and columns
xbnd   = [-1 1]; % bounds of both variables

```

From the above setup, define columns and rows set points, where $k_l = 20$ and $q_l = 20$. In detail (notice that theoretically any arrangement is possible):

- $p_c\{1\}$ are the $[^1\lambda_1, \dots, ^1\lambda_{k_1}]$,
- $p_c\{2\}$ are the $[^2\lambda_1, \dots, ^2\lambda_{k_2}]$,
- $p_r\{1\}$ are the $[^1\mu_1, \dots, ^1\mu_{q_1}]$,
- $p_r\{2\}$ are the $[^2\mu_1, \dots, ^1\mu_{q_2}]$.

```

%%% Interpolation points (IP) columns and rows (as Section 3, eq. 13–15)
for ii = 1:n
    p_c{ii} = linspace(xbnd(1),xbnd(2),Nip);
    dx      = abs(p_c{ii}(end)-p_c{ii}(end-1))/2;
    p_r{ii} = p_c{ii}+dx;
end

```

Check that interpolation points are disjoint and construct the 2-D tensor tableau $\mathbf{tab}_2 \in \mathbb{R}^{(q_1+q_2) \times (k_1+k_2)}$.

```

%%% Elementary ingredients
% Check that column/row IP are disjoint (Section 3)
ok = mlf.check(p_c,p_r);
% Construct tab_n (Section 3)
tab = mlf.make_tab(H,p_c,p_r,true);
%
size(tab)
ans =
    40     40

```

Now, following [3, Alg. 1], it is possible to estimate the order along each variables.

```

%%% Estimate orders along each variables and select a subset of IP
tol_ord          = 1e-7;
ord              = mlf.compute_order(p_c,p_r,tab,tol_ord,[],5,true);
[pc,pr,W,V,tab_red] = mlf.points_selection(p_c,p_r,tab,ord,true);
w                = mlf.mat2vec(W);
pc =
    1x2 cell array
    {[ -1 1]}     {[ -1 -0.0526 1]}
pr =
    1x2 cell array
    {[ -0.9474 1.0526]}     {1x3 double}
w =
    -1.0000
    -0.0028
    -1.0000
    1.0000
    0.0028
    1.0000

```

The following Figure 3 is reported. It shows the single-variable Loewner matrix normalized singular values. In this very simple case, x_1 is of dimension $d_1 = 1$ while x_2 is of dimension $d_2 = 2$, thus requiring $\{k_1, k_2\} = \{2, 3\}$ column interpolation points. This implies a barycentric vector of dimension $2 \times 3 = 6 = N$. Adding more interpolation points would lead to **overfitting**.

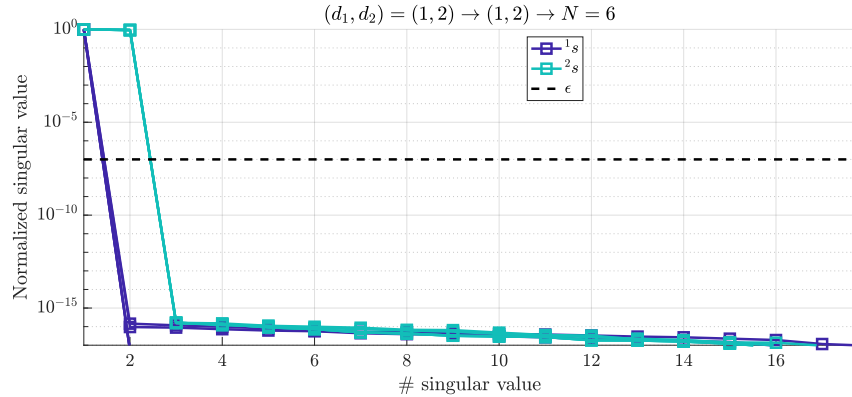


Figure 3: Single variable Loewner matrices normalized singular values (order detection).

Now, following [3, Thm. 5.3] (or Theorem 1 and Theorem 2), one may compute the barycentric coefficients, being the null space \mathbf{c}_2 of the 2-D Loewner matrix (not constructed !), as follows:

```
%>>> %% Recursive null-space computation (Section 5, Theorem 5.3)
[c, info] = mlf.loewner_null_rec(pc, pr, tab_red, 'svd0');
c =
-1.1111
2.1111
-1.0000
1.1111
-2.1111
1.0000
```

Then, following [3, Thm. 5.5 & Thm. 5.6] (or Theorem 3 and Theorem 4), the following computational and storage efforts can be reported.

```
%>>> %% Curse of dimensionality (Section 5, Theorem 5.5 & Theorem 5.6)
fprintf('FLOPS\n')
fprintf(' * recursive: %d\n', info.nflop)
fprintf(' * full.    : %d\n', length(c)^3) % At least !
fprintf('MEMORY\n')
fprintf(' * recursive: %d MB\n', max(ord+1)^2/2^20)
fprintf(' * full.    : %d MB\n', prod(ord+1)^2/2^20)
FLOPS
* recursive: 62
* full.    : 216
MEMORY
* recursive: 8.583069e-06 MB
* full.    : 3.433228e-05 MB
```

The above numbers clearly show how much, even in such a very simple case, the complexity and computational load is reduced. This is why we claim for taming the curse of dimensionality. Then, the following code suggests a way to visualize the evaluation of both \mathbf{H} and \mathbf{G} , as well as the mismatch absolute error (in a log-scale).

```
%>>> %% Compute the responses along first and second variables
x1      = linspace(min(p_r{1}),max(p_r{1}),40)+rand(1)/10;
x2      = linspace(min(p_r{1}),max(p_r{1}),41)+rand(1)/10;
[X,Y]   = meshgrid(x1,x2);
for ii = 1:numel(x1)
    for jj = 1:numel(x2)
        tab_ref(jj,ii) = H(x1(ii),x2(jj));
        tab_app(jj,ii) = mlf.eval_lagrangian(pc,w,c,[x1(ii) x2(jj)],false);
```

```

    end
end
%% 2D surfaces plot and mismatch
figure
subplot(1,2,1); hold on, grid on, axis tight,
surf(X,Y,tab_app , 'EdgeColor','none')
surf(X,Y,tab_ref , 'EdgeColor','k','FaceColor','none')
xlabel('$x_1$', 'Interpreter', 'latex')
ylabel('$x_2$', 'Interpreter', 'latex')
set(gca, 'TickLabelInterpreter', 'latex')
title('Original vs. Approximation', 'Interpreter', 'latex'), view(-30,40)
subplot(1,2,2); hold on, grid on, axis tight
imagesc(log10(abs(tab_ref-tab_app)), 'XData',x1, 'YData',x2)
xlabel('$x_1$', 'Interpreter', 'latex')
ylabel('$x_2$', 'Interpreter', 'latex')
set(gca, 'TickLabelInterpreter', 'latex')
title('{\bf log }(abs. err.)', 'Interpreter', 'latex'), colorbar ,

```

Figure 4 compares the evaluation of original model \mathbf{H} that generated the tensor data \mathbf{tab}_n with the reconstruction surrogate model \mathbf{G} (left), and the mismatch error in logarithmic scale (right). Error is at machine precision. In this case, the function is also recovered.

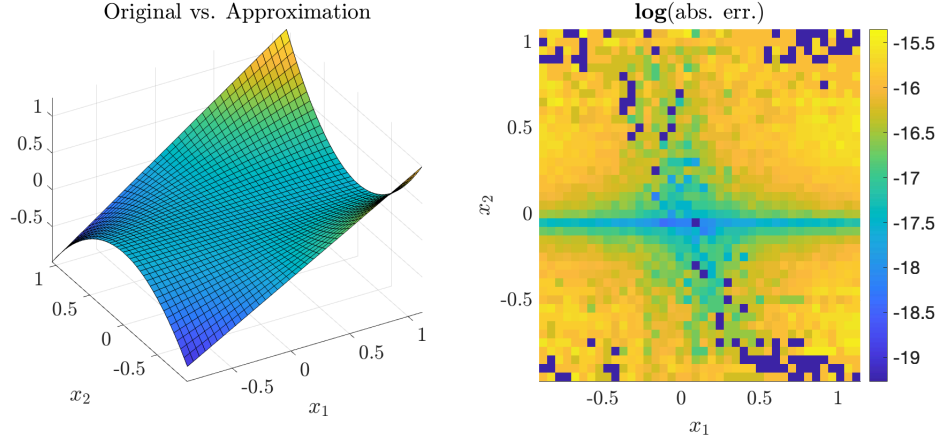


Figure 4: Left: original \mathbf{H} (grid) and approximated \mathbf{G} (colored surface) models. Right: absolute mismatch error (in log-scale).

2.5 Summary

In the contribution [3], thanks to the **cascaded (or recursive) null space construction**, we provide a equivalent alternative to the standard brute force null space computation of multivariate Loewner matrices. Through this recursive null space construction, we avoid the costly intermediate large n -D Loewner matrix construction, thus saving a lot of disk access time and memory and thus taming the C-o-D. In addition, the n -D rational function construction problem is recast as a collection of 1-D problems, **simpler to store and solve in practice**, and leading to overall more accurate results. This statement also shows how much **the variables decoupling is intrinsically achieved by this process**. By this, in addition to the data-driven multivariate rational approximation feature, we believe we also provide a viable solution to tensor approximation via rational functions. Finally, by connecting this result to the **Kolmogorov Superposition Theorem**, it also contributes in bridging the gap between **Neural Networks** and **rational approximation** fields. In the rest of the document, these features are illustrated through a collection of 46 examples.

3 Overview of the results

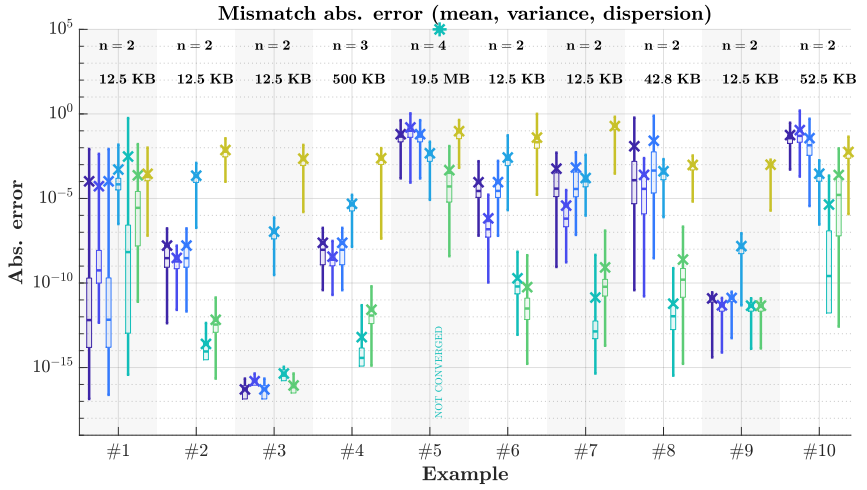
3.1 Approximation performances statistics

For each #1 to #46 examples, Figures 5a, 6a, 7a, 8a, 9a, show the RMSE related statistics obtained for the 500 of random experiments (i.e. input variables draw) applied on \mathbf{G}_m (i.e. the best surrogate candidate). More specifically, the average (crosses), the median (horizontal lines), first quartile (thick bar) and minimal and maximal values (vertical line) are reported for each method. Similarly, Figures 5b, 6b, 7b, 8b, 9b, and 5c, 6c, 7c, 8c, 9c, show the model construction computational time and resulting model complexity, respectively. In each figure, the number of variables n and the data tensor \mathbf{tab}_n size are also recalled.

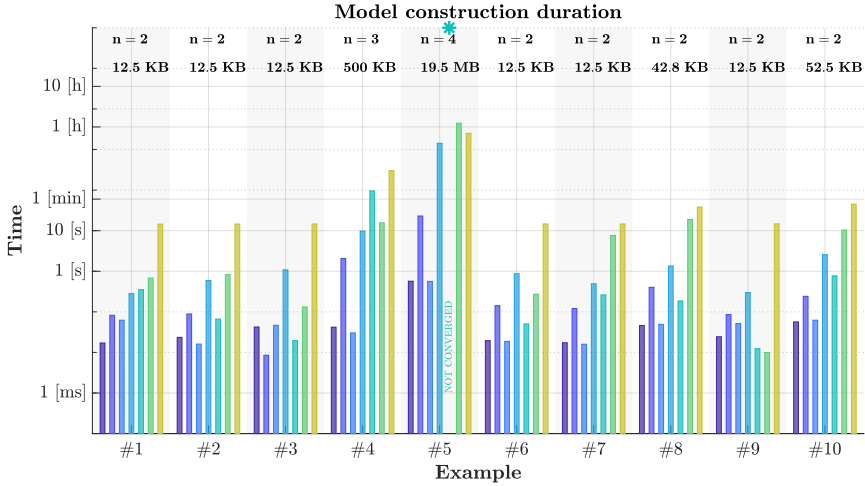
For each block, colors represent methods M1 [3, Alg. 1], M2 [3, Alg. 2], M3 [10], M4 [12, KAN], M5 [5, pAAA] and M6 [5, LR-pAAA], and M7 [1, MLP by Tensor Flow], respectively.

Remark 7 (NaN values) *For some examples, especially ones involving high dimensional tensors, some methods either do not converge or were stopped by as they were stuck or crashed because of memory limitations. Therefore we conclude that scalability limits were reached and report mentioned "not converged" instead. Obviously, we remain open to comments and solutions from readers.*

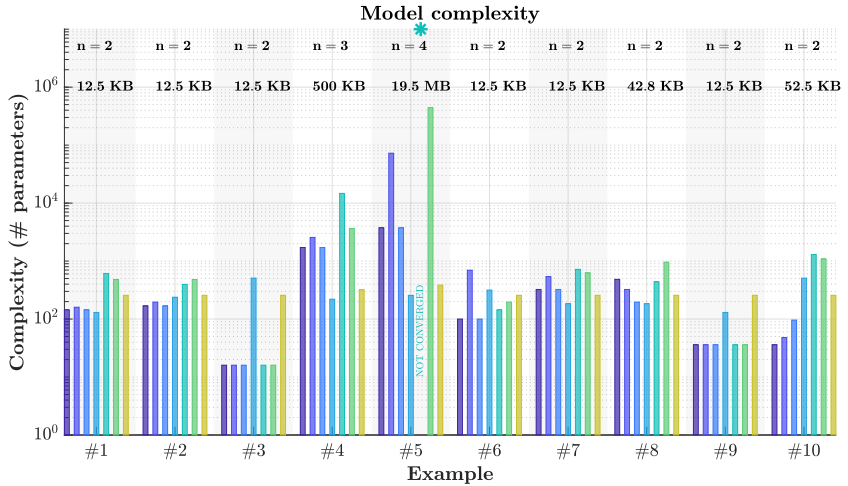
Remark 8 (Feedback to authors) *This report is aimed at being regularly updated and improved. Please send any feedback or suggestions to charles.poussot-vassal@onera.fr.*



(a) Mismatch absolute error $|\mathbf{G}_m - \mathbf{H}|$ of the best configuration only (log-scale).

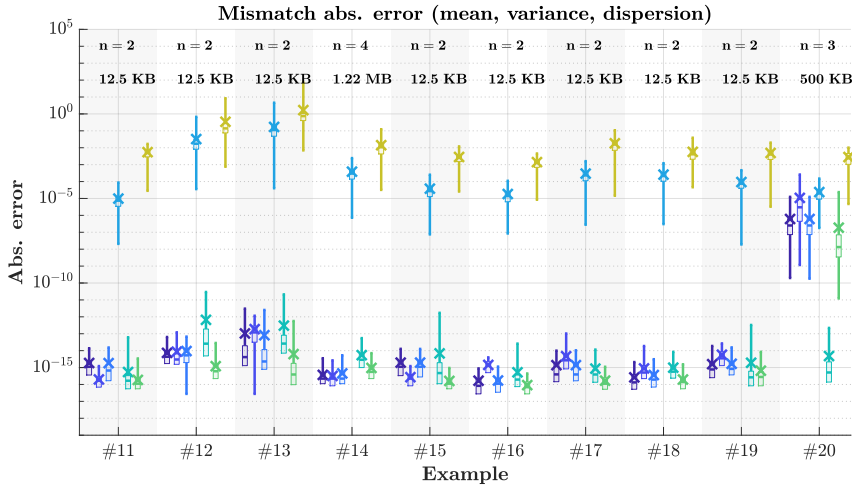


(b) Model \mathbf{G}_m computation time of the best configuration only (log-scale).

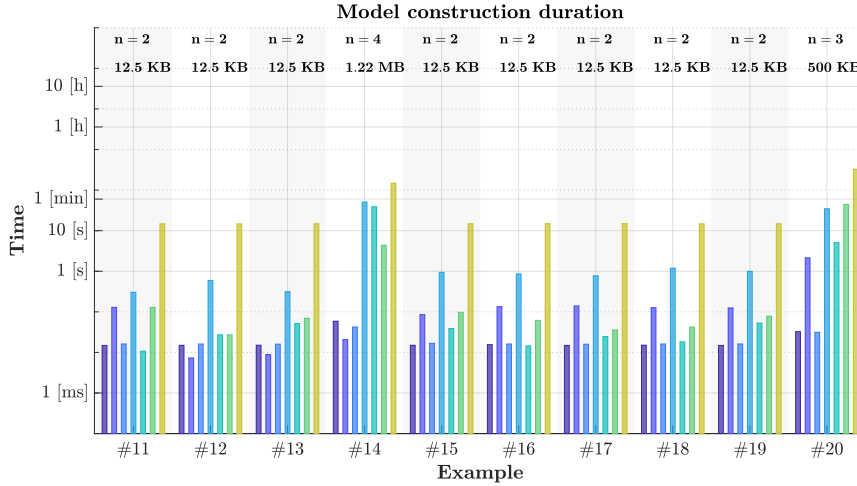


(c) Model \mathbf{G}_m complexity of the best configuration only (log-scale).

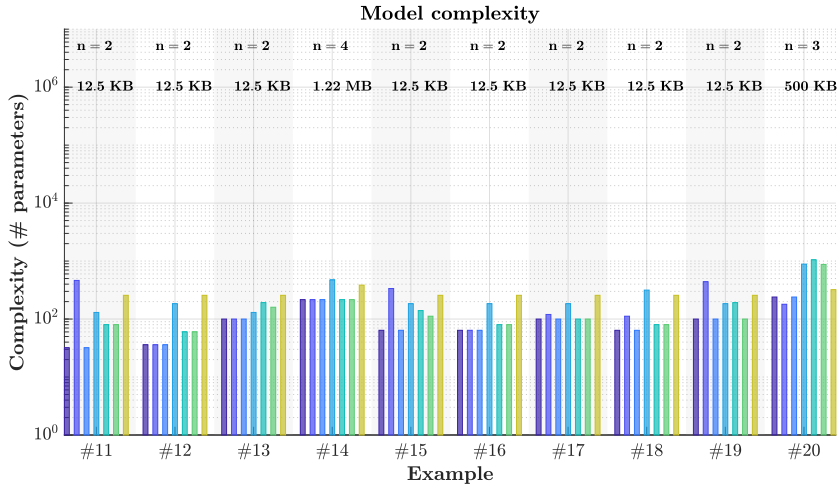
Figure 5: Examples set 1.



(a) Mismatch absolute error $|\mathbf{G}_m - \mathbf{H}|$ of the best configuration only (log-scale).

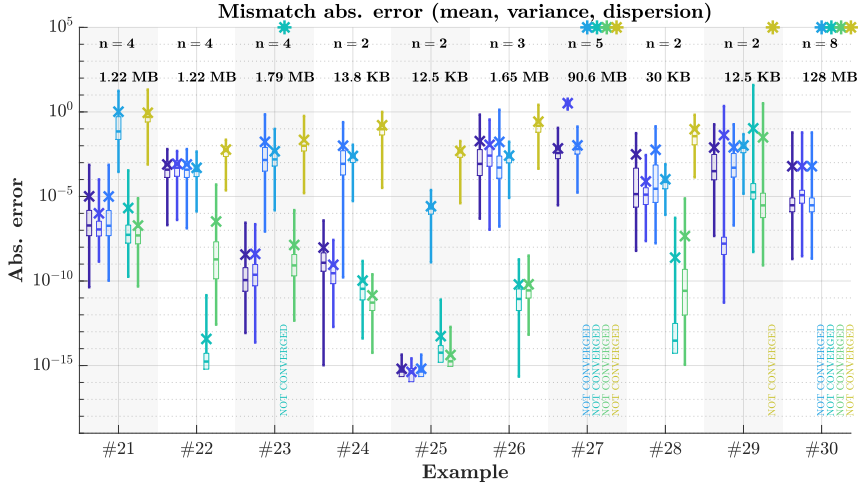


(b) Model \mathbf{G}_m computation time of the best configuration only (log-scale).

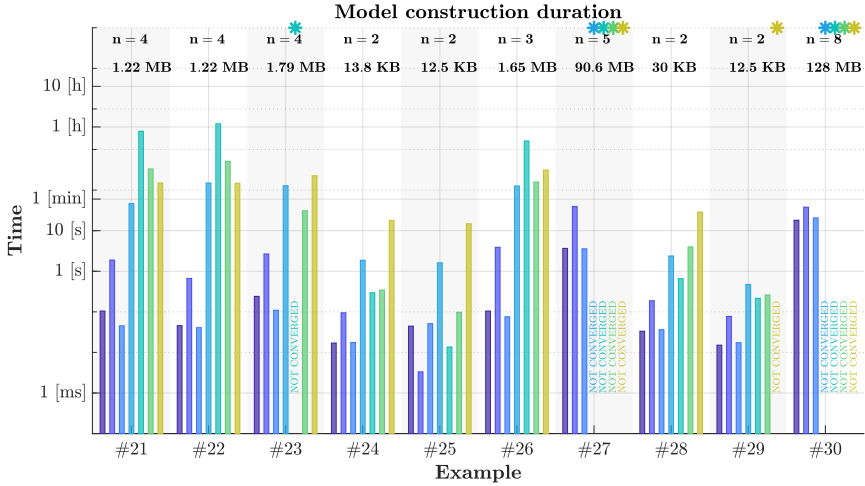


(c) Model \mathbf{G}_m complexity of the best configuration only (log-scale).

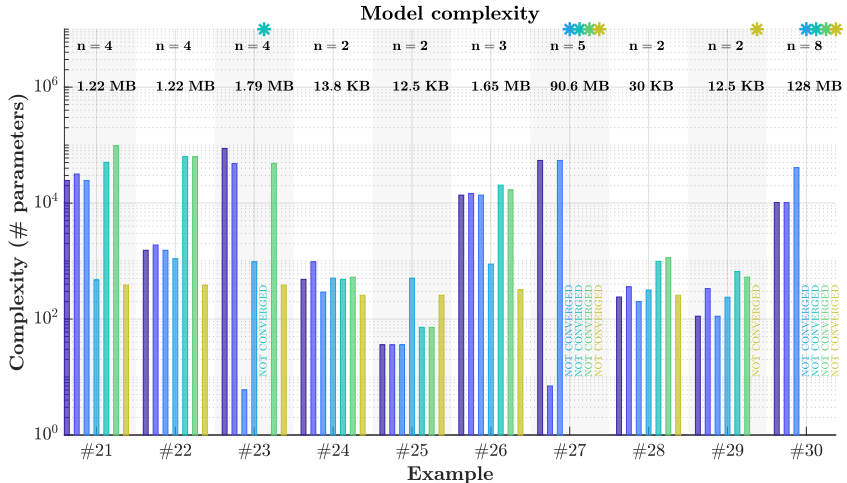
Figure 6: Examples set 2.



(a) Mismatch absolute error $|\mathbf{G}_m - \mathbf{H}|$ of the best configuration only (log-scale).

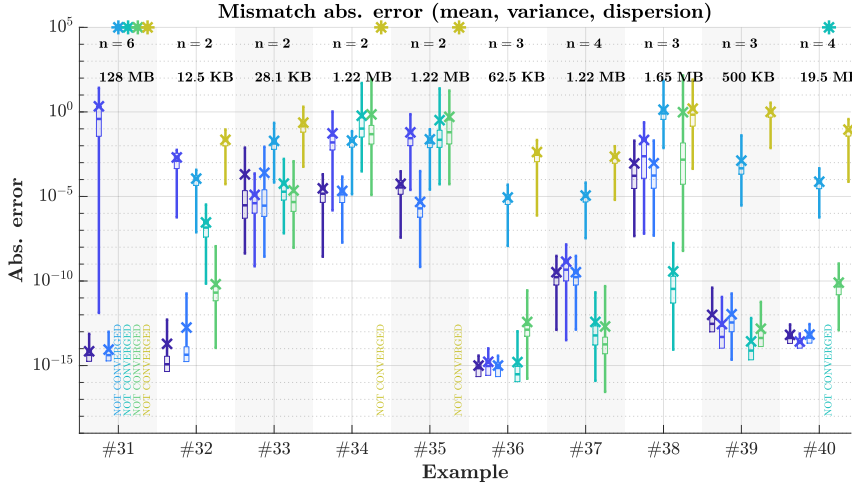


(b) Model \mathbf{G}_m computation time of the best configuration only (log-scale).

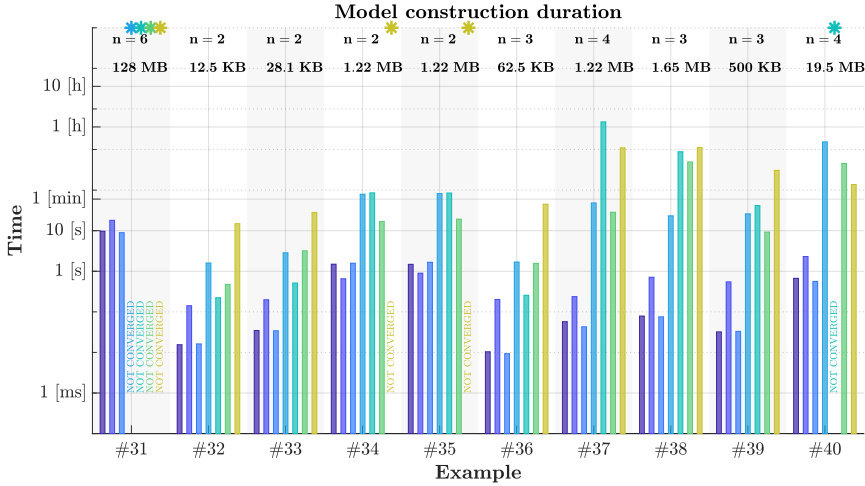


(c) Model \mathbf{G}_m complexity of the best configuration only (log-scale).

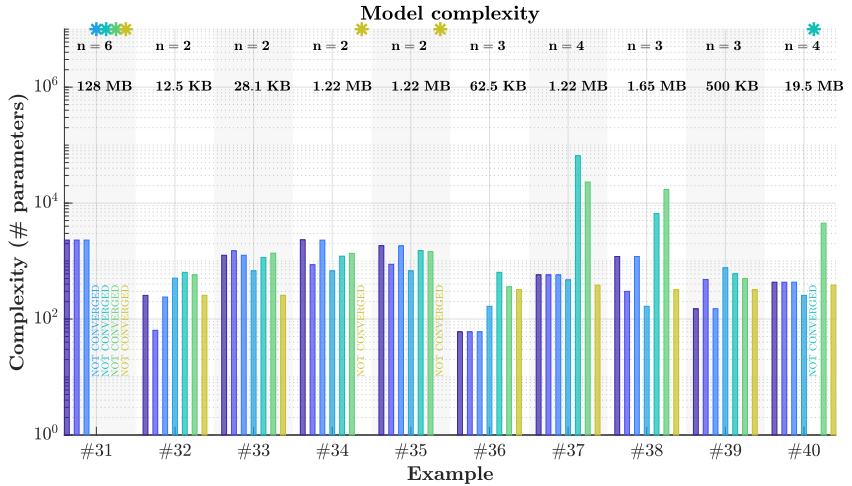
Figure 7: Examples set 3.



(a) Mismatch absolute error $|\mathbf{G}_m - \mathbf{H}|$ of the best configuration only (log-scale).

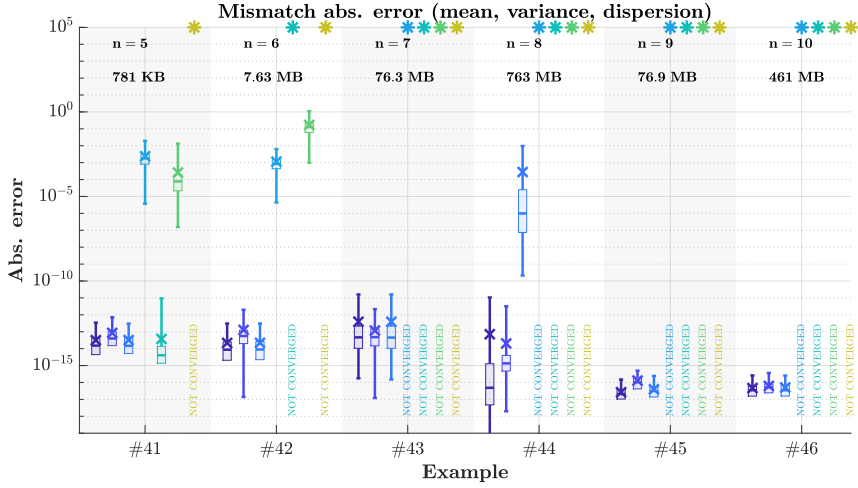


(b) Model \mathbf{G}_m computation time of the best configuration only (log-scale).

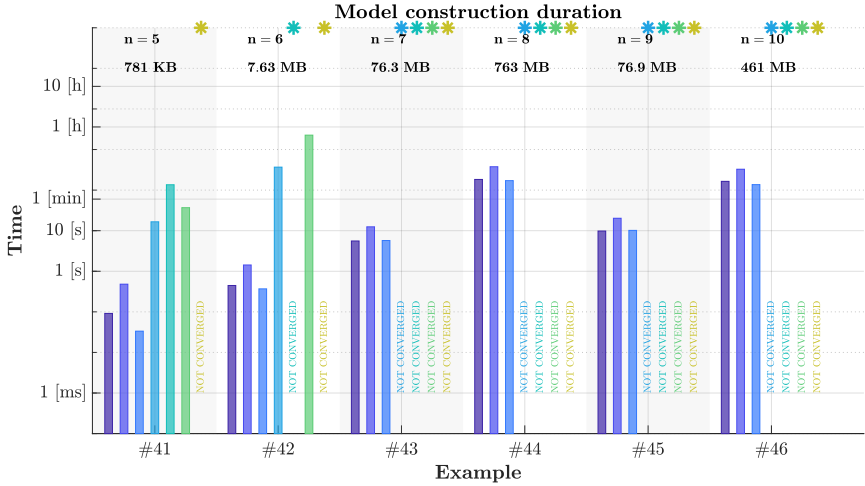


(c) Model \mathbf{G}_m complexity of the best configuration only (log-scale).

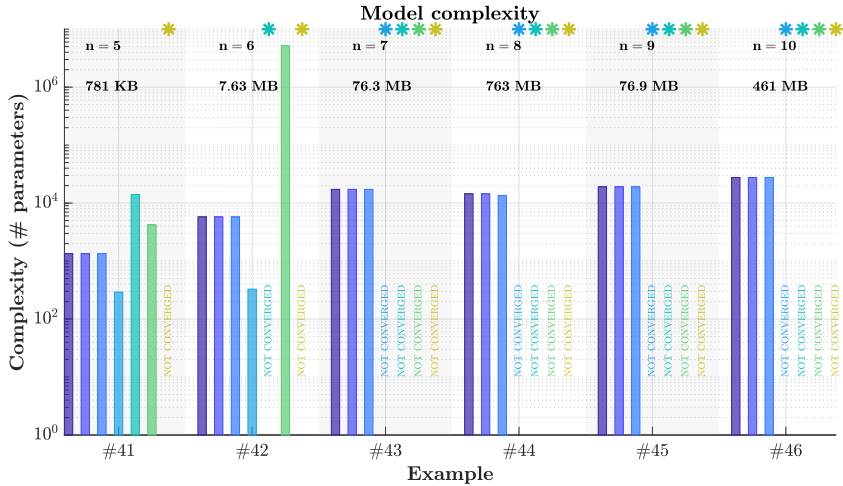
Figure 8: Examples set 4.



(a) Mismatch absolute error $|\mathbf{G}_m - \mathbf{H}|$ of the best configuration only (log-scale).



(b) Model \mathbf{G}_m computation time of the best configuration only (log-scale).



(c) Model \mathbf{G}_m complexity of the best configuration only (log-scale).

Figure 9: Examples set 5.

Next, Figure 10 reports the average (over all method parameterization configurations) computation time for each method as a function of the original tensor \mathbf{tab}_n size.

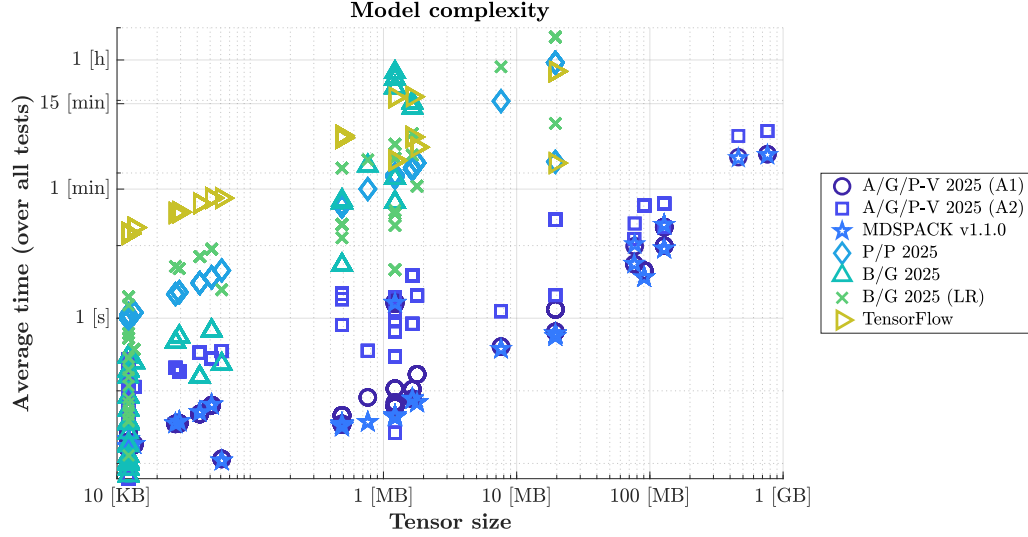


Figure 10: Average \mathbf{G}_m model construction computation time vs. \mathbf{tab}_n tensor size.

3.2 Preliminary remarks

Velocity and scalability. By inspecting Figures 5b, 6b, 7b, 8b, 9b, it is clear that M1, M2 and M3 provide a very fast solution to the tensor approximation problem, with computational times way faster than the other methods. In addition with reference to Figure 10 we demonstrate that these methods are able to address high dimensional tensors, where others fail or lead to prohibitive computational time. This is an essential feature to the perspective of taming the C-o-D. We claim that **the recursive null space computation proposed in [3] is a cutting edge solution to both the scalability issue and the user experience improvement.**

Tuning parameters. Remembering that each method has multiple tunable parameters, finding the adequate/optimal parameter set is not a trivial task. Indeed, in the next section we show how the "optimal" parameters vary from an example to an other. And thus there is no clear optimal tuning parameter set for all functions. We believe this still is an open research question, not only from an engineering point of view, but also from a theoretical one. From our experience, it is still not so clear which parameters play an important role in the success or failure of some methods. While in the single variable case (stopping) criteria are quite well understood (e.g. Loewner rank, singularities/eigenvalues, root mean square error, complexity, etc.), in the multivariate case, such criteria still need to be defined, analyzed and adjusted. This collection of examples gives some insight of issues encountered and potential solutions, but a rather generic solution needs to be discovered. This will be the purpose of future investigations from our group, and hopefully from the community. One interesting argument for M1, M2 and M3, is that the fast computational process allows for multiple (greedy) iterations on the tuning parameter configurations.

Accuracy. By inspecting Figures 5a, 6a, 7a, 8a, 9a, one may also notice that some models obtained with M1, M2, M3, M5 and M6 lead to RMSE close or even below machine precision. This means that the underlying model generating the tensor has been recovered (or discovered) from data only. This property is (always) verified when the generating system \mathbf{H} is a rational model. Indeed the barycentric form of the surrogate model fits the rational form. When the generating function \mathbf{H} is irrational, machine precision mismatch error may not be obtained, or

at the price of a very complex surrogate. Even if machine precision is not reached, one should point that all methods perform well overall, which is important to point out, giving also credit to third parties software. However, when the tensor size or the number of variables n increases, M4, M5, M6 and M7, which do not benefit for the recursive scheme, fail due to with memory issues or prohibitive computational time. This highlight the scalability issue, levered by the proposed contribution in [3].

Complexity. By inspecting Figures 5c, 6c, 7c, 8c, 9c, we may first notice an overall homogeneity in the complexity of the achieved models. However a precise inspection (see detailed sub-sections) reveals that M4, M5 and M6 (and sometimes M2) tend to overfit by constructing models with too many variables. This is especially true when the original function is a rational function, which complexity and minimality can be evaluated exactly. Regarding M7, no conclusion can be made since one single configuration has been tested.

Comments on KAN and MLP based methods. M4 is an algorithm implementing KAN-based models, while M7 is an algorithm implementing MLP-based models. In both cases, the topology of the network is an argument for the optimizer, that is fed by the user. As non expert in network modeling, we humbly chose some configurations that are amendable. Please feel free to test your own configuration and send us improved directions and parameterizations.

4 Detailed examples exposition and results

The collection of 46 examples is now reported in what follows. We believe this stands as a relatively exhaustive evaluation of different methods over different functions. However, results remain amendable and open to improvements. In addition, when possible, i.e. when complexity of the constructed model \mathbf{G}_1 (obtained by M1), is simple, additional detailed informations are also given; the ambition is also to provide a clear understanding of the method M1 detailed in [3], and briefly recalled in Section 2. This collection will be enriched with time.

4.1 Function #1 ($n = 2$ variables, tensor size: 12.5 KB)

$$\text{ReLU}(x_1) + \frac{1}{100}x_2$$

4.1.1 Setup and results overview

- Reference: Personal communication, [none]
- Domain: \mathbb{R}
- Tensor size: 12.5 **KB** (40^2 points)
- Bounds: $(-1 \ 1) \times (-1 \ -\frac{1}{10000000000})$

#	Alg.	Parameters	Dim.	CPU [s]	RMSE	min err.	max err.
1	A/G/P-V 2025 (A1)	1e-11,3	144	0.0171	0.000699	1.39e - 17	0.00841
	A/G/P-V 2025 (A2)	1e-15,3	160	0.0823	0.000389	4.49e-13	0.00434
	MDSPACK v1.1.0	1e-11,1e-06	144	0.0623	0.000699	2.43e-17	0.00841
	P/P 2025	1,0.95,50,0.01,4,6,9	130	0.282	0.0017	3.08e-07	0.0152
	B/G 2025	0.001,20	612	0.353	0.0288	3.75e-16	0.567
	B/G 2025 (LR)	0.001,20,4	480	0.678	0.00147	7.82e-12	0.0164
	TensorFlow		257	14.6	0.00074	6.31e-08	0.0102

Table 2: Function #1: best model configuration and performances per methods.

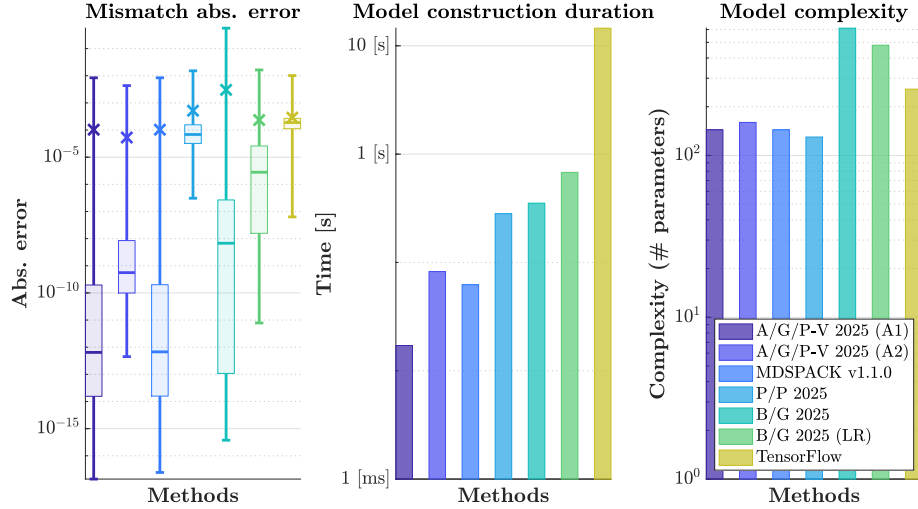


Figure 11: Function #1: graphical view of the best model performances.

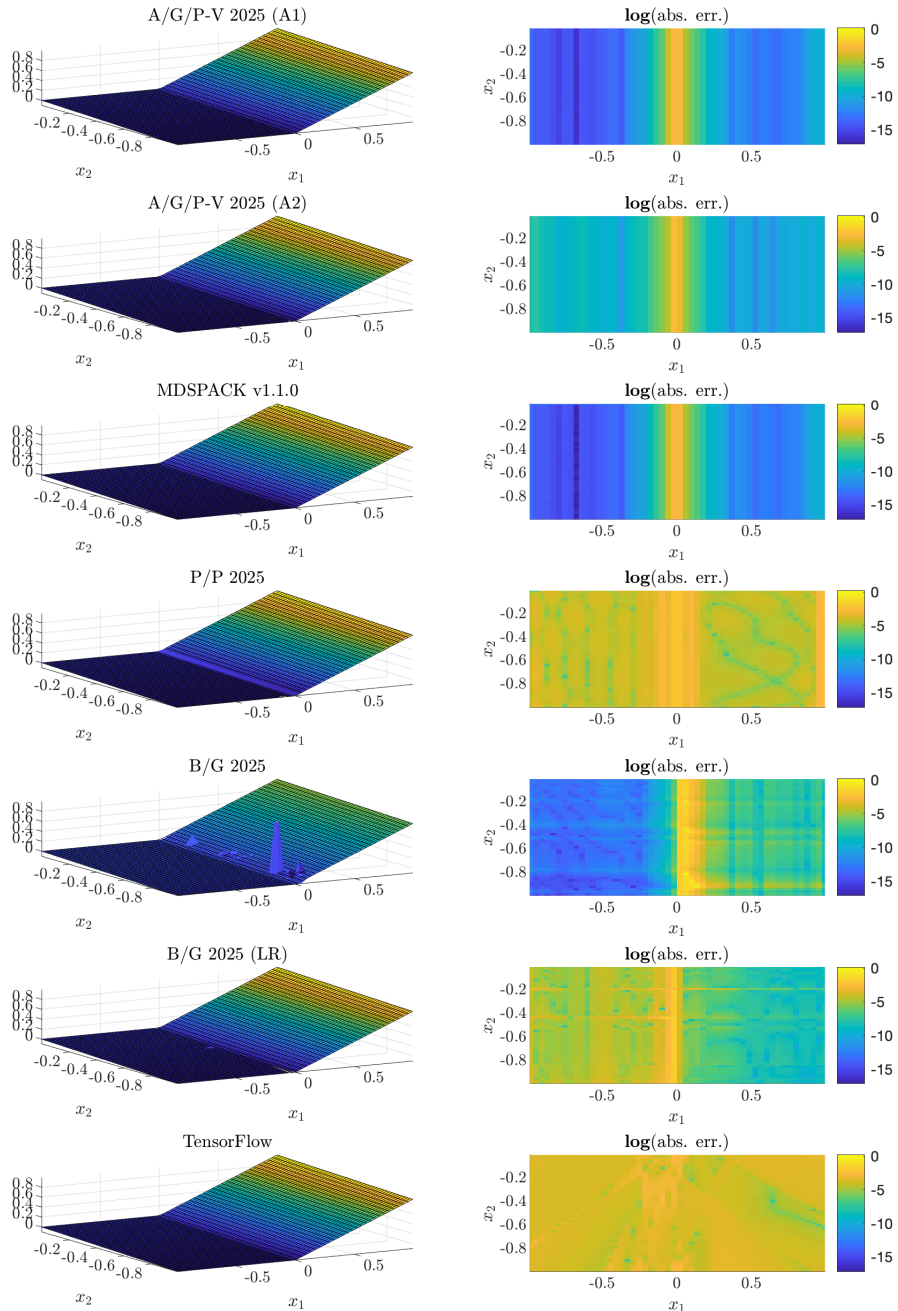


Figure 12: Function #1: left side, evaluation of the original (mesh) vs. approximated (coloured surface) and right side, absolute errors (in log-scale).

4.1.2 mLFB detailed informations (M1)

Right interpolation points: $k_l = \begin{pmatrix} 18 & 2 \end{pmatrix}$, where $l = 1, \dots, n$.

$$\begin{aligned} {}^1\lambda_{j_1} &\in \mathbb{C}^{18}, \text{ linearly spaced between bounds} \\ {}^2\lambda_{j_2} &\in \mathbb{C}^2, \text{ linearly spaced between bounds} \end{aligned}$$

n-D Loewner matrix, barycentric weights and Lagrangian basis:

$$\begin{aligned} \mathbb{L} &\in \mathbb{C}^{36 \times 36} \\ \mathbf{c} &\in \mathbb{C}^{36} \\ \mathbf{w} &\in \mathbb{C}^{36} \\ \mathbf{c} \cdot \mathbf{w} &\in \mathbb{C}^{36} \\ \mathbf{Lag}(x_1, x_2) &\in \mathbb{C}^{36} \end{aligned}$$

4.2 Function #2 ($n = 2$ variables, tensor size: 12.5 KB)

$$\exp(\sin(x_1) + x_2^2)$$

4.2.1 Setup and results overview

- Reference: L/al. 2024, [8]
- Domain: \mathbb{R}
- Tensor size: 12.5 KB (40² points)
- Bounds: $(-1 \ 1) \times (-1 \ 1)$

#	Alg.	Parameters	Dim.	CPU [s]	RMSE	min err.	max err.
2	A/G/P-V 2025 (A1)	1e-06,1	168	0.0235	3.36e-08	4.2e-13	1.7e-07
	A/G/P-V 2025 (A2)	1e-15,1	196	0.0888	4.48e-09	2.58e-12	1.62e-08
	MDSPACK v1.1.0	1e-06,0.0001	168	0.0161	3.36e-08	2.09e-12	1.7e-07
	P/P 2025	1,1,50,0.01,6,6,13	238	0.591	0.000287	1.84e-07	0.00126
	B/G 2025	1e-09,20	396	0.0665	4.88e - 14	0	4.32e - 13
	B/G 2025 (LR)	1e-09,20,3	480	0.827	1.29e-12	2.22e-16	1.38e-11
	TensorFlow		257	14.6	0.00937	9.75e-05	0.0361

Table 3: Function #2: best model configuration and performances per methods.

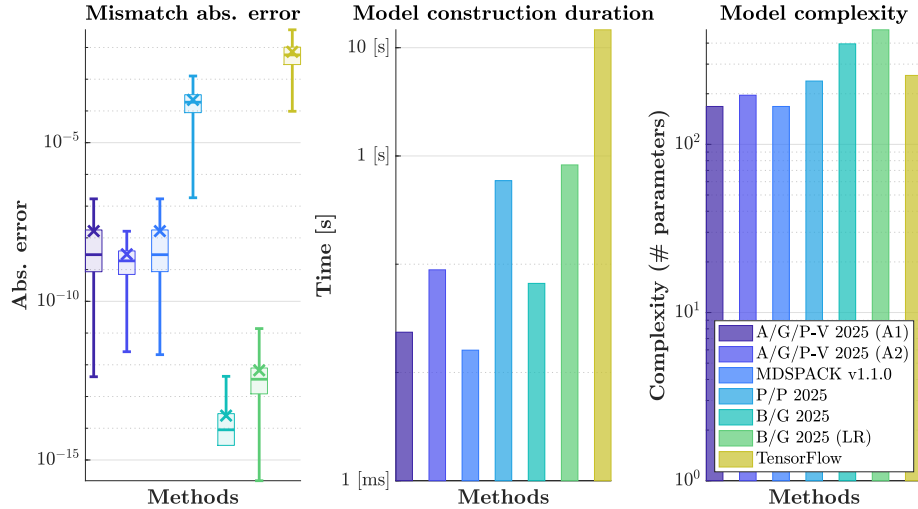


Figure 13: Function #2: graphical view of the best model performances.

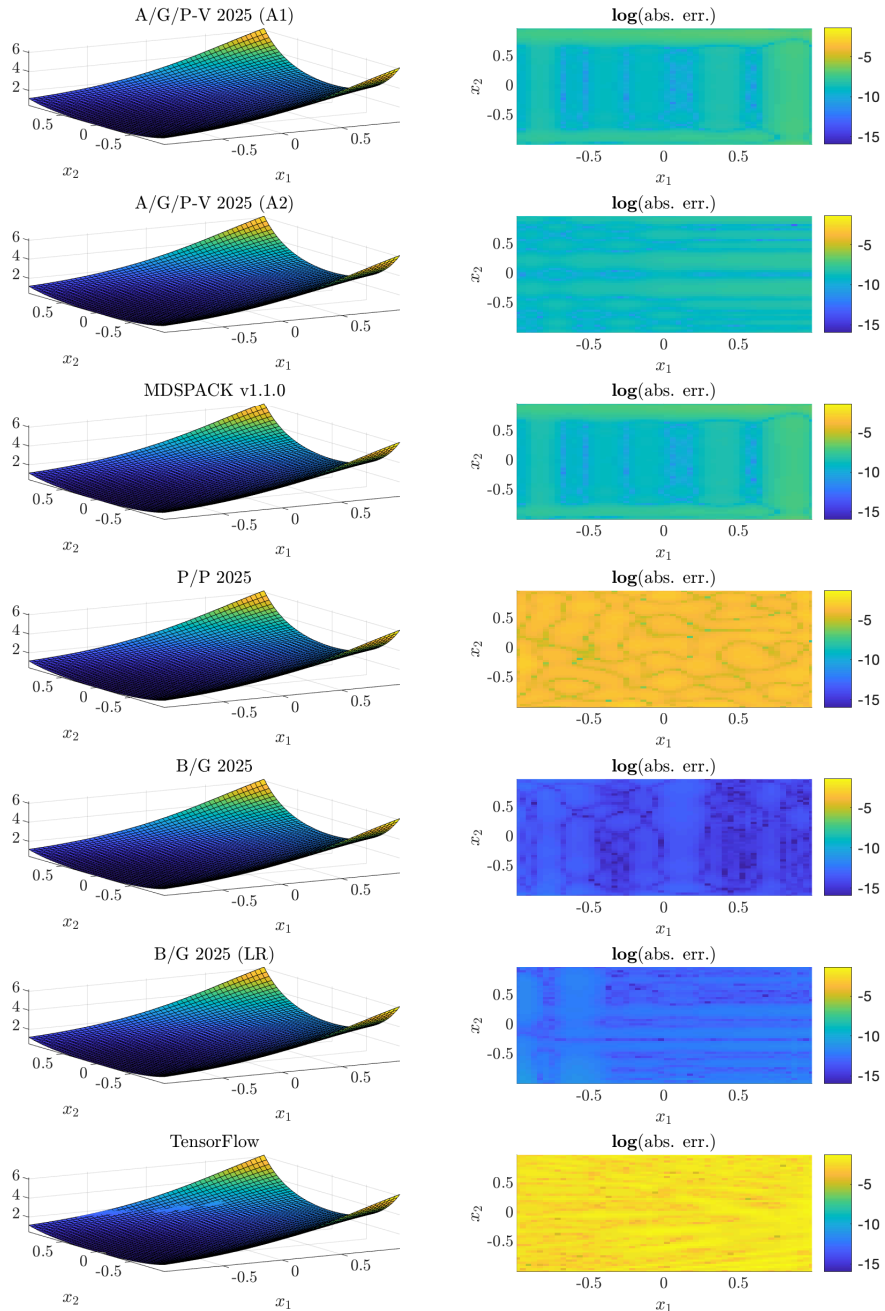


Figure 14: Function #2: left side, evaluation of the original (mesh) vs. approximated (coloured surface) and right side, absolute errors (in log-scale).

4.2.2 mLFB detailed informations (M1)

Right interpolation points: $k_l = \begin{pmatrix} 6 & 7 \end{pmatrix}$, where $l = 1, \dots, n$.

$$\begin{aligned} {}^1\lambda_{j_1} &\in \mathbb{C}^6, \text{ linearly spaced between bounds} \\ {}^2\lambda_{j_2} &\in \mathbb{C}^7, \text{ linearly spaced between bounds} \end{aligned}$$

n-D Loewner matrix, barycentric weights and Lagrangian basis:

$$\begin{aligned} \mathbb{L} &\in \mathbb{C}^{42 \times 42} \\ \mathbf{c} &\in \mathbb{C}^{42} \\ \mathbf{w} &\in \mathbb{C}^{42} \\ \mathbf{c} \cdot \mathbf{w} &\in \mathbb{C}^{42} \\ \mathbf{Lag}(x_1, x_2) &\in \mathbb{C}^{42} \end{aligned}$$

4.3 Function #3 ($n = 2$ variables, tensor size: 12.5 KB)

$$x_1 \cdot x_2$$

4.3.1 Setup and results overview

- Reference: L/al. 2024, [8]
- Domain: \mathbb{R}
- Tensor size: 12.5 **KB** (40^2 points)
- Bounds: $(-1 \ 1) \times (-1 \ 1)$

#	Alg.	Parameters	Dim.	CPU [s]	RMSE	min err.	max err.
3	A/G/P-V 2025 (A1)	0.5,1	16	0.0423	6.8e - 17	0	2.22e - 16
	A/G/P-V 2025 (A2)	1e-15,1	16	0.00854	1.8e-16	0	4.44e-16
	MDSPACK v1.1.0	0.5,0.01	16	0.0467	6.8e-17	0	2.22e-16
	P/P 2025	1,0.95,50,0.01,10,4,21	508	1.08	1.4e-07	2.97e-10	7.41e-07
	B/G 2025	0.001,20	16	0.0196	5.46e-16	0	1.11e-15
	B/G 2025 (LR)	0.001,20,5	16	0.132	1.11e-16	0	4.44e-16
	TensorFlow		257	14.7	0.00296	1.58e-06	0.0147

Table 4: Function #3: best model configuration and performances per methods.

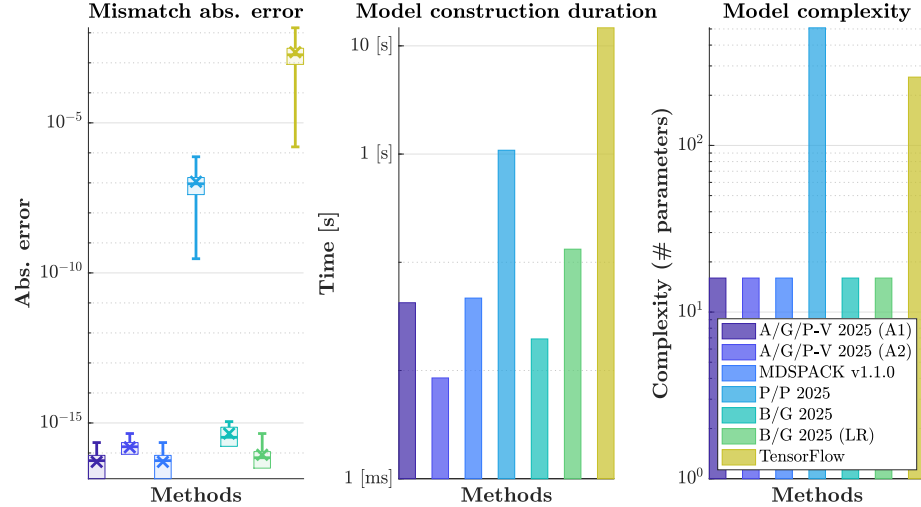


Figure 15: Function #3: graphical view of the best model performances.

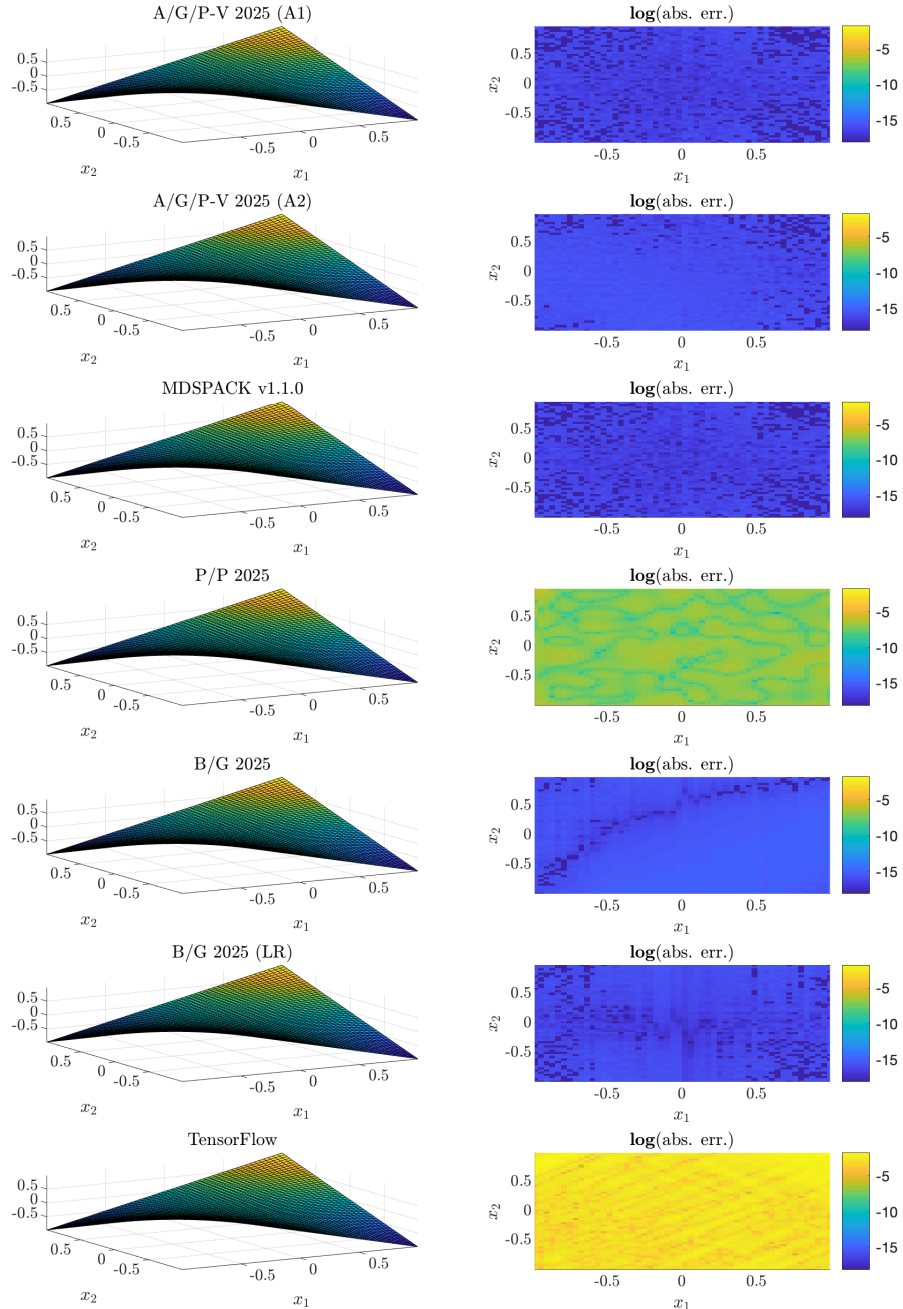


Figure 16: Function #3: left side, evaluation of the original (mesh) vs. approximated (coloured surface) and right side, absolute errors (in log-scale).

4.3.2 mLF detailed informations (M1)

Right interpolation points: $k_l = \begin{pmatrix} 2 & 2 \end{pmatrix}$, where $l = 1, \dots, n$.

$$\begin{aligned} {}^1\lambda_{j_1} &= \begin{pmatrix} -1 & 1 \end{pmatrix} \\ {}^2\lambda_{j_2} &= \begin{pmatrix} -1 & 1 \end{pmatrix} \end{aligned}$$

Lagrangian weights, data and supports (Lagrangian basis):

$$\begin{pmatrix} \mathbf{c} & \mathbf{w} & \mathbf{c} \cdot \mathbf{w} & \mathbf{Lag} \\ 1.0 & 1.0 & 1.0 & \frac{1}{(x_1+1.0)(x_2+1.0)} \\ -1.0 & -1.0 & 1.0 & \frac{1}{(x_1+1.0)(x_2-1.0)} \\ -1.0 & -1.0 & 1.0 & \frac{1}{(x_1-1.0)(x_2+1.0)} \\ 1.0 & 1.0 & 1.0 & \frac{1}{(x_1-1.0)(x_2-1.0)} \end{pmatrix}$$

KST equivalent decoupling pattern

Barycentric weights:

$$\begin{aligned} \mathbf{c}^{x_2} &= \text{vec} \begin{pmatrix} -1.0 & -1.0 \\ 1.0 & 1.0 \end{pmatrix} \quad \text{and } \mathbf{Bary}_{x_2} = \mathbf{c}^{x_2} \otimes \mathbf{1}_1 \\ \mathbf{c}^{x_1} &= \begin{pmatrix} -1.0 \\ 1.0 \end{pmatrix} \quad \text{and } \mathbf{Bary}_{x_1} = \mathbf{c}^{x_1} \otimes \mathbf{1}_2 \\ \mathbf{c} &= \mathbf{c}^{x_n} \odot (\mathbf{c}^{x_{n-1}} \otimes \mathbf{1}_{k_n}) \odot (\mathbf{c}^{x_{n-2}} \otimes \mathbf{1}_{k_n k_{n-1}}) \odot \dots \odot (\mathbf{c}^{x_1} \otimes \mathbf{1}_{k_n \dots k_2}) \\ &= \mathbf{Bary}_{x_n} \odot \mathbf{Bary}_{x_{n-1}} \odot \dots \odot \mathbf{Bary}_{x_1} \end{aligned}$$

Data weights:

$$\begin{aligned} \mathbf{w}^{x_2} &= \text{vec} \begin{pmatrix} 1.0 & -1.0 \\ -1.0 & 1.0 \end{pmatrix} \quad \text{and } \mathbf{W}_{x_2} = \mathbf{c}^{x_2} \otimes \mathbf{1}_1 \\ \mathbf{w}^{x_1} &= \begin{pmatrix} -1.0 \\ 1.0 \end{pmatrix} \quad \text{and } \mathbf{W}_{x_1} = \mathbf{c}^{x_1} \otimes \mathbf{1}_2 \\ \mathbf{w} &= \mathbf{w}^{x_n} \odot (\mathbf{w}^{x_{n-1}} \otimes \mathbf{1}_{k_n}) \odot (\mathbf{w}^{x_{n-2}} \otimes \mathbf{1}_{k_n k_{n-1}}) \odot \dots \odot (\mathbf{w}^{x_1} \otimes \mathbf{1}_{k_n \dots k_2}) \\ &= \mathbf{W}_{x_n} \odot \mathbf{W}_{x_{n-1}} \odot \dots \odot \mathbf{W}_{x_1} \end{aligned}$$

Barycentric denominator univariate vector-wise functions (KST equivalent functions):

$$\mathbf{D} = \begin{pmatrix} \mathbf{c}^{x_1} \cdot \mathbf{Lag}(x_1) & \mathbf{c}^{x_2} \cdot \mathbf{Lag}(x_2) \\ -\frac{1.0}{x_1+1.0} & -\frac{1.0}{x_2+1.0} \\ -\frac{1.0}{x_1+1.0} & \frac{1}{x_2-1.0} \\ \frac{1}{x_1-1.0} & -\frac{1.0}{x_2+1.0} \\ \frac{1}{x_1-1.0} & \frac{1}{x_2-1.0} \end{pmatrix}$$

Equivalent denominator and numerator read:

$$\sum_{i\text{-th row}} \prod_{j\text{-th col}} [\mathbf{D}]_{i,j} \quad \text{and} \quad \sum_{i\text{-th row}} \mathbf{w} \cdot \prod_{j\text{-th col}} [\mathbf{D}]_{i,j}$$

Connection with Neural Networks (equivalent denominator representation):

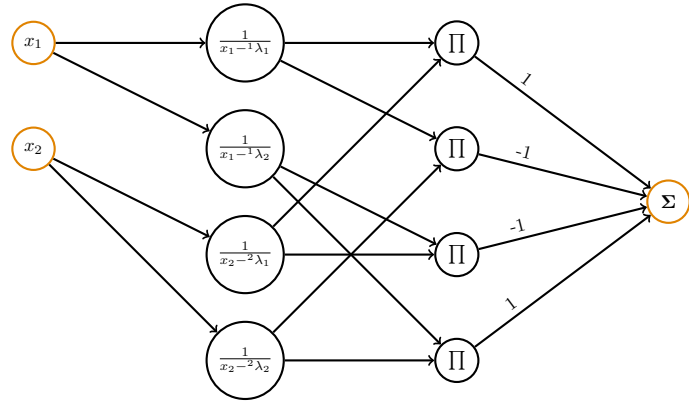


Figure 17: Equivalent NN representation of the denominator \mathbf{D} .

4.4 Function #4 ($n = 3$ variables, tensor size: 500 KB)

$$\frac{1}{3} \sum_{i=1}^3 \sin(\pi x_i/2)^2$$

4.4.1 Setup and results overview

- Reference: L/al. 2024, [8]
- Domain: \mathbb{R}
- Tensor size: 500 KB (40^3 points)
- Bounds: $(-1 \ 1) \times (-1 \ 1) \times (-1 \ 1)$

#	Alg.	Parameters	Dim.	CPU [s]	RMSE	min err.	max err.
4	A/G/P-V 2025 (A1)	1e-06,3	1.72e+03	0.0419	4e-08	3.81e-11	1.82e-07
	A/G/P-V 2025 (A2)	1e-15,1	2.56e+03	2.07	5.24e-09	1.97e-11	3.06e-08
	MDSPACK v1.1.0	1e-06,1e-06	1.72e+03	0.0303	4e-08	3.77e-11	1.82e-07
	P/P 2025	1,0.95,50,0.01,4,12,9	220	9.74	6.11e-06	1.39e-08	1.64e-05
	B/G 2025	1e-09,20	1.47e+04	95.7	3.28e - 13	0	4.86e - 12
	B/G 2025 (LR)	1e-09,20,3	3.64e+03	15.7	5.2e-12	1.3e-15	6.37e-11
	TensorFlow		321	304	0.003	4.23e-08	0.00946

Table 5: Function #4: best model configuration and performances per methods.

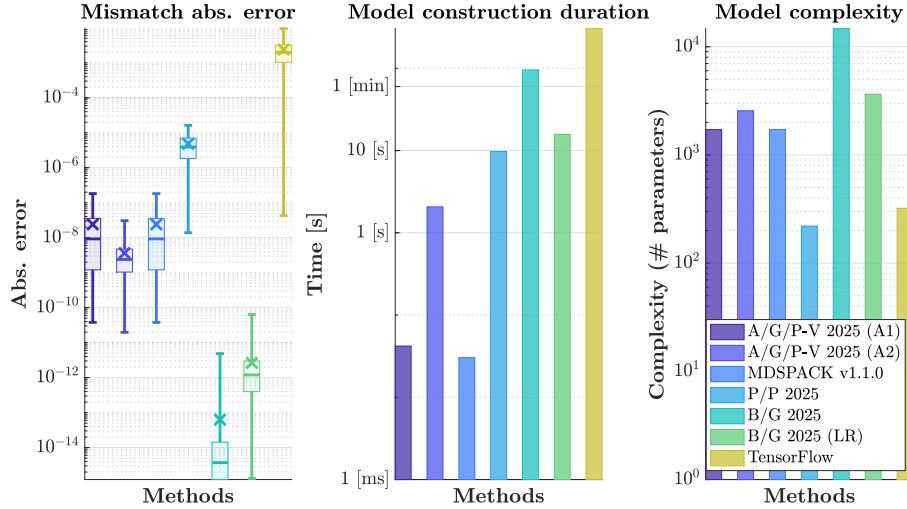


Figure 18: Function #4: graphical view of the best model performances.

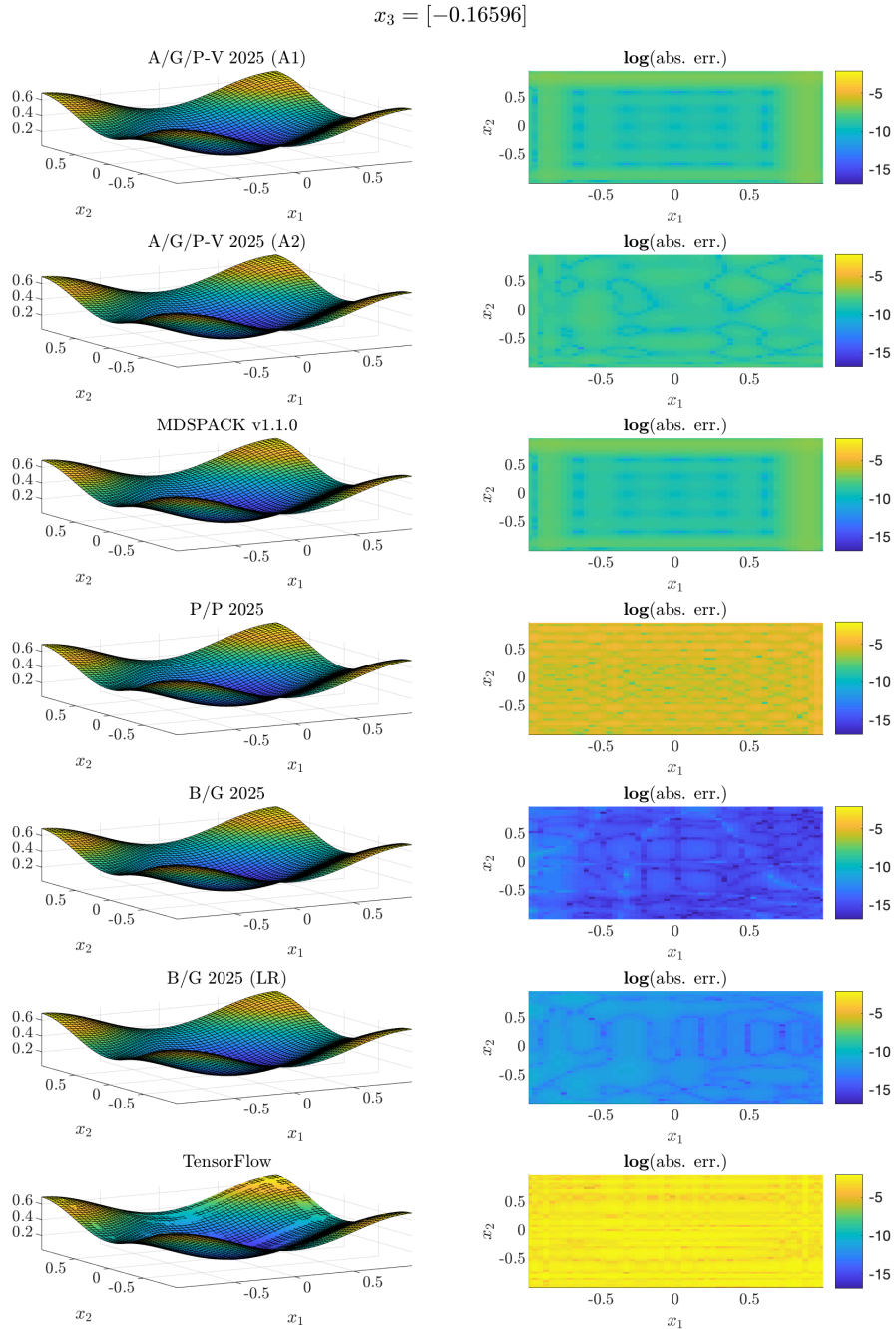


Figure 19: Function #4: left side, evaluation of the original (mesh) vs. approximated (coloured surface) and right side, absolute errors (in log-scale).

4.4.2 mLFI detailed informations (M1)

Right interpolation points: $k_l = (\begin{array}{ccc} 7 & 7 & 7 \end{array})$, where $l = 1, \dots, n$.

$$\begin{aligned} {}^1\lambda_{j_1} &\in \mathbb{C}^7, \text{ linearly spaced between bounds} \\ {}^2\lambda_{j_2} &\in \mathbb{C}^7, \text{ linearly spaced between bounds} \\ {}^3\lambda_{j_3} &\in \mathbb{C}^7, \text{ linearly spaced between bounds} \end{aligned}$$

n -D Loewner matrix, barycentric weights and Lagrangian basis:

$$\begin{aligned} \mathbb{L} &\in \mathbb{C}^{343 \times 343} \\ \mathbf{c} &\in \mathbb{C}^{343} \\ \mathbf{w} &\in \mathbb{C}^{343} \\ \mathbf{c} \cdot \mathbf{w} &\in \mathbb{C}^{343} \\ \text{Lag}(x_1, x_2, x_3) &\in \mathbb{C}^{343} \end{aligned}$$

4.5 Function #5 ($n = 4$ variables, tensor size: 19.5 MB)

$$\exp\left(1/2 \left(\sin(\pi(x_1^2 + x_2^2) + \sin(\pi(x_3^2 + x_4^2))\right)\right)$$

4.5.1 Setup and results overview

- Reference: L/al. 2024, [8]
- Domain: \mathbb{R}
- Tensor size: 19.5 MB (40^4 points)
- Bounds: $(-1 \ 1) \times (-1 \ 1) \times (-1 \ 1) \times (-1 \ 1)$

#	Alg.	Parameters	Dim.	CPU [s]	RMSE	min err.	max err.
5	A/G/P-V 2025 (A1)	0.5,3	3.75e+03	0.568	0.085	0.000155	0.428
	A/G/P-V 2025 (A2)	1e-15,1	7.26e+04	23	0.238	8.67e-05	1.08
	MDSPACK v1.1.0	0.5,0.0001	3.75e+03	0.563	0.085	0.000153	0.428
	P/P 2025	1,0.95,50,0.01,4,12,9	256	1.43e+03	0.00615	8.31e-06	0.0226
	B/G 2025	NaN	NaN	NaN	NaN	NaN	NaN
	B/G 2025 (LR)	1e-09,20,3	4.44e+05	4.46e+03	0.00131	3.86e - 09	0.0126
	TensorFlow		385	2.51e+03	0.12	0.000653	0.439

Table 6: Function #5: best model configuration and performances per methods.

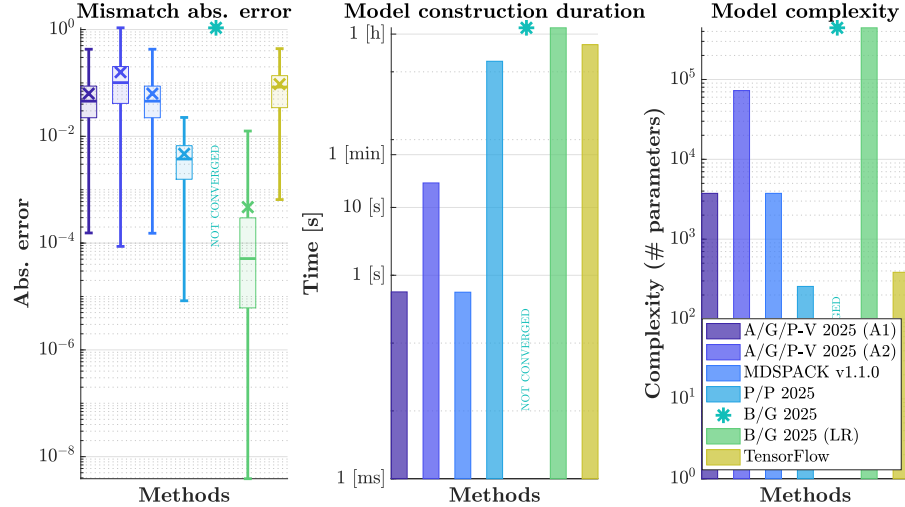


Figure 20: Function #5: graphical view of the best model performances.

$$x_{3\ldots 4} = [-0.16596; -0.99977]$$

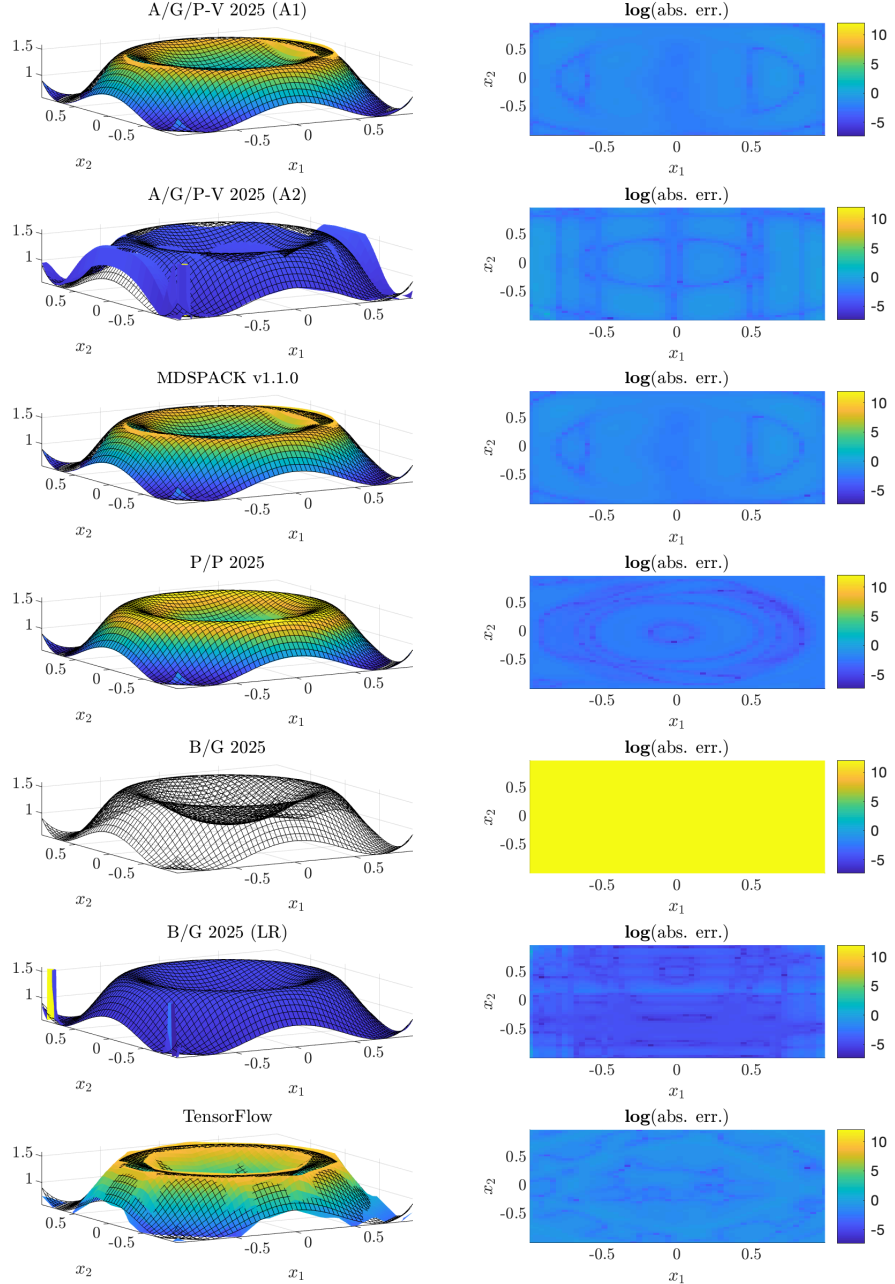


Figure 21: Function #5: left side, evaluation of the original (mesh) vs. approximated (coloured surface) and right side, absolute errors (in log-scale).

4.5.2 mLFI detailed informations (M1)

Right interpolation points: $k_l = (5 \ 5 \ 5 \ 5)$, where $l = 1, \dots, n$.

$$\begin{aligned} {}^1\lambda_{j_1} &\in \mathbb{C}^5, \text{ linearly spaced between bounds} \\ {}^2\lambda_{j_2} &\in \mathbb{C}^5, \text{ linearly spaced between bounds} \\ {}^3\lambda_{j_3} &\in \mathbb{C}^5, \text{ linearly spaced between bounds} \\ {}^4\lambda_{j_4} &\in \mathbb{C}^5, \text{ linearly spaced between bounds} \end{aligned}$$

n-D Loewner matrix, barycentric weights and Lagrangian basis:

$$\begin{aligned} \mathbb{L} &\in \mathbb{C}^{625 \times 625} \\ \mathbf{c} &\in \mathbb{C}^{625} \\ \mathbf{w} &\in \mathbb{C}^{625} \\ \mathbf{c} \cdot \mathbf{w} &\in \mathbb{C}^{625} \\ \mathbf{Lag}(x_1, x_2, x_3, x_4) &\in \mathbb{C}^{625} \end{aligned}$$

4.6 Function #6 ($n = 2$ variables, tensor size: 12.5 KB)

$$\frac{\exp(x_1 x_2)}{(x_1^2 - 1.44)(x_2^2 - 1.44)}$$

4.6.1 Setup and results overview

- Reference: A/al. 2021 (A.5.1), [4]
- Domain: \mathbb{R}
- Tensor size: 12.5 **KB** (40^2 points)
- Bounds: $(-1 \ 1) \times (-1 \ 1)$

#	Alg.	Parameters	Dim.	CPU [s]	RMSE	min err.	max err.
6	A/G/P-V 2025 (A1)	1e-06,3	100	0.0195	0.000187	6.31e-08	0.0016
	A/G/P-V 2025 (A2)	1e-15,3	696	0.142	1.86e-06	1.08e-10	1.67e-05
	MDSPACK v1.1.0	1e-06,0.0001	100	0.0187	0.000192	6.2e-08	0.00167
	P/P 2025	1,0.95,50,0.01,6,12,13	316	0.871	0.00448	2.05e-06	0.0539
	B/G 2025	1e-09,20	144	0.0504	5.66e-10	8.69e-14	7.03e-09
	B/G 2025 (LR)	1e-09,20,5	196	0.273	3.3e - 10	1.67e - 15	4.39e - 09
	TensorFlow		257	14.7	0.0984	1.66e-05	1.01

Table 7: Function #6: best model configuration and performances per methods.

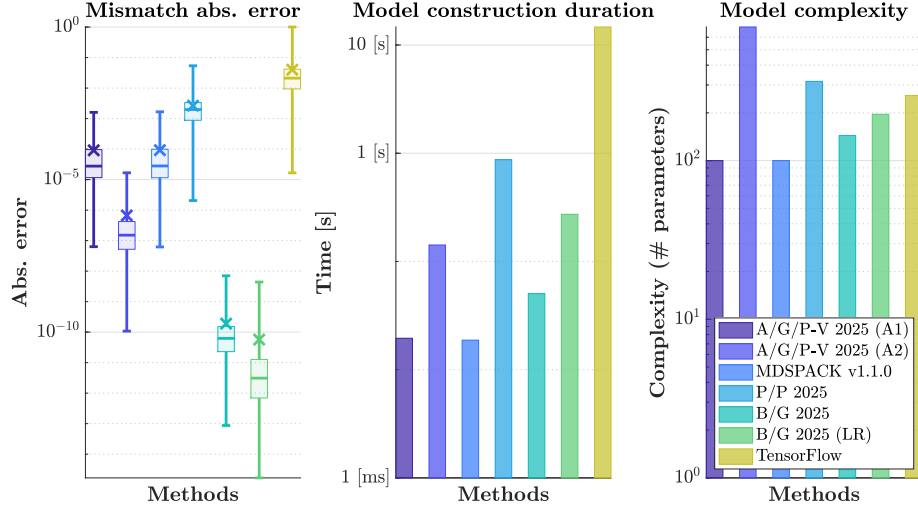


Figure 22: Function #6: graphical view of the best model performances.

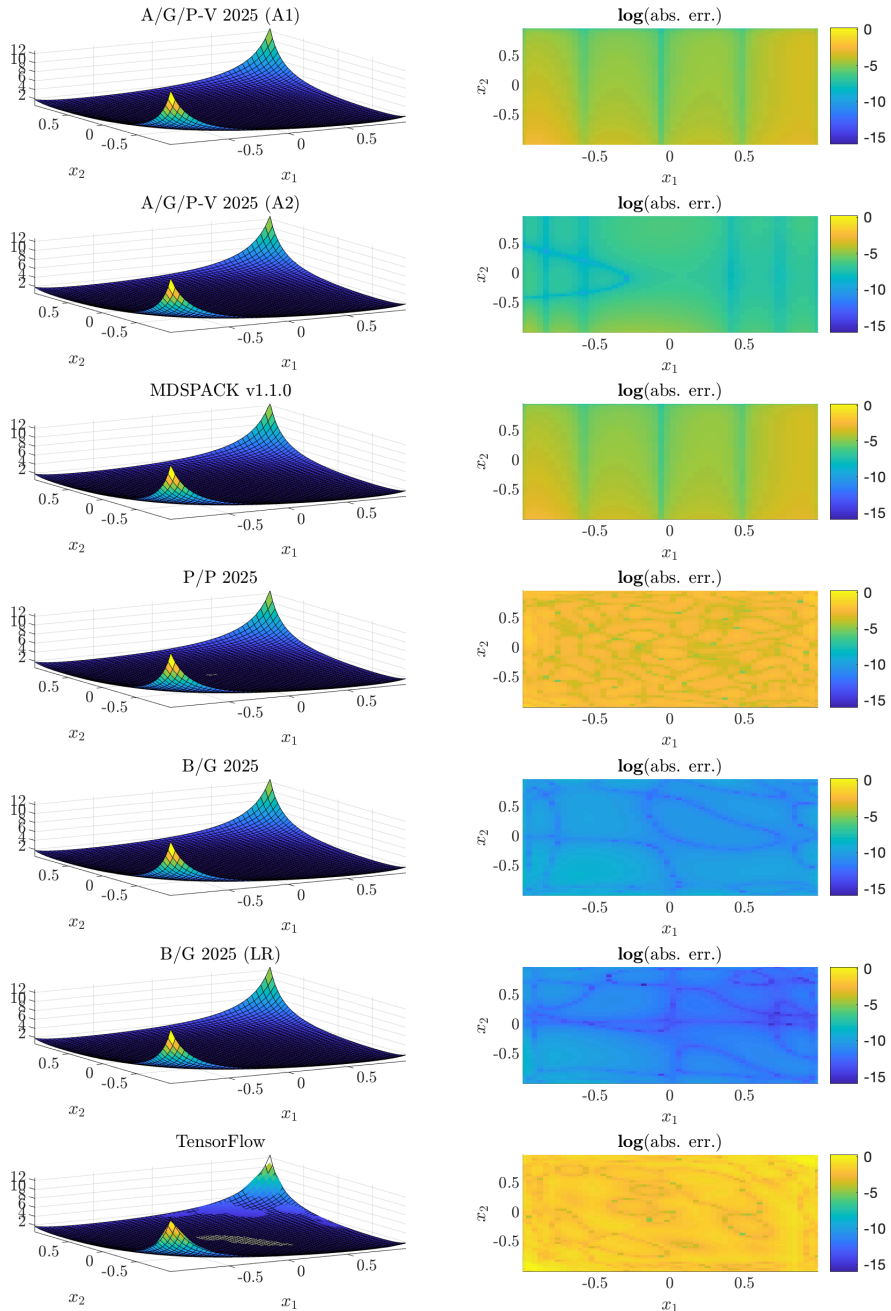


Figure 23: Function #6: left side, evaluation of the original (mesh) vs. approximated (coloured surface) and right side, absolute errors (in log-scale).

4.6.2 mLFI detailed informations (M1)

Right interpolation points: $k_l = \begin{pmatrix} 5 & 5 \end{pmatrix}$, where $l = 1, \dots, n$.

$$\begin{aligned} {}^1\lambda_{j_1} &\in \mathbb{C}^5, \text{ linearly spaced between bounds} \\ {}^2\lambda_{j_2} &\in \mathbb{C}^5, \text{ linearly spaced between bounds} \end{aligned}$$

n-D Loewner matrix, barycentric weights and Lagrangian basis:

$$\begin{aligned} \mathbb{L} &\in \mathbb{C}^{25 \times 25} \\ \mathbf{c} &\in \mathbb{C}^{25} \\ \mathbf{w} &\in \mathbb{C}^{25} \\ \mathbf{c} \cdot \mathbf{w} &\in \mathbb{C}^{25} \\ \mathbf{Lag}(x_1, x_2) &\in \mathbb{C}^{25} \end{aligned}$$

4.7 Function #7 ($n = 2$ variables, tensor size: 12.5 KB)

$$\log(2.25 - x_1^2 - x_2^2)$$

4.7.1 Setup and results overview

- Reference: A/al. 2021 (A.5.2), [4]
- Domain: \mathbb{R}
- Tensor size: 12.5 **KB** (40^2 points)
- Bounds: $(-1 \ 1) \times (-1 \ 1)$

#	Alg.	Parameters	Dim.	CPU [s]	RMSE	min err.	max err.
7	A/G/P-V 2025 (A1)	1e-06,2	324	0.0173	0.00128	8.92e-10	0.00511
	A/G/P-V 2025 (A2)	1e-15,1	540	0.121	7.39e-06	1.68e-09	3.15e-05
	MDSPACK v1.1.0	1e-06,1e-09	324	0.0159	0.00149	7.01e-08	0.00543
	P/P 2025	1,1,50,0.01,4,12,9	184	0.493	0.000313	9.73e-07	0.0038
	B/G 2025	1e-09,20	720	0.263	2.08e - 10	4.44e - 16	4.6e - 09
	B/G 2025 (LR)	1e-09,20,4	624	7.6	6.93e-09	1.95e-14	1.25e-07
	TensorFlow		257	14.7	0.214	0.000296	0.677

Table 8: Function #7: best model configuration and performances per methods.

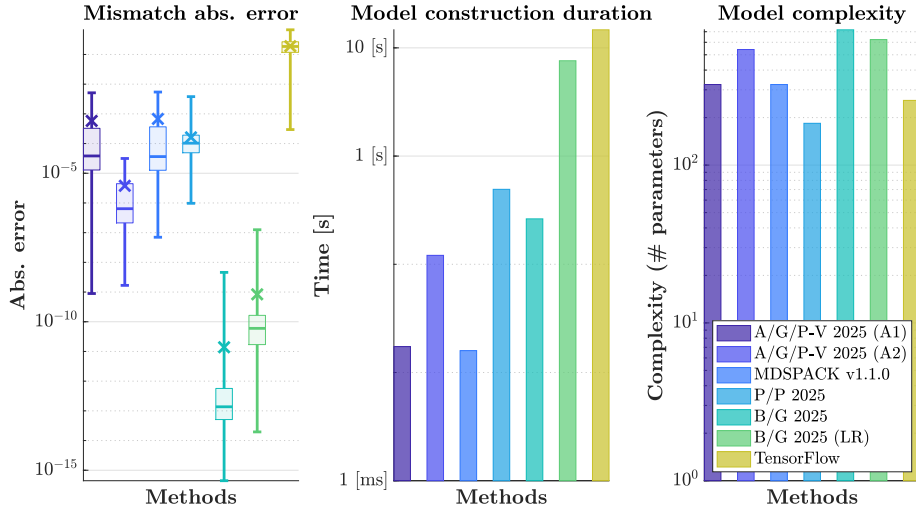


Figure 24: Function #7: graphical view of the best model performances.

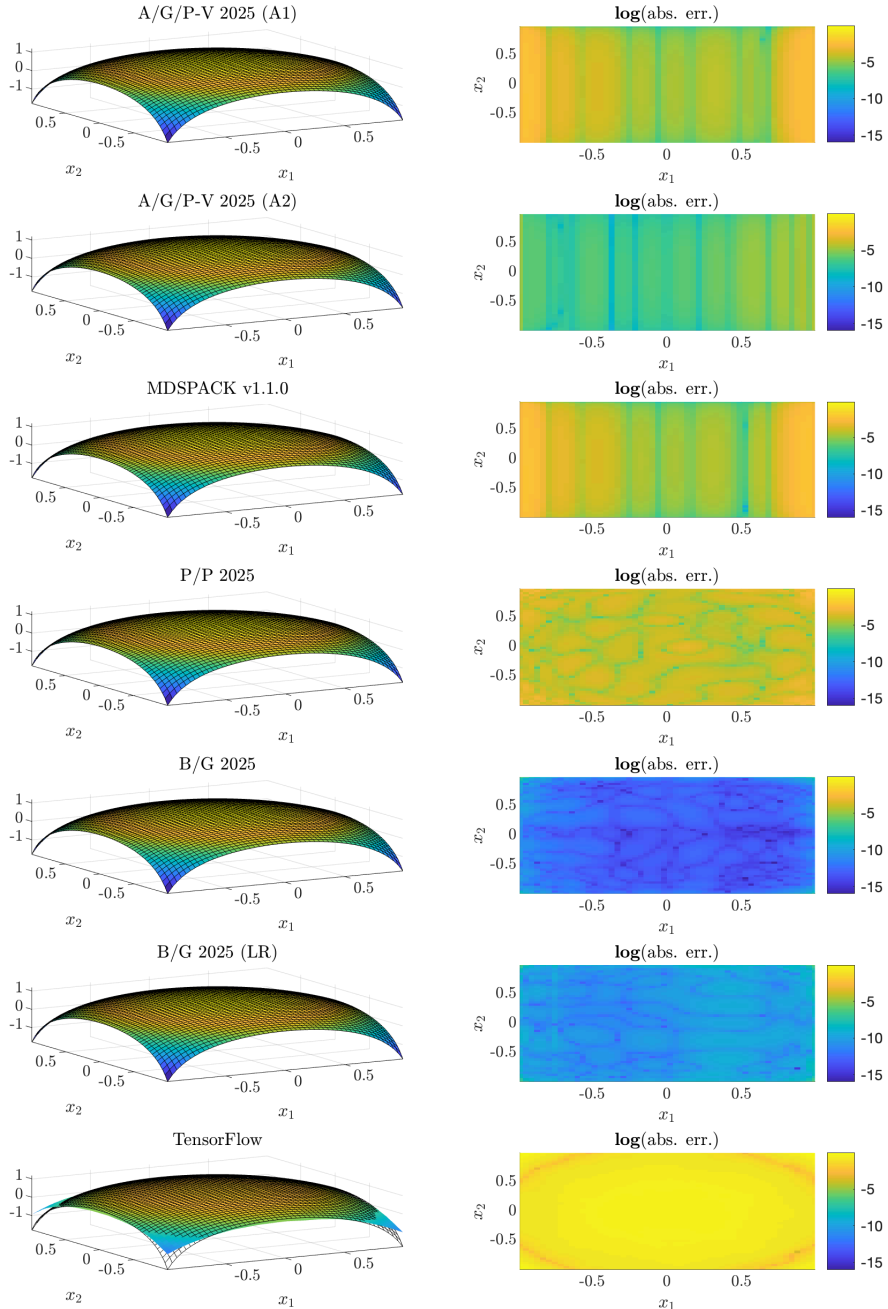


Figure 25: Function #7: left side, evaluation of the original (mesh) vs. approximated (coloured surface) and right side, absolute errors (in log-scale).

4.7.2 mLFI detailed informations (M1)

Right interpolation points: $k_l = \begin{pmatrix} 9 & 9 \end{pmatrix}$, where $l = 1, \dots, n$.

$$\begin{aligned} {}^1\lambda_{j_1} &\in \mathbb{C}^9, \text{ linearly spaced between bounds} \\ {}^2\lambda_{j_2} &\in \mathbb{C}^9, \text{ linearly spaced between bounds} \end{aligned}$$

n-D Loewner matrix, barycentric weights and Lagrangian basis:

$$\begin{aligned} \mathbb{L} &\in \mathbb{C}^{81 \times 81} \\ \mathbf{c} &\in \mathbb{C}^{81} \\ \mathbf{w} &\in \mathbb{C}^{81} \\ \mathbf{c} \cdot \mathbf{w} &\in \mathbb{C}^{81} \\ \mathbf{Lag}(x_1, x_2) &\in \mathbb{C}^{81} \end{aligned}$$

4.8 Function #8 ($n = 2$ variables, tensor size: 42.8 KB)

$$\tanh(4(x_1 - x_2))$$

4.8.1 Setup and results overview

- Reference: A/al. 2021 (A.5.3), [4]
- Domain: \mathbb{R}
- Tensor size: 42.8 KB (74² points)
- Bounds: $(-1 \ 1) \times (-1 \ 1)$

#	Alg.	Parameters	Dim.	CPU [s]	RMSE	min err.	max err.
8	A/G/P-V 2025 (A1)	1e-12,2	484	0.046	0.0543	3.78e-11	0.603
	A/G/P-V 2025 (A2)	1e-15,3	324	0.403	0.000511	1.63e-11	0.00244
	MDSPACK v1.1.0	1e-06,0.0001	196	0.0493	0.0972	2.93e-09	0.783
	P/P 2025	1,1,50,0.01,4,12,9	184	1.35	0.000545	7.93e-07	0.00212
	B/G 2025	1e-09,20	440	0.186	3.47e - 11	3.33e - 16	7.51e - 10
	B/G 2025 (LR)	1e-09,20,5	960	19	1.46e-08	1.67e-15	2.16e-07
	TensorFlow		257	38.2	0.00116	6.58e-06	0.00348

Table 9: Function #8: best model configuration and performances per methods.

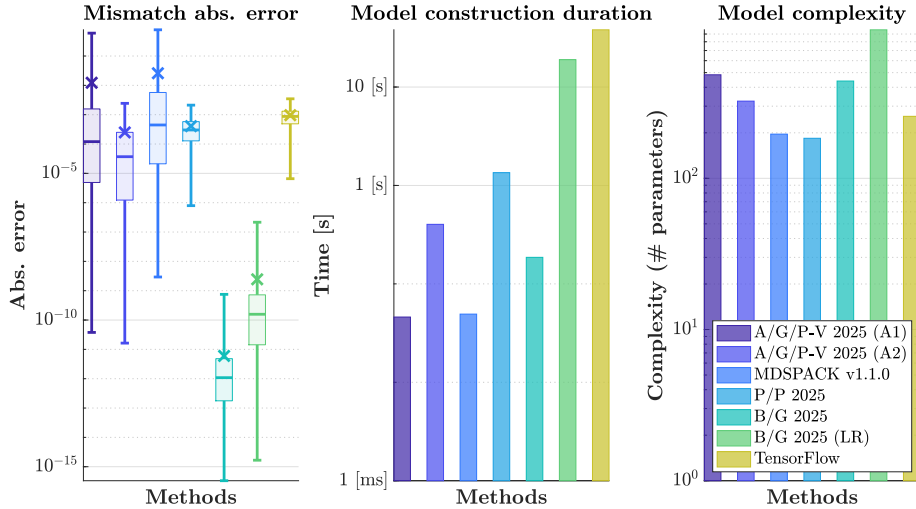


Figure 26: Function #8: graphical view of the best model performances.

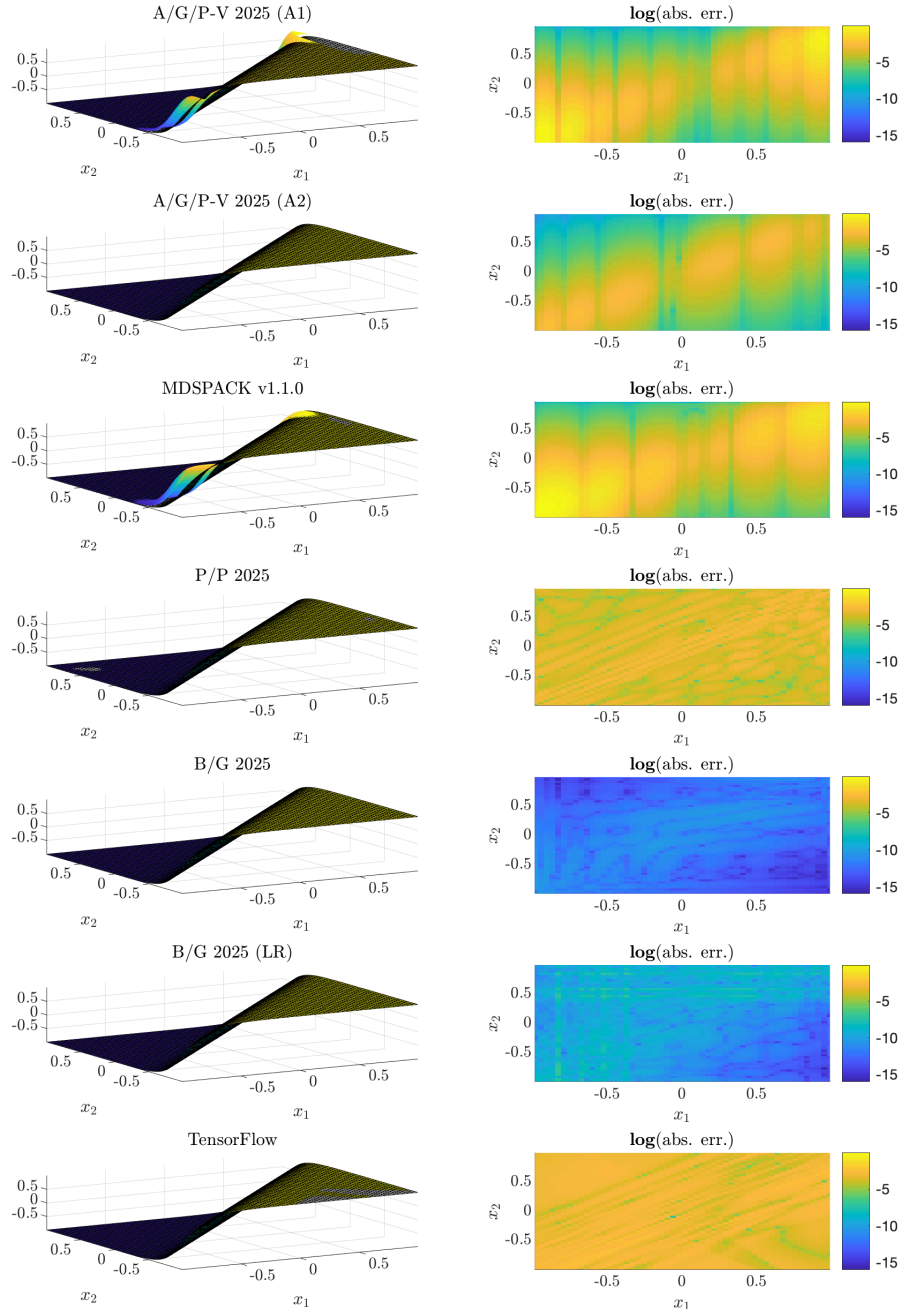


Figure 27: Function #8: left side, evaluation of the original (mesh) vs. approximated (coloured surface) and right side, absolute errors (in log-scale).

4.8.2 mLFI detailed informations (M1)

Right interpolation points: $k_l = \begin{pmatrix} 1 & 1 \end{pmatrix}$, where $l = 1, \dots, n$.

$$\begin{aligned} {}^1\lambda_{j_1} &\in \mathbb{C}^{11}, \text{ linearly spaced between bounds} \\ {}^2\lambda_{j_2} &\in \mathbb{C}^{11}, \text{ linearly spaced between bounds} \end{aligned}$$

n-D Loewner matrix, barycentric weights and Lagrangian basis:

$$\begin{aligned} \mathbb{L} &\in \mathbb{C}^{121 \times 121} \\ \mathbf{c} &\in \mathbb{C}^{121} \\ \mathbf{w} &\in \mathbb{C}^{121} \\ \mathbf{c} \cdot \mathbf{w} &\in \mathbb{C}^{121} \\ \mathbf{Lag}(x_1, x_2) &\in \mathbb{C}^{121} \end{aligned}$$

4.9 Function #9 ($n = 2$ variables, tensor size: 12.5 KB)

$$\exp\left(\frac{-(x_1^2 + x_2^2)}{1000}\right)$$

4.9.1 Setup and results overview

- Reference: A/al. 2021 (A.5.4), [4]
- Domain: \mathbb{R}
- Tensor size: 12.5 KB (40^2 points)
- Bounds: $(-1 \ 1) \times (-1 \ 1)$

#	Alg.	Parameters	Dim.	CPU [s]	RMSE	min err.	max err.
9	A/G/P-V 2025 (A1)	0.5,2	36	0.0244	1.38e-11	4e - 15	2.81e-11
	A/G/P-V 2025 (A2)	1e-15,3	36	0.0856	5.74e-12	7.77e-15	1.31e-11
	MDSPACK v1.1.0	0.5,0.01	36	0.0515	1.46e-11	5.5e-14	3.05e-11
	P/P 2025	1,0.95,50,0.01,4,6,9	130	0.299	2.06e-08	4.8e-12	8.73e-08
	B/G 2025	0.001,20	36	0.0124	5.43e-12	1.29e-14	1.25e-11
	B/G 2025 (LR)	0.001,20,4	36	0.00996	5.43e - 12	1.35e-14	1.25e - 11
	TensorFlow		257	14.8	0.00108	1.92e-06	0.00198

Table 10: Function #9: best model configuration and performances per methods.

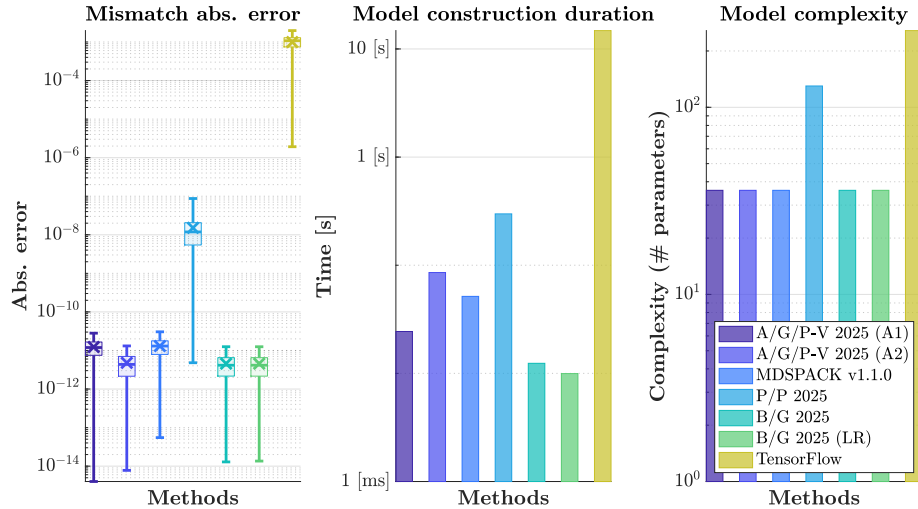


Figure 28: Function #9: graphical view of the best model performances.

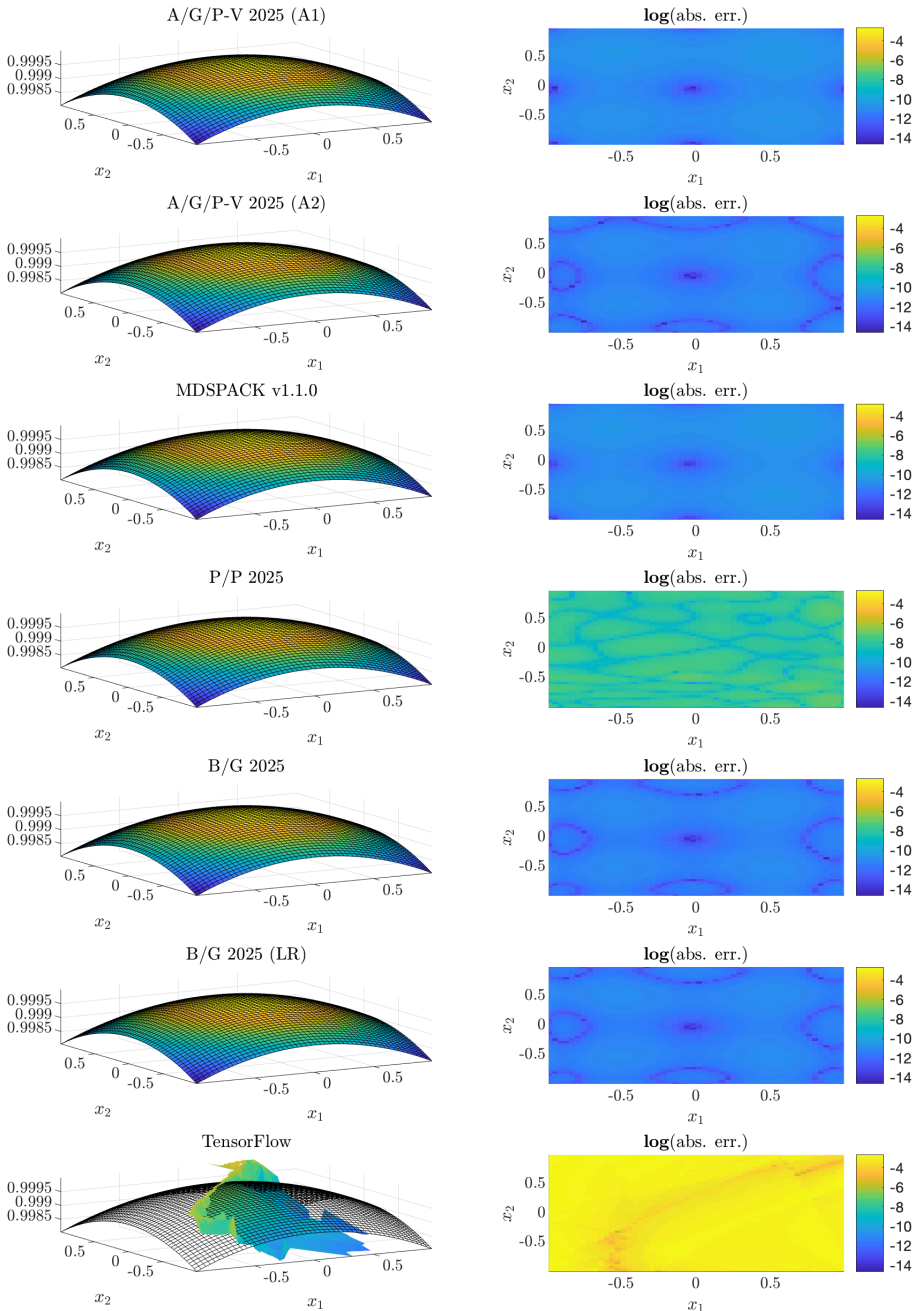


Figure 29: Function #9: left side, evaluation of the original (mesh) vs. approximated (coloured surface) and right side, absolute errors (in log-scale).

4.9.2 mLF detailed informations (M1)

Right interpolation points: $k_l = (3 \ 3)$, where $l = 1, \dots, n$.

$$\begin{aligned} {}^1\lambda_{j_1} &= \left(\begin{array}{ccc} -1 & -\frac{1}{19} & 1 \\ -1 & -\frac{1}{19} & 1 \end{array} \right) \\ {}^2\lambda_{j_2} &= \left(\begin{array}{ccc} 1 & \frac{1}{(x_1+1.0)(x_2+1.0)} \\ 1 & \frac{1}{(x_1+1.0)(x_2+0.053)} \\ 1 & \frac{1}{(x_1+1.0)(x_2-1.0)} \\ 1 & \frac{1}{(x_2+1.0)(x_1+0.053)} \\ 1 & \frac{1}{(x_1+0.053)(x_2+0.053)} \\ 1 & \frac{1}{(x_2-1.0)(x_1+0.053)} \\ 1 & \frac{1}{(x_1-1.0)(x_2+1.0)} \\ 1 & \frac{1}{(x_1-1.0)(x_2+0.053)} \\ 1 & \frac{1}{(x_1-1.0)(x_2-1.0)} \end{array} \right) \end{aligned}$$

Lagrangian weights, data and supports (Lagrangian basis):

$$\left(\begin{array}{cccc} \mathbf{c} & \mathbf{w} & \mathbf{c} \cdot \mathbf{w} & \text{Lag} \\ -0.59 & 1.0 & -0.58 & \frac{1}{(x_1+1.0)(x_2+1.0)} \\ 1.1 & 1.0 & 1.1 & \frac{1}{(x_1+1.0)(x_2+0.053)} \\ -0.53 & 1.0 & -0.53 & \frac{1}{(x_1+1.0)(x_2-1.0)} \\ 1.1 & 1.0 & 1.1 & \frac{1}{(x_2+1.0)(x_1+0.053)} \\ -2.1 & 1.0 & -2.1 & \frac{1}{(x_1+0.053)(x_2+0.053)} \\ 1.0 & 1.0 & 1.0 & \frac{1}{(x_2-1.0)(x_1+0.053)} \\ -0.53 & 1.0 & -0.53 & \frac{1}{(x_1-1.0)(x_2+1.0)} \\ 1.0 & 1.0 & 1.0 & \frac{1}{(x_1-1.0)(x_2+0.053)} \\ -0.47 & 1.0 & -0.47 & \frac{1}{(x_1-1.0)(x_2-1.0)} \end{array} \right)$$

KST equivalent decoupling pattern

Barycentric weights:

$$\begin{aligned} \mathbf{c}^{x_2} &= \text{vec} \begin{pmatrix} 1.1 & 1.1 & 1.1 \\ -2.1 & -2.1 & -2.1 \\ 1.0 & 1.0 & 1.0 \end{pmatrix} \quad \text{and } \mathbf{Bary}_{x_2} = \mathbf{c}^{x_2} \otimes \mathbf{1}_1 \\ \mathbf{c}^{x_1} &= \begin{pmatrix} -0.53 \\ 1.0 \\ -0.47 \end{pmatrix} \quad \text{and } \mathbf{Bary}_{x_1} = \mathbf{c}^{x_1} \otimes \mathbf{1}_3 \end{aligned}$$

$$\begin{aligned} \mathbf{c} &= \mathbf{c}^{x_n} \odot (\mathbf{c}^{x_{n-1}} \otimes \mathbf{1}_{k_n}) \odot (\mathbf{c}^{x_{n-2}} \otimes \mathbf{1}_{k_n k_{n-1}}) \odot \cdots \odot (\mathbf{c}^{x_1} \otimes \mathbf{1}_{k_n \dots k_2}) \\ &= \mathbf{Bary}_{x_n} \odot \mathbf{Bary}_{x_{n-1}} \odot \cdots \odot \mathbf{Bary}_{x_1} \end{aligned}$$

Data weights:

$$\begin{aligned} \mathbf{w}^{x_2} &= \text{vec} \begin{pmatrix} 1.0 & 1.0 & 1.0 \\ 1.0 & 1.0 & 1.0 \\ 1.0 & 1.0 & 1.0 \end{pmatrix} \quad \text{and } \mathbf{W}_{x_2} = \mathbf{c}^{x_2} \otimes \mathbf{1}_1 \\ \mathbf{w}^{x_1} &= \begin{pmatrix} 1.0 \\ 1.0 \\ 1.0 \end{pmatrix} \quad \text{and } \mathbf{W}_{x_1} = \mathbf{c}^{x_1} \otimes \mathbf{1}_3 \end{aligned}$$

$$\begin{aligned} \mathbf{w} &= \mathbf{w}^{x_n} \odot (\mathbf{w}^{x_{n-1}} \otimes \mathbf{1}_{k_n}) \odot (\mathbf{w}^{x_{n-2}} \otimes \mathbf{1}_{k_n k_{n-1}}) \odot \cdots \odot (\mathbf{w}^{x_1} \otimes \mathbf{1}_{k_n \dots k_2}) \\ &= \mathbf{W}_{x_n} \odot \mathbf{W}_{x_{n-1}} \odot \cdots \odot \mathbf{W}_{x_1} \end{aligned}$$

Barycentric denominator univariate vector-wise functions (KST equivalent functions):

$$\mathbf{D} = \begin{pmatrix} \mathbf{c}^{x_1} \cdot \text{Lag}(x_1) & \mathbf{c}^{x_2} \cdot \text{Lag}(x_2) \\ -\frac{0.53}{x_1+1.0} & -\frac{1.1}{x_2+1.0} \\ -\frac{0.53}{x_1+1.0} & -\frac{2.1}{x_2+0.053} \\ -\frac{0.53}{x_1+1.0} & -\frac{1}{x_2-1.0} \\ \frac{1}{x_1+0.053} & -\frac{x_2+1.0}{2.1} \\ \frac{1}{x_1+0.053} & -\frac{x_2+0.053}{1} \\ \frac{1}{x_1+0.053} & -\frac{x_2-1.0}{1} \\ -\frac{0.47}{x_1-1.0} & -\frac{x_2+1.0}{2.1} \\ -\frac{0.47}{x_1-1.0} & -\frac{x_2+0.053}{1} \\ -\frac{0.47}{x_1-1.0} & -\frac{x_2-1.0}{1} \end{pmatrix}$$

Equivalent denominator and numerator read:

$$\sum_{i\text{-th row}} \prod_{j\text{-th col}} [\mathbf{D}]_{i,j} \text{ and } \sum_{i\text{-th row}} \mathbf{w} \cdot \prod_{j\text{-th col}} [\mathbf{D}]_{i,j}$$

Connection with Neural Networks (equivalent denominator representation):

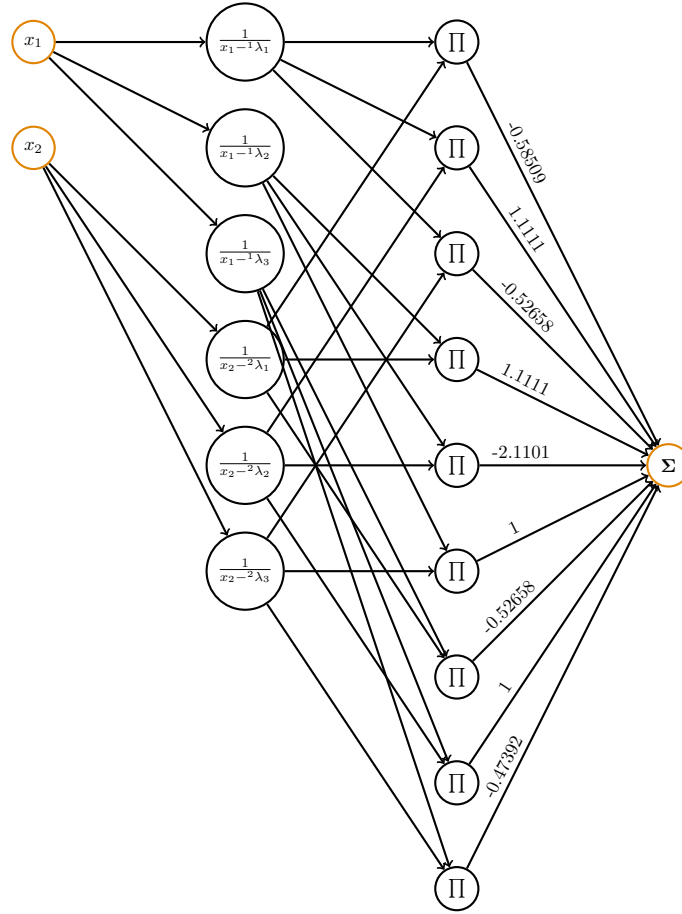


Figure 30: Equivalent NN representation of the denominator \mathbf{D} .

4.10 Function #10 ($n = 2$ variables, tensor size: 52.5 KB)

$$|x_1 - x_2|^3$$

4.10.1 Setup and results overview

- Reference: A/al. 2021 (A.5.5), [4]
- Domain: \mathbb{R}
- Tensor size: 52.5 KB (82² points)
- Bounds: $(-1 \ 1) \times (-1 \ 1)$

#	Alg.	Parameters	Dim.	CPU [s]	RMSE	min err.	max err.
10	A/G/P-V 2025 (A1)	0.5,3	36	0.0565	0.0834	0.000514	0.301
	A/G/P-V 2025 (A2)	1e-15,3	48	0.242	0.205	0.000197	1.57
	MDSPACK v1.1.0	0.01,0.0001	96	0.0623	0.0707	3.57e-06	0.518
	P/P 2025	1,1,50,0.01,10,4,21	508	2.57	0.000397	2.87e-07	0.00181
	B/G 2025	1e-06,20	1.3e+03	0.774	1.72e - 05	0	0.000225
	B/G 2025 (LR)	1e-09,20,3	1.09e+03	10.4	0.00074	2.65e-13	0.00911
	TensorFlow		257	45.3	0.00754	1.19e-06	0.045

Table 11: Function #10: best model configuration and performances per methods.

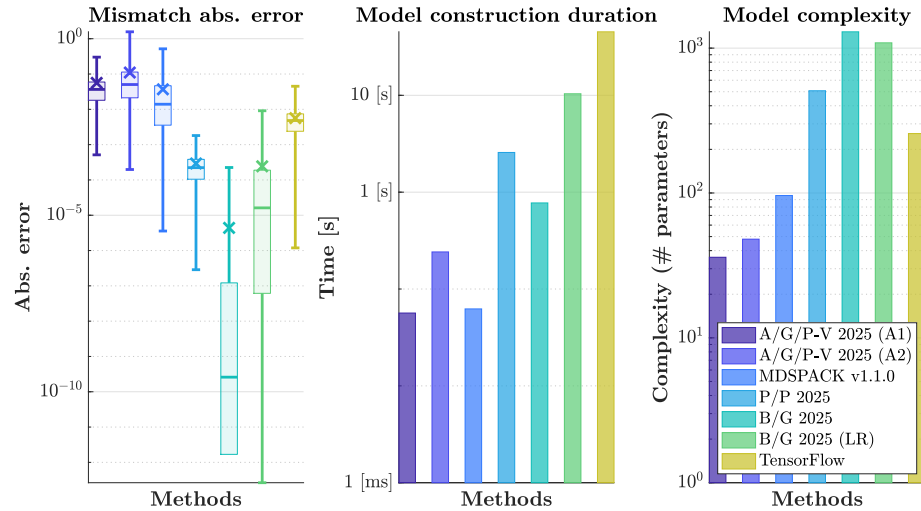


Figure 31: Function #10: graphical view of the best model performances.

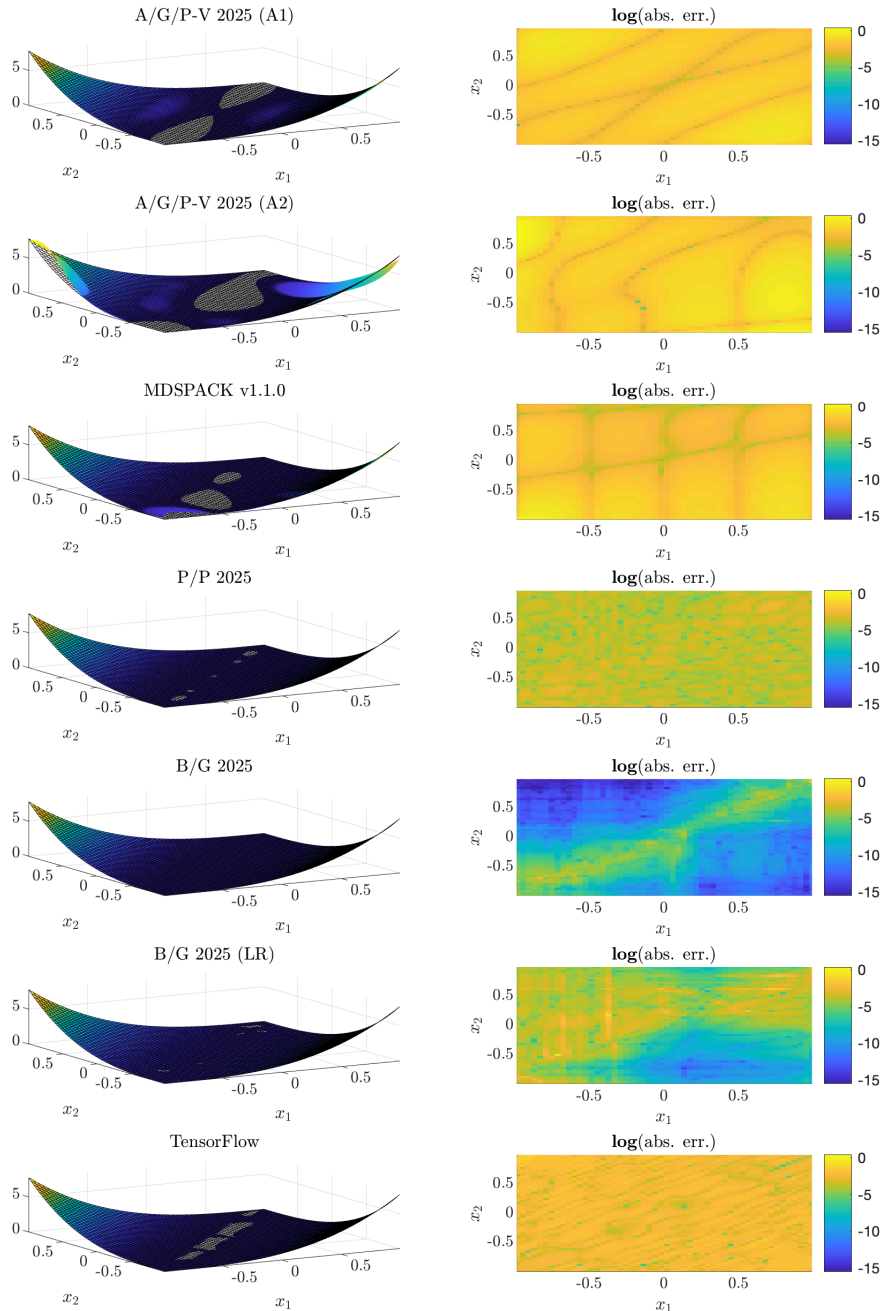


Figure 32: Function #10: left side, evaluation of the original (mesh) vs. approximated (coloured surface) and right side, absolute errors (in log-scale).

4.10.2 mLF detailed informations (M1)

Right interpolation points: $k_l = (3 \ 3)$, where $l = 1, \dots, n$.

$$\begin{aligned} {}^1\lambda_{j_1} &= \begin{pmatrix} -1 & 0 & 1 \end{pmatrix} \\ {}^2\lambda_{j_2} &= \begin{pmatrix} -1 & 0 & 1 \end{pmatrix} \end{aligned}$$

Lagrangian weights, data and supports (Lagrangian basis):

$$\left(\begin{array}{cccc} \mathbf{c} & \mathbf{w} & \mathbf{c} \cdot \mathbf{w} & \text{Lag} \\ -0.9 & 0 & 0 & \frac{1}{(x_1+1.0)(x_2+1.0)} \\ 0.98 & 1.0 & 0.98 & \frac{1}{x_2(x_1+1.0)} \\ -0.28 & 8.0 & -2.2 & \frac{1}{(x_1+1.0)(x_2-1.0)} \\ 0.99 & 1.0 & 0.99 & \frac{1}{x_1(x_2+1.0)} \\ -3.0 & 0 & 0 & \frac{1}{x_1x_2} \\ 1.0 & 1.0 & 1.0 & \frac{1}{x_1(x_2-1.0)} \\ -0.28 & 8.0 & -2.2 & \frac{1}{(x_1-1.0)(x_2+1.0)} \\ 1.0 & 1.0 & 1.0 & \frac{1}{x_2(x_1-1.0)} \\ -0.94 & 0 & 0 & \frac{1}{(x_1-1.0)(x_2-1.0)} \end{array} \right)$$

KST equivalent decoupling pattern

Barycentric weights:

$$\begin{aligned} \mathbf{c}^{x_2} &= \text{vec} \begin{pmatrix} 3.3 & 0.99 & 0.3 \\ -3.6 & -3.0 & -1.1 \\ 1.0 & 1.0 & 1.0 \end{pmatrix} \quad \text{and } \mathbf{Bary}_{x_2} = \mathbf{c}^{x_2} \otimes \mathbf{1}_1 \\ \mathbf{c}^{x_1} &= \begin{pmatrix} -0.28 \\ 1.0 \\ -0.94 \end{pmatrix} \quad \text{and } \mathbf{Bary}_{x_1} = \mathbf{c}^{x_1} \otimes \mathbf{1}_3 \end{aligned}$$

$$\begin{aligned} \mathbf{c} &= \mathbf{c}^{x_n} \odot (\mathbf{c}^{x_{n-1}} \otimes \mathbf{1}_{k_n}) \odot (\mathbf{c}^{x_{n-2}} \otimes \mathbf{1}_{k_n k_{n-1}}) \odot \cdots \odot (\mathbf{c}^{x_1} \otimes \mathbf{1}_{k_n \dots k_2}) \\ &= \mathbf{Bary}_{x_n} \odot \mathbf{Bary}_{x_{n-1}} \odot \cdots \odot \mathbf{Bary}_{x_1} \end{aligned}$$

Data weights:

$$\begin{aligned} \mathbf{w}^{x_2} &= \text{vec} \begin{pmatrix} 0 & 1.0 & 8.0 \\ 1.0 & 0 & 1.0 \\ 8.0 & 1.0 & 0 \end{pmatrix} \quad \text{and } \mathbf{W}_{x_2} = \mathbf{c}^{x_2} \otimes \mathbf{1}_1 \\ \mathbf{w}^{x_1} &= \begin{pmatrix} 8.0 \\ 1.0 \\ 0 \end{pmatrix} \quad \text{and } \mathbf{W}_{x_1} = \mathbf{c}^{x_1} \otimes \mathbf{1}_3 \end{aligned}$$

$$\begin{aligned} \mathbf{w} &= \mathbf{w}^{x_n} \odot (\mathbf{w}^{x_{n-1}} \otimes \mathbf{1}_{k_n}) \odot (\mathbf{w}^{x_{n-2}} \otimes \mathbf{1}_{k_n k_{n-1}}) \odot \cdots \odot (\mathbf{w}^{x_1} \otimes \mathbf{1}_{k_n \dots k_2}) \\ &= \mathbf{W}_{x_n} \odot \mathbf{W}_{x_{n-1}} \odot \cdots \odot \mathbf{W}_{x_1} \end{aligned}$$

Barycentric denominator univariate vector-wise functions (KST equivalent functions):

$$\mathbf{D} = \begin{pmatrix} \mathbf{c}^{x_1} \cdot \text{Lag}(x_1) & \mathbf{c}^{x_2} \cdot \text{Lag}(x_2) \\ -\frac{0.28}{x_1+1.0} & \frac{3.3}{x_2+1.0} \\ -\frac{0.28}{x_1+1.0} & -\frac{3.6}{x_2} \\ -\frac{0.28}{x_1+1.0} & \frac{1}{x_2-1.0} \\ \frac{1}{x_1} & \frac{0.99}{x_2+1.0} \\ \frac{1}{x_1} & -\frac{x_2}{3.0} \\ \frac{1}{x_1} & \frac{1}{x_2-1.0} \\ -\frac{0.94}{x_1-1.0} & \frac{0.3}{x_2+1.0} \\ -\frac{0.94}{x_1-1.0} & -\frac{1.1}{x_2} \\ -\frac{0.94}{x_1-1.0} & \frac{x_2}{x_2-1.0} \end{pmatrix}$$

Equivalent denominator and numerator read:

$$\sum_{i\text{-th row}} \prod_{j\text{-th col}} [\mathbf{D}]_{i,j} \quad \text{and} \quad \sum_{i\text{-th row}} \mathbf{w} \cdot \prod_{j\text{-th col}} [\mathbf{D}]_{i,j}$$

Connection with Neural Networks (equivalent denominator representation):

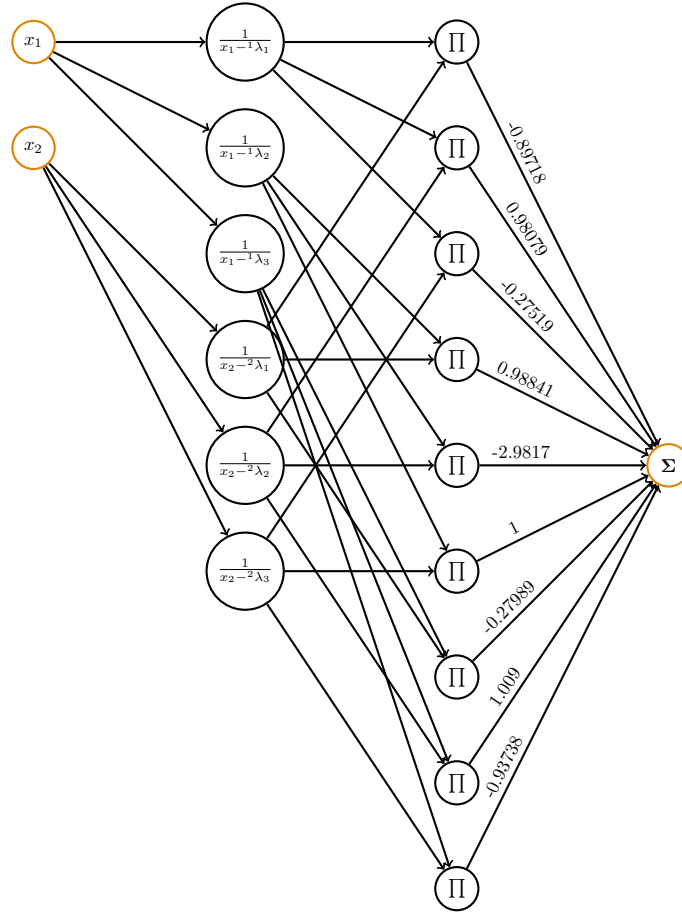


Figure 33: Equivalent NN representation of the denominator \mathbf{D} .

4.11 Function #11 ($n = 2$ variables, tensor size: 12.5 KB)

$$\frac{x_1 + x_2^3}{x_1 x_2^2 + 2}$$

4.11.1 Setup and results overview

- Reference: A/al. 2021 (A.5.6), [4]
- Domain: \mathbb{R}
- Tensor size: 12.5 **KB** (40^2 points)
- Bounds: $(\frac{1}{10000000000}, 1) \times (\frac{1}{10000000000}, 1)$

#	Alg.	Parameters	Dim.	CPU [s]	RMSE	min err.	max err.
11	A/G/P-V 2025 (A1)	0.01,2	32	0.0149	3.09e-15	0	1.38e-14
	A/G/P-V 2025 (A2)	1e-15,3	464	0.129	2.7e - 16	0	1.22e - 15
	MDSPACK v1.1.0	0.01,0.01	32	0.0162	3.48e-15	0	1.53e-14
	P/P 2025	1,0.95,50,0.01,4,6,9	130	0.303	1.4e-05	2.07e-08	8.74e-05
	B/G 2025	0.001,20	80	0.0107	3.16e-15	0	6.17e-14
	B/G 2025 (LR)	1e-09,20,4	80	0.128	3.22e-16	0	3.44e-15
	TensorFlow		257	14.8	0.00655	2.84e-05	0.0169

Table 12: Function #11: best model configuration and performances per methods.

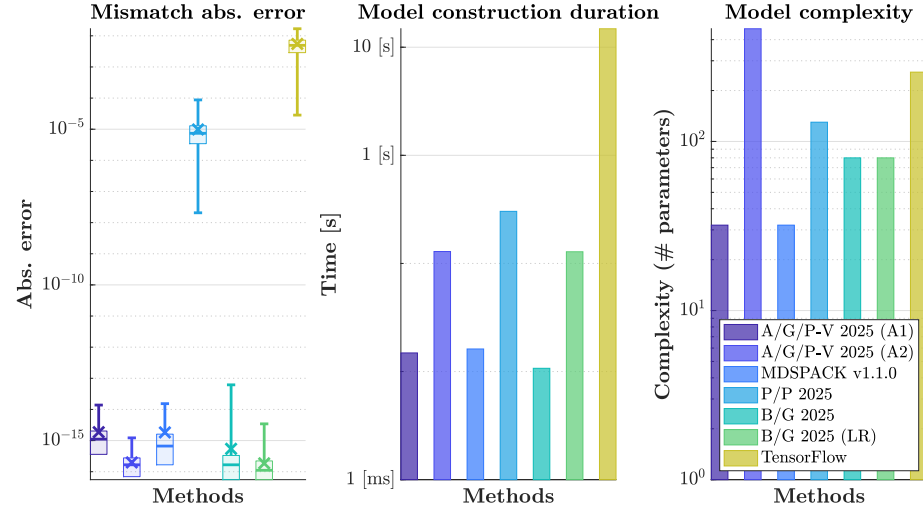


Figure 34: Function #11: graphical view of the best model performances.

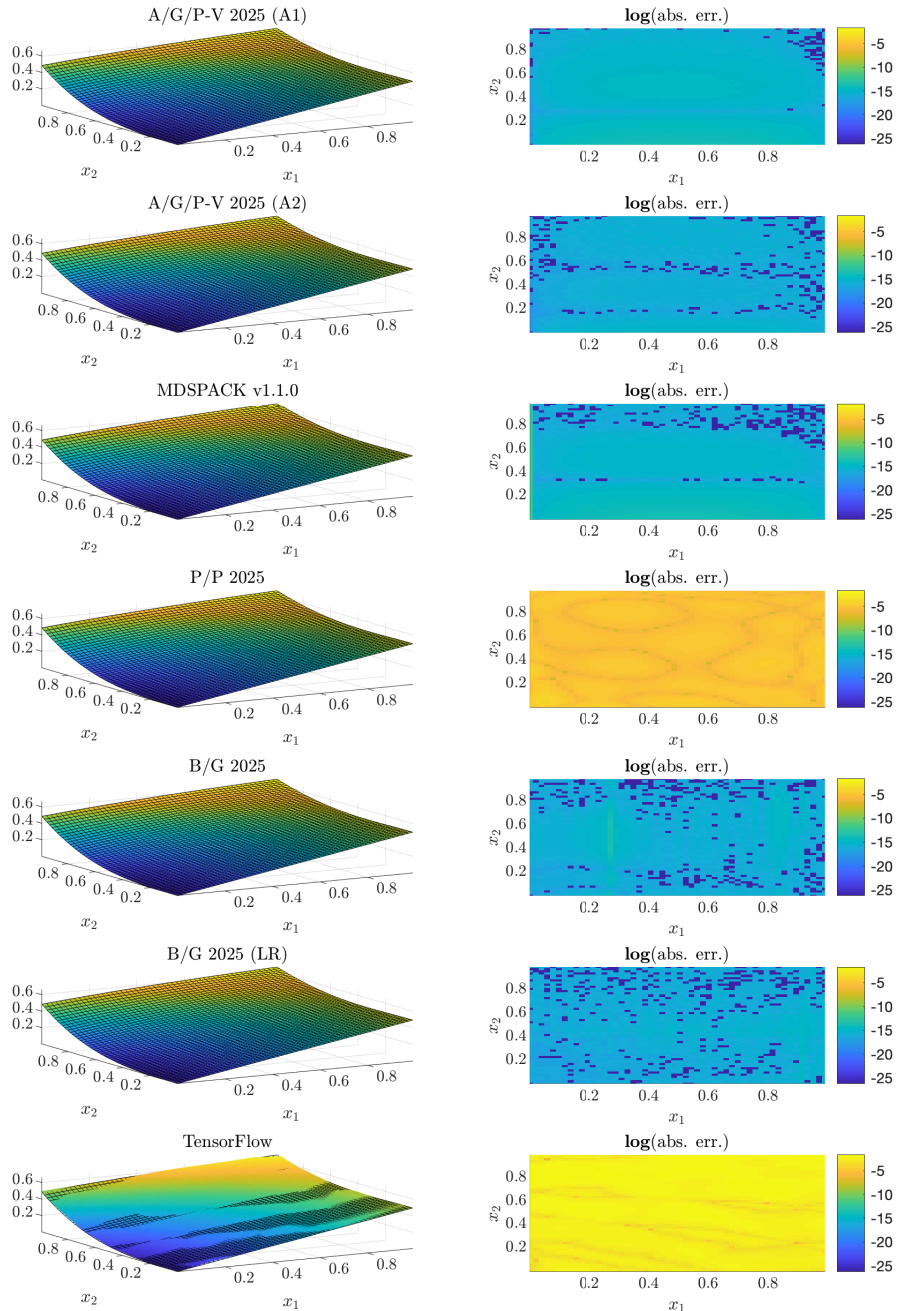


Figure 35: Function #11: left side, evaluation of the original (mesh) vs. approximated (coloured surface) and right side, absolute errors (in log-scale).

4.11.2 mLF detailed informations (M1)

Right interpolation points: $k_l = (2 \ 4)$, where $l = 1, \dots, n$.

$$\begin{aligned} {}^1\lambda_{j_1} &= \left(\frac{1}{10000000000} \quad 1 \right) \\ {}^2\lambda_{j_2} &= \left(\frac{1}{10000000000} \quad \frac{5688757425279507}{18014398509481984} \quad \frac{5688757424378787}{9007199254740992} \quad 1 \right) \end{aligned}$$

Lagrangian weights, data and supports (Lagrangian basis):

$$\left(\begin{array}{cccc} \mathbf{c} & \mathbf{w} & \mathbf{c} \cdot \mathbf{w} & \text{Lag} \\ 0.84 & 5.0e-11 & 4.2e-11 & \frac{1}{(x_1-1.0e-10)(x_2-1.0e-10)} \\ -2.5 & 0.016 & -0.039 & \frac{1}{(x_2-0.32)(x_1-1.0e-10)} \\ 2.3 & 0.13 & 0.29 & \frac{1}{(x_2-0.63)(x_1-1.0e-10)} \\ -0.67 & 0.5 & -0.33 & \frac{1}{(x_2-1.0)(x_1-1.0e-10)} \\ -0.84 & 0.5 & -0.42 & \frac{1}{(x_1-1.0)(x_2-1.0e-10)} \\ 2.6 & 0.49 & 1.3 & \frac{1}{(x_1-1.0)(x_2-0.32)} \\ -2.7 & 0.52 & -1.4 & \frac{1}{(x_1-1.0)(x_2-0.63)} \\ 1.0 & 0.67 & 0.67 & \frac{1}{(x_1-1.0)(x_2-1.0)} \end{array} \right)$$

KST equivalent decoupling pattern

Barycentric weights:

$$\begin{aligned} \mathbf{c}^{x_2} &= \text{vec} \begin{pmatrix} -1.3 & -0.84 \\ 3.7 & 2.6 \\ -3.4 & -2.7 \\ 1.0 & 1.0 \end{pmatrix} \quad \text{and } \mathbf{Bary}_{x_2} = \mathbf{c}^{x_2} \otimes \mathbf{1}_1 \\ \mathbf{c}^{x_1} &= \begin{pmatrix} -0.67 \\ 1.0 \end{pmatrix} \quad \text{and } \mathbf{Bary}_{x_1} = \mathbf{c}^{x_1} \otimes \mathbf{1}_4 \end{aligned}$$

$$\begin{aligned} \mathbf{c} &= \mathbf{c}^{x_n} \odot (\mathbf{c}^{x_{n-1}} \otimes \mathbf{1}_{k_n}) \odot (\mathbf{c}^{x_{n-2}} \otimes \mathbf{1}_{k_n k_{n-1}}) \odot \cdots \odot (\mathbf{c}^{x_1} \otimes \mathbf{1}_{k_n \cdots k_2}) \\ &= \mathbf{Bary}_{x_n} \odot \mathbf{Bary}_{x_{n-1}} \odot \cdots \odot \mathbf{Bary}_{x_1} \end{aligned}$$

Data weights:

$$\begin{aligned} \mathbf{w}^{x_2} &= \text{vec} \begin{pmatrix} 5.0e-11 & 0.5 \\ 0.016 & 0.49 \\ 0.13 & 0.52 \\ 0.5 & 0.67 \end{pmatrix} \quad \text{and } \mathbf{W}_{x_2} = \mathbf{c}^{x_2} \otimes \mathbf{1}_1 \\ \mathbf{w}^{x_1} &= \begin{pmatrix} 0.5 \\ 0.67 \end{pmatrix} \quad \text{and } \mathbf{W}_{x_1} = \mathbf{c}^{x_1} \otimes \mathbf{1}_4 \end{aligned}$$

$$\begin{aligned} \mathbf{w} &= \mathbf{w}^{x_n} \odot (\mathbf{w}^{x_{n-1}} \otimes \mathbf{1}_{k_n}) \odot (\mathbf{w}^{x_{n-2}} \otimes \mathbf{1}_{k_n k_{n-1}}) \odot \cdots \odot (\mathbf{w}^{x_1} \otimes \mathbf{1}_{k_n \cdots k_2}) \\ &= \mathbf{W}_{x_n} \odot \mathbf{W}_{x_{n-1}} \odot \cdots \odot \mathbf{W}_{x_1} \end{aligned}$$

Barycentric denominator univariate vector-wise functions (KST equivalent functions):

$$\mathbf{D} = \left(\begin{array}{cc} \mathbf{c}^{x_1} \cdot \text{Lag}(x_1) & \mathbf{c}^{x_2} \cdot \text{Lag}(x_2) \\ -\frac{0.67}{x_1-1.0e-10} & -\frac{1.3}{x_2-1.0e-10} \\ -\frac{0.67}{x_1-1.0e-10} & \frac{1.8e+16x_2-5.7e+15}{6.7e+16} \\ -\frac{0.67}{x_1-1.0e-10} & -\frac{3.1e+16}{9.0e+15x_2-5.7e+15} \\ -\frac{1}{x_1-1.0e-10} & \frac{1}{x_2-1.0} \\ \frac{1}{x_1-1.0} & -\frac{0.84}{x_2-1.0e-10} \\ \frac{1}{x_1-1.0} & \frac{1.8e+16x_2-5.7e+15}{4.7e+16} \\ \frac{1}{x_1-1.0} & -\frac{1}{9.0e+15x_2-5.7e+15} \\ \frac{1}{x_1-1.0} & \frac{1}{x_2-1.0} \end{array} \right)$$

Equivalent denominator and numerator read:

$$\sum_{i\text{-th row}} \prod_{j\text{-th col}} [\mathbf{D}]_{i,j} \text{ and } \sum_{i\text{-th row}} \mathbf{w} \cdot \prod_{j\text{-th col}} [\mathbf{D}]_{i,j}$$

Connection with Neural Networks (equivalent denominator representation):

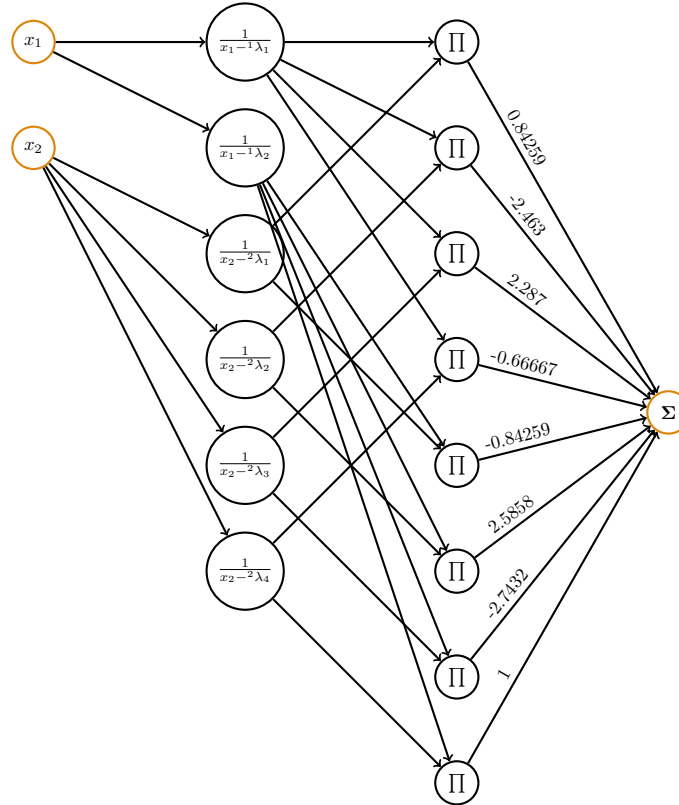


Figure 36: Equivalent NN representation of the denominator \mathbf{D} .

4.12 Function #12 ($n = 2$ variables, tensor size: 12.5 KB)

$$\frac{x_1^2 + x_2^2 + x_1 - x_2 - 1}{(x_1 - 1.1)(x_2 - 1.1)}$$

4.12.1 Setup and results overview

- Reference: A/al. 2021 (A.5.7), [4]
- Domain: \mathbb{R}
- Tensor size: 12.5 **KB** (40^2 points)
- Bounds: $(-1 \ 1) \times (-1 \ 1)$

#	Alg.	Parameters	Dim.	CPU [s]	RMSE	min err.	max err.
12	A/G/P-V 2025 (A1)	0.01,3	36	0.015	1.22e-14	0	6.39e-14
	A/G/P-V 2025 (A2)	1e-15,3	36	0.00732	1.97e-14	0	1.21e-13
	MDSPACK v1.1.0	0.01,0.0001	36	0.0161	1.48e-14	2.78e-17	6.75e-14
	P/P 2025	1,1,50,0.01,4,12,9	184	0.596	0.0667	3.59e-05	0.669
	B/G 2025	0.001,20	60	0.0273	2.84e-12	0	2.94e-11
	B/G 2025 (LR)	1e-09,20,5	60	0.0272	2.57e - 15	0	2.84e - 14
	TensorFlow		257	14.8	0.958	0.000754	8.41

Table 13: Function #12: best model configuration and performances per methods.

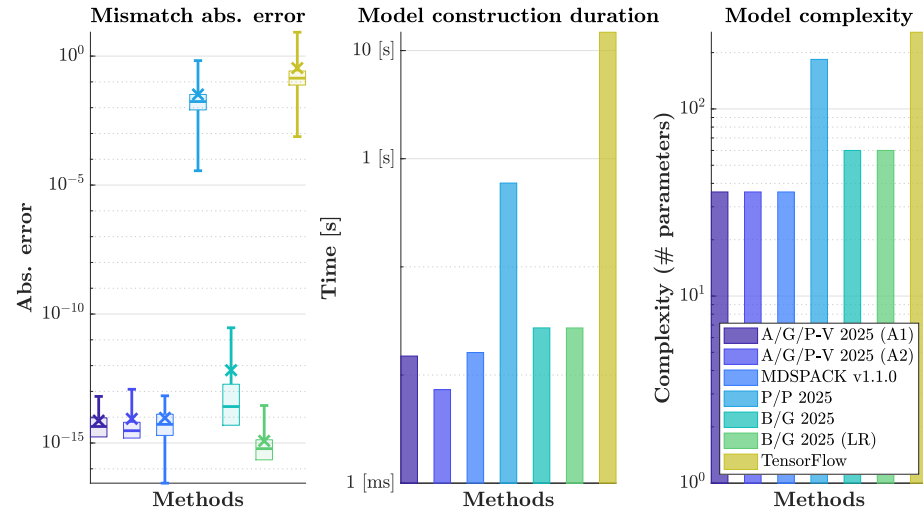


Figure 37: Function #12: graphical view of the best model performances.

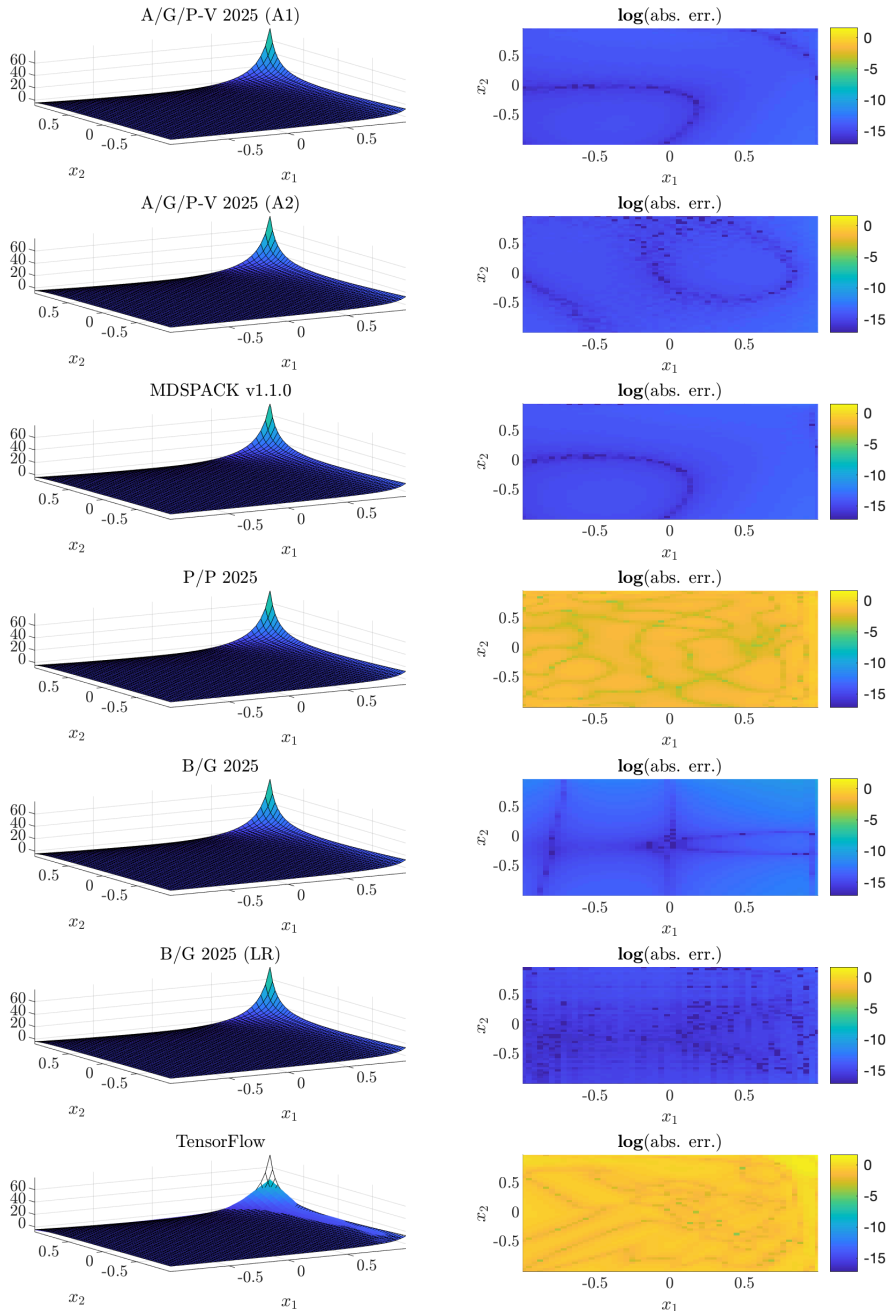


Figure 38: Function #12: left side, evaluation of the original (mesh) vs. approximated (coloured surface) and right side, absolute errors (in log-scale).

4.12.2 mLF detailed informations (M1)

Right interpolation points: $k_l = (3 \ 3)$, where $l = 1, \dots, n$.

$$\begin{aligned} {}^1\lambda_{j_1} &= \left(\begin{array}{ccc} -1 & -\frac{1}{19} & 1 \\ -1 & -\frac{1}{19} & 1 \end{array} \right) \\ {}^2\lambda_{j_2} &= \left(\begin{array}{ccc} 1 & \frac{1}{(x_1+1.0)(x_2+1.0)} \\ 1 & \frac{1}{(x_1+1.0)(x_2+0.053)} \\ 1 & \frac{1}{(x_1+1.0)(x_2-1.0)} \\ 1 & \frac{1}{(x_2+1.0)(x_1+0.053)} \\ 1 & \frac{1}{(x_1+0.053)(x_2+0.053)} \\ 1 & \frac{1}{(x_2-1.0)(x_1+0.053)} \\ 1 & \frac{1}{(x_1-1.0)(x_2+1.0)} \\ 1 & \frac{1}{(x_1-1.0)(x_2+0.053)} \\ 1 & \frac{1}{(x_1-1.0)(x_2-1.0)} \end{array} \right) \end{aligned}$$

Lagrangian weights, data and supports (Lagrangian basis):

$$\left(\begin{array}{cccc} \mathbf{c} & \mathbf{w} & \mathbf{c} \cdot \mathbf{w} & \text{Lag} \\ -22.0 & 0.23 & -5.1 & \frac{1}{(x_1+1.0)(x_2+1.0)} \\ 23.0 & -0.39 & -9.1 & \frac{1}{(x_1+1.0)(x_2+0.053)} \\ -0.96 & -4.8 & 4.6 & \frac{1}{(x_1+1.0)(x_2-1.0)} \\ 23.0 & 0.39 & 9.2 & \frac{1}{(x_2+1.0)(x_1+0.053)} \\ -24.0 & -0.75 & 18.0 & \frac{1}{(x_1+0.053)(x_2+0.053)} \\ 1.0 & -9.1 & -9.1 & \frac{1}{(x_2-1.0)(x_1+0.053)} \\ -0.96 & 14.0 & -14.0 & \frac{1}{(x_1-1.0)(x_2+1.0)} \\ 1.0 & 9.2 & 9.2 & \frac{1}{(x_1-1.0)(x_2+0.053)} \\ -0.041 & 100.0 & -4.1 & \frac{1}{(x_1-1.0)(x_2-1.0)} \end{array} \right)$$

KST equivalent decoupling pattern

Barycentric weights:

$$\begin{aligned} \mathbf{c}^{x_2} &= \text{vec} \begin{pmatrix} 23.0 & 23.0 & 23.0 \\ -24.0 & -24.0 & -24.0 \\ 1.0 & 1.0 & 1.0 \end{pmatrix} \quad \text{and } \mathbf{Bary}_{x_2} = \mathbf{c}^{x_2} \otimes \mathbf{1}_1 \\ \mathbf{c}^{x_1} &= \begin{pmatrix} -0.96 \\ 1.0 \\ -0.041 \end{pmatrix} \quad \text{and } \mathbf{Bary}_{x_1} = \mathbf{c}^{x_1} \otimes \mathbf{1}_3 \\ \mathbf{c} &= \mathbf{c}^{x_n} \odot (\mathbf{c}^{x_{n-1}} \otimes \mathbf{1}_{k_n}) \odot (\mathbf{c}^{x_{n-2}} \otimes \mathbf{1}_{k_n k_{n-1}}) \odot \cdots \odot (\mathbf{c}^{x_1} \otimes \mathbf{1}_{k_n \dots k_2}) \\ &= \mathbf{Bary}_{x_n} \odot \mathbf{Bary}_{x_{n-1}} \odot \cdots \odot \mathbf{Bary}_{x_1} \end{aligned}$$

Data weights:

$$\begin{aligned} \mathbf{w}^{x_2} &= \text{vec} \begin{pmatrix} 0.23 & 0.39 & 14.0 \\ -0.39 & -0.75 & 9.2 \\ -4.8 & -9.1 & 100.0 \end{pmatrix} \quad \text{and } \mathbf{W}_{x_2} = \mathbf{c}^{x_2} \otimes \mathbf{1}_1 \\ \mathbf{w}^{x_1} &= \begin{pmatrix} -4.8 \\ -9.1 \\ 100.0 \end{pmatrix} \quad \text{and } \mathbf{W}_{x_1} = \mathbf{c}^{x_1} \otimes \mathbf{1}_3 \\ \mathbf{w} &= \mathbf{w}^{x_n} \odot (\mathbf{w}^{x_{n-1}} \otimes \mathbf{1}_{k_n}) \odot (\mathbf{w}^{x_{n-2}} \otimes \mathbf{1}_{k_n k_{n-1}}) \odot \cdots \odot (\mathbf{w}^{x_1} \otimes \mathbf{1}_{k_n \dots k_2}) \\ &= \mathbf{W}_{x_n} \odot \mathbf{W}_{x_{n-1}} \odot \cdots \odot \mathbf{W}_{x_1} \end{aligned}$$

Barycentric denominator univariate vector-wise functions (KST equivalent functions):

$$\mathbf{D} = \begin{pmatrix} \mathbf{c}^{x_1} \cdot \text{Lag}(x_1) & \mathbf{c}^{x_2} \cdot \text{Lag}(x_2) \\ -\frac{0.96}{x_1+1.0} & -\frac{23.0}{x_2+1.0} \\ -\frac{0.96}{x_1+1.0} & -\frac{24.0}{x_2+0.053} \\ -\frac{0.96}{x_1+1.0} & -\frac{1}{x_2-1.0} \\ \frac{1}{x_1+0.053} & \frac{23.0}{x_2+1.0} \\ \frac{1}{x_1+0.053} & -\frac{24.0}{x_2+0.053} \\ \frac{1}{x_1+0.053} & -\frac{1}{x_2-1.0} \\ -\frac{0.041}{x_1-1.0} & \frac{23.0}{x_2+1.0} \\ -\frac{0.041}{x_1-1.0} & -\frac{24.0}{x_2+0.053} \\ -\frac{0.041}{x_1-1.0} & -\frac{1}{x_2-1.0} \end{pmatrix}$$

Equivalent denominator and numerator read:

$$\sum_{i\text{-th row}} \prod_{j\text{-th col}} [\mathbf{D}]_{i,j} \quad \text{and} \quad \sum_{i\text{-th row}} \mathbf{w} \cdot \prod_{j\text{-th col}} [\mathbf{D}]_{i,j}$$

Connection with Neural Networks (equivalent denominator representation):

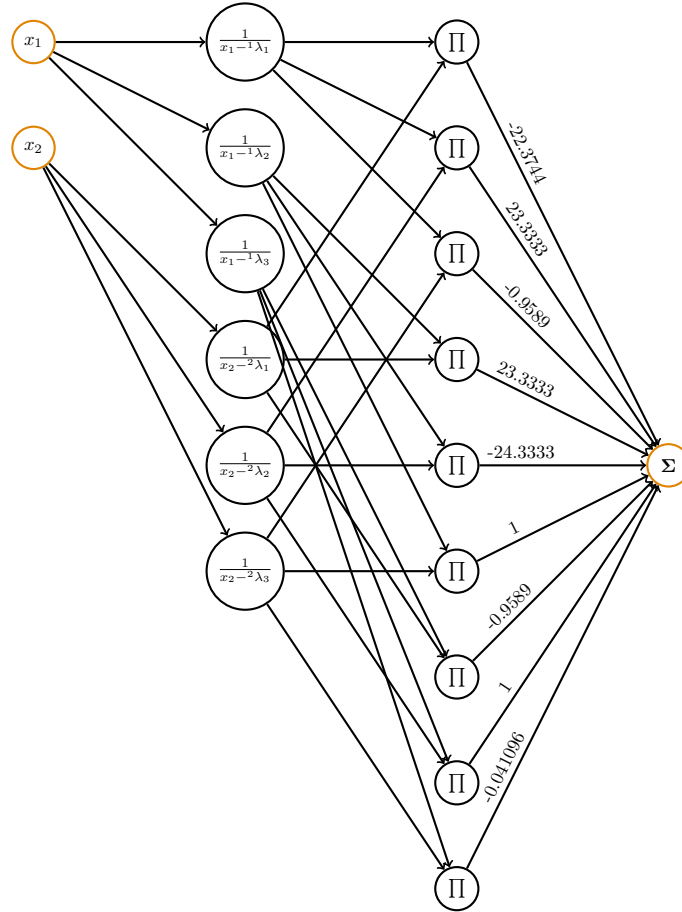


Figure 39: Equivalent NN representation of the denominator \mathbf{D} .

4.13 Function #13 ($n = 2$ variables, tensor size: 12.5 KB)

$$\frac{x_1^4 + x_2^4 + x_1^2x_2^2 + x_1x_2}{(x_1 - 1.1)(y_2 - 1.1)}$$

4.13.1 Setup and results overview

- Reference: A/al. 2021 (A.5.8), [4]
- Domain: \mathbb{R}
- Tensor size: 12.5 **KB** (40^2 points)
- Bounds: $(-1 \ 1) \times (-1 \ 1)$

#	Alg.	Parameters	Dim.	CPU [s]	RMSE	min err.	max err.
13	A/G/P-V 2025 (A1)	0.001,2	100	0.0151	3.86e-13	0	3.05e-12
	A/G/P-V 2025 (A2)	1e-15,3	100	0.00885	2.78e-13	2.78e-17	1.16e-12
	MDSPACK v1.1.0	0.001,0.0001	100	0.016	3.12e-13	0	2.54e-12
	P/P 2025	1,1,50,0.01,4,6,9	130	0.314	0.339	4.03e-05	4.59
	B/G 2025	0.001,20	192	0.0515	1.45e-12	0	2.12e-11
	B/G 2025 (LR)	0.001,20,5	160	0.0695	3.25e - 14	0	5.64e - 13
	TensorFlow		257	14.8	6	0.00699	72

Table 14: Function #13: best model configuration and performances per methods.

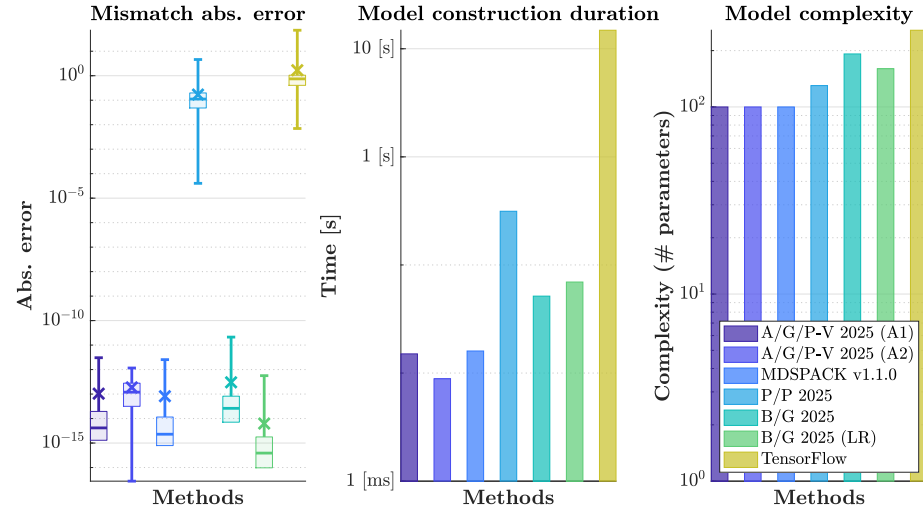


Figure 40: Function #13: graphical view of the best model performances.

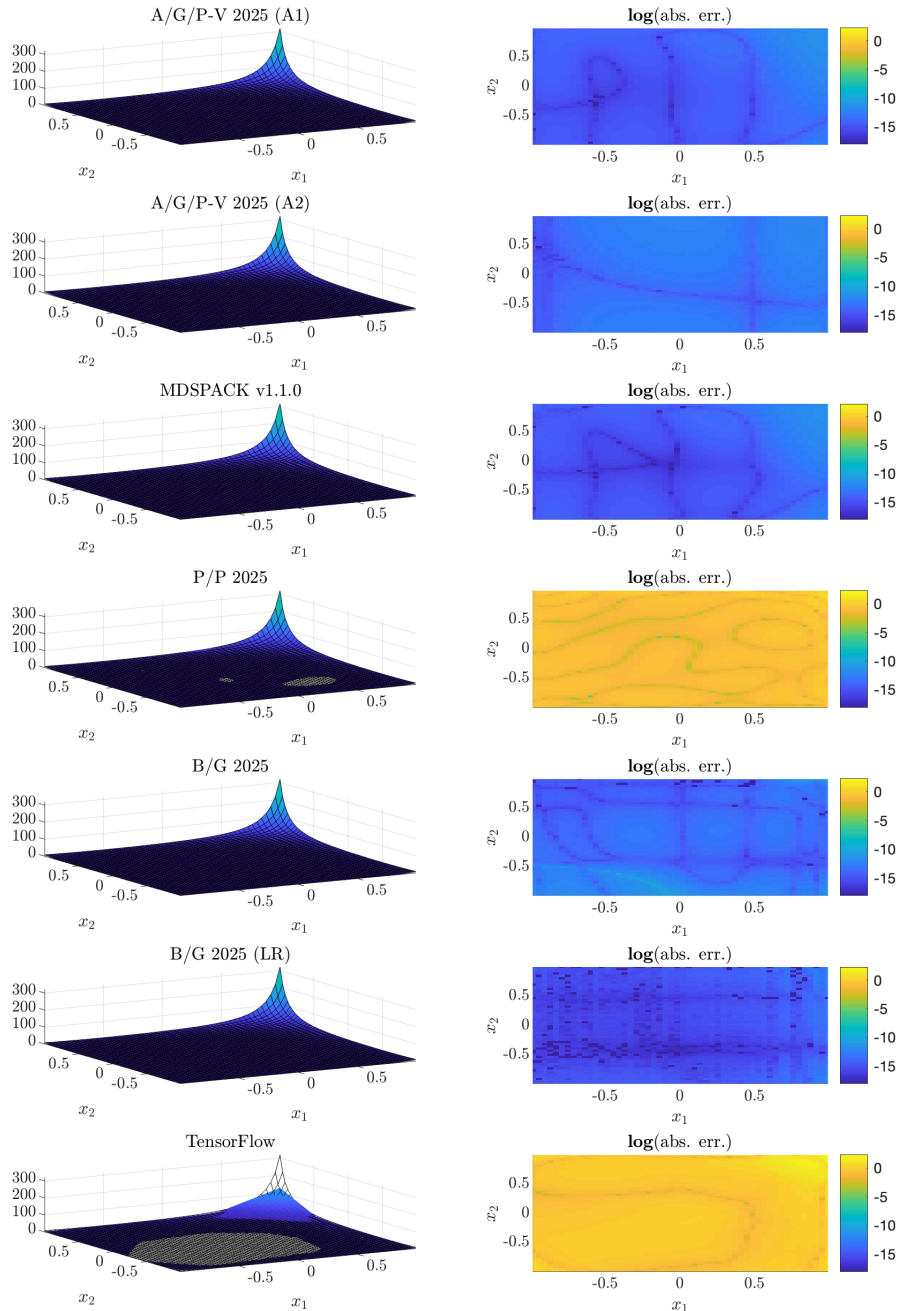


Figure 41: Function #13: left side, evaluation of the original (mesh) vs. approximated (coloured surface) and right side, absolute errors (in log-scale).

4.13.2 mLF detailed informations (M1)

Right interpolation points: $k_l = \begin{pmatrix} 5 & 5 \end{pmatrix}$, where $l = 1, \dots, n$.

$$\begin{aligned} {}^1\lambda_{j_1} &\in \mathbb{C}^5, \text{ linearly spaced between bounds} \\ {}^2\lambda_{j_2} &\in \mathbb{C}^5, \text{ linearly spaced between bounds} \end{aligned}$$

n-D Loewner matrix, barycentric weights and Lagrangian basis:

$$\begin{aligned} \mathbb{L} &\in \mathbb{C}^{25 \times 25} \\ \mathbf{c} &\in \mathbb{C}^{25} \\ \mathbf{w} &\in \mathbb{C}^{25} \\ \mathbf{c} \cdot \mathbf{w} &\in \mathbb{C}^{25} \\ \mathbf{Lag}(x_1, x_2) &\in \mathbb{C}^{25} \end{aligned}$$

4.14 Function #14 ($n = 4$ variables, tensor size: 1.22 MB)

$$\frac{x_1^2 + x_2^2 + x_1 - x_2 + 1}{(x_3 - 1.5)(x_4 - 1.5)}$$

4.14.1 Setup and results overview

- Reference: A/al. 2021 (A.5.9), [4]
- Domain: \mathbb{R}
- Tensor size: 1.22 MB (20^4 points)
- Bounds: $(-1 \ 1) \times (-1 \ 1) \times (-1 \ 1) \times (-1 \ 1)$

#	Alg.	Parameters	Dim.	CPU [s]	RMSE	min err.	max err.
14	A/G/P-V 2025 (A1)	0.1,3	216	0.0587	6.03e-16	0	3.55e-15
	A/G/P-V 2025 (A2)	1e-15,3	216	0.0207	4.76e - 16	0	2.66e - 15
	MDSPACK v1.1.0	0.1,0.0001	216	0.0424	7.49e-16	0	5.33e-15
	P/P 2025	1,0.95,50,0.01,6,12,13	472	50.7	0.000527	7.26e-07	0.00244
	B/G 2025	0.001,20	216	39	9.35e-15	0	5.51e-14
	B/G 2025 (LR)	0.001,20,3	216	4.36	1.43e-15	0	7.11e-15
	TensorFlow		385	148	0.0203	3.22e-05	0.124

Table 15: Function #14: best model configuration and performances per methods.

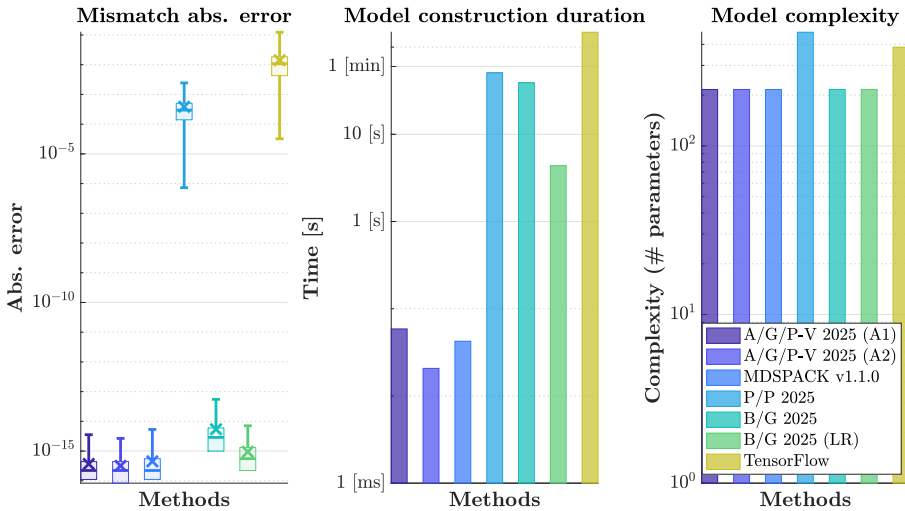


Figure 42: Function #14: graphical view of the best model performances.

$$x_{3\ldots 4} = [-0.16596; -0.99977]$$

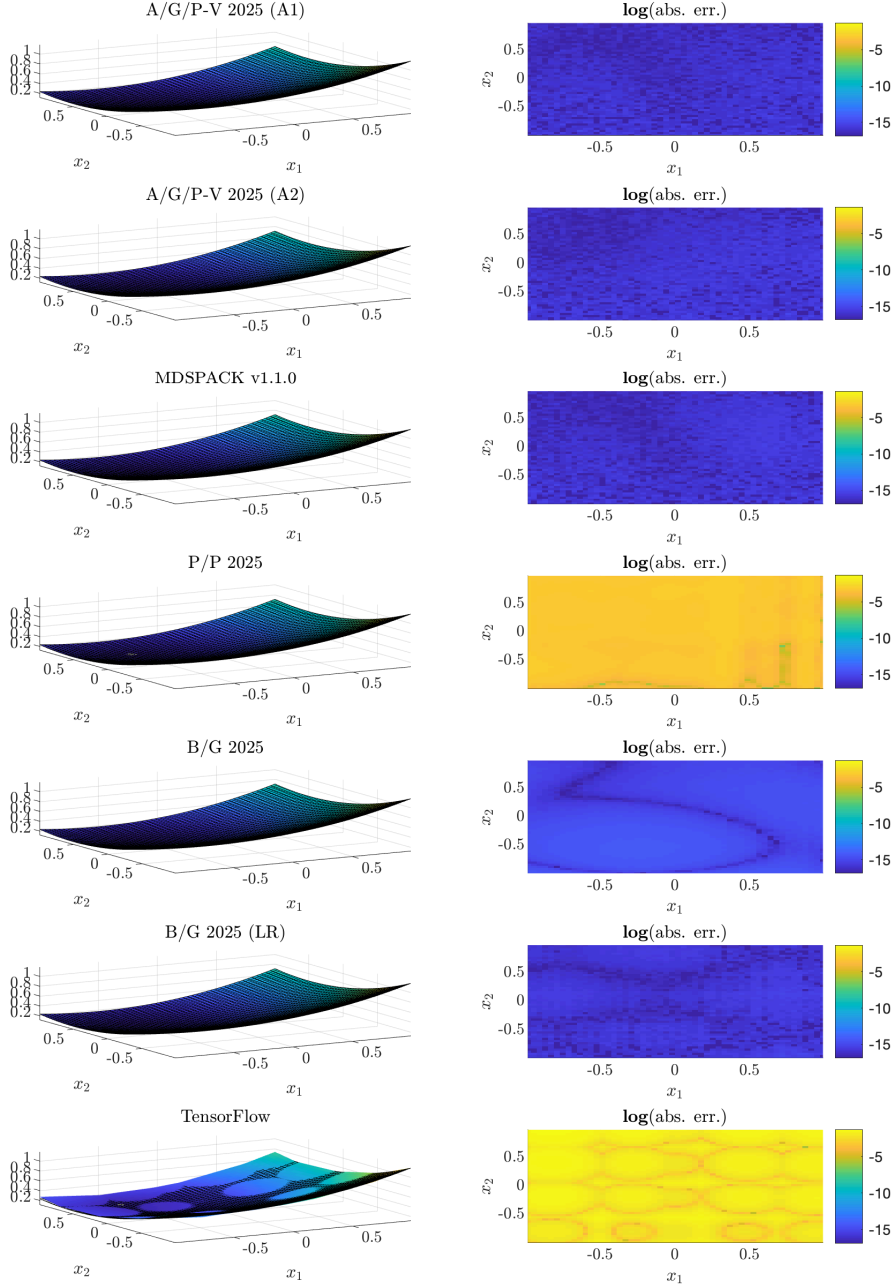


Figure 43: Function #14: left side, evaluation of the original (mesh) vs. approximated (coloured surface) and right side, absolute errors (in log-scale).

4.14.2 mLF detailed informations (M1)

Right interpolation points: $k_l = (3 \ 3 \ 2 \ 2)$, where $l = 1, \dots, n$.

$$\begin{aligned} {}^1\lambda_{j_1} &\in \mathbb{C}^3, \text{ linearly spaced between bounds} \\ {}^2\lambda_{j_2} &\in \mathbb{C}^3, \text{ linearly spaced between bounds} \\ {}^3\lambda_{j_3} &\in \mathbb{C}^2, \text{ linearly spaced between bounds} \\ {}^4\lambda_{j_4} &\in \mathbb{C}^2, \text{ linearly spaced between bounds} \end{aligned}$$

n-D Loewner matrix, barycentric weights and Lagrangian basis:

$$\begin{aligned} \mathbb{L} &\in \mathbb{C}^{36 \times 36} \\ \mathbf{c} &\in \mathbb{C}^{36} \\ \mathbf{w} &\in \mathbb{C}^{36} \\ \mathbf{c} \cdot \mathbf{w} &\in \mathbb{C}^{36} \\ \mathbf{Lag}(x_1, x_2, x_3, x_4) &\in \mathbb{C}^{36} \end{aligned}$$

4.15 Function #15 ($n = 2$ variables, tensor size: 12.5 KB)

$$\frac{x_1^2 + x_2^2 + x_1 - x_2 - 1}{x_1^3 + x_2^3 + 4}$$

4.15.1 Setup and results overview

- Reference: A/al. 2021 (A.5.10), [4]
- Domain: \mathbb{R}
- Tensor size: 12.5 **KB** (40^2 points)
- Bounds: $(-1 \ 1) \times (-1 \ 1)$

#	Alg.	Parameters	Dim.	CPU [s]	RMSE	min err.	max err.
15	A/G/P-V 2025 (A1)	0.01,1	64	0.015	3.11e-15	0	1.28e-14
	A/G/P-V 2025 (A2)	1e-15,3	336	0.0856	3.59e-16	0	1.22e-15
	MDSPACK v1.1.0	0.01,0.01	64	0.0168	3.12e-15	0	1.27e-14
	P/P 2025	1,0.95,50,0.01,4,12,9	184	0.941	5.35e-05	7.53e-08	0.000253
	B/G 2025	0.001,20	140	0.0387	7.86e-14	0	1.72e-12
	B/G 2025 (LR)	0.001,20,5	112	0.0972	2.26e - 16	0	9.44e - 16
	TensorFlow		257	14.9	0.00331	2.57e-05	0.012

Table 16: Function #15: best model configuration and performances per methods.

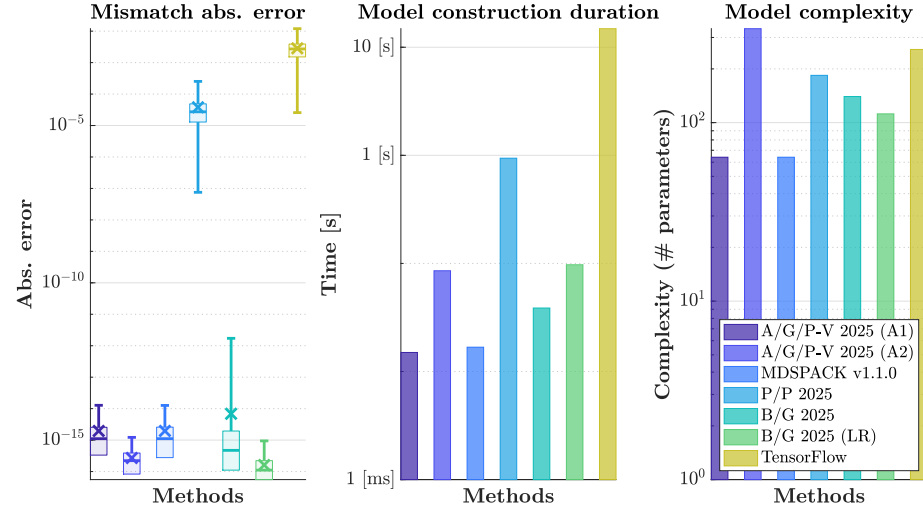


Figure 44: Function #15: graphical view of the best model performances.

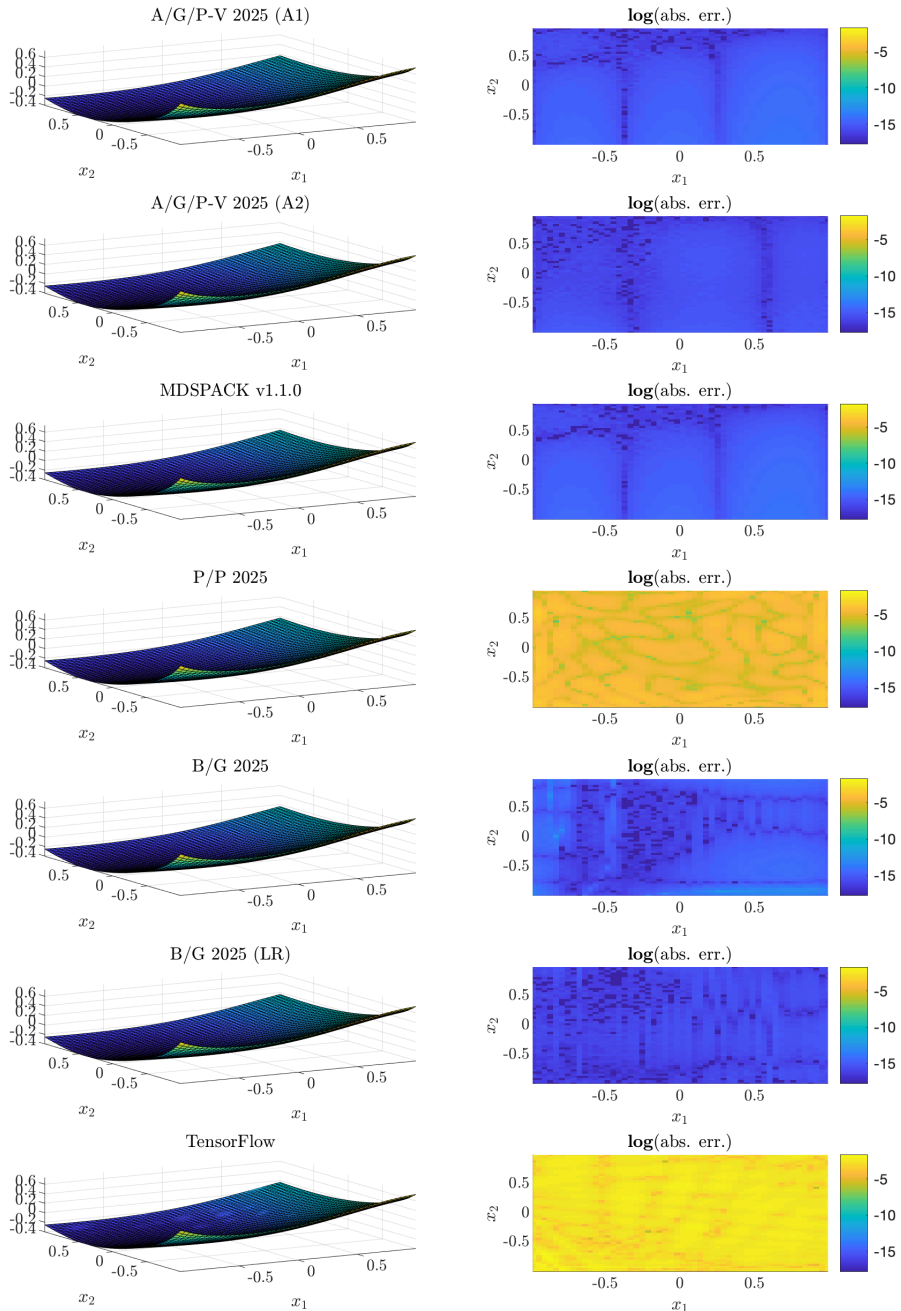


Figure 45: Function #15: left side, evaluation of the original (mesh) vs. approximated (coloured surface) and right side, absolute errors (in log-scale).

4.15.2 mLF detailed informations (M1)

Right interpolation points: $k_l = (4 \quad 4)$, where $l = 1, \dots, n$.

$$\begin{aligned} {}^1\lambda_{j_1} &= \left(-1 \quad -\frac{7}{19} \quad \frac{5}{19} \quad 1 \right) \\ {}^2\lambda_{j_2} &= \left(-1 \quad -\frac{7}{19} \quad \frac{5}{19} \quad 1 \right) \end{aligned}$$

Lagrangian weights, data and supports (Lagrangian basis):

$$\left(\begin{array}{cccc} \mathbf{c} & \mathbf{w} & \mathbf{c} \cdot \mathbf{w} & \text{Lag} \\ 0.17 & 0.5 & 0.087 & \frac{1}{(x_1+1.0)(x_2+1.0)} \\ -0.75 & -0.17 & 0.13 & \frac{1}{(x_1+1.0)(x_2+0.37)} \\ 0.72 & -0.4 & -0.28 & \frac{1}{(x_1+1.0)(x_2-0.26)} \\ -0.28 & -0.25 & 0.069 & \frac{1}{(x_1+1.0)(x_2-1.0)} \\ -0.75 & 0.26 & -0.2 & \frac{1}{(x_2+1.0)(x_1+0.37)} \\ 2.9 & -0.19 & -0.54 & \frac{1}{(x_1+0.37)(x_2+0.37)} \\ -2.8 & -0.36 & 0.99 & \frac{1}{(x_2-0.26)(x_1+0.37)} \\ 1.0 & -0.25 & -0.25 & \frac{1}{(x_2-1.0)(x_1+0.37)} \\ 0.72 & 0.44 & 0.32 & \frac{1}{(x_2+1.0)(x_1-0.26)} \\ -2.8 & -0.041 & 0.11 & \frac{1}{(x_1-0.26)(x_2+0.37)} \\ 2.6 & -0.21 & -0.55 & \frac{1}{(x_1-0.26)(x_2-0.26)} \\ -0.94 & -0.13 & 0.13 & \frac{1}{(x_2-1.0)(x_1-0.26)} \\ -0.28 & 0.75 & -0.21 & \frac{1}{(x_1-1.0)(x_2+1.0)} \\ 1.0 & 0.3 & 0.3 & \frac{1}{(x_1-1.0)(x_2+0.37)} \\ -0.94 & 0.16 & -0.15 & \frac{1}{(x_1-1.0)(x_2-0.26)} \\ 0.33 & 0.17 & 0.055 & \frac{1}{(x_1-1.0)(x_2-1.0)} \end{array} \right)$$

KST equivalent decoupling pattern

Barycentric weights:

$$\begin{aligned} \mathbf{c}^{x_2} &= \text{vec} \begin{pmatrix} -0.63 & -0.75 & -0.76 & -0.84 \\ 2.7 & 2.9 & 2.9 & 3.0 \\ -2.6 & -2.8 & -2.8 & -2.9 \\ 1.0 & 1.0 & 1.0 & 1.0 \end{pmatrix} \quad \text{and } \mathbf{Bary}_{x_2} = \mathbf{c}^{x_2} \otimes \mathbf{1}_1 \\ \mathbf{c}^{x_1} &= \begin{pmatrix} -0.28 \\ 1.0 \\ -0.94 \\ 0.33 \end{pmatrix} \quad \text{and } \mathbf{Bary}_{x_1} = \mathbf{c}^{x_1} \otimes \mathbf{1}_4 \\ \mathbf{c} &= \mathbf{c}^{x_n} \odot (\mathbf{c}^{x_{n-1}} \otimes \mathbf{1}_{k_n}) \odot (\mathbf{c}^{x_{n-2}} \otimes \mathbf{1}_{k_n k_{n-1}}) \odot \cdots \odot (\mathbf{c}^{x_1} \otimes \mathbf{1}_{k_n \cdots k_2}) \\ &= \mathbf{Bary}_{x_n} \odot \mathbf{Bary}_{x_{n-1}} \odot \cdots \odot \mathbf{Bary}_{x_1} \end{aligned}$$

Data weights:

$$\begin{aligned} \mathbf{w}^{x_2} &= \text{vec} \begin{pmatrix} 0.5 & 0.26 & 0.44 & 0.75 \\ -0.17 & -0.19 & -0.041 & 0.3 \\ -0.4 & -0.36 & -0.21 & 0.16 \\ -0.25 & -0.25 & -0.13 & 0.17 \end{pmatrix} \quad \text{and } \mathbf{W}_{x_2} = \mathbf{c}^{x_2} \otimes \mathbf{1}_1 \\ \mathbf{w}^{x_1} &= \begin{pmatrix} -0.25 \\ -0.25 \\ -0.13 \\ 0.17 \end{pmatrix} \quad \text{and } \mathbf{W}_{x_1} = \mathbf{c}^{x_1} \otimes \mathbf{1}_4 \\ \mathbf{w} &= \mathbf{w}^{x_n} \odot (\mathbf{w}^{x_{n-1}} \otimes \mathbf{1}_{k_n}) \odot (\mathbf{w}^{x_{n-2}} \otimes \mathbf{1}_{k_n k_{n-1}}) \odot \cdots \odot (\mathbf{w}^{x_1} \otimes \mathbf{1}_{k_n \cdots k_2}) \\ &= \mathbf{W}_{x_n} \odot \mathbf{W}_{x_{n-1}} \odot \cdots \odot \mathbf{W}_{x_1} \end{aligned}$$

Barycentric denominator univariate vector-wise functions (KST equivalent functions):

$$\mathbf{D} = \begin{pmatrix} \mathbf{c}^{x_1} \cdot \mathbf{Lag}(x_1) & \mathbf{c}^{x_2} \cdot \mathbf{Lag}(x_2) \\ -\frac{0.28}{x_1+1.0} & -\frac{0.63}{x_2+1.0} \\ -\frac{0.28}{x_1+1.0} & -\frac{2.7}{x_2+0.37} \\ -\frac{0.28}{x_1+1.0} & -\frac{2.6}{x_2-0.26} \\ -\frac{1}{x_1+0.37} & -\frac{0.75}{x_2-1.0} \\ \frac{1}{x_1+0.37} & -\frac{x_2+1.0}{2.9} \\ \frac{1}{x_1+0.37} & -\frac{x_2+0.37}{2.8} \\ \frac{1}{x_1+0.37} & -\frac{x_2-0.26}{1} \\ -\frac{0.94}{x_1-0.26} & -\frac{x_2-1.0}{0.76} \\ -\frac{0.94}{x_1-0.26} & -\frac{x_2+1.0}{2.9} \\ -\frac{0.94}{x_1-0.26} & -\frac{x_2+0.37}{2.8} \\ -\frac{0.94}{x_1-0.26} & -\frac{x_2-0.26}{1} \\ -\frac{0.33}{x_1-1.0} & -\frac{x_2-1.0}{0.84} \\ \frac{0.33}{x_1-1.0} & -\frac{x_2+1.0}{3.0} \\ \frac{0.33}{x_1-1.0} & -\frac{x_2+0.37}{2.9} \\ \frac{0.33}{x_1-1.0} & -\frac{x_2-0.26}{1} \\ x_1-1.0 & x_2-1.0 \end{pmatrix}$$

Equivalent denominator and numerator read:

$$\sum_{i\text{-th row}} \prod_{j\text{-th col}} [\mathbf{D}]_{i,j} \text{ and } \sum_{i\text{-th row}} \mathbf{w} \cdot \prod_{j\text{-th col}} [\mathbf{D}]_{i,j}$$

Connection with Neural Networks (equivalent denominator representation):

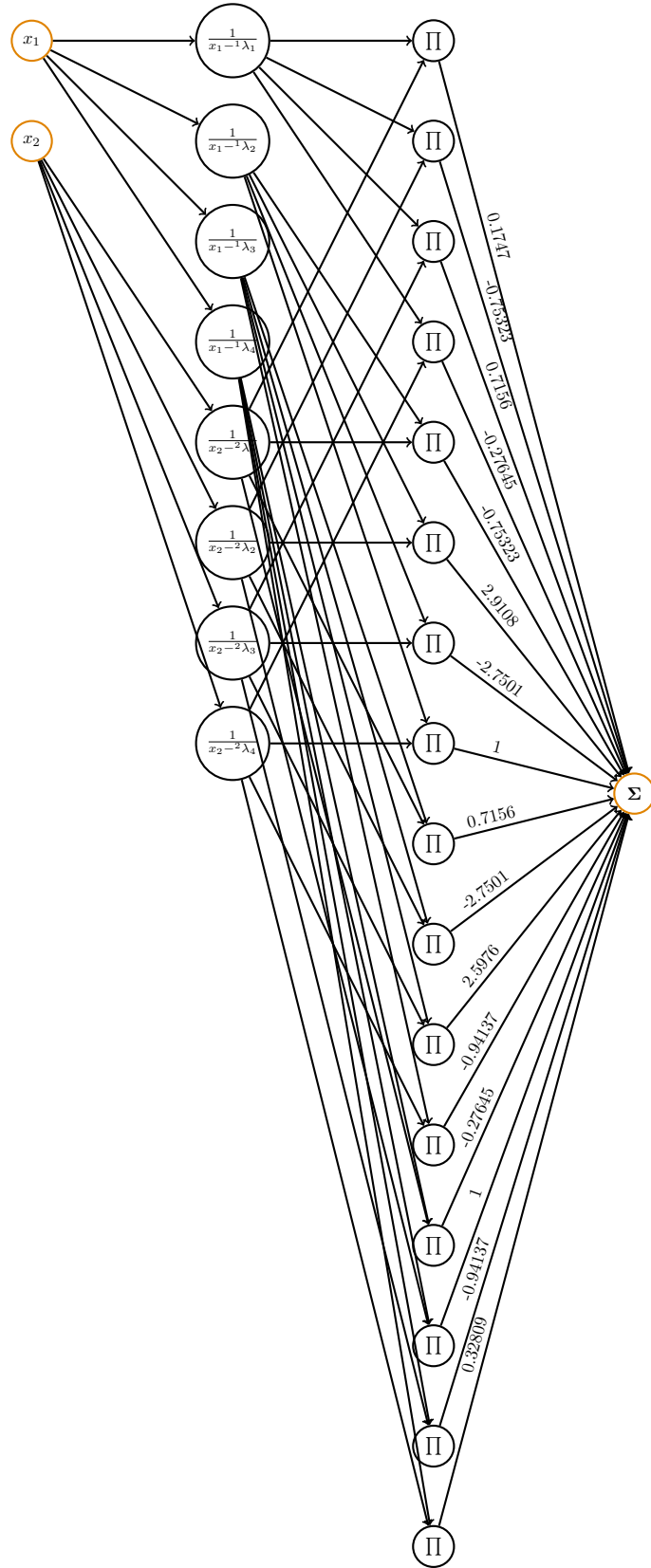


Figure 46: Equivalent NN representation of the denominator \mathbf{D} .

4.16 Function #16 ($n = 2$ variables, tensor size: 12.5 KB)

$$\frac{x_1^3 + x_2^3}{x_1^2 + x_2^2 + 3}$$

4.16.1 Setup and results overview

- Reference: A/al. 2021 (A.5.11), [4]
- Domain: \mathbb{R}
- Tensor size: 12.5 **KB** (40^2 points)
- Bounds: $(-1 \ 1) \times (-1 \ 1)$

#	Alg.	Parameters	Dim.	CPU [s]	RMSE	min err.	max err.
16	A/G/P-V 2025 (A1)	0.1,2	64	0.0156	2.61e-16	0	8.88e-16
	A/G/P-V 2025 (A2)	1e-15,2	64	0.135	1.74e-15	0	4e-15
	MDSPACK v1.1.0	0.1,0.01	64	0.0161	2.69e-16	0	1.14e-15
	P/P 2025	1,1,50,0.01,4,12,9	184	0.86	2.44e-05	8.52e-08	0.00011
	B/G 2025	0.001,20	80	0.0145	2.09e-15	0	2.6e-14
	B/G 2025 (LR)	1e-06,20,4	80	0.0617	1.22e - 16	0	4.44e - 16
	TensorFlow		257	14.9	0.00167	8.43e-06	0.00454

Table 17: Function #16: best model configuration and performances per methods.

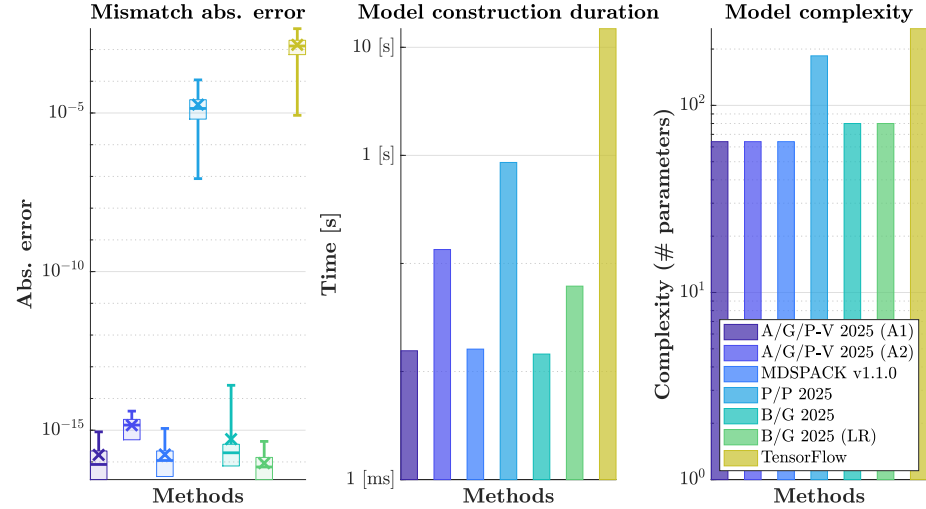


Figure 47: Function #16: graphical view of the best model performances.

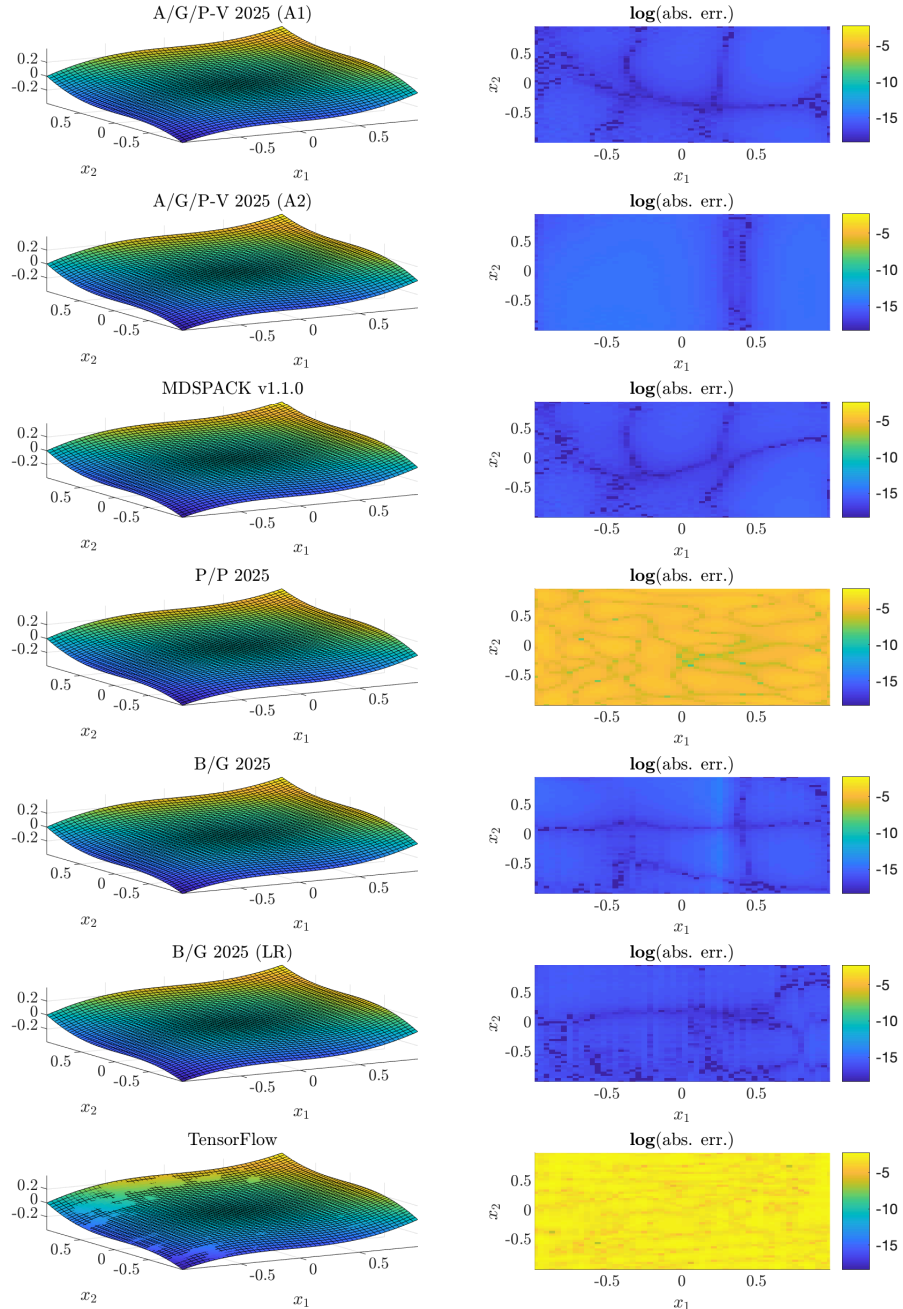


Figure 48: Function #16: left side, evaluation of the original (mesh) vs. approximated (coloured surface) and right side, absolute errors (in log-scale).

4.16.2 mLF detailed informations (M1)

Right interpolation points: $k_l = (4 \quad 4)$, where $l = 1, \dots, n$.

$$\begin{aligned} {}^1\lambda_{j_1} &= \left(\begin{array}{cccc} -1 & -\frac{7}{19} & \frac{5}{19} & 1 \\ -1 & -\frac{1}{19} & \frac{5}{19} & 1 \end{array} \right) \\ {}^2\lambda_{j_2} &= \left(\begin{array}{cccc} -1 & -\frac{7}{19} & \frac{5}{19} & 1 \\ -1 & -\frac{1}{19} & \frac{5}{19} & 1 \end{array} \right) \end{aligned}$$

Lagrangian weights, data and supports (Lagrangian basis):

c	w	c · w	Lag
0.52	-0.4	-0.21	$\frac{1}{(x_1+1.0)(x_2+1.0)}$
-1.3	-0.25	0.32	$\frac{1}{(x_1+1.0)(x_2+0.37)}$
1.2	-0.24	-0.28	$\frac{1}{(x_1+1.0)(x_2-0.26)}$
-0.41	0	0	$\frac{1}{(x_1+1.0)(x_2-1.0)}$
-1.3	-0.25	0.32	$\frac{1}{(x_2+1.0)(x_1+0.37)}$
2.9	-0.031	-0.089	$\frac{1}{(x_1+0.37)(x_2+0.37)}$
-2.7	$-9.9e-3$	0.026	$\frac{1}{(x_2-0.26)(x_1+0.37)}$
1.0	0.23	0.23	$\frac{1}{(x_2-1.0)(x_1+0.37)}$
1.2	-0.24	-0.28	$\frac{1}{(x_2+1.0)(x_1-0.26)}$
-2.7	$-9.9e-3$	0.026	$\frac{1}{(x_1-0.26)(x_2+0.37)}$
2.4	0.012	0.028	$\frac{1}{(x_1-0.26)(x_2-0.26)}$
-0.91	0.25	-0.23	$\frac{1}{(x_2-1.0)(x_1-0.26)}$
-0.41	0	0	$\frac{1}{(x_1-1.0)(x_2+1.0)}$
1.0	0.23	0.23	$\frac{1}{(x_1-1.0)(x_2+0.37)}$
-0.91	0.25	-0.23	$\frac{1}{(x_1-1.0)(x_2-0.26)}$
0.33	0.4	0.13	$\frac{1}{(x_1-1.0)(x_2-1.0)}$

KST equivalent decoupling pattern

Barycentric weights:

$$\mathbf{c}^{x_2} = \text{vec} \begin{pmatrix} -1.3 & -1.3 & -1.3 & -1.3 \\ 3.1 & 2.9 & 2.9 & 3.1 \\ -2.8 & -2.7 & -2.6 & -2.8 \\ 1.0 & 1.0 & 1.0 & 1.0 \end{pmatrix} \quad \text{and } \mathbf{Bary}_{x_2} = \mathbf{c}^{x_2} \otimes \mathbf{1}_1$$

$$\mathbf{c}^{x_1} = \begin{pmatrix} -0.41 \\ 1.0 \\ -0.91 \\ 0.33 \end{pmatrix} \quad \text{and } \mathbf{Bary}_{x_1} = \mathbf{c}^{x_1} \otimes \mathbf{1}_4$$

$$\begin{aligned} \mathbf{c} &= \mathbf{c}^{x_n} \odot (\mathbf{c}^{x_{n-1}} \otimes \mathbf{1}_{k_n}) \odot (\mathbf{c}^{x_{n-2}} \otimes \mathbf{1}_{k_n k_{n-1}}) \odot \cdots \odot (\mathbf{c}^{x_1} \otimes \mathbf{1}_{k_n \cdots k_2}) \\ &= \mathbf{Bary}_{x_n} \odot \mathbf{Bary}_{x_{n-1}} \odot \cdots \odot \mathbf{Bary}_{x_1} \end{aligned}$$

Data weights:

$$\mathbf{w}^{x_2} = \text{vec} \begin{pmatrix} -0.4 & -0.25 & -0.24 & 0 \\ -0.25 & -0.031 & -9.9e-3 & 0.23 \\ -0.24 & -9.9e-3 & 0.012 & 0.25 \\ 0 & 0.23 & 0.25 & 0.4 \end{pmatrix} \quad \text{and } \mathbf{W}_{x_2} = \mathbf{c}^{x_2} \otimes \mathbf{1}_1$$

$$\mathbf{w}^{x_1} = \begin{pmatrix} 0 \\ 0.23 \\ 0.25 \\ 0.4 \end{pmatrix} \quad \text{and } \mathbf{W}_{x_1} = \mathbf{c}^{x_1} \otimes \mathbf{1}_4$$

$$\begin{aligned} \mathbf{w} &= \mathbf{w}^{x_n} \odot (\mathbf{w}^{x_{n-1}} \otimes \mathbf{1}_{k_n}) \odot (\mathbf{w}^{x_{n-2}} \otimes \mathbf{1}_{k_n k_{n-1}}) \odot \cdots \odot (\mathbf{w}^{x_1} \otimes \mathbf{1}_{k_n \cdots k_2}) \\ &= \mathbf{W}_{x_n} \odot \mathbf{W}_{x_{n-1}} \odot \cdots \odot \mathbf{W}_{x_1} \end{aligned}$$

Barycentric denominator univariate vector-wise functions (KST equivalent functions):

$$\mathbf{D} = \begin{pmatrix} \mathbf{c}^{x_1} \cdot \mathbf{Lag}(x_1) & \mathbf{c}^{x_2} \cdot \mathbf{Lag}(x_2) \\ -\frac{0.41}{x_1+1.0} & -\frac{1.3}{x_2+1.0} \\ -\frac{0.41}{x_1+1.0} & -\frac{3.1}{x_2+0.37} \\ -\frac{0.41}{x_1+1.0} & -\frac{2.8}{x_2-0.26} \\ -\frac{0.41}{x_1+1.0} & -\frac{1}{x_2-1.0} \\ -\frac{1}{x_1+0.37} & -\frac{1.3}{x_2+1.0} \\ -\frac{1}{x_1+0.37} & -\frac{2.9}{x_2+0.37} \\ -\frac{1}{x_1+0.37} & -\frac{2.7}{x_2-0.26} \\ -\frac{0.91}{x_1-0.26} & -\frac{1.0}{x_2-1.3} \\ -\frac{0.91}{x_1-0.26} & -\frac{x_2+1.0}{2.9} \\ -\frac{0.91}{x_1-0.26} & -\frac{x_2+0.37}{2.6} \\ -\frac{0.91}{x_1-0.26} & -\frac{x_2-0.26}{1} \\ -\frac{0.33}{x_1-1.0} & -\frac{x_2-1.0}{1.3} \\ -\frac{0.33}{x_1-1.0} & -\frac{x_2+1.0}{3.1} \\ -\frac{0.33}{x_1-1.0} & -\frac{x_2+0.37}{2.8} \\ -\frac{0.33}{x_1-1.0} & -\frac{x_2-0.26}{1} \\ x_1-1.0 & -\frac{x_2-1.0}{x_2-1.0} \end{pmatrix}$$

Equivalent denominator and numerator read:

$$\sum_{i\text{-th row}} \prod_{j\text{-th col}} [\mathbf{D}]_{i,j} \text{ and } \sum_{i\text{-th row}} \mathbf{w} \cdot \prod_{j\text{-th col}} [\mathbf{D}]_{i,j}$$

Connection with Neural Networks (equivalent denominator representation):

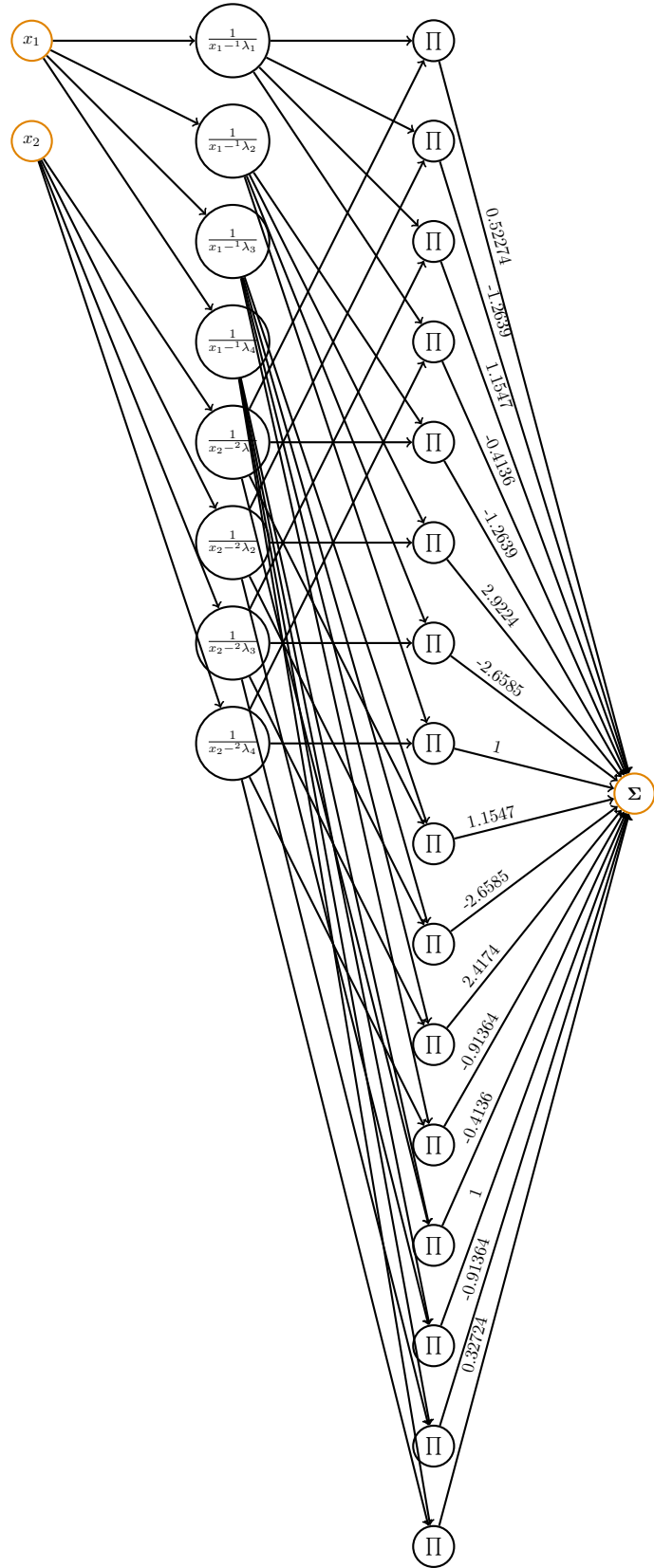


Figure 49: Equivalent NN representation of the denominator \mathbf{D} .

4.17 Function #17 ($n = 2$ variables, tensor size: 12.5 KB)

$$\frac{x_1^4 + x_2^4 + x_1^2x_2^2 + x_1x_2}{x_1^2x_2^2 - 2x_1^2 - 2x_2^2 + 4}$$

4.17.1 Setup and results overview

- Reference: A/al. 2021 (A.5.12), [4]
- Domain: \mathbb{R}
- Tensor size: 12.5 **KB** (40^2 points)
- Bounds: $(-1 \ 1) \times (-1 \ 1)$

#	Alg.	Parameters	Dim.	CPU [s]	RMSE	min err.	max err.
17	A/G/P-V 2025 (A1)	0.01,3	100	0.0149	2.45e-15	0	9.99e-15
	A/G/P-V 2025 (A2)	1e-15,1	120	0.14	8.71e-15	0	1.03e-13
	MDSPACK v1.1.0	0.01,0.0001	100	0.016	2.5e-15	0	1.04e-14
	P/P 2025	1,1,50,0.01,4,12,9	184	0.776	0.000392	2.81e-07	0.0016
	B/G 2025	0.001,20	100	0.0246	1.67e-15	0	1.15e-14
	B/G 2025 (LR)	1e-06,20,5	100	0.0358	2.37e - 16	0	1.11e - 15
	TensorFlow		257	14.9	0.0234	1.45e-05	0.108

Table 18: Function #17: best model configuration and performances per methods.

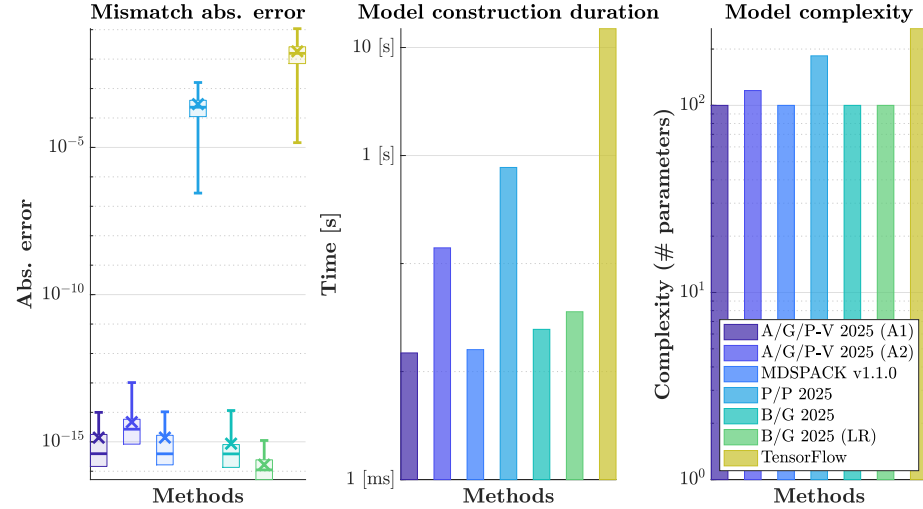


Figure 50: Function #17: graphical view of the best model performances.

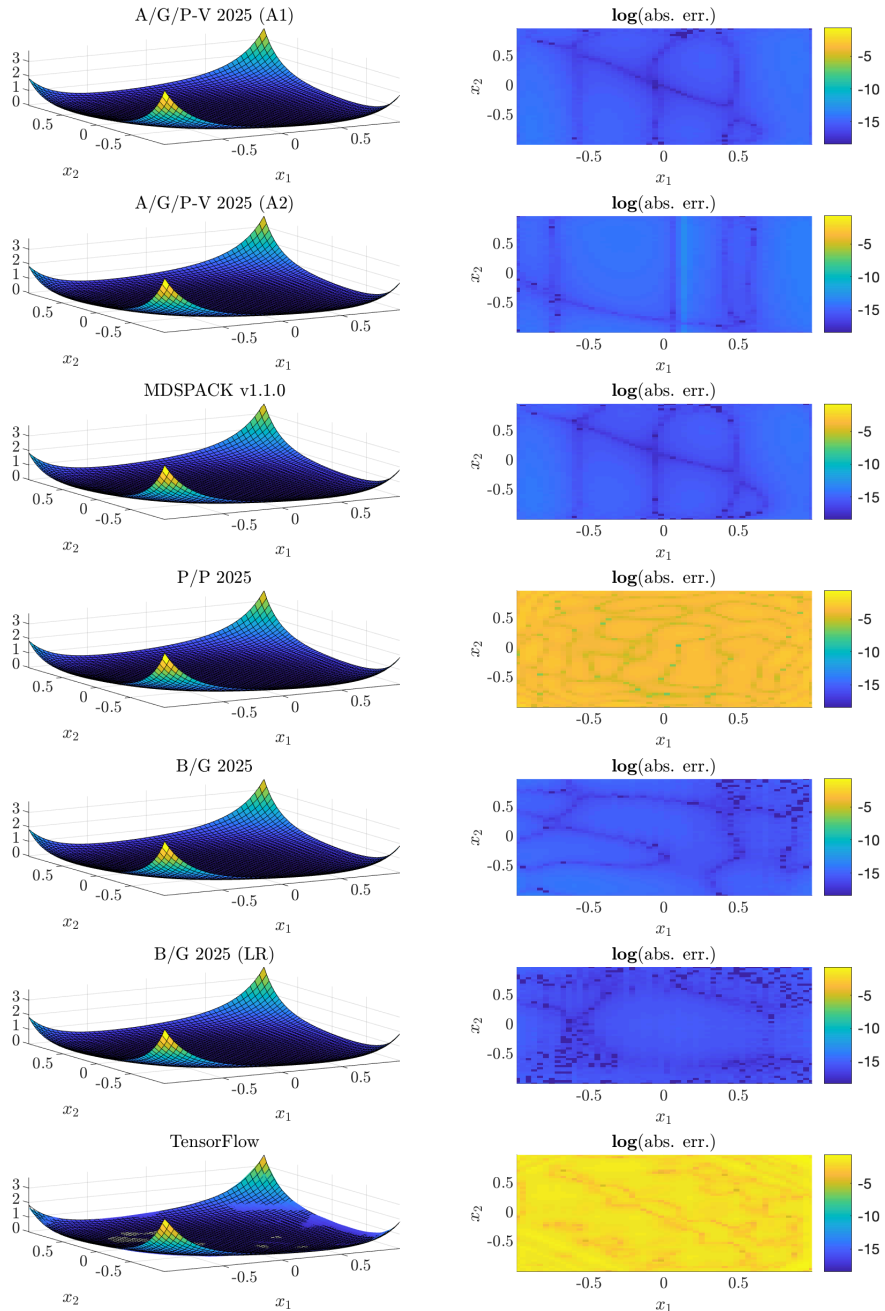


Figure 51: Function #17: left side, evaluation of the original (mesh) vs. approximated (coloured surface) and right side, absolute errors (in log-scale).

4.17.2 mLF detailed informations (M1)

Right interpolation points: $k_l = \begin{pmatrix} 5 & 5 \end{pmatrix}$, where $l = 1, \dots, n$.

$$\begin{aligned} {}^1\lambda_{j_1} &\in \mathbb{C}^5, \text{ linearly spaced between bounds} \\ {}^2\lambda_{j_2} &\in \mathbb{C}^5, \text{ linearly spaced between bounds} \end{aligned}$$

n-D Loewner matrix, barycentric weights and Lagrangian basis:

$$\begin{aligned} \mathbb{L} &\in \mathbb{C}^{25 \times 25} \\ \mathbf{c} &\in \mathbb{C}^{25} \\ \mathbf{w} &\in \mathbb{C}^{25} \\ \mathbf{c} \cdot \mathbf{w} &\in \mathbb{C}^{25} \\ \mathbf{Lag}(x_1, x_2) &\in \mathbb{C}^{25} \end{aligned}$$

4.18 Function #18 ($n = 2$ variables, tensor size: 12.5 KB)

$$\frac{x_1^3 + x_2^3}{x_1^2 x_2^2 - 2x_1^2 - 2x_2^2 + 4}$$

4.18.1 Setup and results overview

- Reference: A/al. 2021 (A.5.13), [4]
- Domain: \mathbb{R}
- Tensor size: 12.5 **KB** (40^2 points)
- Bounds: $(-1 \ 1) \times (-1 \ 1)$

#	Alg.	Parameters	Dim.	CPU [s]	RMSE	min err.	max err.
18	A/G/P-V 2025 (A1)	0.1,3	64	0.0151	4.08e-16	0	2.11e-15
	A/G/P-V 2025 (A2)	1e-15,2	112	0.127	1.48e-15	0	1.88e-14
	MDSPACK v1.1.0	0.1,0.01	64	0.0162	5.82e-16	0	3.11e-15
	P/P 2025	1,0.95,50,0.01,6,12,13	316	1.19	0.000331	3.05e-07	0.00122
	B/G 2025	0.001,20	80	0.0183	1.54e-15	0	8.44e-15
	B/G 2025 (LR)	1e-06,20,4	80	0.0423	2.83e - 16	0	1.55e - 15
	TensorFlow		257	14.8	0.00819	4.62e-05	0.039

Table 19: Function #18: best model configuration and performances per methods.

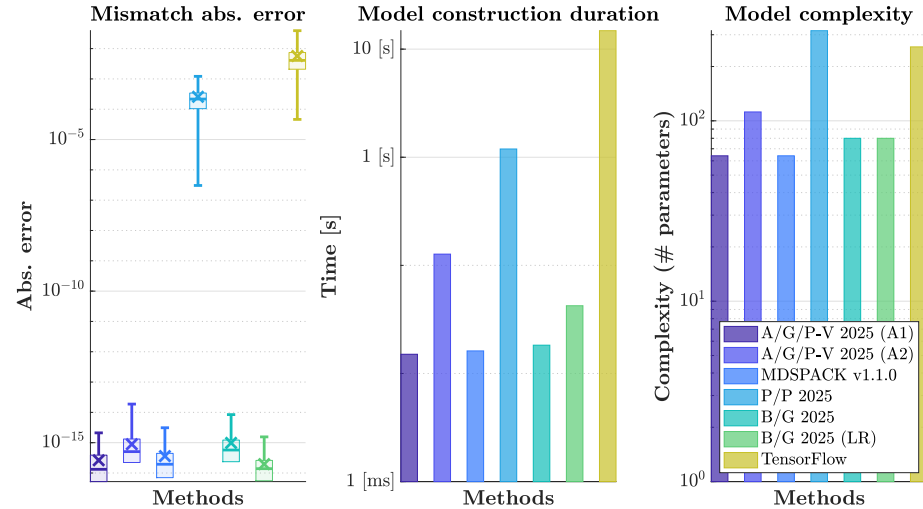


Figure 52: Function #18: graphical view of the best model performances.

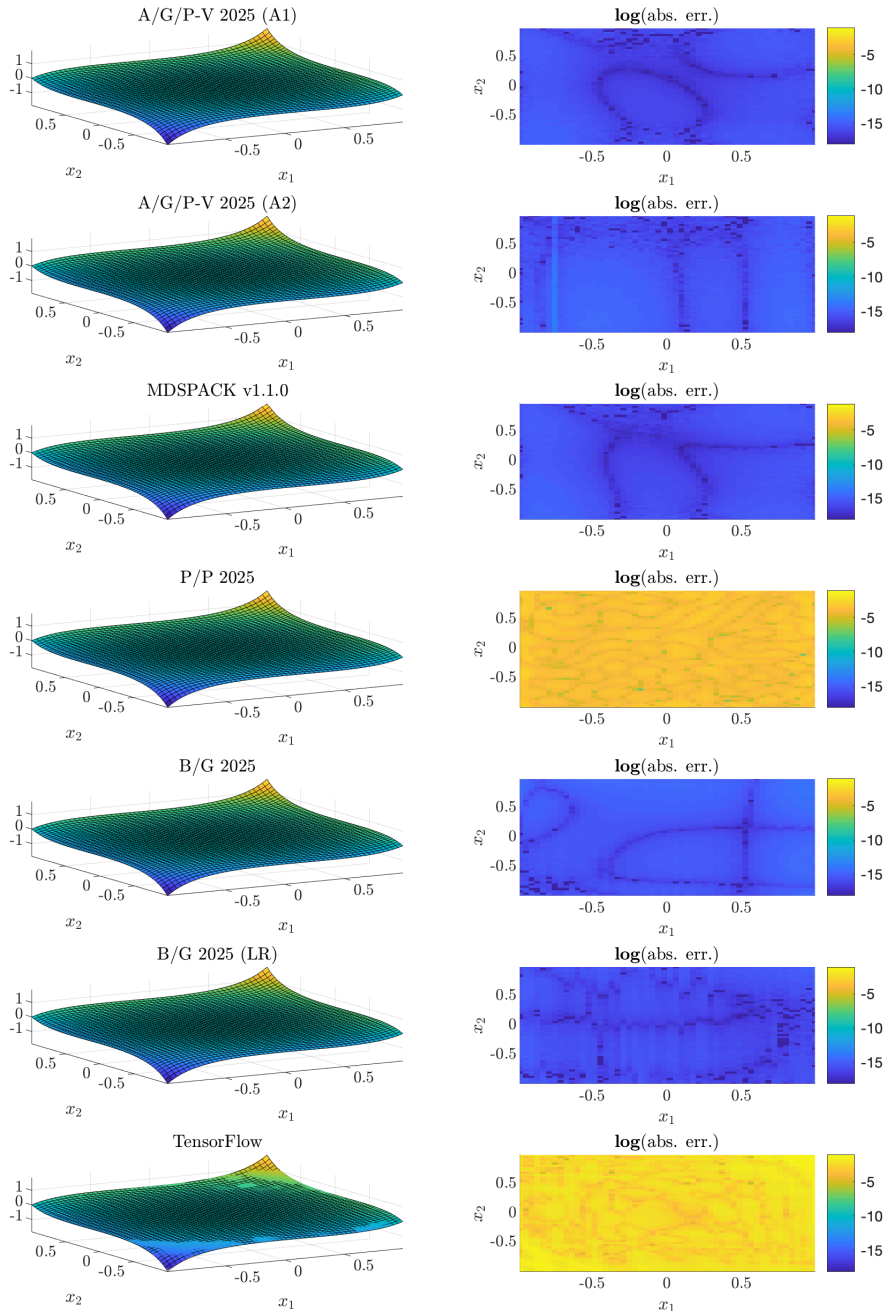


Figure 53: Function #18: left side, evaluation of the original (mesh) vs. approximated (coloured surface) and right side, absolute errors (in log-scale).

4.18.2 mLF detailed informations (M1)

Right interpolation points: $k_l = (4 \quad 4)$, where $l = 1, \dots, n$.

$$\begin{aligned} {}^1\lambda_{j_1} &= \left(\begin{array}{cccc} -1 & -\frac{7}{19} & \frac{5}{19} & 1 \\ -1 & -\frac{7}{19} & \frac{5}{19} & 1 \end{array} \right) \\ {}^2\lambda_{j_2} &= \left(\begin{array}{cccc} -1 & -\frac{7}{19} & \frac{5}{19} & 1 \\ -1 & -\frac{7}{19} & \frac{5}{19} & 1 \end{array} \right) \end{aligned}$$

Lagrangian weights, data and supports (Lagrangian basis):

c	w	c · w	Lag
0.23	-2.0	-0.46	$\frac{1}{(x_1+1.0)(x_2+1.0)}$
-1.3	-0.56	0.71	$\frac{1}{(x_1+1.0)(x_2+0.37)}$
1.2	-0.51	-0.62	$\frac{1}{(x_1+1.0)(x_2-0.26)}$
-0.18	0	0	$\frac{1}{(x_1+1.0)(x_2-1.0)}$
-1.3	-0.56	0.71	$\frac{1}{(x_2+1.0)(x_1+0.37)}$
6.9	-0.029	-0.2	$\frac{1}{(x_1+0.37)(x_2+0.37)}$
-6.6	$-8.8e-3$	0.058	$\frac{1}{(x_2-0.26)(x_1+0.37)}$
1.0	0.51	0.51	$\frac{1}{(x_2-1.0)(x_1+0.37)}$
1.2	-0.51	-0.62	$\frac{1}{(x_2+1.0)(x_1-0.26)}$
-6.6	$-8.8e-3$	0.058	$\frac{1}{(x_1-0.26)(x_2+0.37)}$
6.4	$9.8e-3$	0.062	$\frac{1}{(x_1-0.26)(x_2-0.26)}$
-0.96	0.53	-0.51	$\frac{1}{(x_2-1.0)(x_1-0.26)}$
-0.18	0	0	$\frac{1}{(x_1-1.0)(x_2+1.0)}$
1.0	0.51	0.51	$\frac{1}{(x_1-1.0)(x_2+0.37)}$
-0.96	0.53	-0.51	$\frac{1}{(x_1-1.0)(x_2-0.26)}$
0.15	2.0	0.29	$\frac{1}{(x_1-1.0)(x_2-1.0)}$

KST equivalent decoupling pattern

Barycentric weights:

$$\begin{aligned} \mathbf{c}^{x_2} &= \text{vec} \begin{pmatrix} -1.3 & -1.3 & -1.3 & -1.3 \\ 6.9 & 6.9 & 6.9 & 6.9 \\ -6.6 & -6.6 & -6.6 & -6.6 \\ 1.0 & 1.0 & 1.0 & 1.0 \end{pmatrix} \quad \text{and } \mathbf{Bary}_{x_2} = \mathbf{c}^{x_2} \otimes \mathbf{1}_1 \\ \mathbf{c}^{x_1} &= \begin{pmatrix} -0.18 \\ 1.0 \\ -0.96 \\ 0.15 \end{pmatrix} \quad \text{and } \mathbf{Bary}_{x_1} = \mathbf{c}^{x_1} \otimes \mathbf{1}_4 \\ \mathbf{c} &= \mathbf{c}^{x_n} \odot (\mathbf{c}^{x_{n-1}} \otimes \mathbf{1}_{k_n}) \odot (\mathbf{c}^{x_{n-2}} \otimes \mathbf{1}_{k_n k_{n-1}}) \odot \cdots \odot (\mathbf{c}^{x_1} \otimes \mathbf{1}_{k_n \cdots k_2}) \\ &= \mathbf{Bary}_{x_n} \odot \mathbf{Bary}_{x_{n-1}} \odot \cdots \odot \mathbf{Bary}_{x_1} \end{aligned}$$

Data weights:

$$\begin{aligned} \mathbf{w}^{x_2} &= \text{vec} \begin{pmatrix} -2.0 & -0.56 & -0.51 & 0 \\ -0.56 & -0.029 & -8.8e-3 & 0.51 \\ -0.51 & -8.8e-3 & 9.8e-3 & 0.53 \\ 0 & 0.51 & 0.53 & 2.0 \end{pmatrix} \quad \text{and } \mathbf{W}_{x_2} = \mathbf{c}^{x_2} \otimes \mathbf{1}_1 \\ \mathbf{w}^{x_1} &= \begin{pmatrix} 0 \\ 0.51 \\ 0.53 \\ 2.0 \end{pmatrix} \quad \text{and } \mathbf{W}_{x_1} = \mathbf{c}^{x_1} \otimes \mathbf{1}_4 \\ \mathbf{w} &= \mathbf{w}^{x_n} \odot (\mathbf{w}^{x_{n-1}} \otimes \mathbf{1}_{k_n}) \odot (\mathbf{w}^{x_{n-2}} \otimes \mathbf{1}_{k_n k_{n-1}}) \odot \cdots \odot (\mathbf{w}^{x_1} \otimes \mathbf{1}_{k_n \cdots k_2}) \\ &= \mathbf{W}_{x_n} \odot \mathbf{W}_{x_{n-1}} \odot \cdots \odot \mathbf{W}_{x_1} \end{aligned}$$

Barycentric denominator univariate vector-wise functions (KST equivalent functions):

$$\mathbf{D} = \begin{pmatrix} \mathbf{c}^{x_1} \cdot \mathbf{Lag}(x_1) & \mathbf{c}^{x_2} \cdot \mathbf{Lag}(x_2) \\ -\frac{0.18}{x_1+1.0} & -\frac{1.3}{x_2+1.0} \\ -\frac{0.18}{x_1+1.0} & -\frac{6.9}{x_2+0.37} \\ -\frac{0.18}{x_1+1.0} & -\frac{6.6}{x_2-0.26} \\ -\frac{1}{x_1+1.0} & -\frac{1}{x_2-1.0} \\ \frac{1}{x_1+0.37} & -\frac{1.3}{x_2+1.0} \\ \frac{1}{x_1+0.37} & -\frac{6.9}{x_2+0.37} \\ \frac{1}{x_1+0.37} & -\frac{6.6}{x_2-0.26} \\ \frac{1}{x_1+0.37} & -\frac{1}{x_2-1.0} \\ -\frac{0.96}{x_1-0.26} & -\frac{1.3}{x_2+1.0} \\ -\frac{0.96}{x_1-0.26} & -\frac{6.9}{x_2+0.37} \\ -\frac{0.96}{x_1-0.26} & -\frac{6.6}{x_2-0.26} \\ -\frac{0.96}{x_1-0.26} & -\frac{1}{x_2-1.0} \\ \frac{0.15}{x_1-1.0} & -\frac{1.3}{x_2+1.0} \\ \frac{0.15}{x_1-1.0} & -\frac{6.9}{x_2+0.37} \\ \frac{0.15}{x_1-1.0} & -\frac{6.6}{x_2-0.26} \\ \frac{0.15}{x_1-1.0} & -\frac{1}{x_2-1.0} \end{pmatrix}$$

Equivalent denominator and numerator read:

$$\sum_{i\text{-th row}} \prod_{j\text{-th col}} [\mathbf{D}]_{i,j} \text{ and } \sum_{i\text{-th row}} \mathbf{w} \cdot \prod_{j\text{-th col}} [\mathbf{D}]_{i,j}$$

Connection with Neural Networks (equivalent denominator representation):

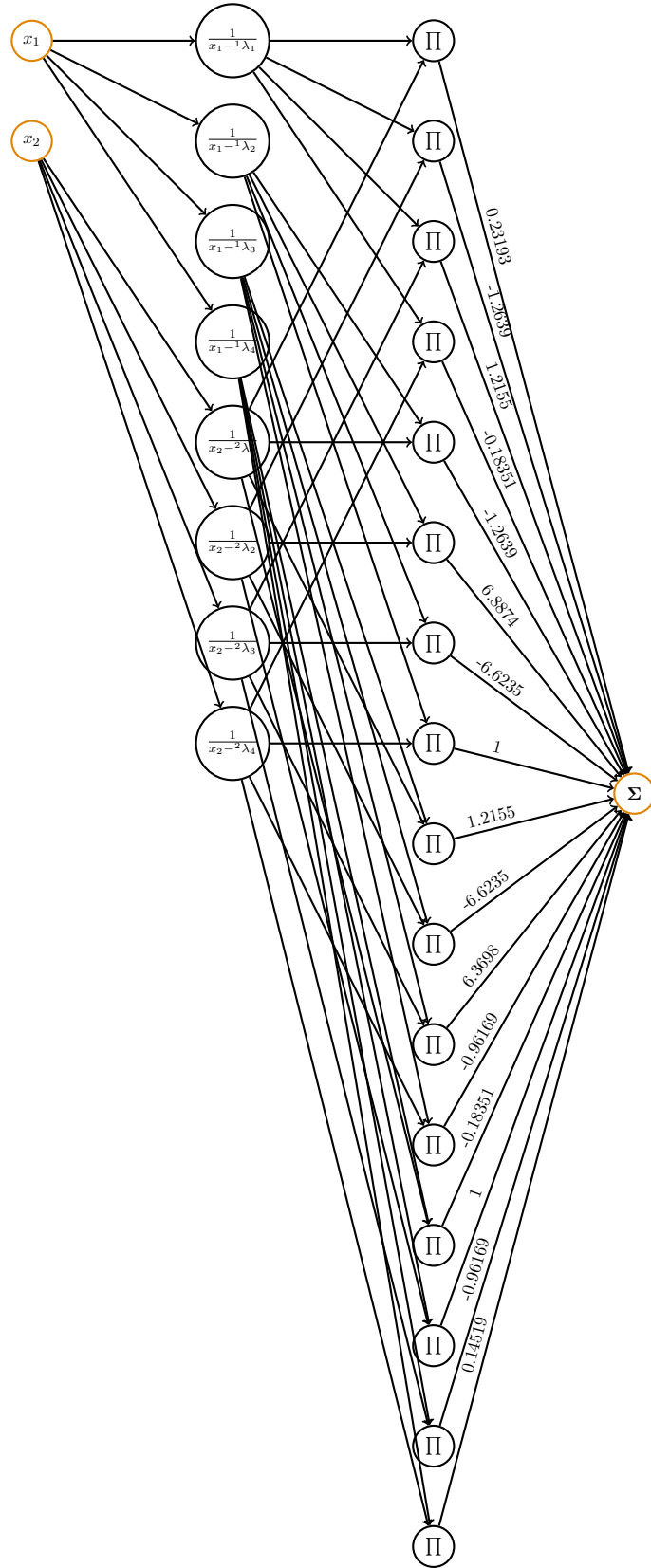


Figure 54: Equivalent NN representation of the denominator \mathbf{D} .

4.19 Function #19 ($n = 2$ variables, tensor size: 12.5 KB)

$$\frac{x_1^4 + x_2^4 + x_1^2x_2^2 + x_1x_2}{x_1^3 + x_2^3 + 4}$$

4.19.1 Setup and results overview

- Reference: A/al. 2021 (A.5.14), [4]
- Domain: \mathbb{R}
- Tensor size: 12.5 **KB** (40^2 points)
- Bounds: $(-1 \ 1) \times (-1 \ 1)$

#	Alg.	Parameters	Dim.	CPU [s]	RMSE	min err.	max err.
19	A/G/P-V 2025 (A1)	0.01,2	100	0.0149	2.69e-15	0	1.89e-14
	A/G/P-V 2025 (A2)	1e-15,3	440	0.125	7.98e-15	0	2.67e-14
	MDSPACK v1.1.0	0.01,0.01	100	0.0162	2.73e-15	0	1.55e-14
	P/P 2025	1,0.95,50,0.01,4,12,9	184	0.995	0.00012	1.91e-08	0.000468
	B/G 2025	0.001,20	192	0.0528	1.61e-14	0	3.29e-13
	B/G 2025 (LR)	1e-09,20,3	100	0.0782	1.35e - 15	0	8.49e - 15
	TensorFlow		257	14.9	0.00622	3.25e-06	0.0201

Table 20: Function #19: best model configuration and performances per methods.

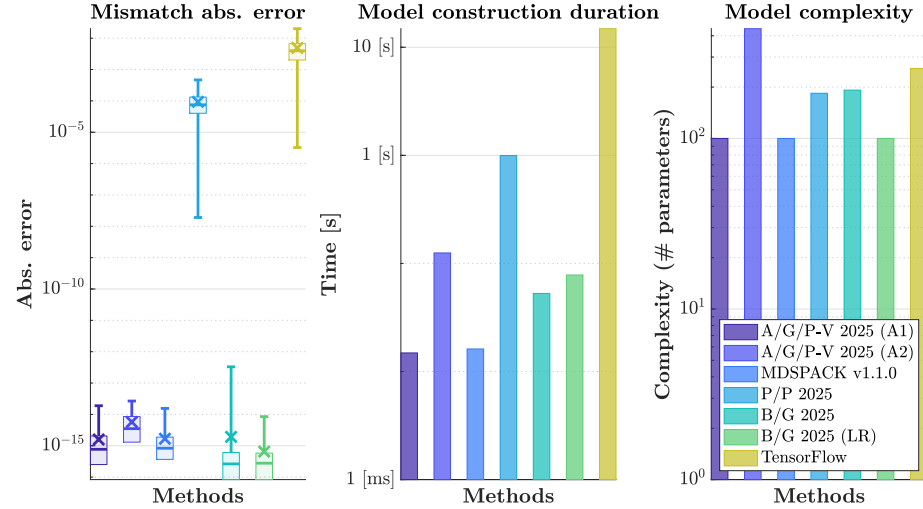


Figure 55: Function #19: graphical view of the best model performances.

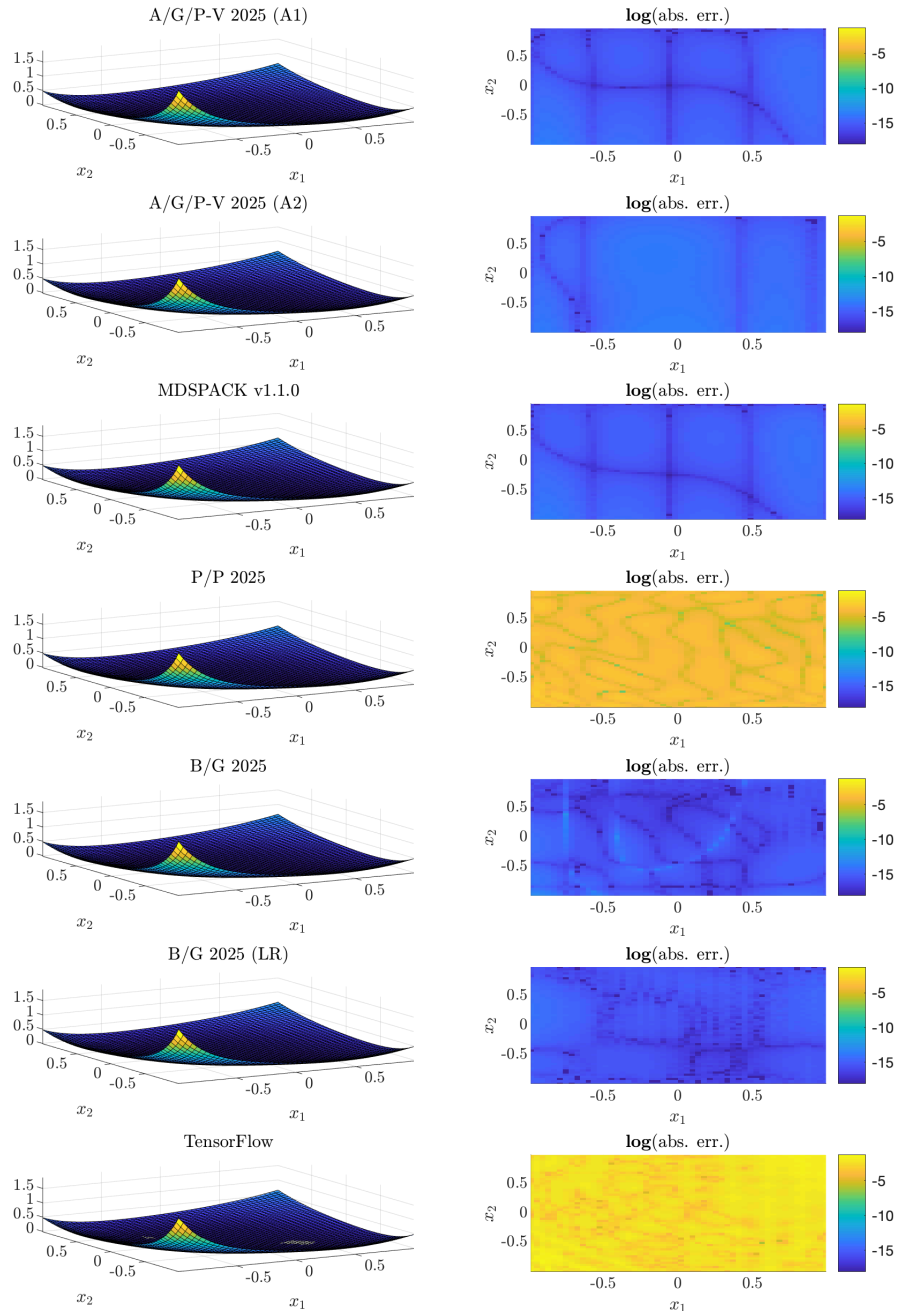


Figure 56: Function #19: left side, evaluation of the original (mesh) vs. approximated (coloured surface) and right side, absolute errors (in log-scale).

4.19.2 mLF detailed informations (M1)

Right interpolation points: $k_l = \begin{pmatrix} 5 & 5 \end{pmatrix}$, where $l = 1, \dots, n$.

$$\begin{aligned} {}^1\lambda_{j_1} &\in \mathbb{C}^5, \text{ linearly spaced between bounds} \\ {}^2\lambda_{j_2} &\in \mathbb{C}^5, \text{ linearly spaced between bounds} \end{aligned}$$

n-D Loewner matrix, barycentric weights and Lagrangian basis:

$$\begin{aligned} \mathbb{L} &\in \mathbb{C}^{25 \times 25} \\ \mathbf{c} &\in \mathbb{C}^{25} \\ \mathbf{w} &\in \mathbb{C}^{25} \\ \mathbf{c} \cdot \mathbf{w} &\in \mathbb{C}^{25} \\ \mathbf{Lag}(x_1, x_2) &\in \mathbb{C}^{25} \end{aligned}$$

4.20 Function #20 ($n = 3$ variables, tensor size: 500 KB)

Breit Wigner function

4.20.1 Setup and results overview

- Reference: A/al. 2021 (A.5.15), [4]
- Domain: \mathbb{R}
- Tensor size: 500 KB (40^3 points)
- Bounds: $(80 \quad 100) \times (5 \quad 10) \times (90 \quad 93)$

#	Alg.	Parameters	Dim.	CPU [s]	RMSE	min err.	max err.
20	A/G/P-V 2025 (A1)	1e-06,2	240	0.0325	1.25e-06	1.98e-10	1.24e-05
	A/G/P-V 2025 (A2)	1e-15,3	180	2.15	2.66e-05	1.16e-09	0.000259
	MDSPACK v1.1.0	1e-06,0.01	240	0.0314	1.25e-06	1.8e-10	1.24e-05
	P/P 2025	1,1,50,0.01,10,12,21	886	34.7	3.14e-05	1.8e-07	0.00015
	B/G 2025	1e-06,20	1.05e+03	5.09	1.66e - 14	0	2.2e - 13
	B/G 2025 (LR)	0.001,20,5	875	44.5	1.24e-06	1.23e-11	2.38e-05
	TensorFlow		321	327	0.00348	4.72e-06	0.0101

Table 21: Function #20: best model configuration and performances per methods.

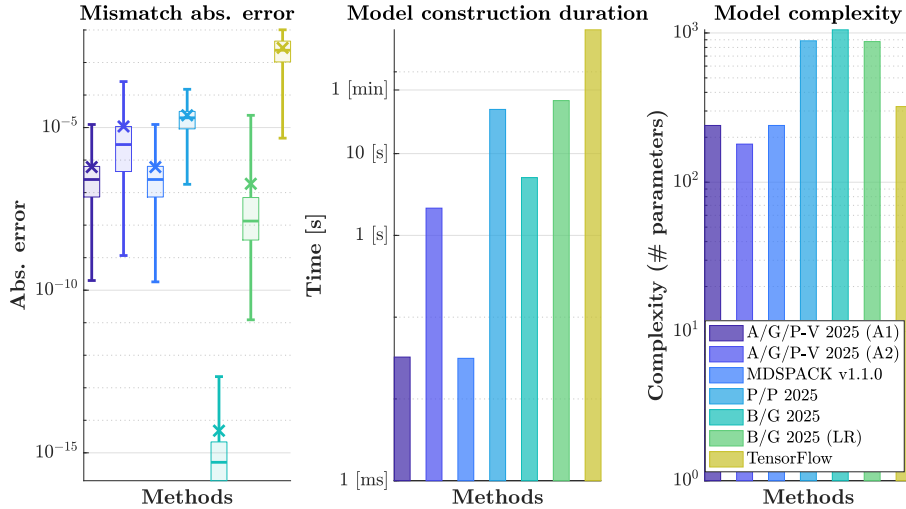


Figure 57: Function #20: graphical view of the best model performances.

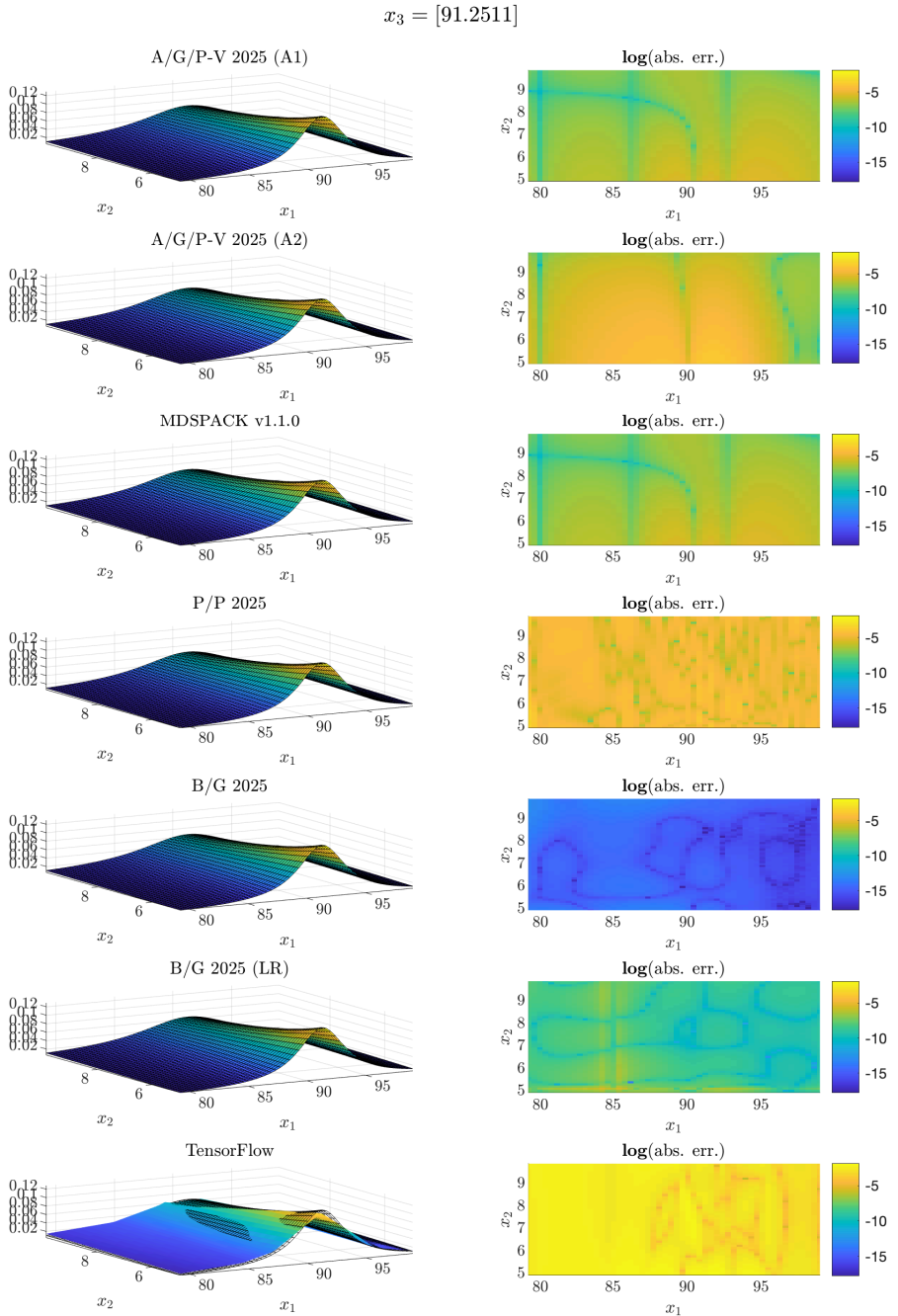


Figure 58: Function #20: left side, evaluation of the original (mesh) vs. approximated (coloured surface) and right side, absolute errors (in log-scale).

4.20.2 mLF detailed informations (M1)

Right interpolation points: $k_l = (4 \quad 4 \quad 3)$, where $l = 1, \dots, n$.

$$\begin{aligned} {}^1\lambda_{j_1} &\in \mathbb{C}^4, \text{ linearly spaced between bounds} \\ {}^2\lambda_{j_2} &\in \mathbb{C}^4, \text{ linearly spaced between bounds} \\ {}^3\lambda_{j_3} &\in \mathbb{C}^3, \text{ linearly spaced between bounds} \end{aligned}$$

n -D Loewner matrix, barycentric weights and Lagrangian basis:

$$\begin{aligned} \mathbb{L} &\in \mathbb{C}^{48 \times 48} \\ \mathbf{c} &\in \mathbb{C}^{48} \\ \mathbf{w} &\in \mathbb{C}^{48} \\ \mathbf{c} \cdot \mathbf{w} &\in \mathbb{C}^{48} \\ \mathbf{Lag}(x_1, x_2, x_3) &\in \mathbb{C}^{48} \end{aligned}$$

4.21 Function #21 ($n = 4$ variables, tensor size: 1.22 MB)

$$\frac{\sum_{i=1}^4 \tan(x_i)}{x_1^2 x_2^2 - x_1^2 - x_2^2 + 1}$$

4.21.1 Setup and results overview

- Reference: A/al. 2021 (A.5.16), [4]
- Domain: \mathbb{R}
- Tensor size: 1.22 MB (20^4 points)
- Bounds: $(-\frac{19}{20}, \frac{19}{20}) \times (-\frac{19}{20}, \frac{19}{20}) \times (-\frac{19}{20}, \frac{19}{20}) \times (-\frac{19}{20}, \frac{19}{20})$

#	Alg.	Parameters	Dim.	CPU [s]	RMSE	min err.	max err.
21	A/G/P-V 2025 (A1)	1e-09,3	2.46e+04	0.105	6.36e-05	4.3e - 11	0.000739
	A/G/P-V 2025 (A2)	1e-15,3	3.18e+04	1.89	5.59e-06	1.4e-09	0.000102
	MDSPACK v1.1.0	1e-09,1e-09	2.46e+04	0.0454	6.1e-05	1.05e-10	0.000743
	P/P 2025	1,0.95,50,0.01,6,12,13	472	46.5	2.66	0.000284	17.5
	B/G 2025	1e-06,20	5.05e+04	2.82e+03	1.78e-05	1.79e-10	0.000349
	B/G 2025 (LR)	1e-06,20,5	9.73e+04	332	5.83e - 07	4.76e-11	7.85e - 06
	TensorFlow		385	150	1.91	0.000778	20.9

Table 22: Function #21: best model configuration and performances per methods.

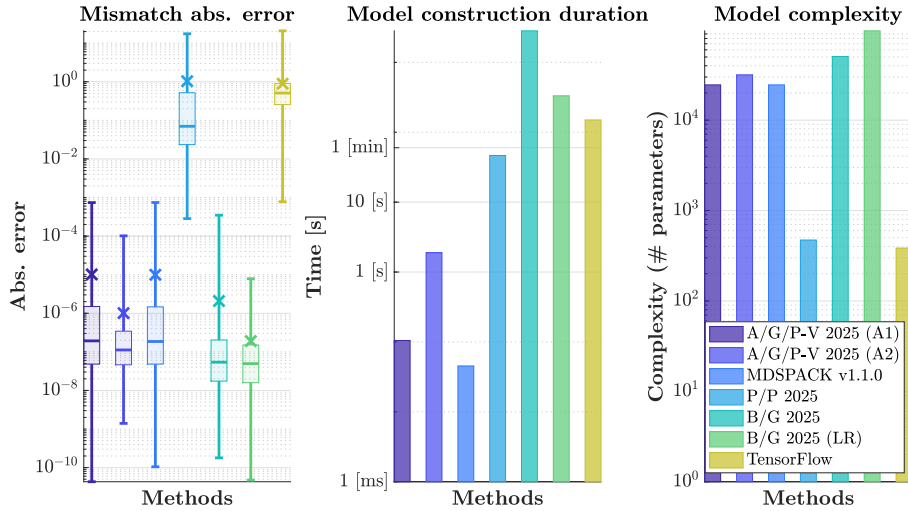


Figure 59: Function #21: graphical view of the best model performances.

$$x_{3\ldots 4} = [-0.15766; -0.94978]$$

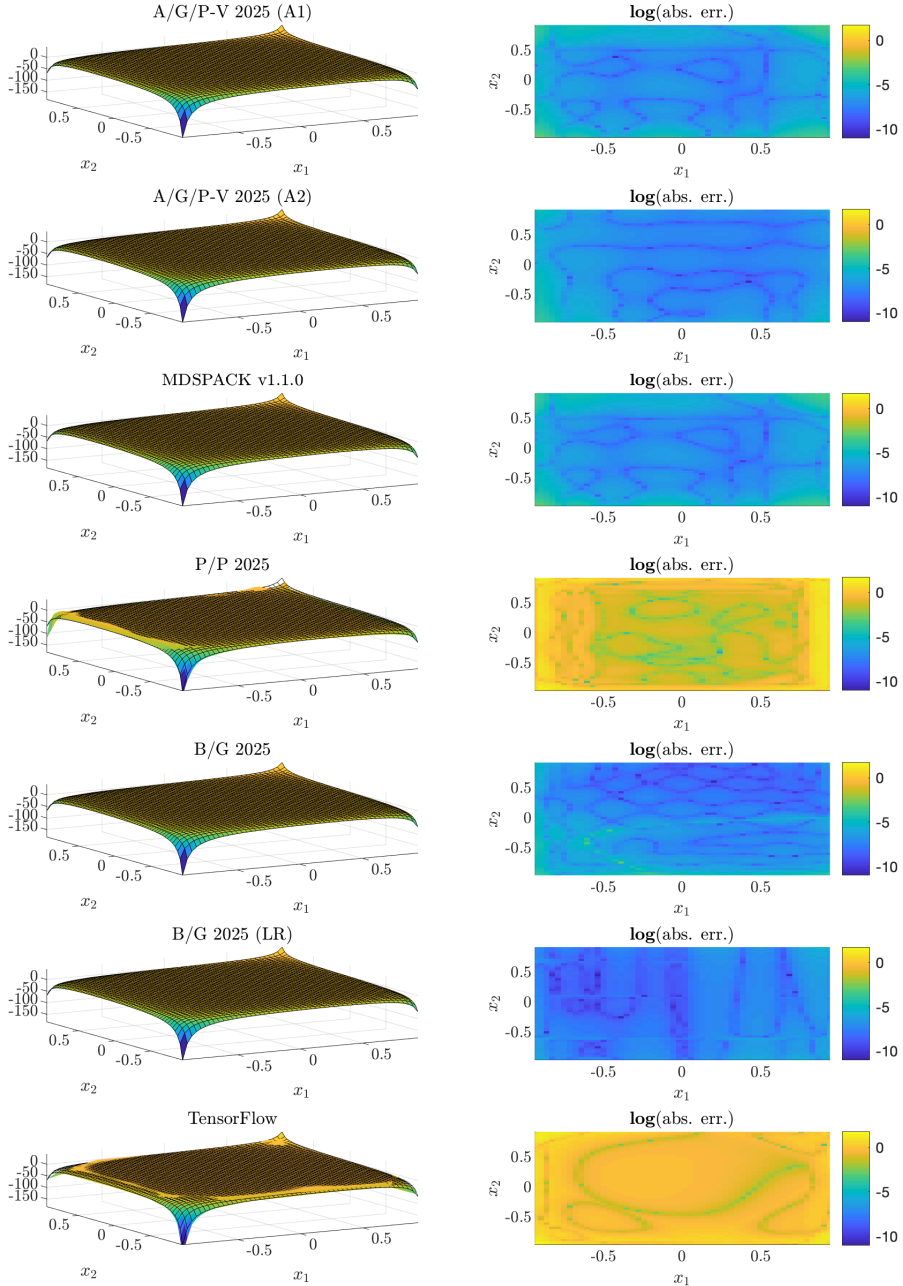


Figure 60: Function #21: left side, evaluation of the original (mesh) vs. approximated (coloured surface) and right side, absolute errors (in log-scale).

4.21.2 mLF detailed informations (M1)

Right interpolation points: $k_l = (8 \ 8 \ 8 \ 8)$, where $l = 1, \dots, n$.

$$\begin{aligned} {}^1\lambda_{j_1} &\in \mathbb{C}^8, \text{ linearly spaced between bounds} \\ {}^2\lambda_{j_2} &\in \mathbb{C}^8, \text{ linearly spaced between bounds} \\ {}^3\lambda_{j_3} &\in \mathbb{C}^8, \text{ linearly spaced between bounds} \\ {}^4\lambda_{j_4} &\in \mathbb{C}^8, \text{ linearly spaced between bounds} \end{aligned}$$

n-D Loewner matrix, barycentric weights and Lagrangian basis:

$$\begin{aligned} \mathbb{L} &\in \mathbb{C}^{4096 \times 4096} \\ \mathbf{c} &\in \mathbb{C}^{4096} \\ \mathbf{w} &\in \mathbb{C}^{4096} \\ \mathbf{c} \cdot \mathbf{w} &\in \mathbb{C}^{4096} \\ \mathbf{Lag}(x_1, x_2, x_3, x_4) &\in \mathbb{C}^{4096} \end{aligned}$$

4.22 Function #22 ($n = 4$ variables, tensor size: 1.22 MB)

$$\frac{\exp(x_1x_2x_3x_4)}{x_1^2 + x_2^2 - x_3x_4 + 3}$$

4.22.1 Setup and results overview

- Reference: A/al. 2021 (A.5.17), [4]
- Domain: \mathbb{R}
- Tensor size: 1.22 MB (20^4 points)
- Bounds: $(-1 \ 1) \times (-1 \ 1) \times (-1 \ 1) \times (-1 \ 1)$

#	Alg.	Parameters	Dim.	CPU [s]	RMSE	min err.	max err.
22	A/G/P-V 2025 (A1)	0.0001,3	1.54e+03	0.0458	0.00125	2.02e-07	0.00633
	A/G/P-V 2025 (A2)	1e-15,2	1.89e+03	0.668	0.00127	4.09e-07	0.00489
	MDSPACK v1.1.0	0.0001,0.0001	1.54e+03	0.0409	0.00125	1.31e-07	0.00633
	P/P 2025	1,1,50,0.01,10,12,21	1.1e+03	150	0.000731	1.3e-06	0.00452
	B/G 2025	1e-09,20	6.34e+04	4.32e+03	6.48e - 13	0	1.45e - 11
	B/G 2025 (LR)	1e-06,20,5	6.34e+04	513	3.08e-06	2.63e-13	5.09e-05
	TensorFlow		385	147	0.0075	2.3e-05	0.0227

Table 23: Function #22: best model configuration and performances per methods.

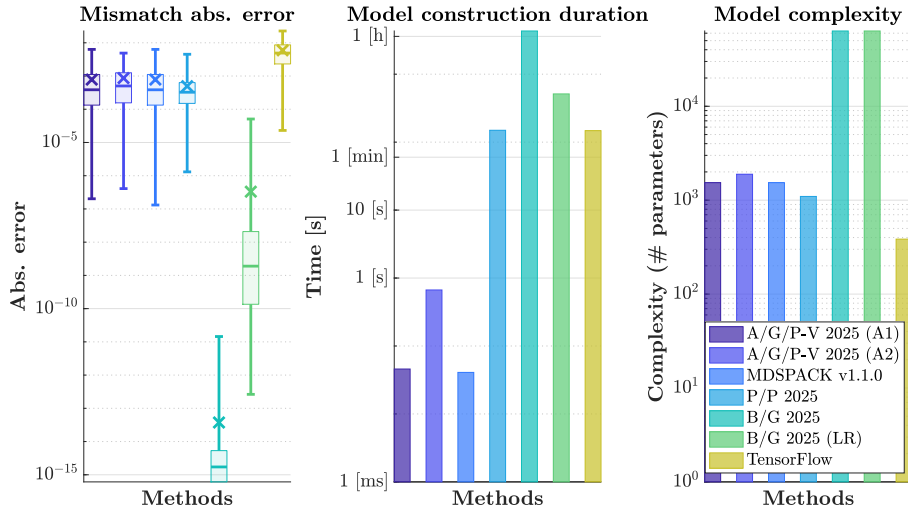


Figure 61: Function #22: graphical view of the best model performances.

$$x_{3\ldots 4} = [-0.16596; -0.99977]$$

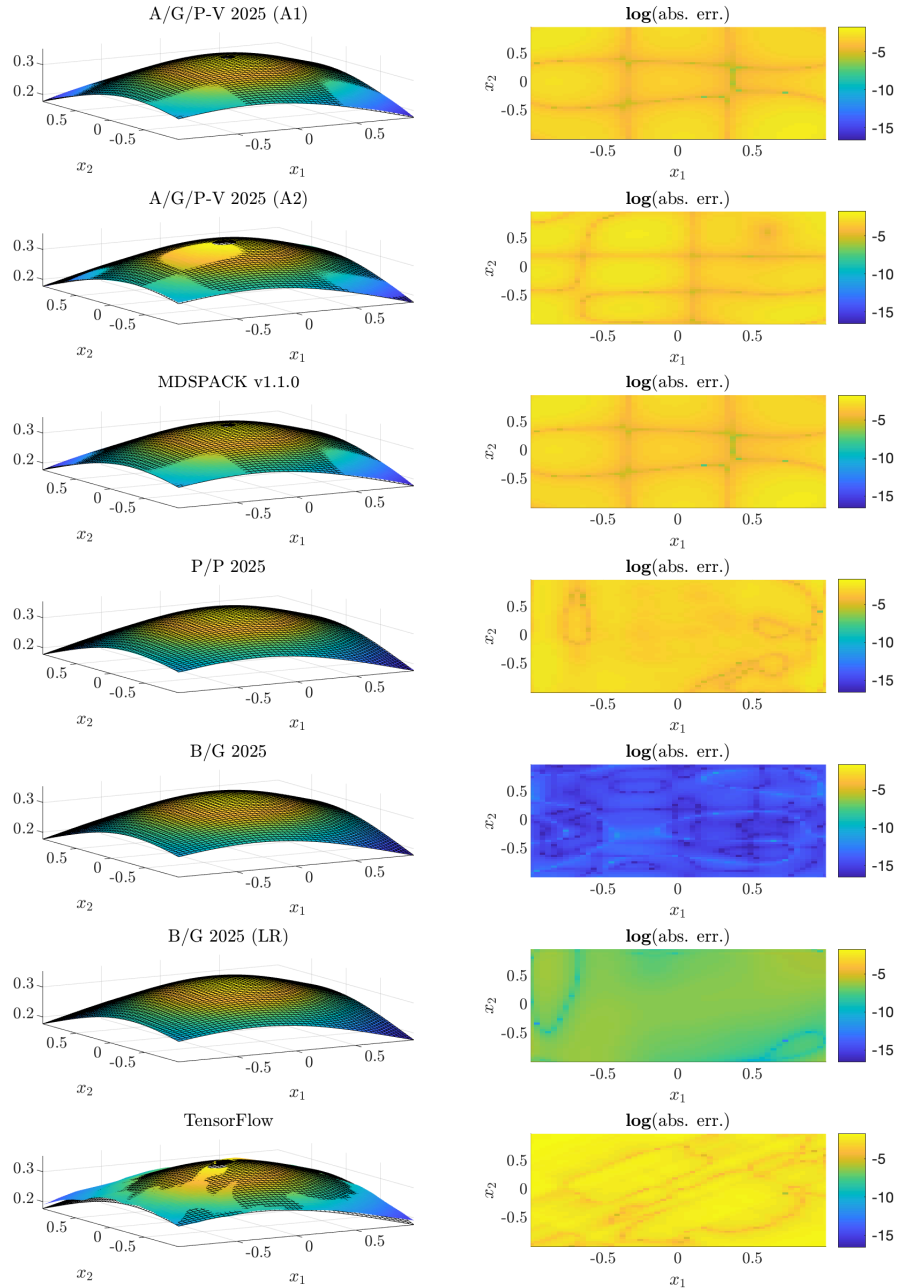


Figure 62: Function #22: left side, evaluation of the original (mesh) vs. approximated (coloured surface) and right side, absolute errors (in log-scale).

4.22.2 mLF detailed informations (M1)

Right interpolation points: $k_l = (4 \ 4 \ 4 \ 4)$, where $l = 1, \dots, n$.

$$\begin{aligned} {}^1\lambda_{j_1} &\in \mathbb{C}^4, \text{ linearly spaced between bounds} \\ {}^2\lambda_{j_2} &\in \mathbb{C}^4, \text{ linearly spaced between bounds} \\ {}^3\lambda_{j_3} &\in \mathbb{C}^4, \text{ linearly spaced between bounds} \\ {}^4\lambda_{j_4} &\in \mathbb{C}^4, \text{ linearly spaced between bounds} \end{aligned}$$

n-D Loewner matrix, barycentric weights and Lagrangian basis:

$$\begin{aligned} \mathbb{L} &\in \mathbb{C}^{256 \times 256} \\ \mathbf{c} &\in \mathbb{C}^{256} \\ \mathbf{w} &\in \mathbb{C}^{256} \\ \mathbf{c} \cdot \mathbf{w} &\in \mathbb{C}^{256} \\ \mathbf{Lag}(x_1, x_2, x_3, x_4) &\in \mathbb{C}^{256} \end{aligned}$$

4.23 Function #23 ($n = 4$ variables, tensor size: 1.79 MB)

$$10 \prod_{i=1}^4 \text{sinc}(x_i)$$

4.23.1 Setup and results overview

- Reference: A/al. 2021 (A.5.18), [4]
- Domain: \mathbb{R}
- Tensor size: 1.79 MB (22^4 points)
- Bounds: $(\frac{1}{1000000}, 4\pi) \times (\frac{1}{1000000}, 4\pi) \times (\frac{1}{1000000}, 4\pi) \times (\frac{1}{1000000}, 4\pi)$

#	Alg.	Parameters	Dim.	CPU [s]	RMSE	min err.	max err.
23	A/G/P-V 2025 (A1)	1e-09,2	8.78e+04	0.241	2.16e-08	8.42e-14	2.8e-07
	A/G/P-V 2025 (A2)	1e-15,1	4.81e+04	2.67	2.01e - 08	2.31e - 14	2.29e - 07
	MDSPACK v1.1.0	0.5,0.01	6	0.109	0.0649	8.43e-08	0.718
	P/P 2025	1,1,50,0.01,10,6,21	970	128	0.0109	1.53e-06	0.0985
	B/G 2025	0.001,20	NaN	NaN	NaN	NaN	NaN
	B/G 2025 (LR)	0.001,20,3	4.86e+04	31	9.8e-08	4.52e-13	1.56e-06
	TensorFlow		385	227	0.0552	1.58e-05	0.576

Table 24: Function #23: best model configuration and performances per methods.

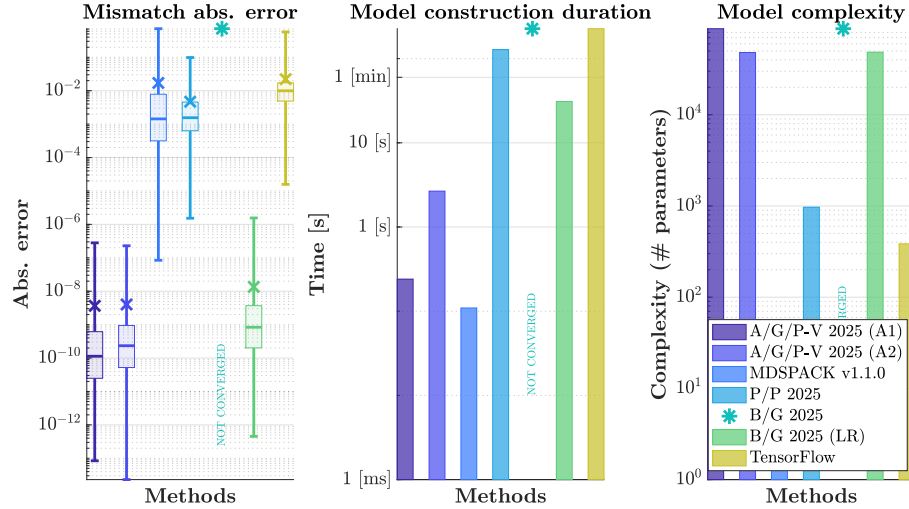


Figure 63: Function #23: graphical view of the best model performances.

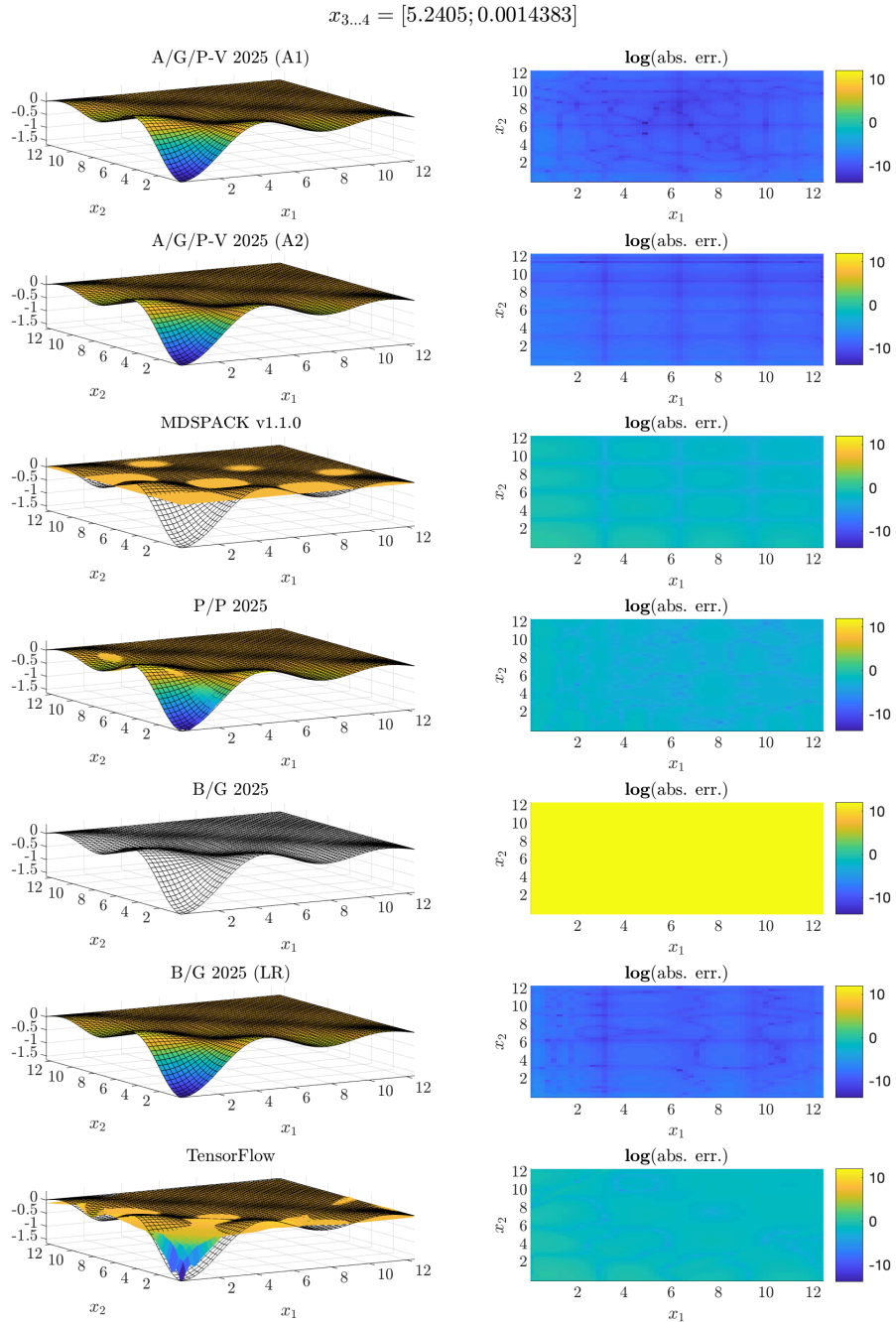


Figure 64: Function #23: left side, evaluation of the original (mesh) vs. approximated (coloured surface) and right side, absolute errors (in log-scale).

4.23.2 mLF detailed informations (M1)

Right interpolation points: $k_l = (11 \ 11 \ 11 \ 11)$, where $l = 1, \dots, n$.

$$\begin{aligned} {}^1\lambda_{j_1} &\in \mathbb{C}^{11}, \text{ linearly spaced between bounds} \\ {}^2\lambda_{j_2} &\in \mathbb{C}^{11}, \text{ linearly spaced between bounds} \\ {}^3\lambda_{j_3} &\in \mathbb{C}^{11}, \text{ linearly spaced between bounds} \\ {}^4\lambda_{j_4} &\in \mathbb{C}^{11}, \text{ linearly spaced between bounds} \end{aligned}$$

n-D Loewner matrix, barycentric weights and Lagrangian basis:

$$\begin{aligned} \mathbb{L} &\in \mathbb{C}^{14641 \times 14641} \\ \mathbf{c} &\in \mathbb{C}^{14641} \\ \mathbf{w} &\in \mathbb{C}^{14641} \\ \mathbf{c} \cdot \mathbf{w} &\in \mathbb{C}^{14641} \\ \mathbf{Lag}(x_1, x_2, x_3, x_4) &\in \mathbb{C}^{14641} \end{aligned}$$

4.24 Function #24 ($n = 2$ variables, tensor size: 13.8 KB)

$$10\text{sinc}(x_1)\text{sinc}(x_2)$$

4.24.1 Setup and results overview

- Reference: A/al. 2021 (A.5.19), [4]
- Domain: \mathbb{R}
- Tensor size: 13.8 **KB** (42^2 points)
- Bounds: $(-\frac{1}{1000000} \quad 4\pi) \times (-\frac{1}{1000000} \quad 4\pi)$

#	Alg.	Parameters	Dim.	CPU [s]	RMSE	min err.	max err.
24	A/G/P-V 2025 (A1)	1e-09,1	484	0.017	3.65e-08	1.05e - 15	3.82e-07
	A/G/P-V 2025 (A2)	1e-15,2	968	0.095	2.11e-09	1.92e-13	2.69e-08
	MDSPACK v1.1.0	1e-06,0.0001	292	0.0175	0.0303	1.64e-10	0.248
	P/P 2025	1,0.95,50,0.01,10,4,21	508	1.87	0.00316	5.36e-06	0.0114
	B/G 2025	1e-09,20,20	484	0.297	2.18e-10	4.02e-14	1.53e-09
	B/G 2025 (LR)	1e-09,20,4	528	0.344	3.19e - 11	5.67e-15	2.5e - 10
	TensorFlow		257	17.7	0.247	3.22e-05	1

Table 25: Function #24: best model configuration and performances per methods.

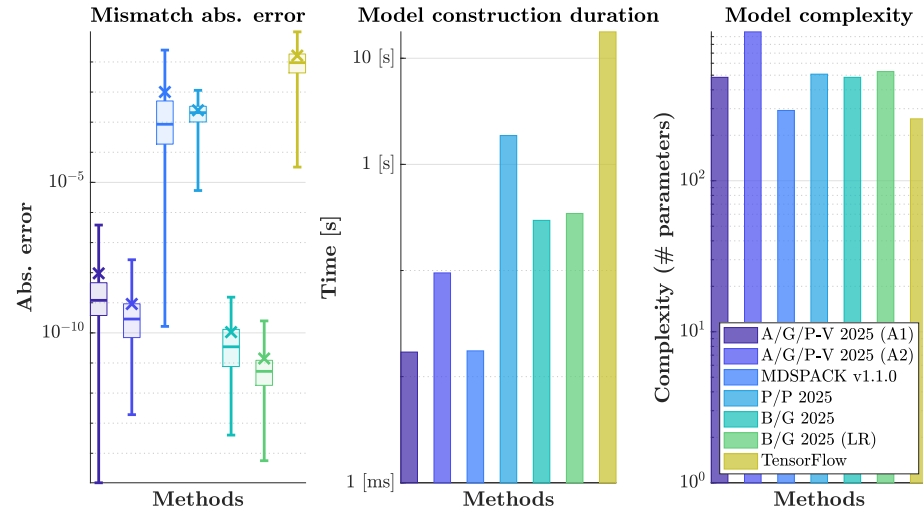


Figure 65: Function #24: graphical view of the best model performances.

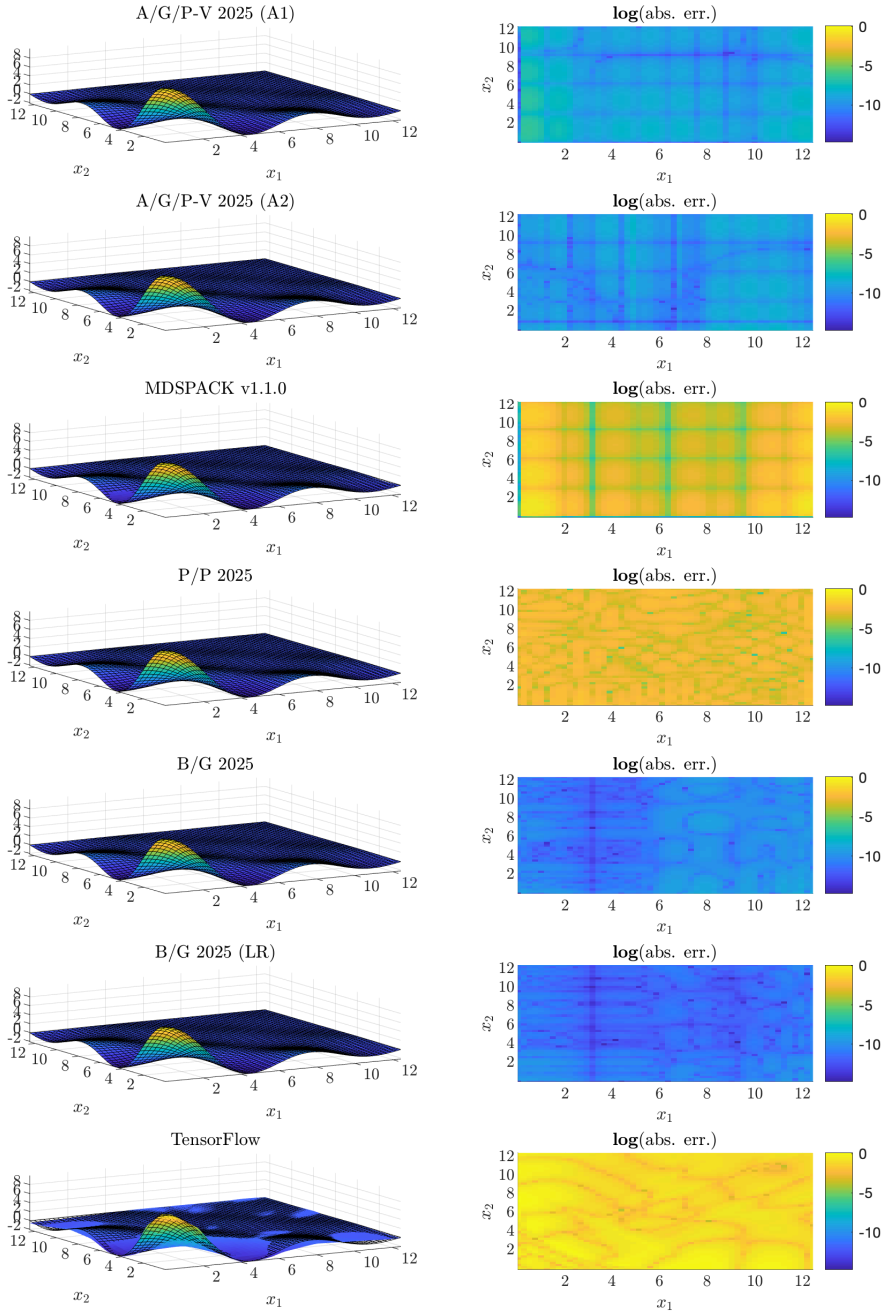


Figure 66: Function #24: left side, evaluation of the original (mesh) vs. approximated (coloured surface) and right side, absolute errors (in log-scale).

4.24.2 mLF detailed informations (M1)

Right interpolation points: $k_l = \begin{pmatrix} 11 & 11 \end{pmatrix}$, where $l = 1, \dots, n$.

$$\begin{aligned} {}^1\lambda_{j_1} &\in \mathbb{C}^{11}, \text{ linearly spaced between bounds} \\ {}^2\lambda_{j_2} &\in \mathbb{C}^{11}, \text{ linearly spaced between bounds} \end{aligned}$$

n-D Loewner matrix, barycentric weights and Lagrangian basis:

$$\begin{aligned} \mathbb{L} &\in \mathbb{C}^{121 \times 121} \\ \mathbf{c} &\in \mathbb{C}^{121} \\ \mathbf{w} &\in \mathbb{C}^{121} \\ \mathbf{c} \cdot \mathbf{w} &\in \mathbb{C}^{121} \\ \mathbf{Lag}(x_1, x_2) &\in \mathbb{C}^{121} \end{aligned}$$

4.25 Function #25 ($n = 2$ variables, tensor size: 12.5 KB)

$$x_1^2 + x_2^2 + x_1 x_2 - x_2 + 1$$

4.25.1 Setup and results overview

- Reference: A/al. 2021 (A.5.20), [4]
- Domain: \mathbb{R}
- Tensor size: 12.5 **KB** (40^2 points)
- Bounds: $(-1 \ 1) \times (-1 \ 1)$

#	Alg.	Parameters	Dim.	CPU [s]	RMSE	min err.	max err.
25	A/G/P-V 2025 (A1)	0.5,1	36	0.0445	9.22e-16	0	4.44e-15
	A/G/P-V 2025 (A2)	1e-15,3	36	0.00333	5.85e - 16	0	2.66e - 15
	MDSPACK v1.1.0	0.5,0.01	36	0.0512	9.39e-16	0	4.44e-15
	P/P 2025	1,0.95,50,0.01,10,4,21	508	1.62	3.65e-06	1.28e-09	2.39e-05
	B/G 2025	0.001,20	72	0.0137	3.8e-13	0	7.92e-12
	B/G 2025 (LR)	0.001,20,3	72	0.0977	1.23e-14	0	1.93e-13
	TensorFlow		257	14.8	0.0062	3.99e-06	0.019

Table 26: Function #25: best model configuration and performances per methods.

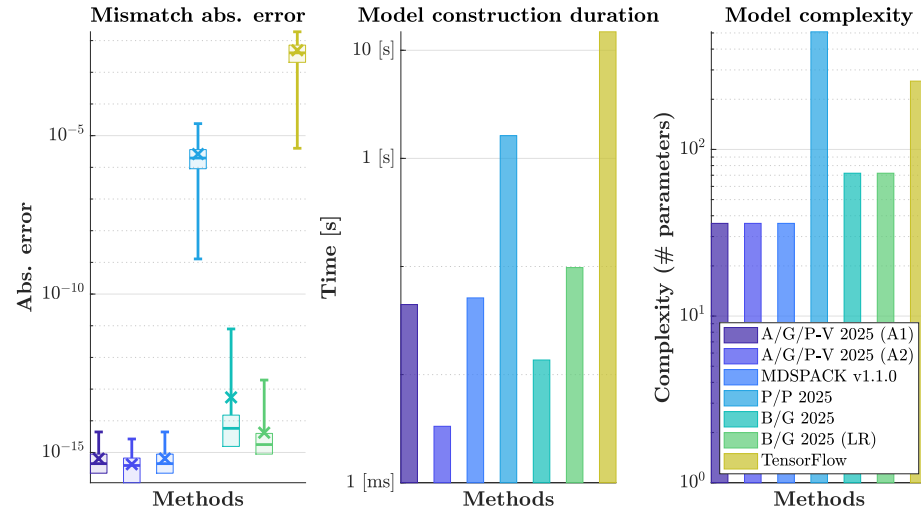


Figure 67: Function #25: graphical view of the best model performances.

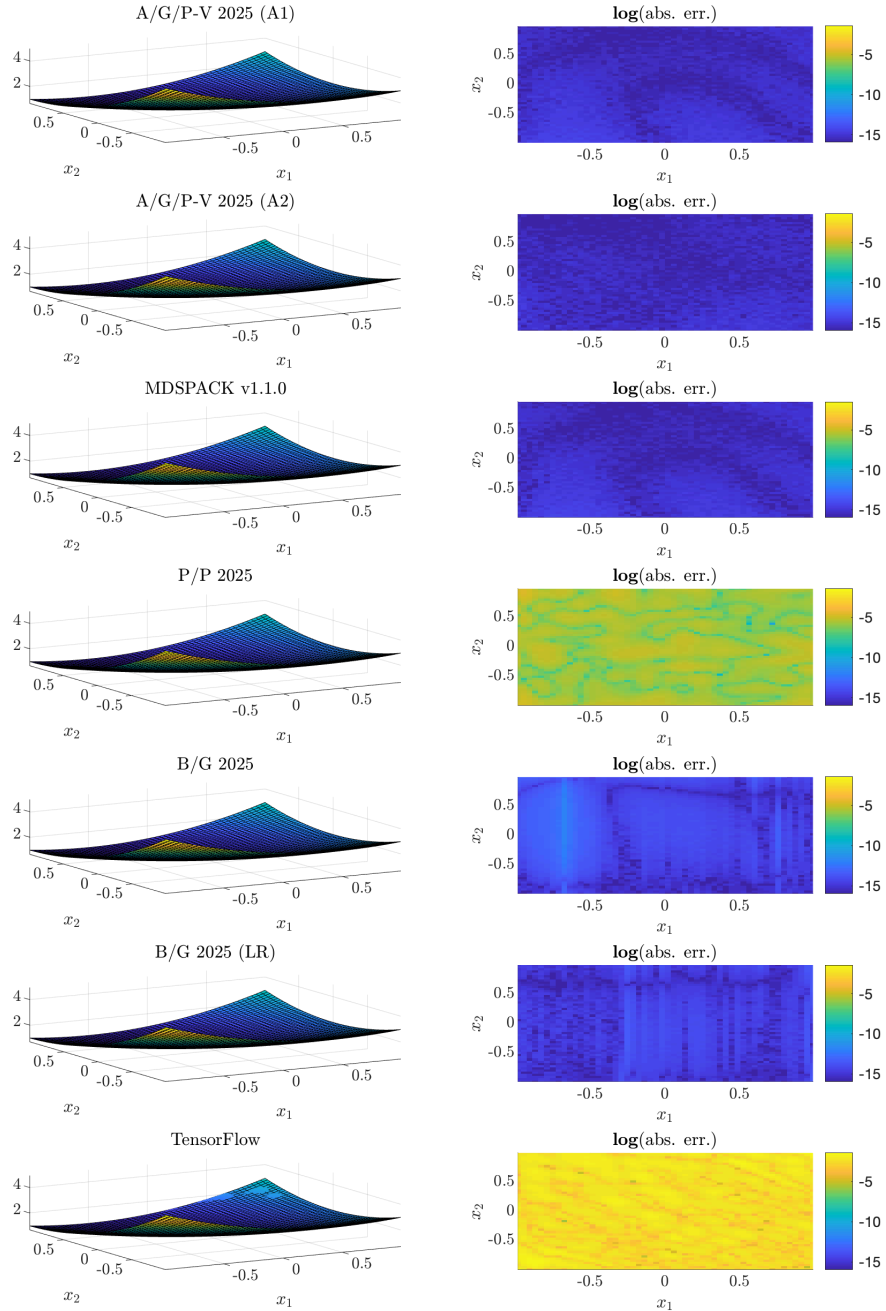


Figure 68: Function #25: left side, evaluation of the original (mesh) vs. approximated (coloured surface) and right side, absolute errors (in log-scale).

4.25.2 mLf detailed informations (M1)

Right interpolation points: $k_l = (3 \ 3)$, where $l = 1, \dots, n$.

$$\begin{aligned} {}^1\lambda_{j_1} &= \left(\begin{array}{ccc} -1 & -\frac{1}{19} & 1 \\ -1 & -\frac{1}{19} & 1 \end{array} \right) \\ {}^2\lambda_{j_2} &= \left(\begin{array}{ccc} 1 & 1 & 1 \\ 1 & 1 & 1 \end{array} \right) \end{aligned}$$

Lagrangian weights, data and supports (Lagrangian basis):

$$\left(\begin{array}{cccc} \mathbf{c} & \mathbf{w} & \mathbf{c} \cdot \mathbf{w} & \text{Lag} \\ -0.58 & 5.0 & -2.9 & \frac{1}{(x_1+1.0)(x_2+1.0)} \\ 1.1 & 2.1 & 2.3 & \frac{1}{(x_1+1.0)(x_2+0.053)} \\ -0.53 & 1.0 & -0.53 & \frac{1}{(x_1+1.0)(x_2-1.0)} \\ 1.1 & 3.1 & 3.4 & \frac{1}{(x_2+1.0)(x_1+0.053)} \\ -2.1 & 1.1 & -2.2 & \frac{1}{(x_1+0.053)(x_2+0.053)} \\ 1.0 & 0.95 & 0.95 & \frac{1}{(x_2-1.0)(x_1+0.053)} \\ -0.53 & 3.0 & -1.6 & \frac{1}{(x_1-1.0)(x_2+1.0)} \\ 1.0 & 2.0 & 2.0 & \frac{1}{(x_1-1.0)(x_2+0.053)} \\ -0.47 & 3.0 & -1.4 & \frac{1}{(x_1-1.0)(x_2-1.0)} \end{array} \right)$$

KST equivalent decoupling pattern

Barycentric weights:

$$\begin{aligned} \mathbf{c}^{x_2} &= \text{vec} \left(\begin{array}{ccc} 1.1 & 1.1 & 1.1 \\ -2.1 & -2.1 & -2.1 \\ 1.0 & 1.0 & 1.0 \end{array} \right) \quad \text{and } \mathbf{Bary}_{x_2} = \mathbf{c}^{x_2} \otimes \mathbf{1}_1 \\ \mathbf{c}^{x_1} &= \left(\begin{array}{c} -0.53 \\ 1.0 \\ -0.47 \end{array} \right) \quad \text{and } \mathbf{Bary}_{x_1} = \mathbf{c}^{x_1} \otimes \mathbf{1}_3 \end{aligned}$$

$$\begin{aligned} \mathbf{c} &= \mathbf{c}^{x_n} \odot (\mathbf{c}^{x_{n-1}} \otimes \mathbf{1}_{k_n}) \odot (\mathbf{c}^{x_{n-2}} \otimes \mathbf{1}_{k_n k_{n-1}}) \odot \cdots \odot (\mathbf{c}^{x_1} \otimes \mathbf{1}_{k_n \dots k_2}) \\ &= \mathbf{Bary}_{x_n} \odot \mathbf{Bary}_{x_{n-1}} \odot \cdots \odot \mathbf{Bary}_{x_1} \end{aligned}$$

Data weights:

$$\begin{aligned} \mathbf{w}^{x_2} &= \text{vec} \left(\begin{array}{ccc} 5.0 & 3.1 & 3.0 \\ 2.1 & 1.1 & 2.0 \\ 1.0 & 0.95 & 3.0 \end{array} \right) \quad \text{and } \mathbf{W}_{x_2} = \mathbf{c}^{x_2} \otimes \mathbf{1}_1 \\ \mathbf{w}^{x_1} &= \left(\begin{array}{c} 1.0 \\ 0.95 \\ 3.0 \end{array} \right) \quad \text{and } \mathbf{W}_{x_1} = \mathbf{c}^{x_1} \otimes \mathbf{1}_3 \end{aligned}$$

$$\begin{aligned} \mathbf{w} &= \mathbf{w}^{x_n} \odot (\mathbf{w}^{x_{n-1}} \otimes \mathbf{1}_{k_n}) \odot (\mathbf{w}^{x_{n-2}} \otimes \mathbf{1}_{k_n k_{n-1}}) \odot \cdots \odot (\mathbf{w}^{x_1} \otimes \mathbf{1}_{k_n \dots k_2}) \\ &= \mathbf{W}_{x_n} \odot \mathbf{W}_{x_{n-1}} \odot \cdots \odot \mathbf{W}_{x_1} \end{aligned}$$

Barycentric denominator univariate vector-wise functions (KST equivalent functions):

$$\mathbf{D} = \left(\begin{array}{cc} \mathbf{c}^{x_1} \cdot \text{Lag}(x_1) & \mathbf{c}^{x_2} \cdot \text{Lag}(x_2) \\ -\frac{0.53}{x_1+1.0} & -\frac{1.1}{x_2+1.0} \\ -\frac{0.53}{x_1+1.0} & -\frac{2.1}{x_2+0.053} \\ -\frac{0.53}{x_1+1.0} & -\frac{1}{x_2-1.0} \\ \frac{1}{x_1+0.053} & -\frac{x_2+1.0}{2.1} \\ \frac{1}{x_1+0.053} & -\frac{x_2+0.053}{1} \\ \frac{1}{x_1+0.053} & -\frac{x_2-1.0}{1.1} \\ -\frac{0.47}{x_1-1.0} & -\frac{x_2+1.0}{2.1} \\ -\frac{0.47}{x_1-1.0} & -\frac{x_2+0.053}{1} \end{array} \right)$$

Equivalent denominator and numerator read:

$$\sum_{i\text{-th row}} \prod_{j\text{-th col}} [\mathbf{D}]_{i,j} \quad \text{and} \quad \sum_{i\text{-th row}} \mathbf{w} \cdot \prod_{j\text{-th col}} [\mathbf{D}]_{i,j}$$

Connection with Neural Networks (equivalent denominator representation):

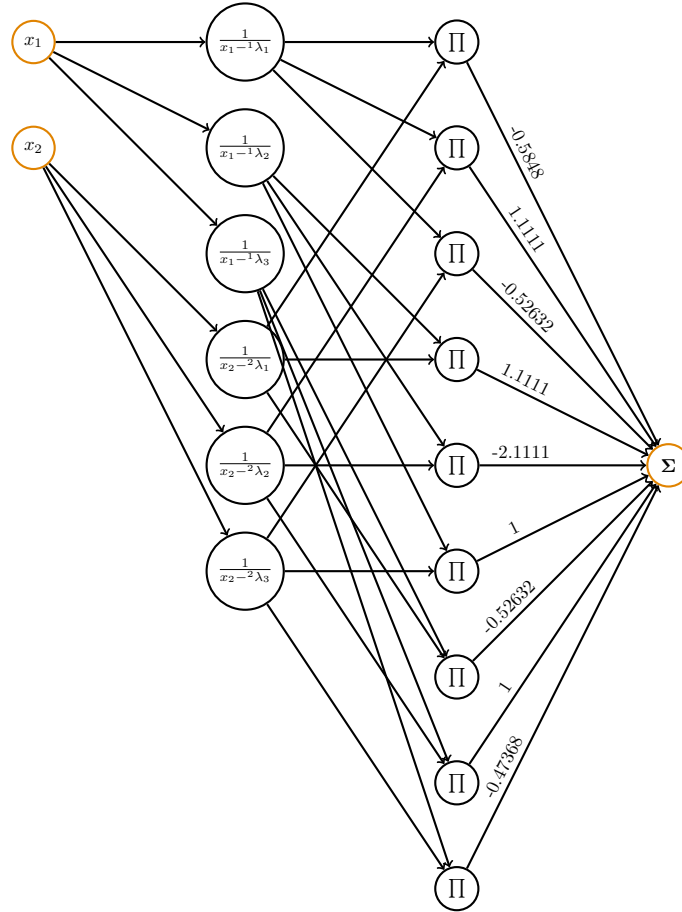


Figure 69: Equivalent NN representation of the denominator \mathbf{D} .

4.26 Function #26 ($n = 3$ variables, tensor size: 1.65 MB)

$$\frac{x_1 + x_2 + x_3}{6 + \cos(x_1) + \cos(x_2) + \cos(x_3)}$$

4.26.1 Setup and results overview

- Reference: B/G 2025, [5]
- Domain: \mathbb{R}
- Tensor size: 1.65 MB (60³ points)
- Bounds: (-10 10) × (-10 10) × (-10 10)

#	Alg.	Parameters	Dim.	CPU [s]	RMSE	min err.	max err.
26	A/G/P-V 2025 (A1)	1e-09,2	1.37e+04	0.105	0.0723	4.88e-07	0.692
	A/G/P-V 2025 (A2)	1e-15,2	1.47e+04	3.9	0.0307	1.08e-07	0.355
	MDSPACK v1.1.0	1e-09,1e-09	1.37e+04	0.0758	0.0944	1.67e-07	1.35
	P/P 2025	1,0.95,50,0.01,10,12,21	886	127	0.00353	8.24e-06	0.0172
	B/G 2025	1e-09,20	2.04e+04	1.63e+03	2.01e-10	2.22e - 16	1.9e - 09
	B/G 2025 (LR)	1e-09,20,4	1.69e+04	158	1.91e - 10	6.66e-14	3.18e-09
	TensorFlow		321	313	0.427	0.000438	2.63

Table 27: Function #26: best model configuration and performances per methods.

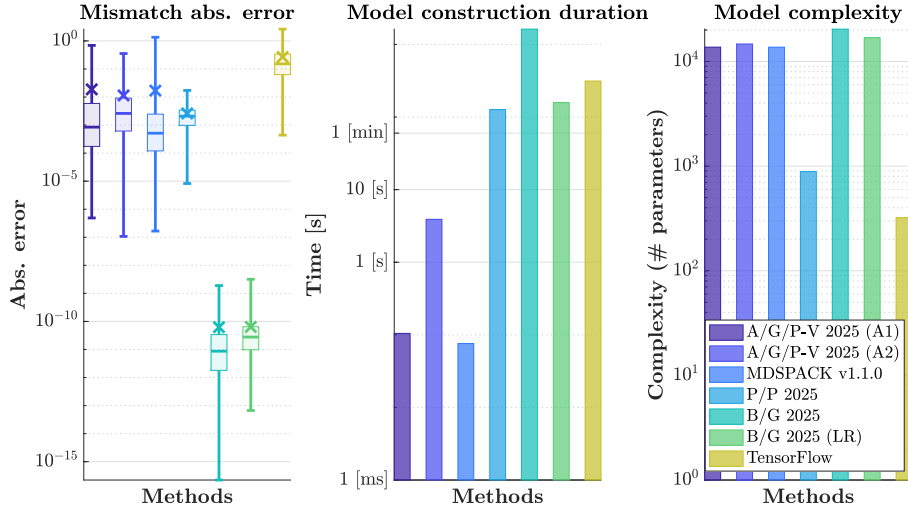


Figure 70: Function #26: graphical view of the best model performances.

$$x_3 = [-1.6596]$$

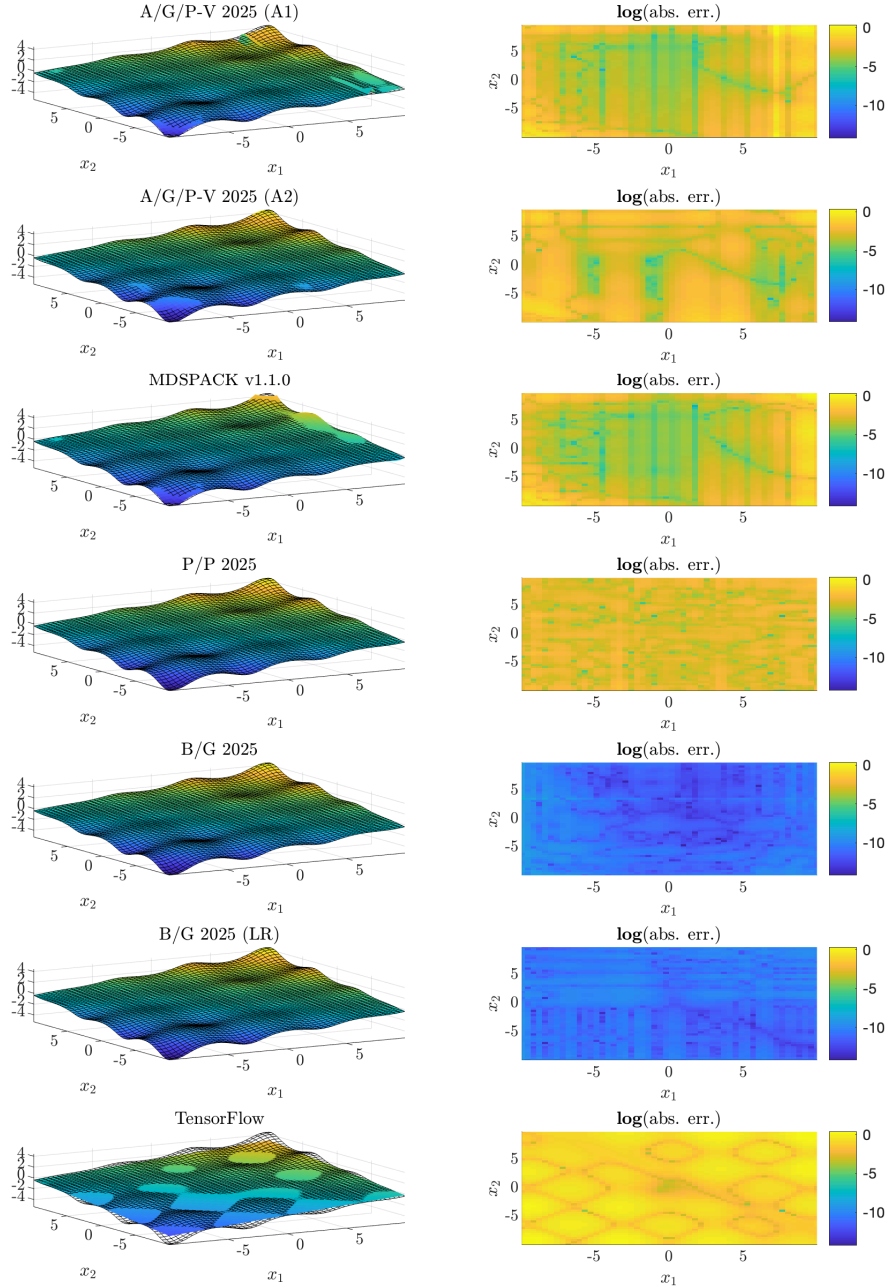


Figure 71: Function #26: left side, evaluation of the original (mesh) vs. approximated (coloured surface) and right side, absolute errors (in log-scale).

4.26.2 mLF detailed informations (M1)

Right interpolation points: $k_l = (14 \quad 14 \quad 14)$, where $l = 1, \dots, n$.

$$\begin{aligned} {}^1\lambda_{j_1} &\in \mathbb{C}^{14}, \text{ linearly spaced between bounds} \\ {}^2\lambda_{j_2} &\in \mathbb{C}^{14}, \text{ linearly spaced between bounds} \\ {}^3\lambda_{j_3} &\in \mathbb{C}^{14}, \text{ linearly spaced between bounds} \end{aligned}$$

n -D Loewner matrix, barycentric weights and Lagrangian basis:

$$\begin{aligned} \mathbb{L} &\in \mathbb{C}^{2744 \times 2744} \\ \mathbf{c} &\in \mathbb{C}^{2744} \\ \mathbf{w} &\in \mathbb{C}^{2744} \\ \mathbf{c} \cdot \mathbf{w} &\in \mathbb{C}^{2744} \\ \mathbf{Lag}(x_1, x_2, x_3) &\in \mathbb{C}^{2744} \end{aligned}$$

4.27 Function #27 ($n = 5$ variables, tensor size: 90.6 MB)

$$\frac{x_1 + x_2 + x_3 + x_4 + x_5}{10 + \cos(x_1) + \cos(x_2) + \cos(x_3) + \cos(x_4) + \cos(x_5)}$$

4.27.1 Setup and results overview

- Reference: B/G 2025, [5]
- Domain: \mathbb{R}
- Tensor size: 90.6 MB (26^5 points)
- Bounds: $(-4 \ 4) \times (-4 \ 4) \times (-4 \ 4) \times (-4 \ 4) \times (-4 \ 4)$

#	Alg.	Parameters	Dim.	CPU [s]	RMSE	min err.	max err.
27	A/G/P-V 2025 (A1)	0.001,3	5.44e+04	3.66	0.0129	3.02e - 06	0.114
	A/G/P-V 2025 (A2)	1e-15,1	7	39.3	3.35	1.38	6.03
	MDSPACK v1.1.0	0.001,1e-06	5.44e+04	3.59	0.0168	1.7e-05	0.136
	P/P 2025	NaN	NaN	NaN	NaN	NaN	NaN
	B/G 2025	NaN	NaN	NaN	NaN	NaN	NaN
	B/G 2025 (LR)	NaN	NaN	NaN	NaN	NaN	NaN
	TensorFlow	NaN	NaN	NaN	NaN	NaN	NaN

Table 28: Function #27: best model configuration and performances per methods.

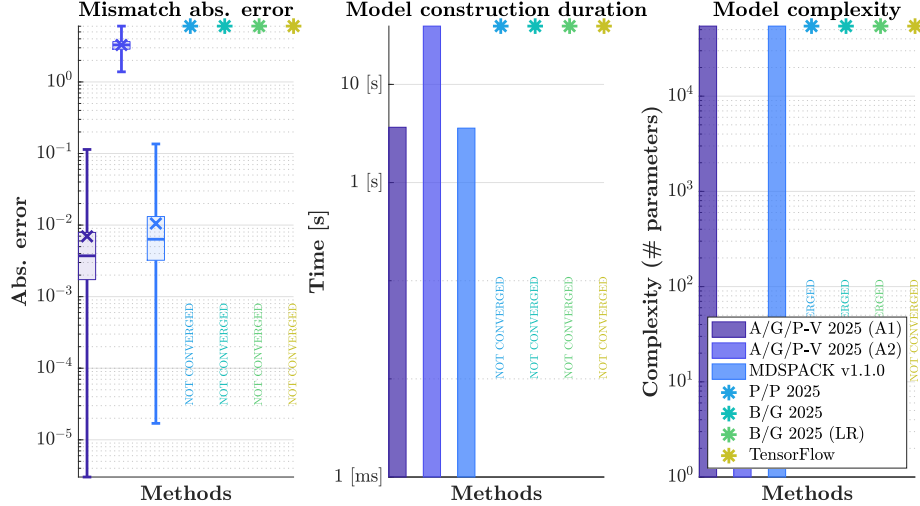


Figure 72: Function #27: graphical view of the best model performances.

$$x_{3..5} = [-0.66382; -3.9991; -2.826]$$

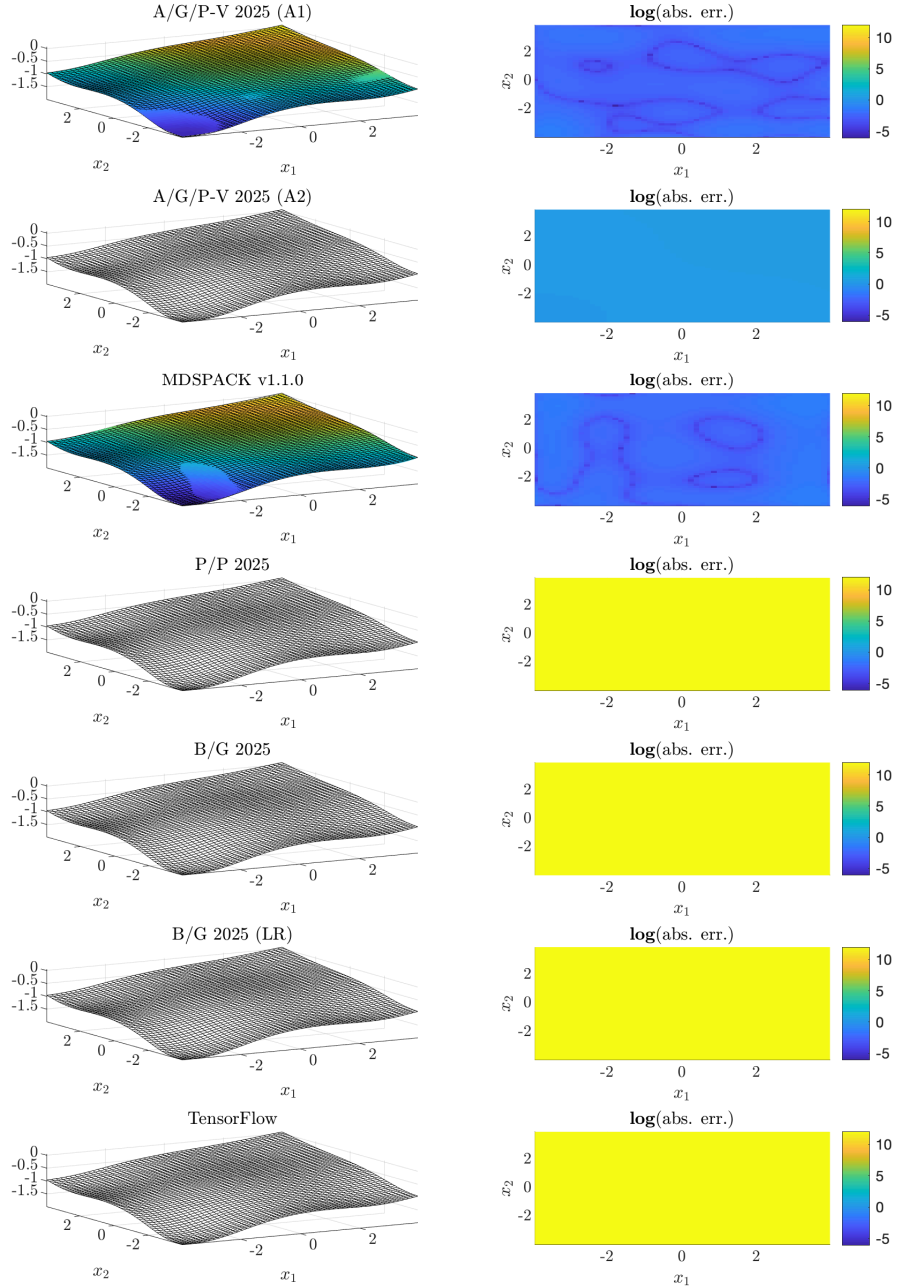


Figure 73: Function #27: left side, evaluation of the original (mesh) vs. approximated (coloured surface) and right side, absolute errors (in log-scale).

4.27.2 mLF detailed informations (M1)

Right interpolation points: $k_l = (\begin{array}{ccccc} 6 & 6 & 6 & 6 & 6 \end{array})$, where $l = 1, \dots, n$.

$$\begin{aligned} {}^1\lambda_{j_1} &\in \mathbb{C}^6, \text{ linearly spaced between bounds} \\ {}^2\lambda_{j_2} &\in \mathbb{C}^6, \text{ linearly spaced between bounds} \\ {}^3\lambda_{j_3} &\in \mathbb{C}^6, \text{ linearly spaced between bounds} \\ {}^4\lambda_{j_4} &\in \mathbb{C}^6, \text{ linearly spaced between bounds} \\ {}^5\lambda_{j_5} &\in \mathbb{C}^6, \text{ linearly spaced between bounds} \end{aligned}$$

n -D Loewner matrix, barycentric weights and Lagrangian basis:

$$\begin{aligned} \mathbb{L} &\in \mathbb{C}^{7776 \times 7776} \\ \mathbf{c} &\in \mathbb{C}^{7776} \\ \mathbf{w} &\in \mathbb{C}^{7776} \\ \mathbf{c} \cdot \mathbf{w} &\in \mathbb{C}^{7776} \\ \mathbf{Lag}(x_1, x_2, x_3, x_4, x_5) &\in \mathbb{C}^{7776} \end{aligned}$$

4.28 Function #28 ($n = 2$ variables, tensor size: 30 KB)

$$\left(\frac{x_1}{x_1+1}\right)^4 (1 + \exp(-x_2^2)) \left(1 + x_2 \cos(x_2) \exp\frac{(-x_1 x_2)}{x_1+1}\right)$$

4.28.1 Setup and results overview

- Reference: J/al. 2024 (Toy function), [none]
- Domain: \mathbb{R}
- Tensor size: 30 **KB** (62^2 points)
- Bounds: $(\frac{1}{10000000000}, 10) \times (\frac{1}{10000000000}, 10)$

#	Alg.	Parameters	Dim.	CPU [s]	RMSE	min err.	max err.
28	A/G/P-V 2025 (A1)	0.0001,1	240	0.0333	0.00928	6.1e-09	0.0554
	A/G/P-V 2025 (A2)	1e-15,3	360	0.188	0.000256	2.31e-08	0.00281
	MDSPACK v1.1.0	0.0001,1e-06	200	0.0365	0.0177	1.71e-08	0.141
	P/P 2025	1,0.95,50,0.01,6,12,13	316	2.38	0.000151	8.18e-07	0.000808
	B/G 2025	1e-09,20	988	0.66	3.05e - 08	0	5.45e - 07
	B/G 2025 (LR)	1e-06,20,3	1.14e+03	3.99	4.42e-07	1.11e-15	7.67e-06
	TensorFlow		257	28.9	0.161	0.000136	0.674

Table 29: Function #28: best model configuration and performances per methods.

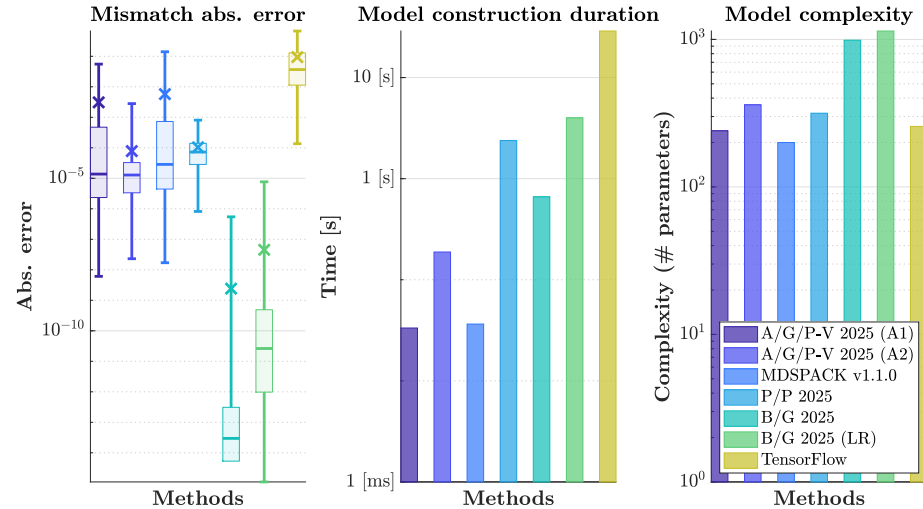


Figure 74: Function #28: graphical view of the best model performances.

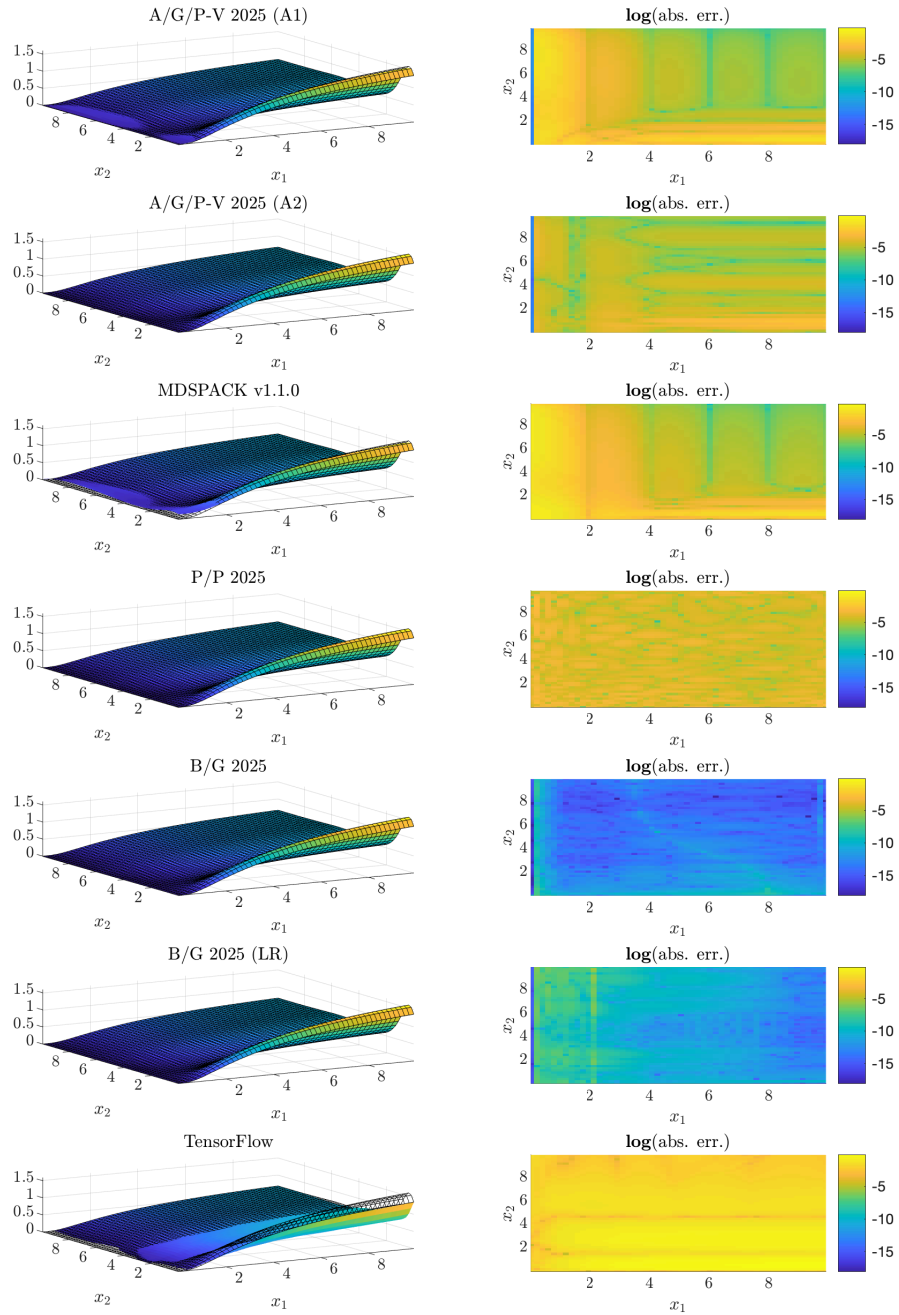


Figure 75: Function #28: left side, evaluation of the original (mesh) vs. approximated (coloured surface) and right side, absolute errors (in log-scale).

4.28.2 mLF detailed informations (M1)

Right interpolation points: $k_l = \begin{pmatrix} 6 & 10 \end{pmatrix}$, where $l = 1, \dots, n$.

$$\begin{aligned} {}^1\lambda_{j_1} &\in \mathbb{C}^6, \text{ linearly spaced between bounds} \\ {}^2\lambda_{j_2} &\in \mathbb{C}^{10}, \text{ linearly spaced between bounds} \end{aligned}$$

n-D Loewner matrix, barycentric weights and Lagrangian basis:

$$\begin{aligned} \mathbb{L} &\in \mathbb{C}^{60 \times 60} \\ \mathbf{c} &\in \mathbb{C}^{60} \\ \mathbf{w} &\in \mathbb{C}^{60} \\ \mathbf{c} \cdot \mathbf{w} &\in \mathbb{C}^{60} \\ \mathbf{Lag}(x_1, x_2) &\in \mathbb{C}^{60} \end{aligned}$$

4.29 Function #29 ($n = 2$ variables, tensor size: 12.5 KB)

$$\min(10|x_1|, 1)\text{sign}(x_1) + \frac{x_1 x_2^3}{10}$$

4.29.1 Setup and results overview

- Reference: Personal communication, [none]
- Domain: \mathbb{R}
- Tensor size: 12.5 **KB** (40^2 points)
- Bounds: $(-1 \ 1) \times (-1 \ 1)$

#	Alg.	Parameters	Dim.	CPU [s]	RMSE	min err.	max err.
29	A/G/P-V 2025 (A1)	0.01,2	112	0.0151	0.0236	4.62e-08	0.185
	A/G/P-V 2025 (A2)	1e-15,2	336	0.0773	0.161	5.26e - 12	2.23
	MDSPACK v1.1.0	0.01,0.01	112	0.0174	0.0238	1.93e-07	0.186
	P/P 2025	4,1,50,0.01,6,6,13	238	0.473	0.0137	1.44e-05	0.0485
	B/G 2025	0.001,20	660	0.216	1.76	5.22e-09	38.9
	B/G 2025 (LR)	0.001,20,5	528	0.26	0.203	8.41e-10	3.24
	TensorFlow	NaN	NaN	NaN	NaN	NaN	NaN

Table 30: Function #29: best model configuration and performances per methods.

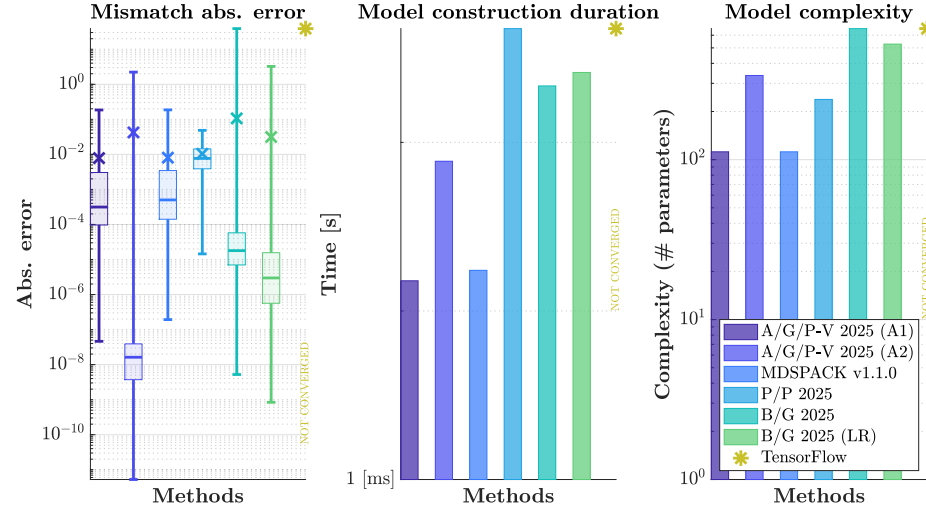


Figure 76: Function #29: graphical view of the best model performances.

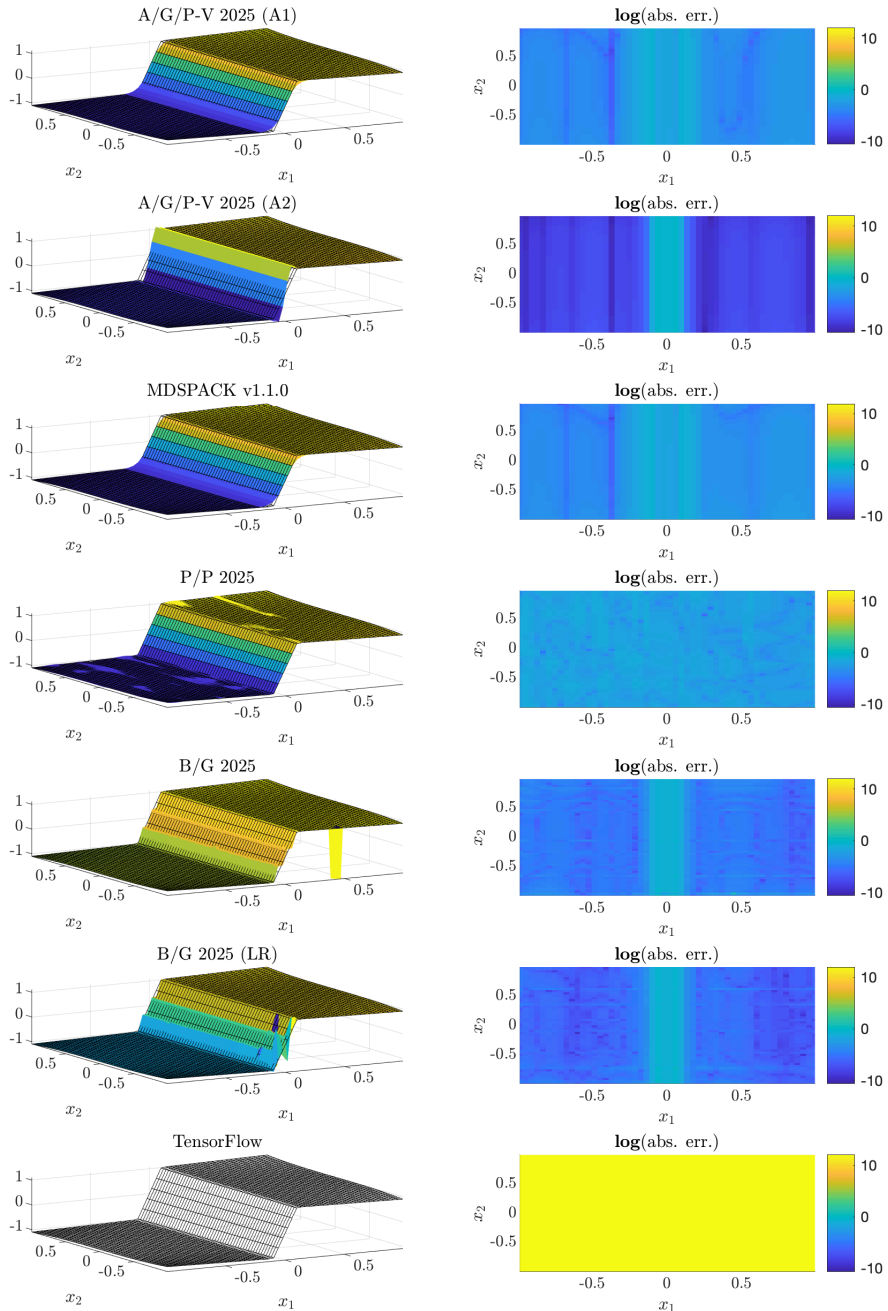


Figure 77: Function #29: left side, evaluation of the original (mesh) vs. approximated (coloured surface) and right side, absolute errors (in log-scale).

4.29.2 mLF detailed informations (M1)

Right interpolation points: $k_l = \begin{pmatrix} 7 & 4 \end{pmatrix}$, where $l = 1, \dots, n$.

$$\begin{aligned} {}^1\lambda_{j_1} &\in \mathbb{C}^7, \text{ linearly spaced between bounds} \\ {}^2\lambda_{j_2} &\in \mathbb{C}^4, \text{ linearly spaced between bounds} \end{aligned}$$

n-D Loewner matrix, barycentric weights and Lagrangian basis:

$$\begin{aligned} \mathbb{L} &\in \mathbb{C}^{28 \times 28} \\ \mathbf{c} &\in \mathbb{C}^{28} \\ \mathbf{w} &\in \mathbb{C}^{28} \\ \mathbf{c} \cdot \mathbf{w} &\in \mathbb{C}^{28} \\ \mathbf{Lag}(x_1, x_2) &\in \mathbb{C}^{28} \end{aligned}$$

4.30 Function #30 ($n = 8$ variables, tensor size: 128 MB)

$$f(r_w, r, T_u, H_u, T_l, H_l, L, K_w) = \frac{2\pi T_u (H_u - H_l)}{\ln\left(\frac{r}{r_w}\right) \left(1 + \frac{2LT_u}{\ln(r/r_w)r_w^2 K_w}\right) + \frac{T_u}{T_l}}$$

4.30.1 Setup and results overview

- Reference: Borehole function, sfu.ca/~ssurjano
- Domain: \mathbb{R}
- Tensor size: 128 MB (8^8 points)
- Bounds: $(\frac{1}{20}, \frac{3}{20}) \times (100, 50000) \times (63070, 115600) \times (990, 1110) \times (\frac{631}{10}, 116) \times (700, 820) \times (1120, 1680) \times (9855, 12045)$

#	Alg.	Parameters	Dim.	CPU [s]	RMSE	min err.	max err.
30	A/G/P-V 2025 (A1)	1e-09,1	1.02e + 04	18.1	0.00455	2e - 09	0.061
	A/G/P-V 2025 (A2)	1e-15,2	1.02e+04	38	0.00456	2.93e-09	0.0611
	MDSPACK v1.1.0	1e-13,-1	4.1e+04	20.7	0.00455	2.1e-09	0.061
	P/P 2025	NaN	NaN	NaN	NaN	NaN	NaN
	B/G 2025	NaN	NaN	NaN	NaN	NaN	NaN
	B/G 2025 (LR)	NaN	NaN	NaN	NaN	NaN	NaN
	TensorFlow	NaN	NaN	NaN	NaN	NaN	NaN

Table 31: Function #30: best model configuration and performances per methods.

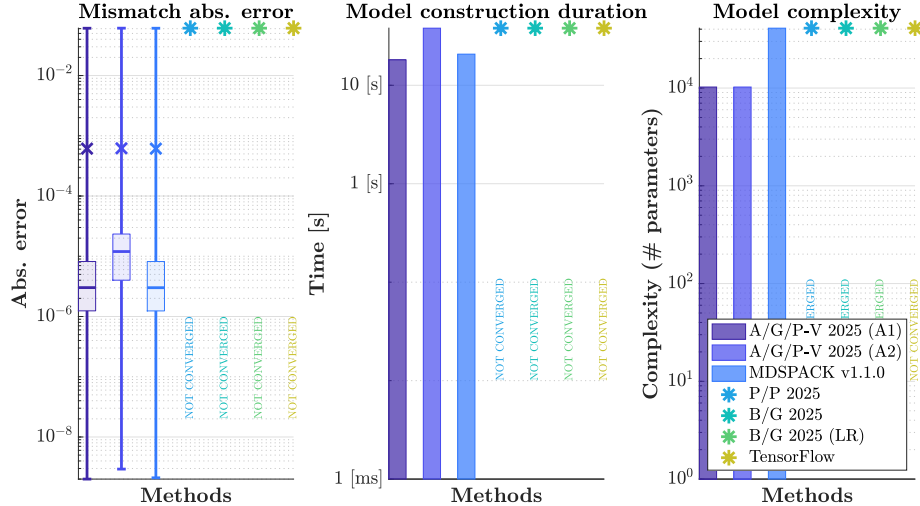


Figure 78: Function #30: graphical view of the best model performances.

$$x_{3..8} = [84976.1659; 990.0137; 70.8634; 722.3512; 1342.1898; 10773.036]$$

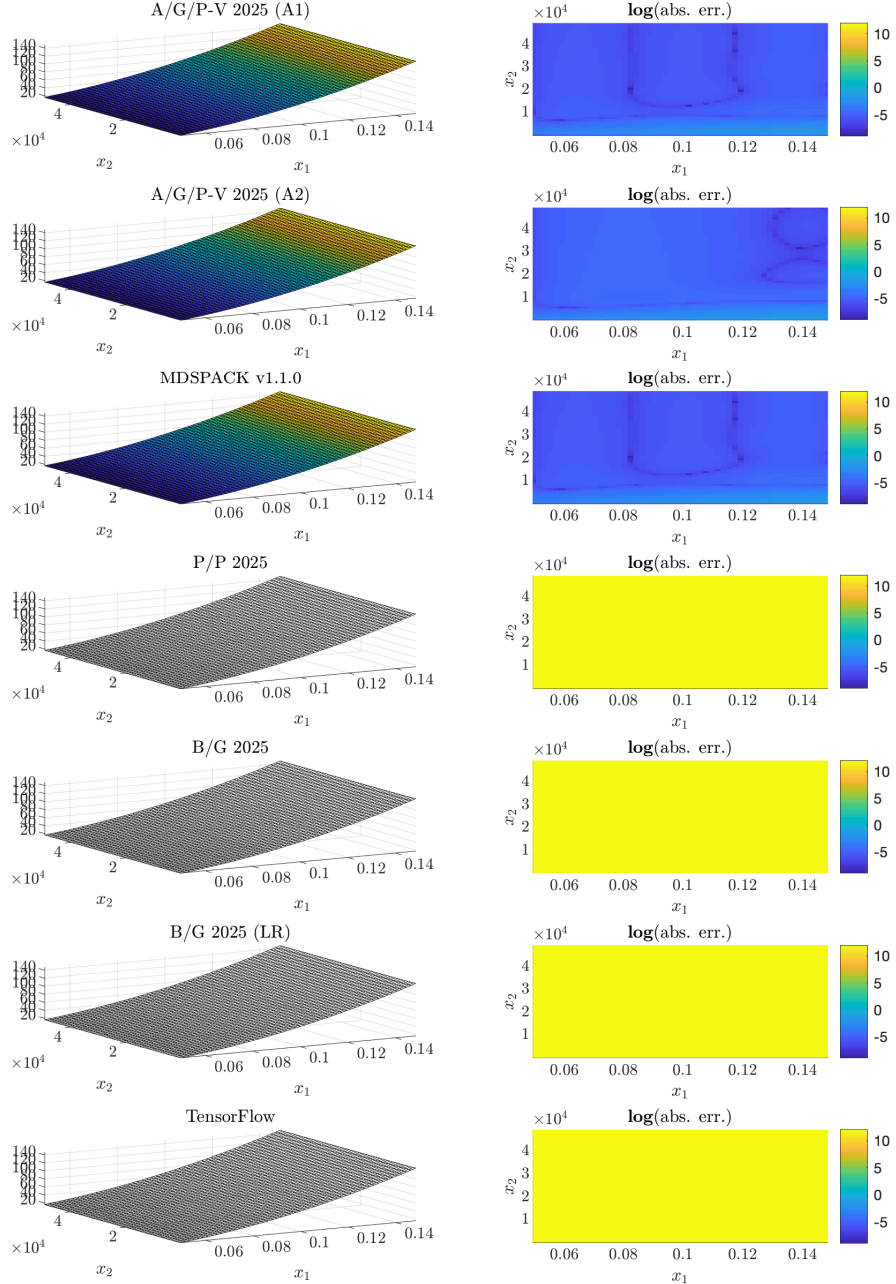


Figure 79: Function #30: left side, evaluation of the original (mesh) vs. approximated (coloured surface) and right side, absolute errors (in log-scale).

4.30.2 mLF detailed informations (M1)

Right interpolation points: $k_l = (4 \ 4 \ 2 \ 2 \ 2 \ 2 \ 2 \ 2)$, where $l = 1, \dots, n$.

$$\begin{aligned} {}^1\lambda_{j_1} &\in \mathbb{C}^4, \text{ linearly spaced between bounds} \\ {}^2\lambda_{j_2} &\in \mathbb{C}^4, \text{ linearly spaced between bounds} \\ {}^3\lambda_{j_3} &\in \mathbb{C}^2, \text{ linearly spaced between bounds} \\ {}^4\lambda_{j_4} &\in \mathbb{C}^2, \text{ linearly spaced between bounds} \\ {}^5\lambda_{j_5} &\in \mathbb{C}^2, \text{ linearly spaced between bounds} \\ {}^6\lambda_{j_6} &\in \mathbb{C}^2, \text{ linearly spaced between bounds} \\ {}^7\lambda_{j_7} &\in \mathbb{C}^2, \text{ linearly spaced between bounds} \\ {}^8\lambda_{j_8} &\in \mathbb{C}^2, \text{ linearly spaced between bounds} \end{aligned}$$

n-D Loewner matrix, barycentric weights and Lagrangian basis:

$$\begin{aligned} \mathbb{L} &\in \mathbb{C}^{1024 \times 1024} \\ \mathbf{c} &\in \mathbb{C}^{1024} \\ \mathbf{w} &\in \mathbb{C}^{1024} \\ \mathbf{c} \cdot \mathbf{w} &\in \mathbb{C}^{1024} \\ \mathbf{Lag}(x_1, x_2, x_3, x_4, x_5, x_6, x_7, x_8) &\in \mathbb{C}^{1024} \end{aligned}$$

4.31 Function #31 ($n = 6$ variables, tensor size: 128 MB)

$$x_1^2 x_2^3 x_3 x_4 - x_5^2 + x_6$$

4.31.1 Setup and results overview

- Reference: Personal communication, [none]
- Domain: \mathbb{R}
- Tensor size: 128 **MB** (16^6 points)
- Bounds: $(-2 \ 2) \times (-2 \ 2)$

#	Alg.	Parameters	Dim.	CPU [s]	RMSE	min err.	max err.
31	A/G/P-V 2025 (A1)	0.1,3	2.3e + 03	9.69	1.18e - 14	0	7.46e - 14
	A/G/P-V 2025 (A2)	1e-15,2	2.3e+03	18	4.42	1.3e-12	26.6
	MDSPACK v1.1.0	0.1,0.01	2.3e+03	8.95	1.68e-14	0	9.95e-14
	P/P 2025	NaN	NaN	NaN	NaN	NaN	NaN
	B/G 2025	NaN	NaN	NaN	NaN	NaN	NaN
	B/G 2025 (LR)	NaN	NaN	NaN	NaN	NaN	NaN
	TensorFlow	NaN	NaN	NaN	NaN	NaN	NaN

Table 32: Function #31: best model configuration and performances per methods.

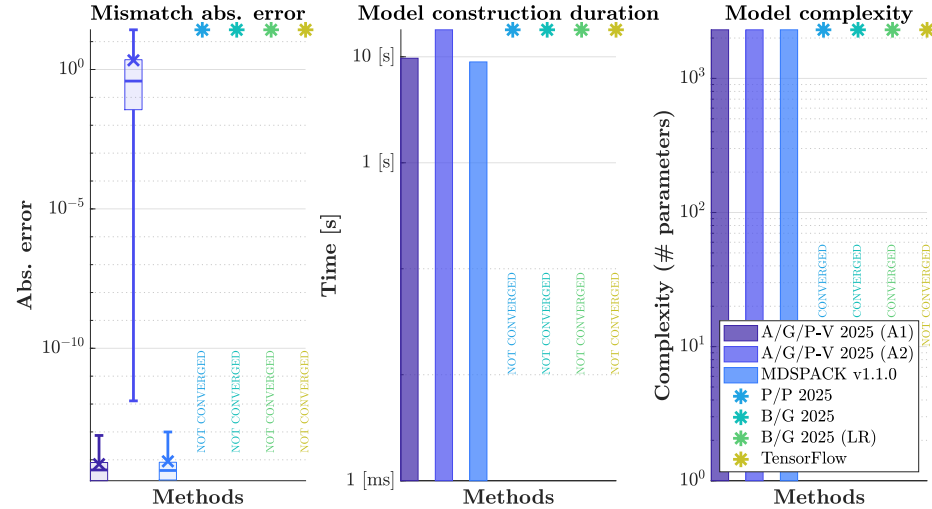


Figure 80: Function #31: graphical view of the best model performances.

$$x_{3..6} = [-0.33191; -1.9995; -1.413; -1.255]$$

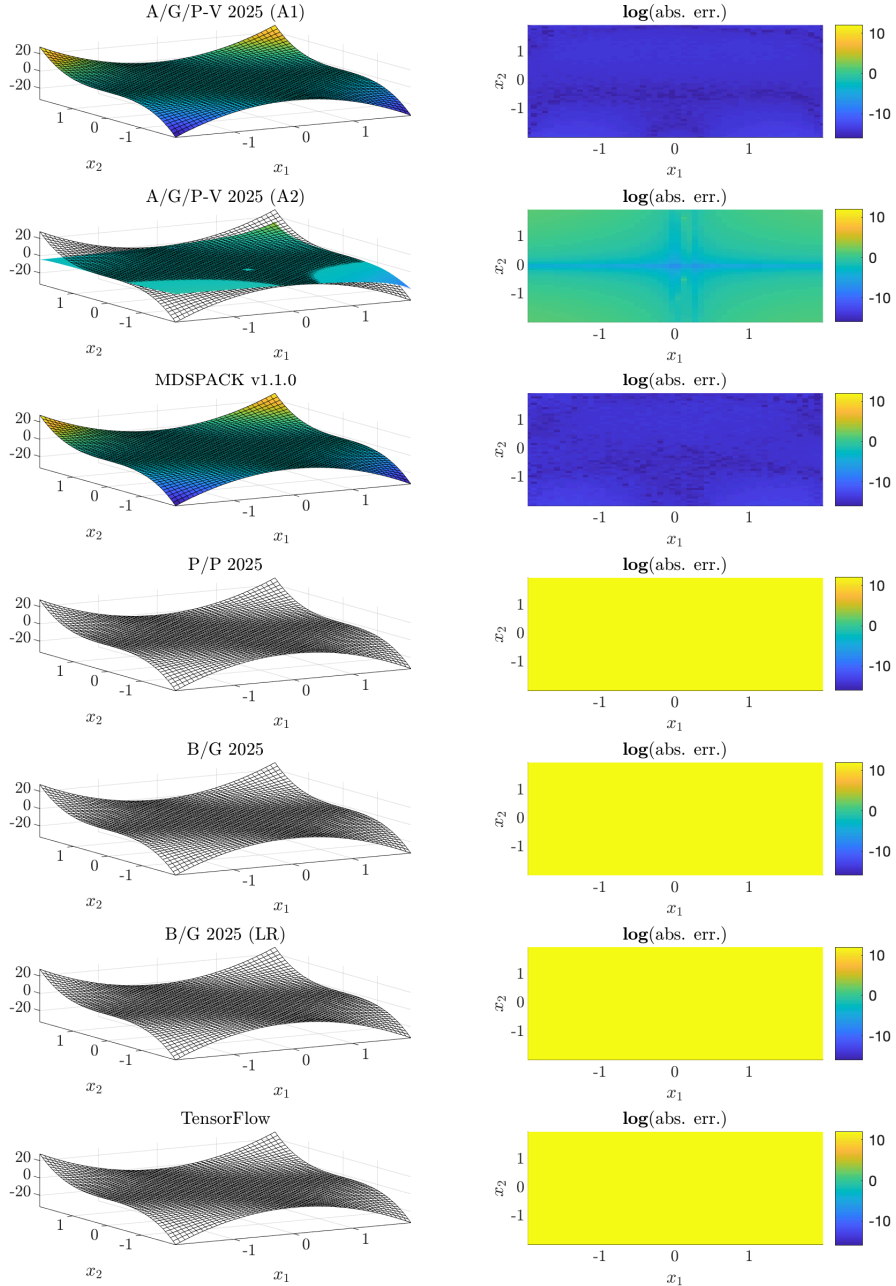


Figure 81: Function #31: left side, evaluation of the original (mesh) vs. approximated (coloured surface) and right side, absolute errors (in log-scale).

4.31.2 mLF detailed informations (M1)

Right interpolation points: $k_l = (3 \ 4 \ 2 \ 2 \ 3 \ 2)$, where $l = 1, \dots, n$.

- ${}^1\lambda_{j_1} \in \mathbb{C}^3$, linearly spaced between bounds
- ${}^2\lambda_{j_2} \in \mathbb{C}^4$, linearly spaced between bounds
- ${}^3\lambda_{j_3} \in \mathbb{C}^2$, linearly spaced between bounds
- ${}^4\lambda_{j_4} \in \mathbb{C}^2$, linearly spaced between bounds
- ${}^5\lambda_{j_5} \in \mathbb{C}^3$, linearly spaced between bounds
- ${}^6\lambda_{j_6} \in \mathbb{C}^2$, linearly spaced between bounds

n -D Loewner matrix, barycentric weights and Lagrangian basis:

$$\begin{aligned}\mathbb{L} &\in \mathbb{C}^{288 \times 288} \\ \mathbf{c} &\in \mathbb{C}^{288} \\ \mathbf{w} &\in \mathbb{C}^{288} \\ \mathbf{c} \cdot \mathbf{w} &\in \mathbb{C}^{288} \\ \mathbf{Lag}(x_1, x_2, x_3, x_4, x_5, x_6) &\in \mathbb{C}^{288}\end{aligned}$$

4.32 Function #32 ($n = 2$ variables, tensor size: 12.5 KB)

$$\text{atan}(x_1) + x_2^3$$

4.32.1 Setup and results overview

- Reference: Personal communication, [none]
- Domain: \mathbb{R}
- Tensor size: 12.5 **KB** (40^2 points)
- Bounds: $(-2 \ 2) \times (-2 \ 2)$

#	Alg.	Parameters	Dim.	CPU [s]	RMSE	min err.	max err.
32	A/G/P-V 2025 (A1)	1e-14,3	256	0.0155	8.25e - 14	0	5.21e - 13
	A/G/P-V 2025 (A2)	1e-15,1	64	0.142	0.00275	5.84e-07	0.00569
	MDSPACK v1.1.0	1e-14,0.0001	240	0.0162	1.18e-12	0	1.82e-11
	P/P 2025	1,1,50,0.01,10,4,21	508	1.6	0.00014	7.62e-08	0.000377
	B/G 2025	1e-09,20	640	0.223	4.6e-07	6.98e-11	3.33e-06
	B/G 2025 (LR)	1e-09,20,5	576	0.476	5.17e-10	1.11e-14	1.14e-08
	TensorFlow		257	14.9	0.028	5.36e-05	0.0912

Table 33: Function #32: best model configuration and performances per methods.

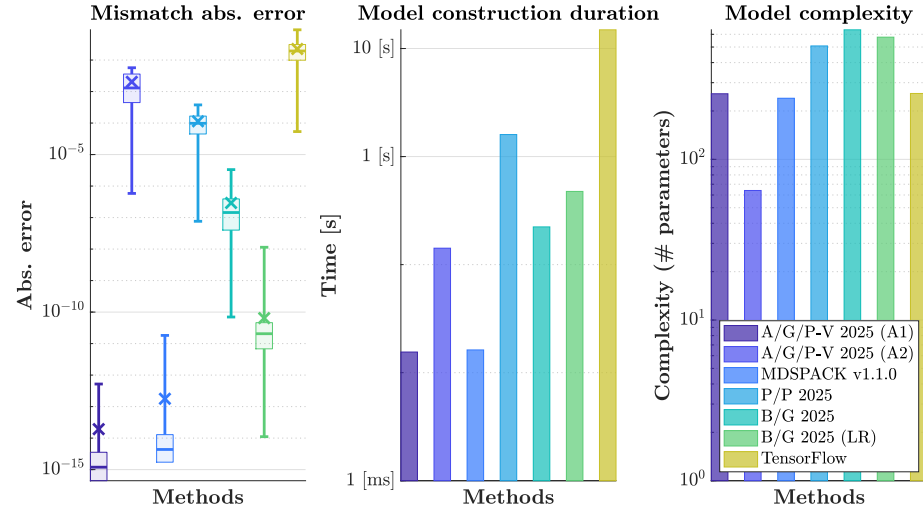


Figure 82: Function #32: graphical view of the best model performances.

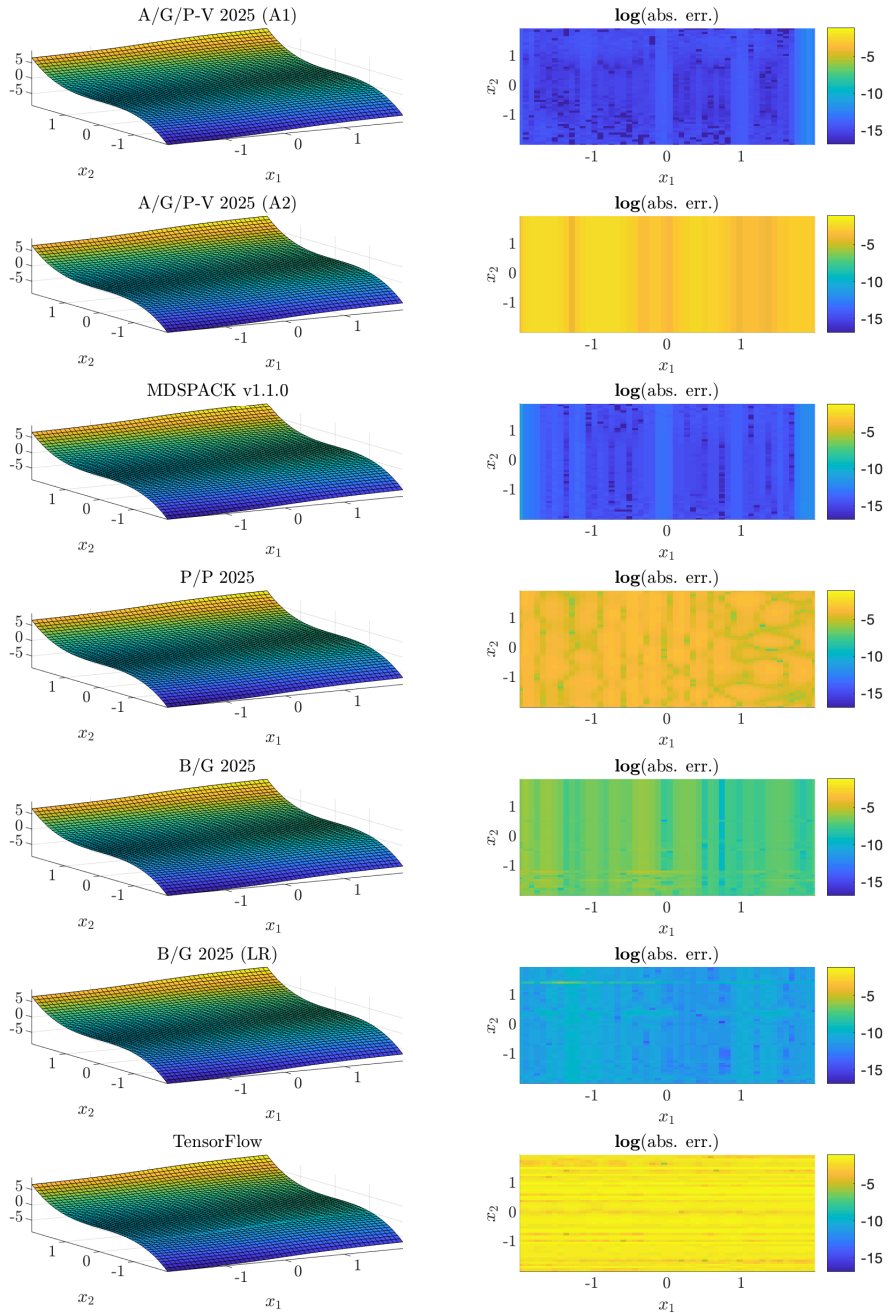


Figure 83: Function #32: left side, evaluation of the original (mesh) vs. approximated (coloured surface) and right side, absolute errors (in log-scale).

4.32.2 mLF detailed informations (M1)

Right interpolation points: $k_l = \begin{pmatrix} 16 & 4 \end{pmatrix}$, where $l = 1, \dots, n$.

$$\begin{aligned} {}^1\lambda_{j_1} &\in \mathbb{C}^{16}, \text{ linearly spaced between bounds} \\ {}^2\lambda_{j_2} &\in \mathbb{C}^4, \text{ linearly spaced between bounds} \end{aligned}$$

n-D Loewner matrix, barycentric weights and Lagrangian basis:

$$\begin{aligned} \mathbb{L} &\in \mathbb{C}^{64 \times 64} \\ \mathbf{c} &\in \mathbb{C}^{64} \\ \mathbf{w} &\in \mathbb{C}^{64} \\ \mathbf{c} \cdot \mathbf{w} &\in \mathbb{C}^{64} \\ \mathbf{Lag}(x_1, x_2) &\in \mathbb{C}^{64} \end{aligned}$$

4.33 Function #33 ($n = 2$ variables, tensor size: 28.1 KB)

$$\frac{x_1 + x_2}{\cos(x_1)^2 + \cos(x_2) + 3}$$

4.33.1 Setup and results overview

- Reference: Personal communication, [none]
- Domain: \mathbb{R}
- Tensor size: 28.1 **KB** (60^2 points)
- Bounds: $(-10 \ 10) \times (-10 \ 10)$

#	Alg.	Parameters	Dim.	CPU [s]	RMSE	min err.	max err.
33	A/G/P-V 2025 (A1)	1e-09,1	1.26e+03	0.0347	0.000805	4.28e-09	0.00774
	A/G/P-V 2025 (A2)	1e-15,2	1.5e+03	0.199	2.55e - 05	7.46e - 10	0.000228
	MDSPACK v1.1.0	1e-09,1e-09	1.26e+03	0.0342	0.000978	2.75e-09	0.00864
	P/P 2025	1,0.95,50,0.01,10,12,21	676	2.85	0.0285	6.74e-05	0.224
	B/G 2025	0.001,20	1.16e+03	0.514	0.000134	6.64e-08	0.00166
	B/G 2025 (LR)	1e-09,20,3	1.37e+03	3.2	8.22e-05	9.3e-09	0.00121
	TensorFlow		257	28.2	0.348	0.00057	2.03

Table 34: Function #33: best model configuration and performances per methods.

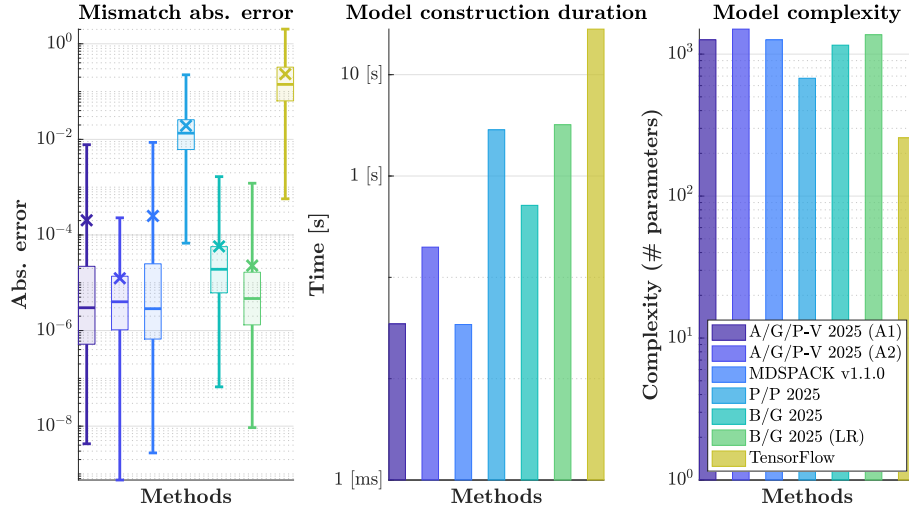


Figure 84: Function #33: graphical view of the best model performances.

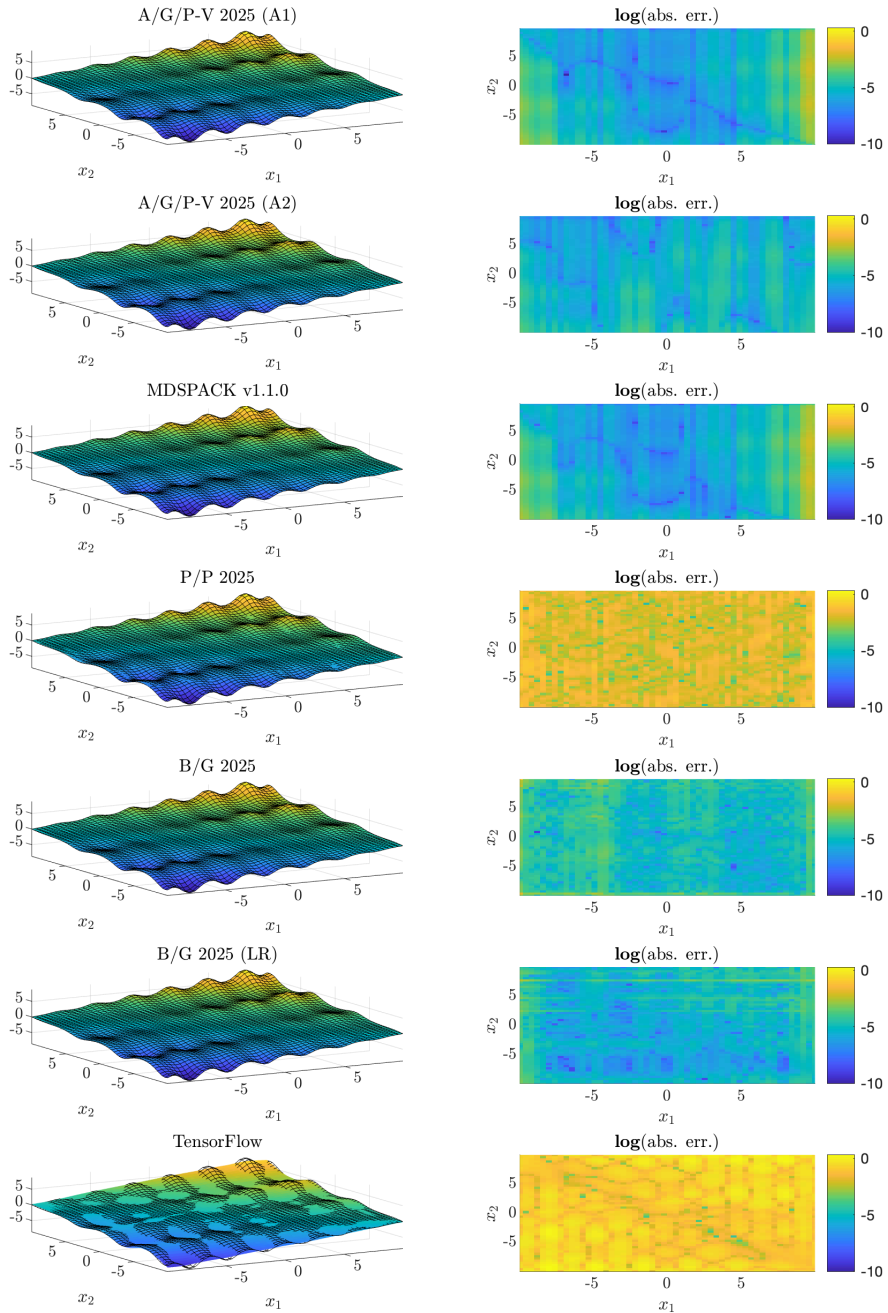


Figure 85: Function #33: left side, evaluation of the original (mesh) vs. approximated (coloured surface) and right side, absolute errors (in log-scale).

4.33.2 mLF detailed informations (M1)

Right interpolation points: $k_l = \begin{pmatrix} 21 & 15 \end{pmatrix}$, where $l = 1, \dots, n$.

$$\begin{aligned} {}^1\lambda_{j_1} &\in \mathbb{C}^{21}, \text{ linearly spaced between bounds} \\ {}^2\lambda_{j_2} &\in \mathbb{C}^{15}, \text{ linearly spaced between bounds} \end{aligned}$$

n-D Loewner matrix, barycentric weights and Lagrangian basis:

$$\begin{aligned} \mathbb{L} &\in \mathbb{C}^{315 \times 315} \\ \mathbf{c} &\in \mathbb{C}^{315} \\ \mathbf{w} &\in \mathbb{C}^{315} \\ \mathbf{c} \cdot \mathbf{w} &\in \mathbb{C}^{315} \\ \mathbf{Lag}(x_1, x_2) &\in \mathbb{C}^{315} \end{aligned}$$

4.34 Function #34 ($n = 2$ variables, tensor size: 1.22 MB)

$$Re(\zeta(x_1 + ix_2))$$

4.34.1 Setup and results overview

- Reference: Riemann ζ function (real part), [none]
- Domain: \mathbb{R}
- Tensor size: 1.22 MB (400² points)
- Bounds: $(\frac{9}{20}, \frac{11}{20}) \times (1, 50)$

#	Alg.	Parameters	Dim.	CPU [s]	RMSE	min err.	max err.
34	A/G/P-V 2025 (A1)	1e-10,2	2.32e+03	1.5	4.86e-05	2.74e - 09	0.000206
	A/G/P-V 2025 (A2)	1e-15,2	864	0.654	0.137	1.51e-06	1.06
	MDSPACK v1.1.0	1e-10,1e-09	2.3e+03	1.58	3.21e - 05	1.87e-08	0.00015
	P/P 2025	1,0.95,50,0.01,10,12,21	676	79	0.0254	1.36e-05	0.0731
	B/G 2025	0.001,20	1.22e+03	85.6	2.53	0.000305	51.2
	B/G 2025 (LR)	1e-06,20,3	1.36e+03	16.9	4.74	1.23e-05	86.8
	TensorFlow	NaN	NaN	NaN	NaN	NaN	NaN

Table 35: Function #34: best model configuration and performances per methods.

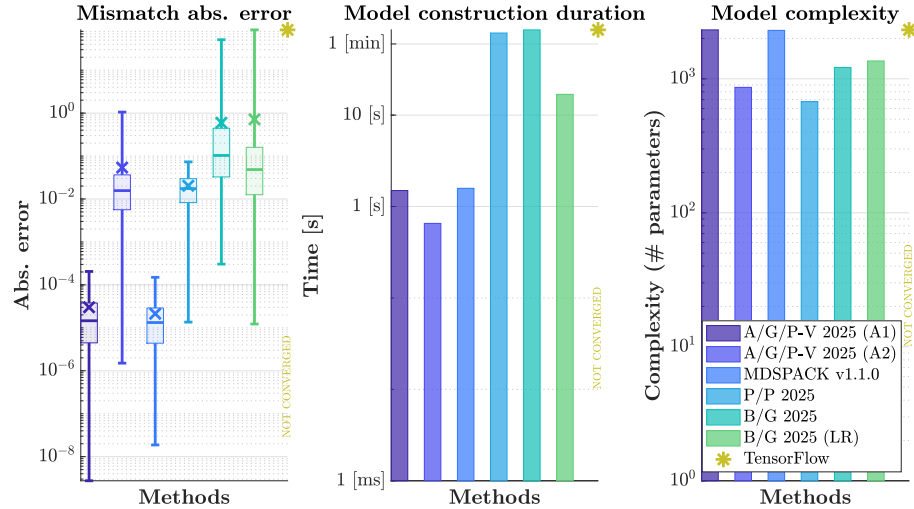


Figure 86: Function #34: graphical view of the best model performances.

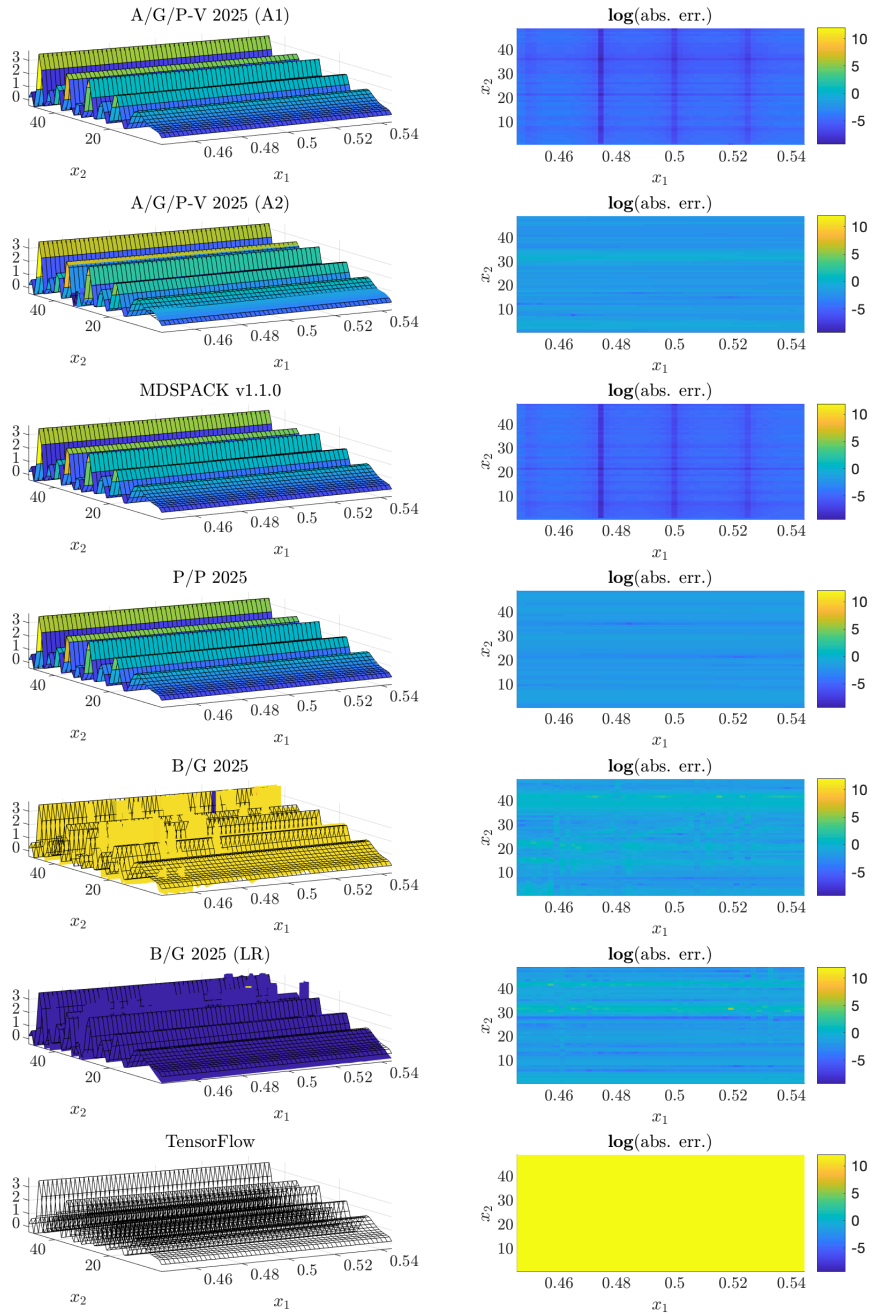


Figure 87: Function #34: left side, evaluation of the original (mesh) vs. approximated (coloured surface) and right side, absolute errors (in log-scale).

4.34.2 mLF detailed informations (M1)

Right interpolation points: $k_l = (5 \quad 116)$, where $l = 1, \dots, n$.

$$\begin{aligned} {}^1\lambda_{j_1} &\in \mathbb{C}^5, \text{ linearly spaced between bounds} \\ {}^2\lambda_{j_2} &\in \mathbb{C}^{116}, \text{ linearly spaced between bounds} \end{aligned}$$

n-D Loewner matrix, barycentric weights and Lagrangian basis:

$$\begin{aligned} \mathbb{L} &\in \mathbb{C}^{580 \times 580} \\ \mathbf{c} &\in \mathbb{C}^{580} \\ \mathbf{w} &\in \mathbb{C}^{580} \\ \mathbf{c} \cdot \mathbf{w} &\in \mathbb{C}^{580} \\ \mathbf{Lag}(x_1, x_2) &\in \mathbb{C}^{580} \end{aligned}$$

4.35 Function #35 ($n = 2$ variables, tensor size: 1.22 MB)

$$Im(\zeta(x_1 + ux_2))$$

4.35.1 Setup and results overview

- Reference: Riemann ζ function (imaginary part), [none]
- Domain: \mathbb{R}
- Tensor size: 1.22 MB (400² points)
- Bounds: $(\frac{9}{20}, \frac{11}{20}) \times (1, 50)$

#	Alg.	Parameters	Dim.	CPU [s]	RMSE	min err.	max err.
35	A/G/P-V 2025 (A1)	1e-09,3	1.84e+03	1.48	8.07e-05	3.69e-08	0.000309
	A/G/P-V 2025 (A2)	1e-15,2	880	0.898	0.108	2.44e-05	0.733
	MDSPACK v1.1.0	1e-09,1e-09	1.82e+03	1.67	1.81e - 05	6.82e - 10	0.000316
	P/P 2025	1,1,50,0.01,10,12,21	676	82	0.032	2.55e-05	0.0943
	B/G 2025	0.001,20	1.52e+03	84.8	1.78	5.26e-05	24.7
	B/G 2025 (LR)	1e-09,20,3	1.44e+03	19.3	1.43	5.34e-05	18.3
	TensorFlow	NaN	NaN	NaN	NaN	NaN	NaN

Table 36: Function #35: best model configuration and performances per methods.

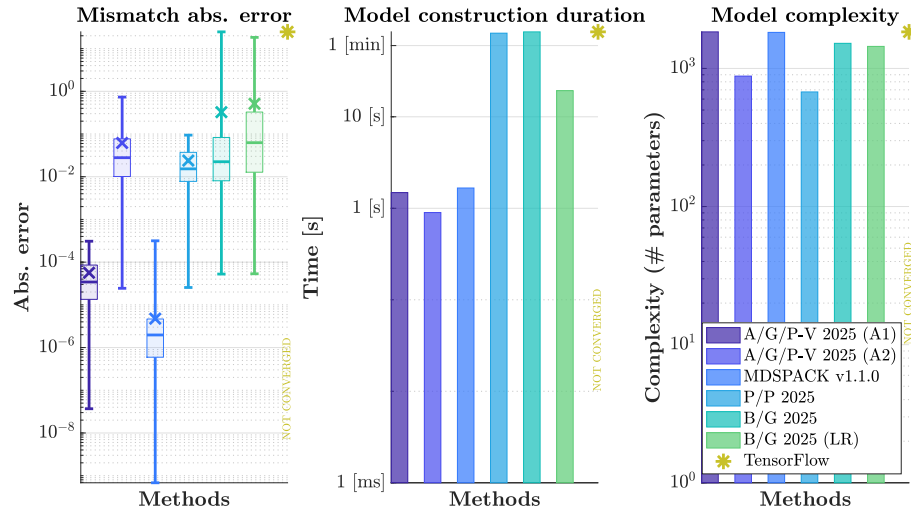


Figure 88: Function #35: graphical view of the best model performances.

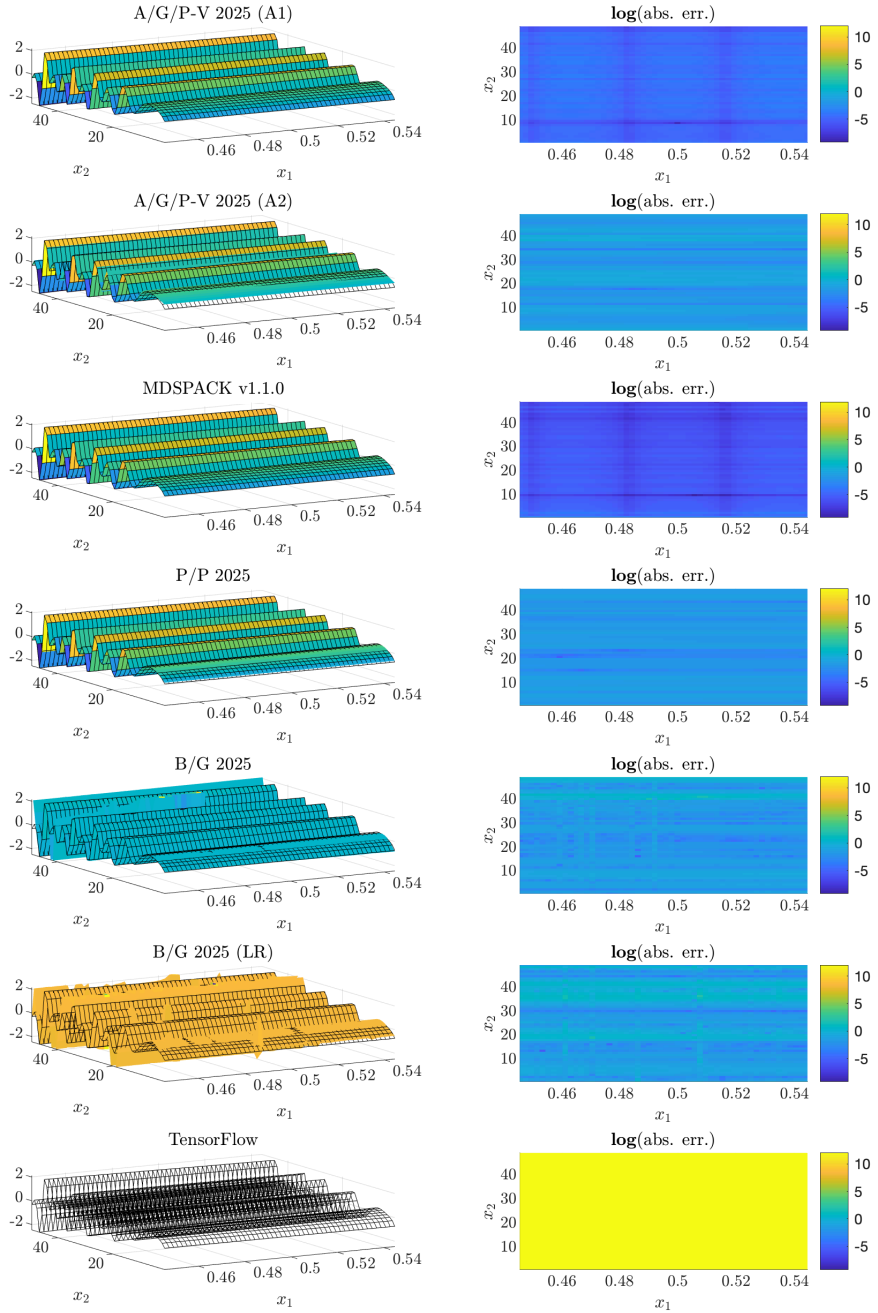


Figure 89: Function #35: left side, evaluation of the original (mesh) vs. approximated (coloured surface) and right side, absolute errors (in log-scale).

4.35.2 mLF detailed informations (M1)

Right interpolation points: $k_l = (4 \quad 115)$, where $l = 1, \dots, n$.

$$\begin{aligned} {}^1\lambda_{j_1} &\in \mathbb{C}^4, \text{ linearly spaced between bounds} \\ {}^2\lambda_{j_2} &\in \mathbb{C}^{115}, \text{ linearly spaced between bounds} \end{aligned}$$

n-D Loewner matrix, barycentric weights and Lagrangian basis:

$$\begin{aligned} \mathbb{L} &\in \mathbb{C}^{460 \times 460} \\ \mathbf{c} &\in \mathbb{C}^{460} \\ \mathbf{w} &\in \mathbb{C}^{460} \\ \mathbf{c} \cdot \mathbf{w} &\in \mathbb{C}^{460} \\ \mathbf{Lag}(x_1, x_2) &\in \mathbb{C}^{460} \end{aligned}$$

4.36 Function #36 ($n = 3$ variables, tensor size: 62.5 KB)

$$\frac{x_2}{3 + 1/3x_2x_1 - x_3^2}$$

4.36.1 Setup and results overview

- Reference: Personal communication, [none]
- Domain: \mathbb{R}
- Tensor size: 62.5 **KB** (20^3 points)
- Bounds: $(\frac{1}{10}, 1) \times (\frac{1}{10}, 1) \times (\frac{1}{10}, 1)$

#	Alg.	Parameters	Dim.	CPU [s]	RMSE	min err.	max err.
36	A/G/P-V 2025 (A1)	0.01,2	60	0.0104	1.35e - 15	0	3.89e-15
	A/G/P-V 2025 (A2)	1e-15,2	60	0.202	2.61e-15	0	1.04e-14
	MDSPACK v1.1.0	0.01,0.01	60	0.00933	1.35e-15	0	3.83e - 15
	P/P 2025	1,1,50,0.01,4,6,9	166	1.69	1.14e-05	1.2e-08	4.96e-05
	B/G 2025	0.001,20	640	0.256	7.47e-15	0	1.06e-13
	B/G 2025 (LR)	1e-09,20,5	360	1.57	1.94e-12	1.67e-16	2.79e-11
	TensorFlow		321	45.1	0.00595	7.52e-07	0.0218

Table 37: Function #36: best model configuration and performances per methods.

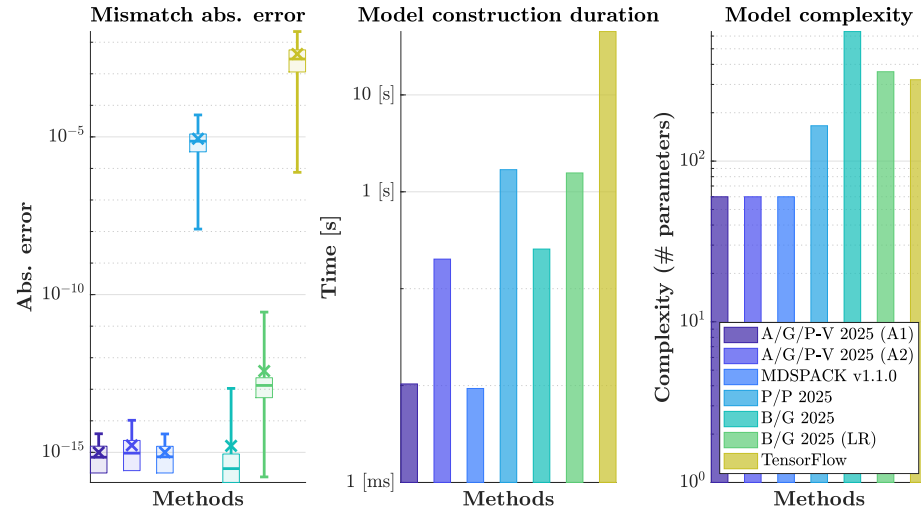


Figure 90: Function #36: graphical view of the best model performances.

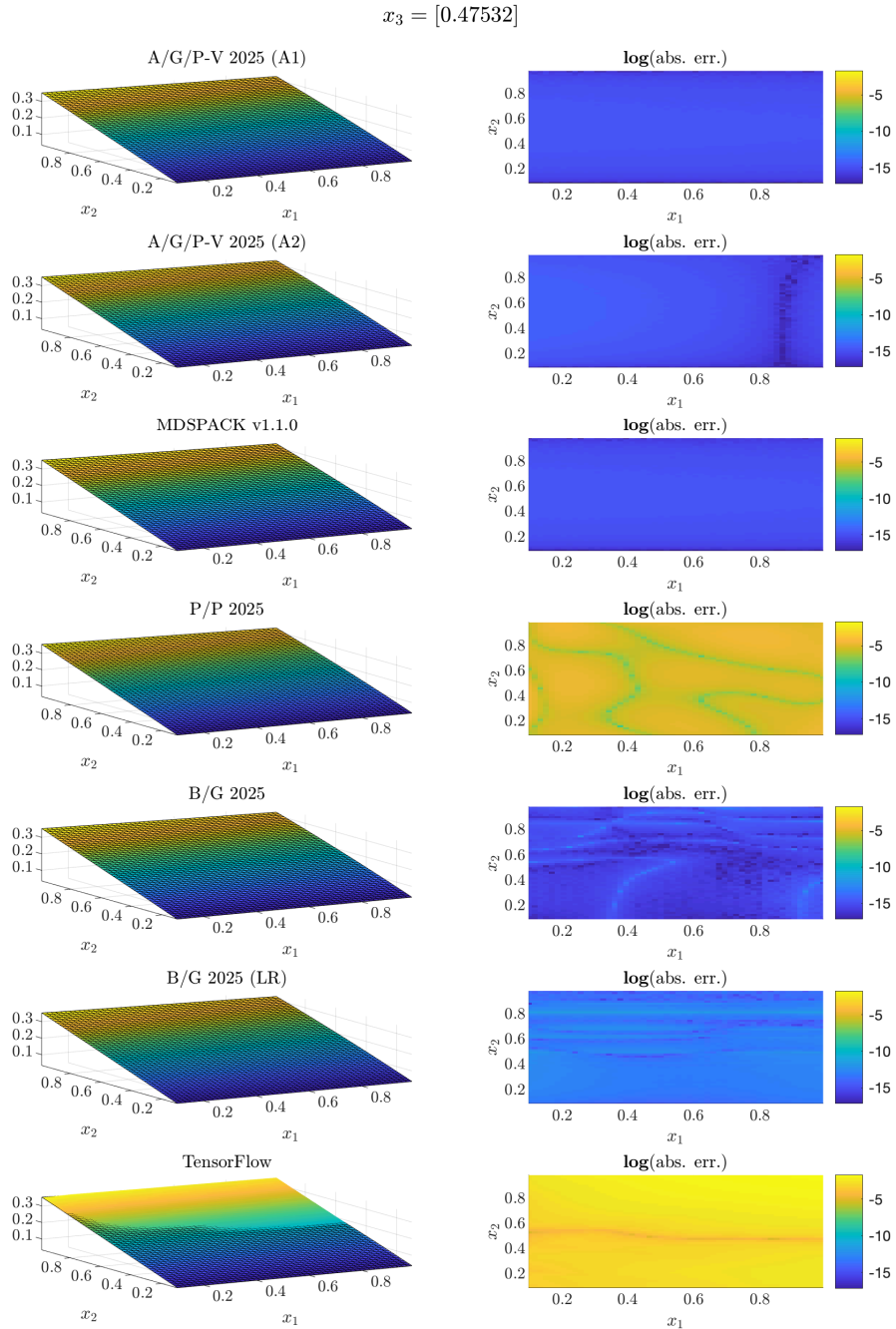


Figure 91: Function #36: left side, evaluation of the original (mesh) vs. approximated (coloured surface) and right side, absolute errors (in log-scale).

4.36.2 mLFI detailed informations (M1)

Right interpolation points: $k_l = (2 \ 2 \ 3)$, where $l = 1, \dots, n$.

$$\begin{aligned} {}^1\lambda_{j_1} &= \left(\begin{array}{cc} \frac{1}{10} & 1 \\ \frac{1}{10} & 1 \end{array} \right) \\ {}^2\lambda_{j_2} &= \left(\begin{array}{c} \frac{1}{10} \\ \frac{1}{10} \end{array} \right) \\ {}^3\lambda_{j_3} &= \left(\begin{array}{ccc} \frac{1}{10} & \frac{1}{2} & 1 \end{array} \right) \end{aligned}$$

Lagrangian weights, data and supports (Lagrangian basis):

c	w	c · w	Lag
1.6	0.033	0.054	$\frac{1}{(x_1-0.1)(x_2-0.1)(x_3-0.1)}$
-2.7	0.036	-0.096	$\frac{1}{(x_3-0.5)(x_1-0.1)(x_2-0.1)}$
0.86	0.05	0.043	$\frac{1}{(x_3-1.0)(x_1-0.1)(x_2-0.1)}$
-1.6	0.33	-0.54	$\frac{1}{(x_2-1.0)(x_1-0.1)(x_3-0.1)}$
2.7	0.36	0.96	$\frac{1}{(x_2-1.0)(x_3-0.5)(x_1-0.1)}$
-0.87	0.49	-0.43	$\frac{1}{(x_2-1.0)(x_3-1.0)(x_1-0.1)}$
-1.6	0.033	-0.054	$\frac{1}{(x_1-1.0)(x_2-0.1)(x_3-0.1)}$
2.7	0.036	0.096	$\frac{1}{(x_1-1.0)(x_3-0.5)(x_2-0.1)}$
-0.87	0.049	-0.043	$\frac{1}{(x_1-1.0)(x_3-1.0)(x_2-0.1)}$
1.8	0.3	0.54	$\frac{1}{(x_1-1.0)(x_2-1.0)(x_3-0.1)}$
-3.0	0.32	-0.96	$\frac{1}{(x_1-1.0)(x_2-1.0)(x_3-0.5)}$
1.0	0.43	0.43	$\frac{1}{(x_1-1.0)(x_2-1.0)(x_3-1.0)}$

KST equivalent decoupling pattern

Barycentric weights:

$$\begin{aligned} \mathbf{c}^{x_3} &= \text{vec} \begin{pmatrix} 1.9 & 1.9 & 1.9 & 1.8 \\ -3.1 & -3.1 & -3.1 & -3.0 \\ 1.0 & 1.0 & 1.0 & 1.0 \end{pmatrix} \quad \text{and } \mathbf{Bary}_{x_3} = \mathbf{c}^{x_3} \otimes \mathbf{1}_1 \\ \mathbf{c}^{x_2} &= \text{vec} \begin{pmatrix} -0.99 & -0.87 \\ 1.0 & 1.0 \end{pmatrix} \quad \text{and } \mathbf{Bary}_{x_2} = \mathbf{c}^{x_2} \otimes \mathbf{1}_3 \\ \mathbf{c}^{x_1} &= \begin{pmatrix} -0.87 \\ 1.0 \end{pmatrix} \quad \text{and } \mathbf{Bary}_{x_1} = \mathbf{c}^{x_1} \otimes \mathbf{1}_6 \\ \mathbf{c} &= \mathbf{c}^{x_n} \odot (\mathbf{c}^{x_{n-1}} \otimes \mathbf{1}_{k_n}) \odot (\mathbf{c}^{x_{n-2}} \otimes \mathbf{1}_{k_n k_{n-1}}) \odot \cdots \odot (\mathbf{c}^{x_1} \otimes \mathbf{1}_{k_n \cdots k_2}) \\ &= \mathbf{Bary}_{x_n} \odot \mathbf{Bary}_{x_{n-1}} \odot \cdots \odot \mathbf{Bary}_{x_1} \end{aligned}$$

Data weights:

$$\begin{aligned} \mathbf{w}^{x_3} &= \text{vec} \begin{pmatrix} 0.033 & 0.33 & 0.033 & 0.3 \\ 0.036 & 0.36 & 0.036 & 0.32 \\ 0.05 & 0.49 & 0.049 & 0.43 \end{pmatrix} \quad \text{and } \mathbf{W}_{x_3} = \mathbf{c}^{x_3} \otimes \mathbf{1}_1 \\ \mathbf{w}^{x_2} &= \text{vec} \begin{pmatrix} 0.05 & 0.049 \\ 0.49 & 0.43 \end{pmatrix} \quad \text{and } \mathbf{W}_{x_2} = \mathbf{c}^{x_2} \otimes \mathbf{1}_3 \\ \mathbf{w}^{x_1} &= \begin{pmatrix} 0.49 \\ 0.43 \end{pmatrix} \quad \text{and } \mathbf{W}_{x_1} = \mathbf{c}^{x_1} \otimes \mathbf{1}_6 \\ \mathbf{w} &= \mathbf{w}^{x_n} \odot (\mathbf{w}^{x_{n-1}} \otimes \mathbf{1}_{k_n}) \odot (\mathbf{w}^{x_{n-2}} \otimes \mathbf{1}_{k_n k_{n-1}}) \odot \cdots \odot (\mathbf{w}^{x_1} \otimes \mathbf{1}_{k_n \cdots k_2}) \\ &= \mathbf{W}_{x_n} \odot \mathbf{W}_{x_{n-1}} \odot \cdots \odot \mathbf{W}_{x_1} \end{aligned}$$

Barycentric denominator univariate vector-wise functions (KST equivalent functions):

$$\mathbf{D} = \begin{pmatrix} \mathbf{c}^{x_1} \cdot \mathbf{Lag}(x_1) & \mathbf{c}^{x_2} \cdot \mathbf{Lag}(x_2) & \mathbf{c}^{x_3} \cdot \mathbf{Lag}(x_3) \\ -\frac{0.87}{x_1-0.1} & -\frac{0.99}{x_2-0.1} & -\frac{1.9}{x_3-0.1} \\ -\frac{x_1-0.1}{0.87} & -\frac{x_2-0.1}{0.99} & -\frac{x_3-0.1}{3.1} \\ -\frac{0.87}{x_1-0.1} & -\frac{0.99}{x_2-0.1} & -\frac{x_3-1.0}{1.9} \\ -\frac{x_1-0.1}{0.87} & -\frac{x_2-1.0}{1} & -\frac{x_3-0.1}{3.1} \\ -\frac{0.87}{x_1-0.1} & -\frac{x_2-1.0}{x_2-1.0} & -\frac{x_3-0.5}{1} \\ -\frac{x_1-0.1}{0.87} & -\frac{1}{x_2-1.0} & -\frac{x_3-1.0}{1.9} \\ -\frac{1}{x_1-0.1} & -\frac{x_2-1.0}{0.87} & -\frac{x_3-1.0}{1.9} \\ -\frac{x_1-1.0}{1} & -\frac{x_2-0.1}{0.87} & -\frac{x_3-0.1}{3.1} \\ -\frac{x_1-1.0}{1} & -\frac{x_2-0.1}{0.87} & -\frac{x_3-0.5}{1} \\ -\frac{x_1-1.0}{1} & -\frac{x_2-0.1}{x_2-0.1} & -\frac{x_3-1.0}{1.8} \\ -\frac{x_1-1.0}{1} & -\frac{1}{x_2-1.0} & -\frac{x_3-0.1}{3.0} \\ -\frac{x_1-1.0}{1} & -\frac{x_2-1.0}{1} & -\frac{x_3-0.5}{1} \\ x_1-1.0 & -\frac{x_2-1.0}{x_2-1.0} & -\frac{x_3-1.0}{1.0} \end{pmatrix}$$

Equivalent denominator and numerator read:

$$\sum_{i\text{-th row}} \prod_{j\text{-th col}} [\mathbf{D}]_{i,j} \text{ and } \sum_{i\text{-th row}} \mathbf{w} \cdot \prod_{j\text{-th col}} [\mathbf{D}]_{i,j}$$

Connection with Neural Networks (equivalent denominator representation):

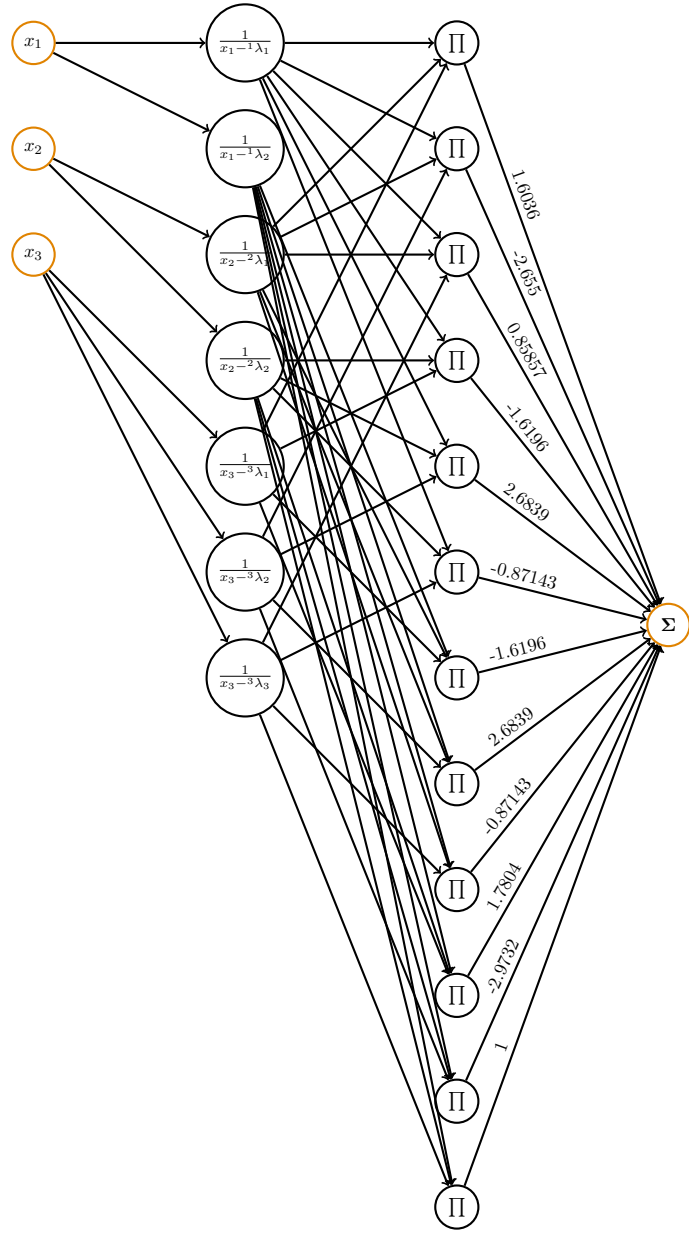


Figure 92: Equivalent NN representation of the denominator \mathbf{D} .

4.37 Function #37 ($n = 4$ variables, tensor size: 1.22 MB)

$$x_1 x_4^3 + \sin(2x_2) x_3$$

4.37.1 Setup and results overview

- Reference: Personal communication, [none]
- Domain: \mathbb{R}
- Tensor size: 1.22 MB (20^4 points)
- Bounds: $(\frac{1}{1000}, 1) \times (\frac{1}{1000}, 1) \times (\frac{1}{1000}, 1) \times (\frac{1}{1000}, 1)$

#	Alg.	Parameters	Dim.	CPU [s]	RMSE	min err.	max err.
37	A/G/P-V 2025 (A1)	1e-09,1	576	0.0574	5.44e-10	1.3e-13	3.04e-09
	A/G/P-V 2025 (A2)	1e-15,3	576	0.237	2.5e-09	3.19e-14	1.45e-08
	MDSPACK v1.1.0	1e-09,0.01	576	0.0429	5.45e-10	1.34e-13	3.05e-09
	P/P 2025	1,0.95,50,0.01,6,12,13	472	48.3	1.44e-05	3.39e-08	6.58e-05
	B/G 2025	1e-06,20	6.55e+04	4.8e+03	1.45e - 12	1.25e-16	2.13e - 11
	B/G 2025 (LR)	1e-09,20,4	2.31e+04	28.5	2.3e-12	2.78e - 17	4.96e-11
	TensorFlow		385	1.1e+03	0.00281	6.32e-06	0.00938

Table 38: Function #37: best model configuration and performances per methods.

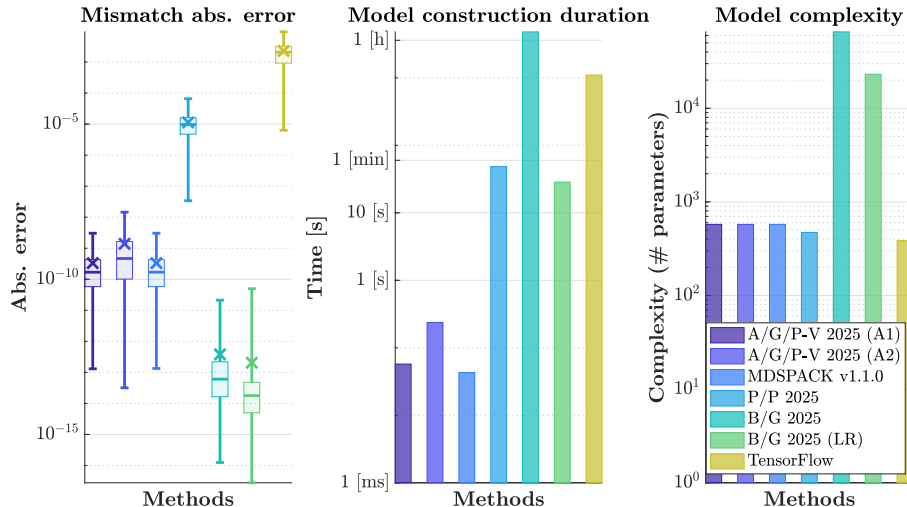


Figure 93: Function #37: graphical view of the best model performances.

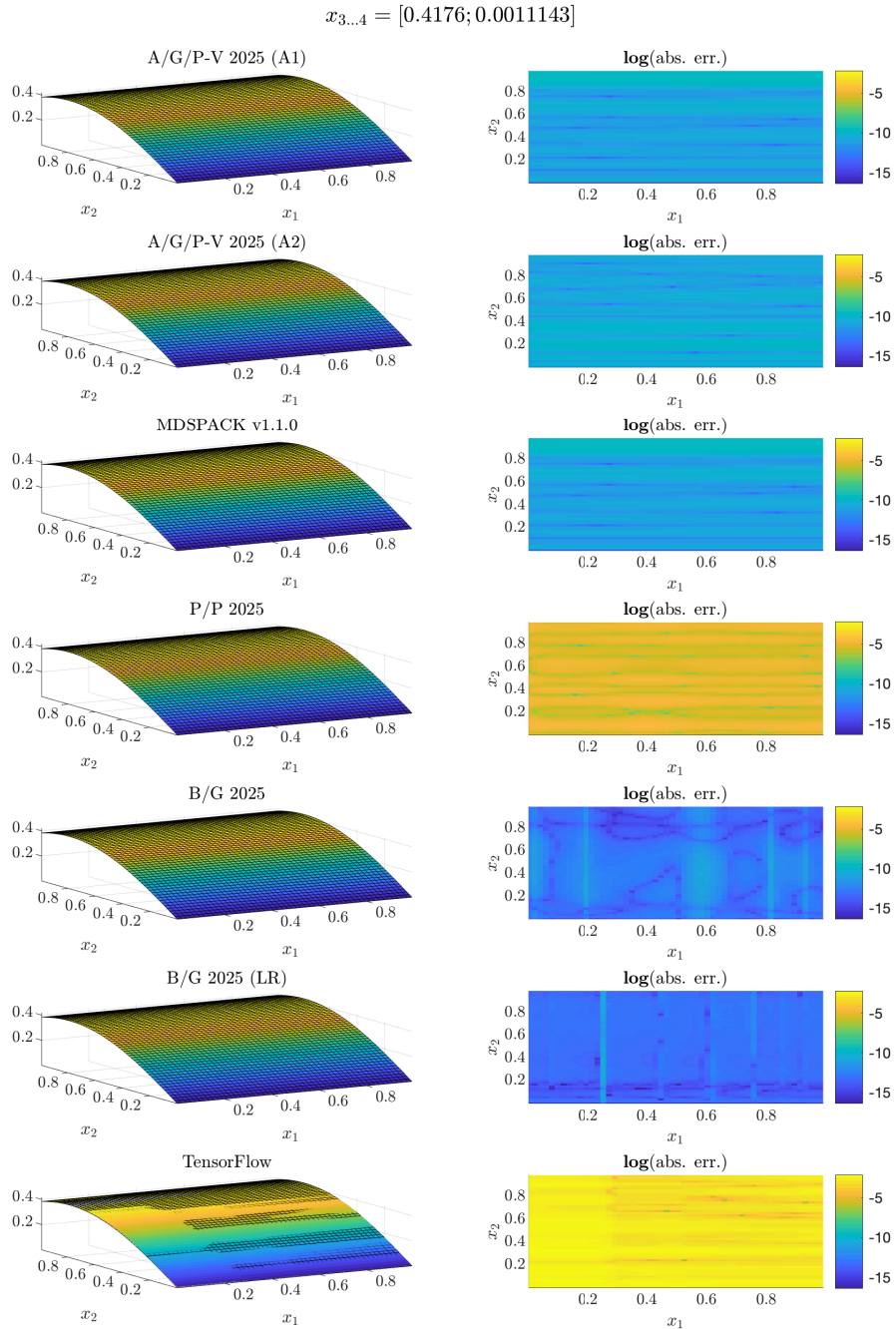


Figure 94: Function #37: left side, evaluation of the original (mesh) vs. approximated (coloured surface) and right side, absolute errors (in log-scale).

4.37.2 mLF detailed informations (M1)

Right interpolation points: $k_l = (2 \ 6 \ 2 \ 4)$, where $l = 1, \dots, n$.

$$\begin{aligned} {}^1\lambda_{j_1} &\in \mathbb{C}^2, \text{ linearly spaced between bounds} \\ {}^2\lambda_{j_2} &\in \mathbb{C}^6, \text{ linearly spaced between bounds} \\ {}^3\lambda_{j_3} &\in \mathbb{C}^2, \text{ linearly spaced between bounds} \\ {}^4\lambda_{j_4} &\in \mathbb{C}^4, \text{ linearly spaced between bounds} \end{aligned}$$

n-D Loewner matrix, barycentric weights and Lagrangian basis:

$$\begin{aligned} \mathbb{L} &\in \mathbb{C}^{96 \times 96} \\ \mathbf{c} &\in \mathbb{C}^{96} \\ \mathbf{w} &\in \mathbb{C}^{96} \\ \mathbf{c} \cdot \mathbf{w} &\in \mathbb{C}^{96} \\ \mathbf{Lag}(x_1, x_2, x_3, x_4) &\in \mathbb{C}^{96} \end{aligned}$$

4.38 Function #38 ($n = 3$ variables, tensor size: 1.65 MB)

$$\frac{x_1^9x_2^7 + x_1^3 + 5x_3^2}{5x_1^4 + 4x_1^2 + x_3x_2^3 + 1}$$

4.38.1 Setup and results overview

- Reference: A.C. Antoulas presentation, [none]
- Domain: \mathbb{R}
- Tensor size: 1.65 MB (60^3 points)
- Bounds: $(-\frac{11}{10}, \frac{11}{10}) \times (-\frac{11}{10}, \frac{11}{10}) \times (-\frac{11}{10}, \frac{11}{10})$

#	Alg.	Parameters	Dim.	CPU [s]	RMSE	min err.	max err.
38	A/G/P-V 2025 (A1)	1e-06,3	1.2e+03	0.0787	0.00237	4.56e-08	0.02
	A/G/P-V 2025 (A2)	1e-15,3	300	0.713	0.0454	6.33e-08	0.243
	MDSPACK v1.1.0	1e-06,0.0001	1.2e+03	0.0755	0.0024	4.84e-08	0.0203
	P/P 2025	1,1,50,0.01,4,6,9	166	23.3	4.04	0.00734	68.7
	B/G 2025	1e-09,20	6.6e+03	883	1.67e - 09	8.74e - 15	1.76e - 08
	B/G 2025 (LR)	1e-06,20,4	1.71e+04	495	9.3	6.07e-09	143
	TensorFlow		321	1.12e+03	4.7	0.000433	81.3

Table 39: Function #38: best model configuration and performances per methods.

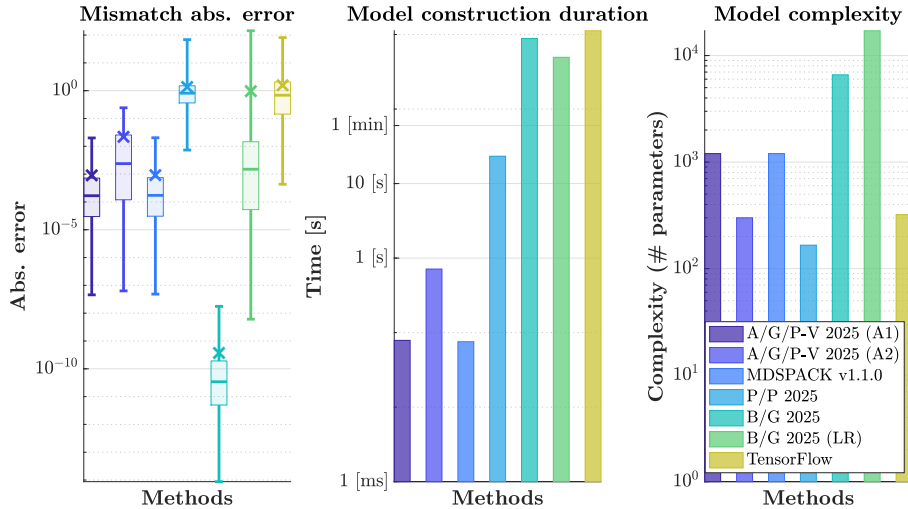


Figure 95: Function #38: graphical view of the best model performances.

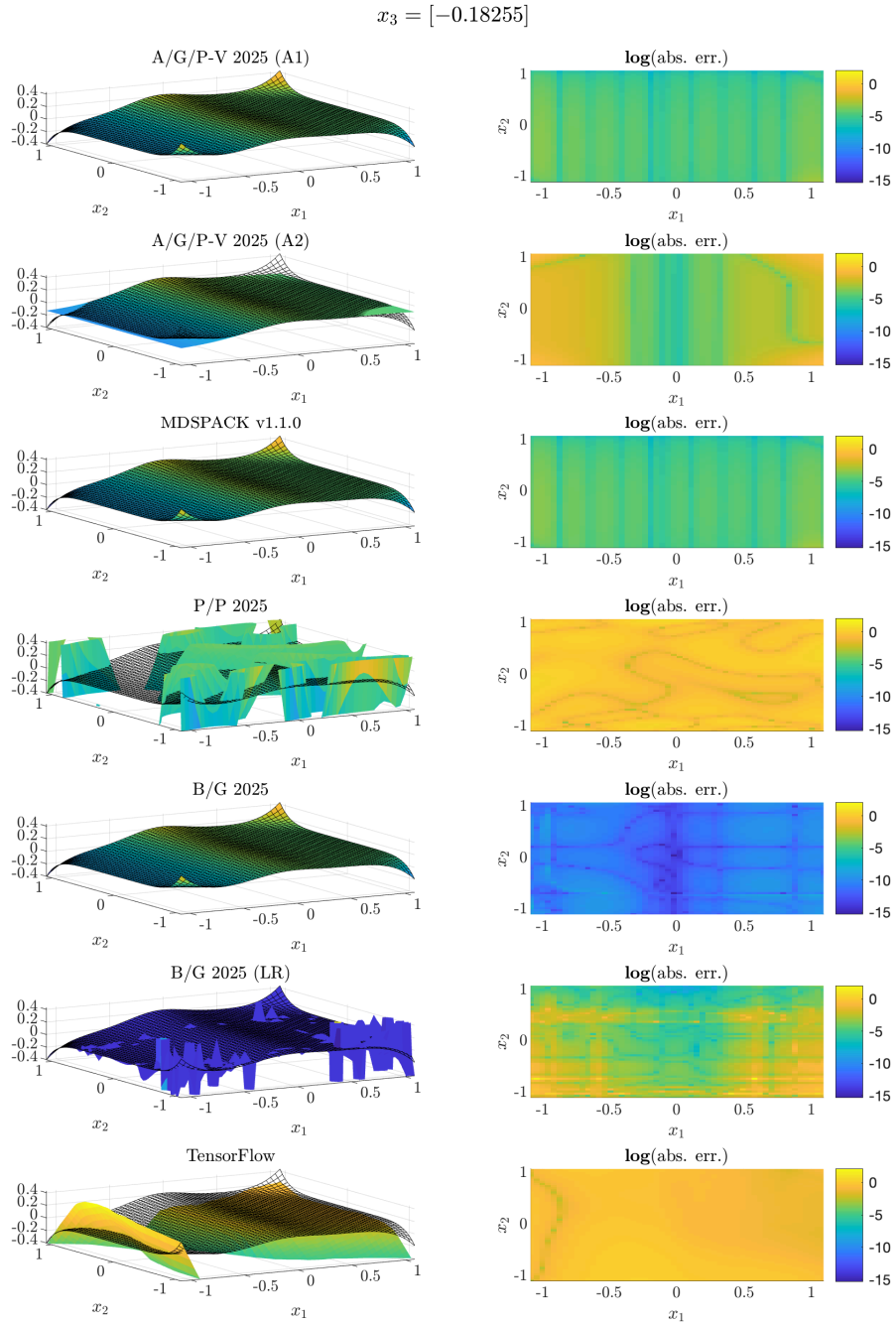


Figure 96: Function #38: left side, evaluation of the original (mesh) vs. approximated (coloured surface) and right side, absolute errors (in log-scale).

4.38.2 mLF detailed informations (M1)

Right interpolation points: $k_l = (10 \quad 8 \quad 3)$, where $l = 1, \dots, n$.

$$\begin{aligned} {}^1\lambda_{j_1} &\in \mathbb{C}^{10}, \text{ linearly spaced between bounds} \\ {}^2\lambda_{j_2} &\in \mathbb{C}^8, \text{ linearly spaced between bounds} \\ {}^3\lambda_{j_3} &\in \mathbb{C}^3, \text{ linearly spaced between bounds} \end{aligned}$$

n -D Loewner matrix, barycentric weights and Lagrangian basis:

$$\begin{aligned} \mathbb{L} &\in \mathbb{C}^{240 \times 240} \\ \mathbf{c} &\in \mathbb{C}^{240} \\ \mathbf{w} &\in \mathbb{C}^{240} \\ \mathbf{c} \cdot \mathbf{w} &\in \mathbb{C}^{240} \\ \mathbf{Lag}(x_1, x_2, x_3) &\in \mathbb{C}^{240} \end{aligned}$$

4.39 Function #39 ($n = 3$ variables, tensor size: 500 KB)

$$\frac{x_3 + x_1^4}{x_1^3 + x_2^2 + 1}$$

4.39.1 Setup and results overview

- Reference: Personal communication, [none]
- Domain: \mathbb{R}
- Tensor size: 500 KB (40^3 points)
- Bounds: $(\frac{1}{10}, 10) \times (\frac{1}{10}, 10) \times (\frac{1}{10}, 10)$

#	Alg.	Parameters	Dim.	CPU [s]	RMSE	min err.	max err.
39	A/G/P-V 2025 (A1)	0.001,2	150	0.0321	2.69e-12	0	4.03e-11
	A/G/P-V 2025 (A2)	1e-15,2	480	0.549	1.06e-12	0	1.14e-11
	MDSPACK v1.1.0	1e-14,0.0001	150	0.033	2.54e-12	2.22e-15	1.82e-11
	P/P 2025	1,1,50,0.01,10,6,21	760	26.1	0.00359	2.94e-06	0.041
	B/G 2025	0.001,20	600	41.7	6.65e - 14	0	6.46e - 13
	B/G 2025 (LR)	1e-06,20,5	500	9.26	5.42e-13	0	5.83e-12
	TensorFlow		321	307	1.23	0.0073	3.52

Table 40: Function #39: best model configuration and performances per methods.

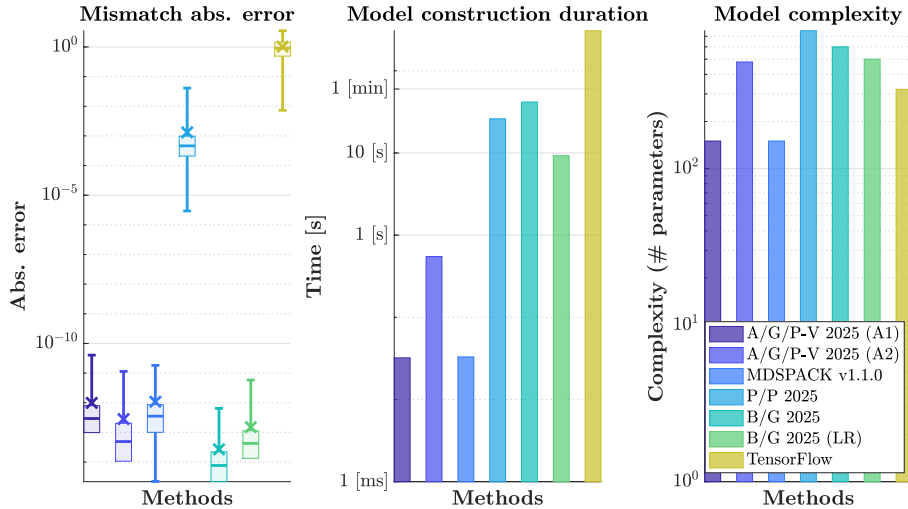


Figure 97: Function #39: graphical view of the best model performances.

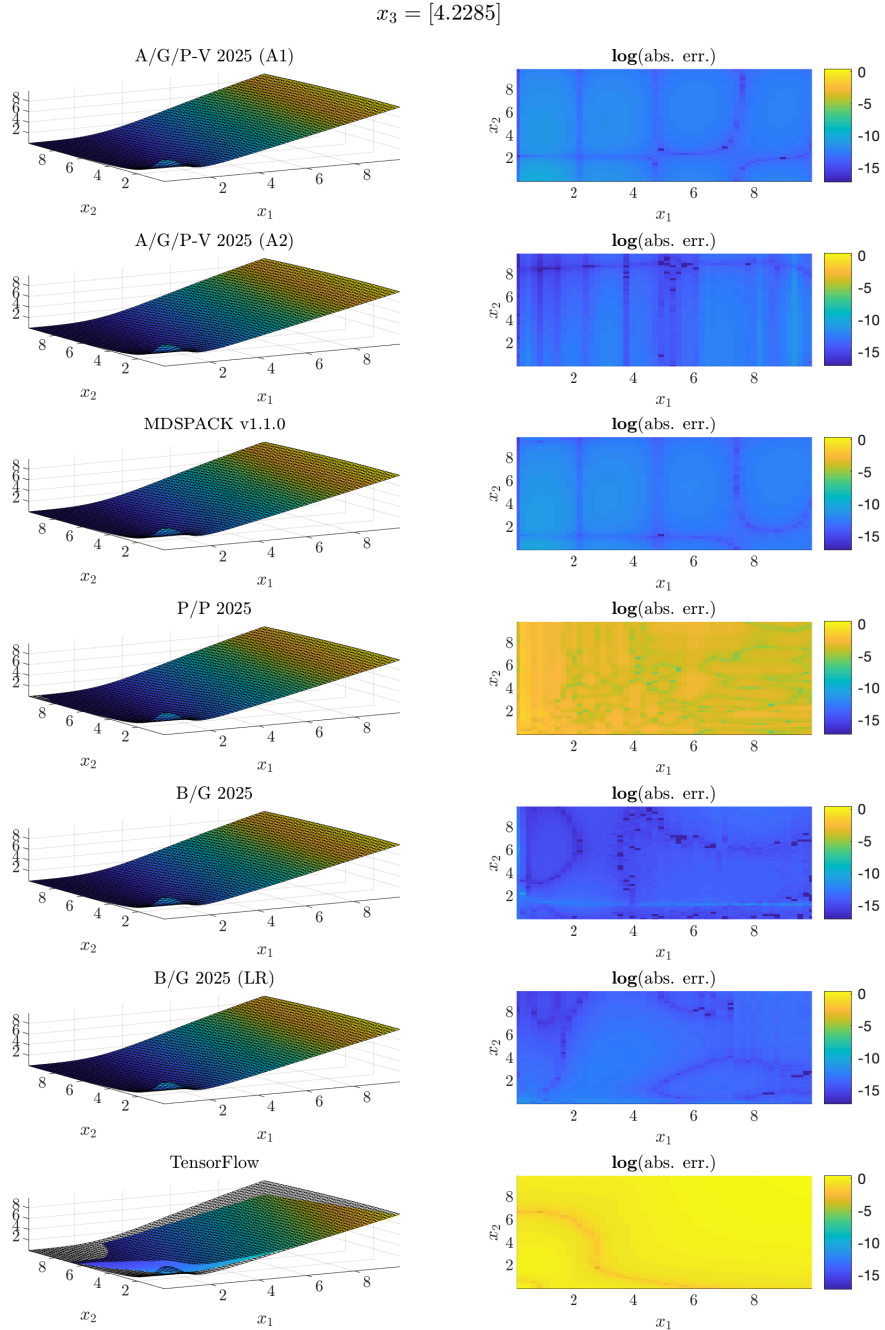


Figure 98: Function #39: left side, evaluation of the original (mesh) vs. approximated (coloured surface) and right side, absolute errors (in log-scale).

4.39.2 mLF detailed informations (M1)

Right interpolation points: $k_l = (\begin{array}{ccc} 5 & 3 & 2 \end{array})$, where $l = 1, \dots, n$.

$$\begin{aligned}\lambda_{j_1} &\in \mathbb{C}^5, \text{ linearly spaced between bounds} \\ \lambda_{j_2} &\in \mathbb{C}^3, \text{ linearly spaced between bounds} \\ \lambda_{j_3} &\in \mathbb{C}^2, \text{ linearly spaced between bounds}\end{aligned}$$

n -D Loewner matrix, barycentric weights and Lagrangian basis:

$$\begin{aligned}\mathbb{L} &\in \mathbb{C}^{30 \times 30} \\ \mathbf{c} &\in \mathbb{C}^{30} \\ \mathbf{w} &\in \mathbb{C}^{30} \\ \mathbf{c} \cdot \mathbf{w} &\in \mathbb{C}^{30} \\ \mathbf{Lag}(x_1, x_2, x_3) &\in \mathbb{C}^{30}\end{aligned}$$

4.40 Function #40 ($n = 4$ variables, tensor size: 19.5 MB)

$$\frac{x_3 x_1}{x_1^2 + x_2 + x_3^2 + 1} + x_4^3$$

4.40.1 Setup and results overview

- Reference: Personal communication, [none]
- Domain: \mathbb{R}
- Tensor size: 19.5 MB (40^4 points)
- Bounds: $(1 \ 4) \times (1 \ 4) \times (1 \ 4) \times (1 \ 4)$

#	Alg.	Parameters	Dim.	CPU [s]	RMSE	min err.	max err.
40	A/G/P-V 2025 (A1)	0.0001,3	432	0.67	9.08e-14	0	2.7e-13
	A/G/P-V 2025 (A2)	1e-15,1	432	2.31	3.2e - 14	0	7.82e - 14
	MDSPACK v1.1.0	0.0001,0.01	432	0.563	9.33e-14	0	2.84e-13
	P/P 2025	1,0.95,50,0.01,4,12,9	256	1.54e+03	9.59e-05	5.78e-07	0.000463
	B/G 2025	NaN	NaN	NaN	NaN	NaN	NaN
	B/G 2025 (LR)	1e-09,20,4	4.5e+03	452	1.24e-10	1.24e-13	1.08e-09
	TensorFlow		385	137	0.113	7.41e-05	0.377

Table 41: Function #40: best model configuration and performances per methods.

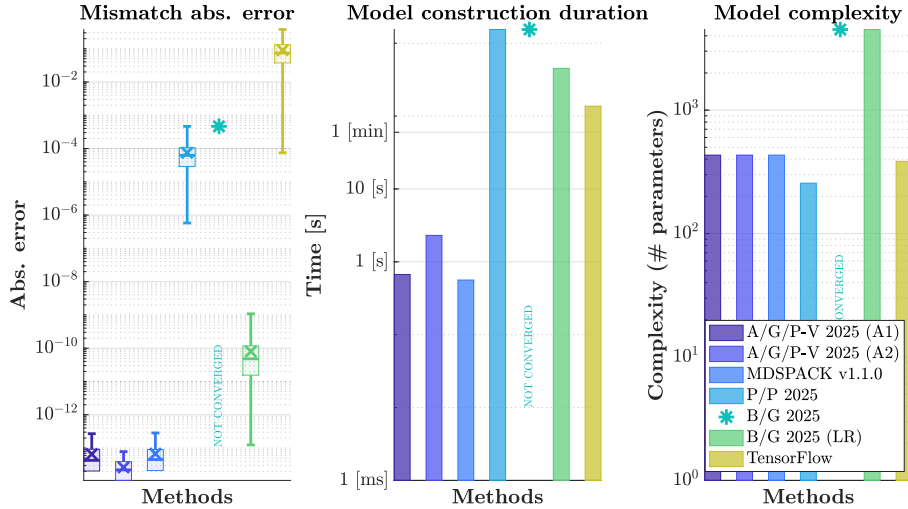


Figure 99: Function #40: graphical view of the best model performances.

$$x_{3..4} = [2.2511; 1.0003]$$

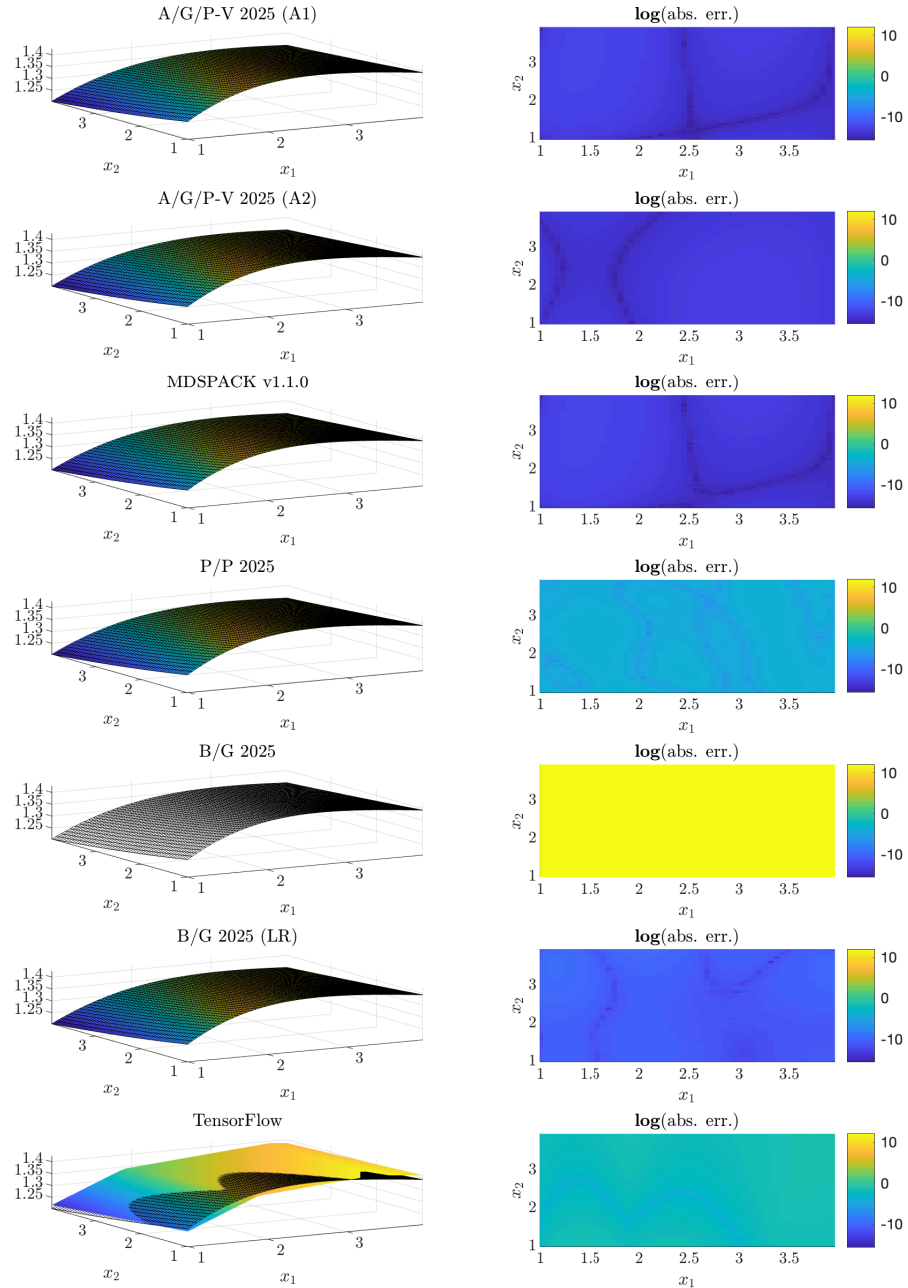


Figure 100: Function #40: left side, evaluation of the original (mesh) vs. approximated (coloured surface) and right side, absolute errors (in log-scale).

4.40.2 mLF detailed informations (M1)

Right interpolation points: $k_l = (3 \ 2 \ 3 \ 4)$, where $l = 1, \dots, n$.

$$\begin{aligned} {}^1\lambda_{j_1} &\in \mathbb{C}^3, \text{ linearly spaced between bounds} \\ {}^2\lambda_{j_2} &\in \mathbb{C}^2, \text{ linearly spaced between bounds} \\ {}^3\lambda_{j_3} &\in \mathbb{C}^3, \text{ linearly spaced between bounds} \\ {}^4\lambda_{j_4} &\in \mathbb{C}^4, \text{ linearly spaced between bounds} \end{aligned}$$

n-D Loewner matrix, barycentric weights and Lagrangian basis:

$$\begin{aligned} \mathbb{L} &\in \mathbb{C}^{72 \times 72} \\ \mathbf{c} &\in \mathbb{C}^{72} \\ \mathbf{w} &\in \mathbb{C}^{72} \\ \mathbf{c} \cdot \mathbf{w} &\in \mathbb{C}^{72} \\ \mathbf{Lag}(x_1, x_2, x_3, x_4) &\in \mathbb{C}^{72} \end{aligned}$$

4.41 Function #41 ($n = 5$ variables, tensor size: 781 KB)

$$\frac{x_5^3 x_3 x_1 + x_3^2}{x_1^3 + x_2 x_3 + x_4}$$

4.41.1 Setup and results overview

- Reference: Personal communication, [none]
- Domain: \mathbb{R}
- Tensor size: 781 KB (10^5 points)
- Bounds: $(\frac{1}{10}, 1) \times (\frac{1}{10}, 1) \times (\frac{1}{10}, 1) \times (\frac{1}{10}, 1) \times (\frac{1}{10}, 1)$

#	Alg.	Parameters	Dim.	CPU [s]	RMSE	min err.	max err.
41	A/G/P-V 2025 (A1)	0.001,3	1.34e+03	0.0915	5.2e - 14	0	3.43e-13
	A/G/P-V 2025 (A2)	1e-15,1	1.34e+03	0.481	1.44e-13	0	7.2e-13
	MDSPACK v1.1.0	0.001,0.0001	1.34e+03	0.0335	5.26e-14	0	3.02e - 13
	P/P 2025	1,1,50,0.01,4,12,9	292	16.6	0.00344	3.73e-06	0.0192
	B/G 2025	0.001,20	1.4e+04	136	4.23e-13	0	9.39e-12
	B/G 2025 (LR)	0.001,20,3	4.2e+03	37	0.000927	1.56e-07	0.0134
	TensorFlow	NaN	NaN	NaN	NaN	NaN	NaN

Table 42: Function #41: best model configuration and performances per methods.

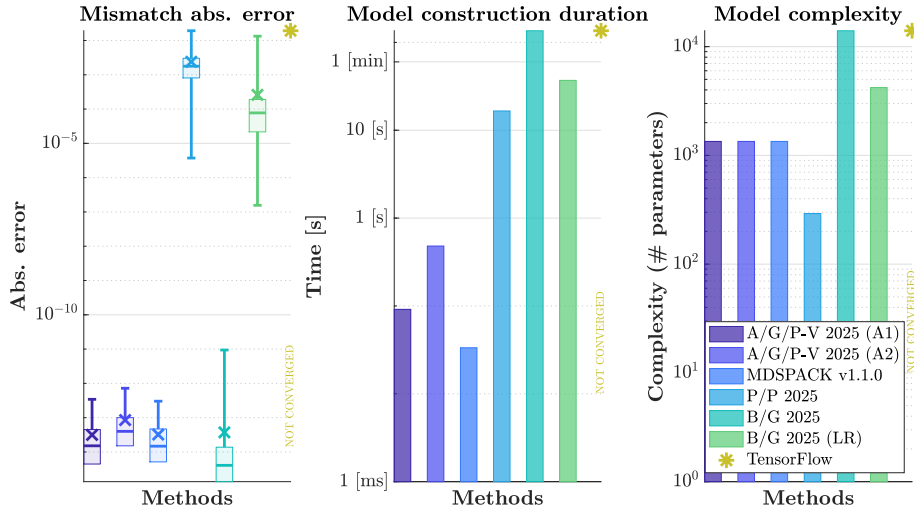


Figure 101: Function #41: graphical view of the best model performances.

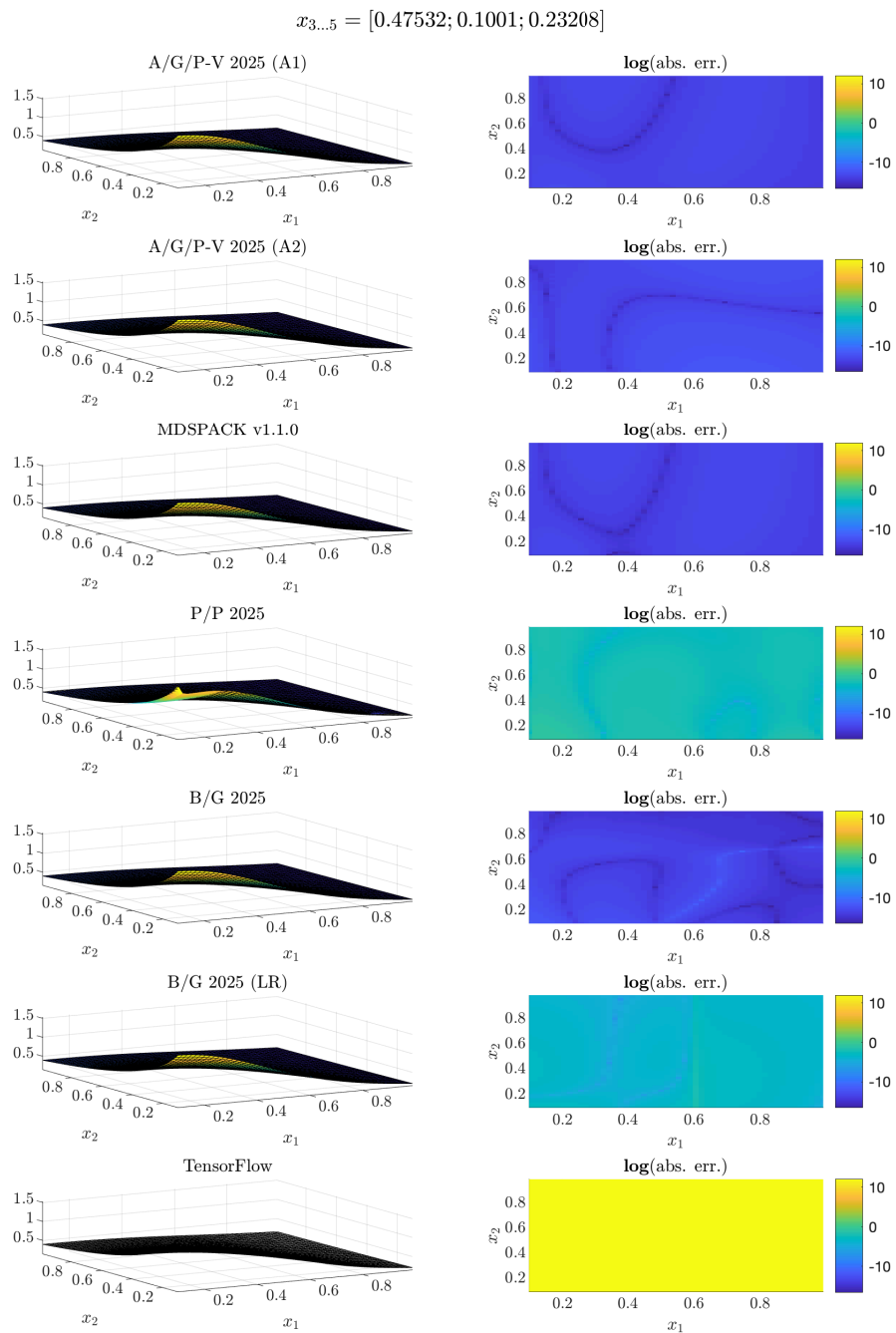


Figure 102: Function #41: left side, evaluation of the original (mesh) vs. approximated (coloured surface) and right side, absolute errors (in log-scale).

4.41.2 mLF detailed informations (M1)

Right interpolation points: $k_l = (4 \ 2 \ 3 \ 2 \ 4)$, where $l = 1, \dots, n$.

$$\begin{aligned} {}^1\lambda_{j_1} &\in \mathbb{C}^4, \text{ linearly spaced between bounds} \\ {}^2\lambda_{j_2} &\in \mathbb{C}^2, \text{ linearly spaced between bounds} \\ {}^3\lambda_{j_3} &\in \mathbb{C}^3, \text{ linearly spaced between bounds} \\ {}^4\lambda_{j_4} &\in \mathbb{C}^2, \text{ linearly spaced between bounds} \\ {}^5\lambda_{j_5} &\in \mathbb{C}^4, \text{ linearly spaced between bounds} \end{aligned}$$

n-D Loewner matrix, barycentric weights and Lagrangian basis:

$$\begin{aligned} \mathbb{L} &\in \mathbb{C}^{192 \times 192} \\ \mathbf{c} &\in \mathbb{C}^{192} \\ \mathbf{w} &\in \mathbb{C}^{192} \\ \mathbf{c} \cdot \mathbf{w} &\in \mathbb{C}^{192} \\ \mathbf{Lag}(x_1, x_2, x_3, x_4, x_5) &\in \mathbb{C}^{192} \end{aligned}$$

4.42 Function #42 ($n = 6$ variables, tensor size: 7.63 MB)

$$\frac{x_1 + x_3 - \sqrt{2}x_6^2}{x_1^4 + x_2x_3 + x_4^3 + x_5^2 + x_6}$$

4.42.1 Setup and results overview

- Reference: Personal communication, [none]
- Domain: \mathbb{R}
- Tensor size: 7.63 MB (10^6 points)
- Bounds: $(\frac{1}{10}, 1) \times (\frac{1}{10}, 1)$

#	Alg.	Parameters	Dim.	CPU [s]	RMSE	min err.	max err.
42	A/G/P-V 2025 (A1)	0.0001,2	5.76e+03	0.446	4.17e - 14	0	3.05e - 13
	A/G/P-V 2025 (A2)	1e-15,1	5.76e+03	1.43	2.59e-13	1.39e-17	1.98e-12
	MDSPACK v1.1.0	0.0001,0.0001	5.76e+03	0.369	4.21e-14	0	3.06e-13
	P/P 2025	1,1,50,0.01,4,12,9	328	368	0.00156	4.4e-06	0.00637
	B/G 2025	NaN	NaN	NaN	NaN	NaN	NaN
	B/G 2025 (LR)	0.001,20,3	5.18e+06	2.26e+03	0.231	0.000987	1.1
	TensorFlow	NaN	NaN	NaN	NaN	NaN	NaN

Table 43: Function #42: best model configuration and performances per methods.

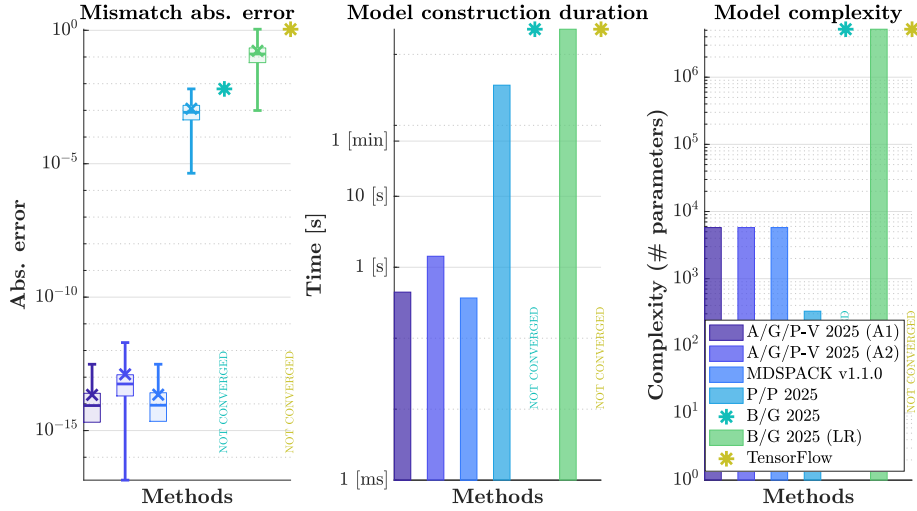


Figure 103: Function #42: graphical view of the best model performances.

$$x_{3..6} = [0.47532; 0.1001; 0.23208; 0.26763]$$

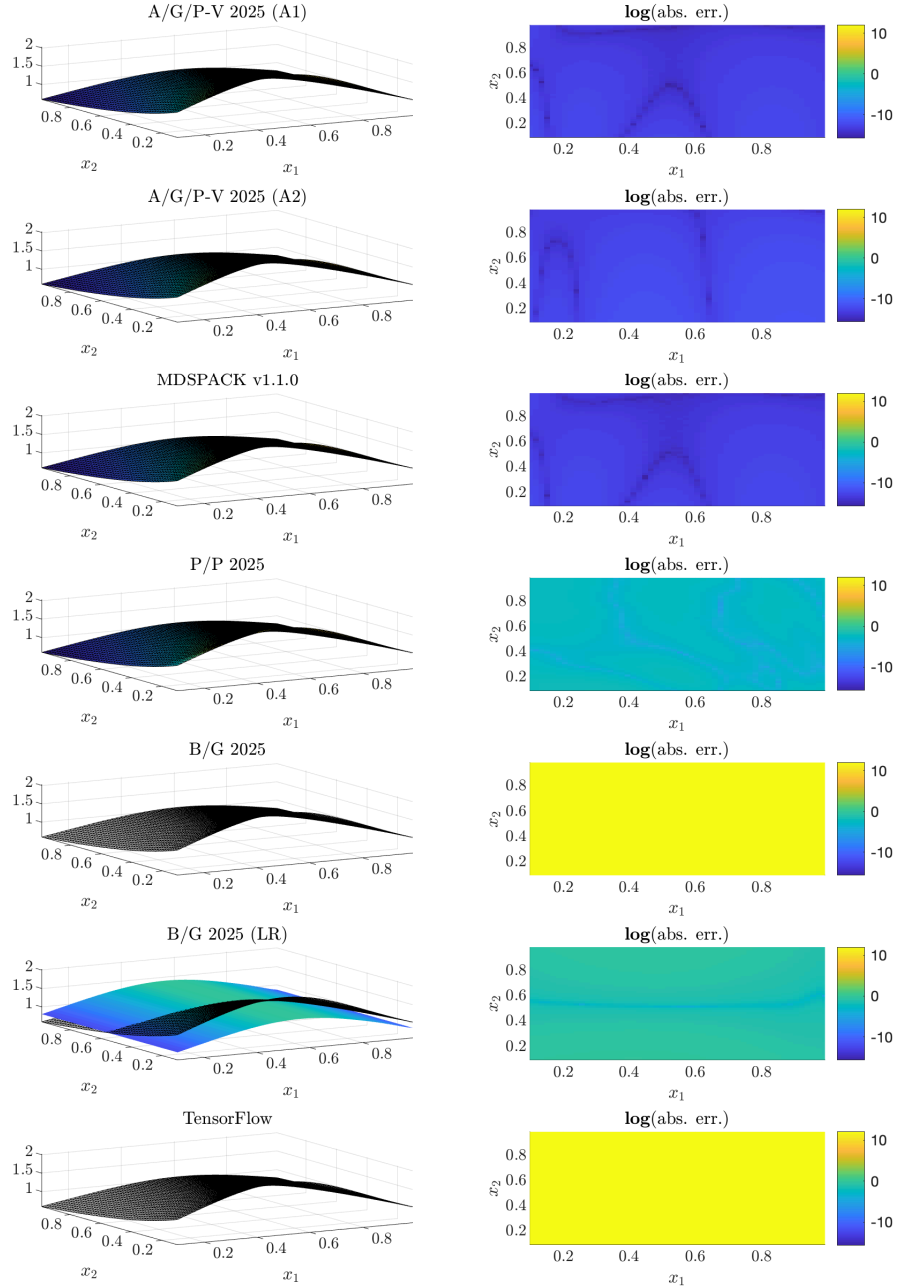


Figure 104: Function #42: left side, evaluation of the original (mesh) vs. approximated (coloured surface) and right side, absolute errors (in log-scale).

4.42.2 mLF detailed informations (M1)

Right interpolation points: $k_l = (5 \ 2 \ 2 \ 4 \ 3 \ 3)$, where $l = 1, \dots, n$.

$$\begin{aligned} {}^1\lambda_{j_1} &\in \mathbb{C}^5, \text{ linearly spaced between bounds} \\ {}^2\lambda_{j_2} &\in \mathbb{C}^2, \text{ linearly spaced between bounds} \\ {}^3\lambda_{j_3} &\in \mathbb{C}^2, \text{ linearly spaced between bounds} \\ {}^4\lambda_{j_4} &\in \mathbb{C}^4, \text{ linearly spaced between bounds} \\ {}^5\lambda_{j_5} &\in \mathbb{C}^3, \text{ linearly spaced between bounds} \\ {}^6\lambda_{j_6} &\in \mathbb{C}^3, \text{ linearly spaced between bounds} \end{aligned}$$

n -D Loewner matrix, barycentric weights and Lagrangian basis:

$$\begin{aligned} \mathbb{L} &\in \mathbb{C}^{720 \times 720} \\ \mathbf{c} &\in \mathbb{C}^{720} \\ \mathbf{w} &\in \mathbb{C}^{720} \\ \mathbf{c} \cdot \mathbf{w} &\in \mathbb{C}^{720} \\ \mathbf{Lag}(x_1, x_2, x_3, x_4, x_5, x_6) &\in \mathbb{C}^{720} \end{aligned}$$

4.43 Function #43 ($n = 7$ variables, tensor size: 76.3 MB)

$$\frac{x_3x_2^3 + 1}{x_1^4 + x_2^2x_3 + x_4^2 + x_5 + x_6^3 + x_7}$$

4.43.1 Setup and results overview

- Reference: Personal communication, [none]
- Domain: \mathbb{R}
- Tensor size: 76.3 MB (10^7 points)
- Bounds: $(1 \ 10) \times (1 \ 10)$

#	Alg.	Parameters	Dim.	CPU [s]	RMSE	min err.	max err.
43	A/G/P-V 2025 (A1)	0.0001,1	1.73e + 04	5.58	1.41e-12	1.76e-16	1.6e-11
	A/G/P-V 2025 (A2)	1e-15,1	1.73e+04	12.5	2.39e - 13	1.21e - 17	2.18e - 12
	MDSPACK v1.1.0	0.0001,1e-06	1.73e+04	5.72	1.4e-12	1.49e-16	1.62e-11
	P/P 2025	NaN	NaN	NaN	NaN	NaN	NaN
	B/G 2025	NaN	NaN	NaN	NaN	NaN	NaN
	B/G 2025 (LR)	NaN	NaN	NaN	NaN	NaN	NaN
	TensorFlow	NaN	NaN	NaN	NaN	NaN	NaN

Table 44: Function #43: best model configuration and performances per methods.

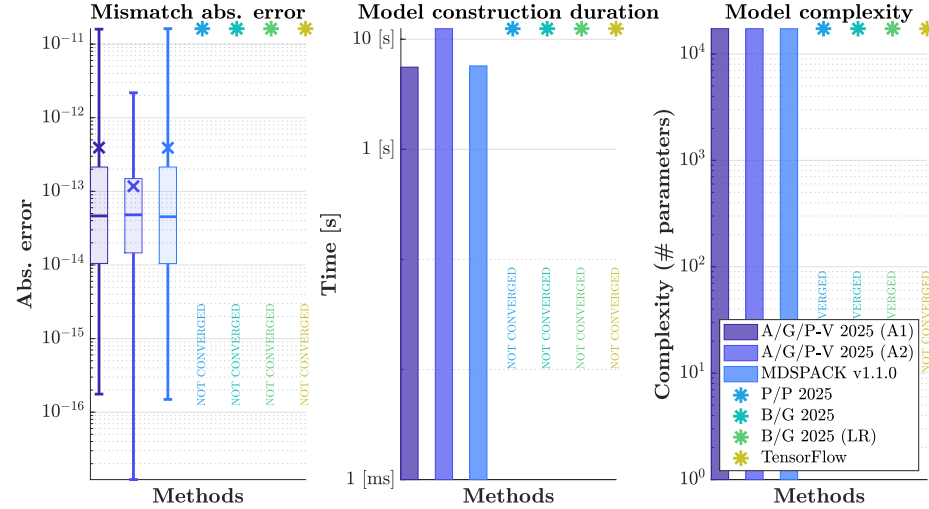


Figure 105: Function #43: graphical view of the best model performances.

$$x_{3..7} = [4.7532; 1.001; 2.3208; 2.6763; 4.5709]$$

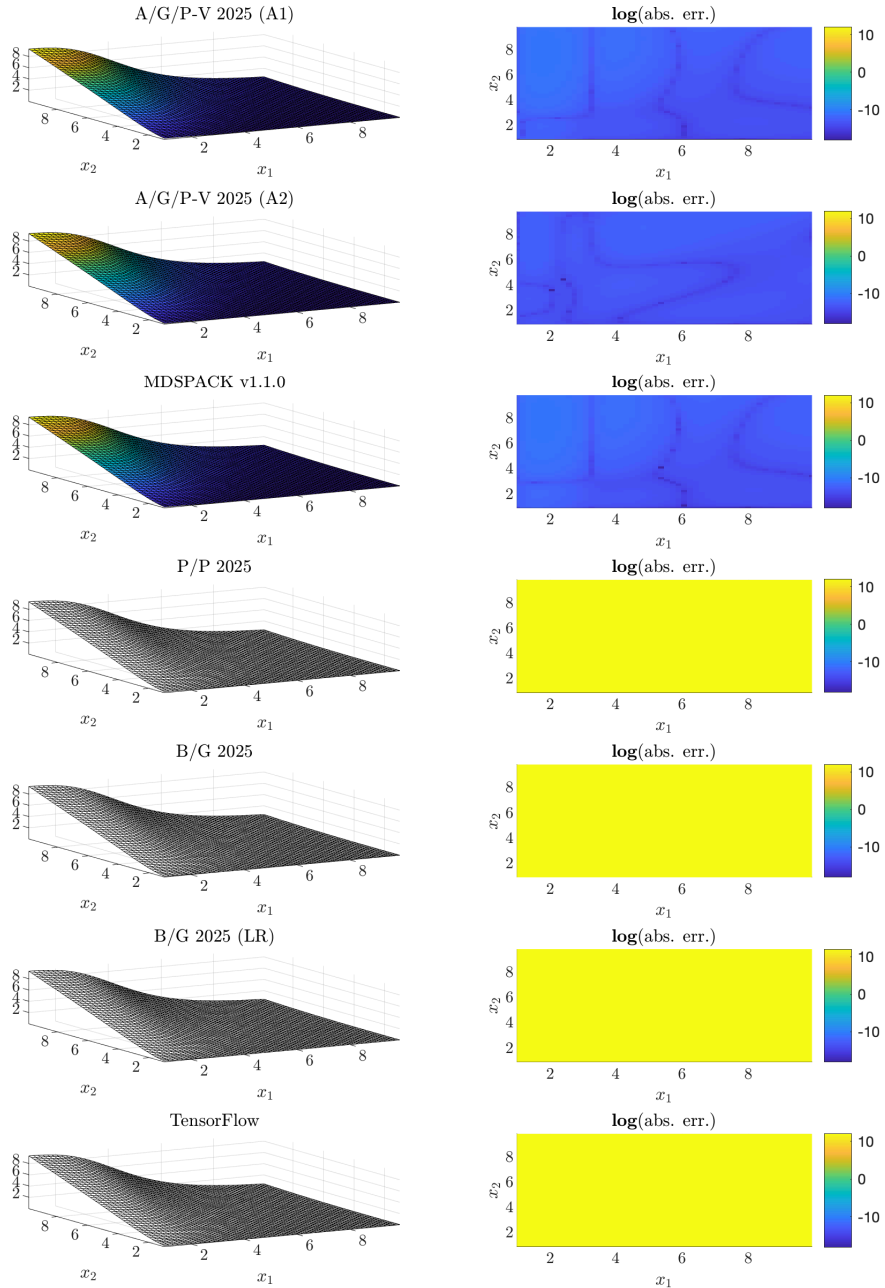


Figure 106: Function #43: left side, evaluation of the original (mesh) vs. approximated (coloured surface) and right side, absolute errors (in log-scale).

4.43.2 mLF detailed informations (M1)

Right interpolation points: $k_l = (5 \ 4 \ 2 \ 3 \ 2 \ 4 \ 2)$, where $l = 1, \dots, n$.

$$\begin{aligned} {}^1\lambda_{j_1} &\in \mathbb{C}^5, \text{ linearly spaced between bounds} \\ {}^2\lambda_{j_2} &\in \mathbb{C}^4, \text{ linearly spaced between bounds} \\ {}^3\lambda_{j_3} &\in \mathbb{C}^2, \text{ linearly spaced between bounds} \\ {}^4\lambda_{j_4} &\in \mathbb{C}^3, \text{ linearly spaced between bounds} \\ {}^5\lambda_{j_5} &\in \mathbb{C}^2, \text{ linearly spaced between bounds} \\ {}^6\lambda_{j_6} &\in \mathbb{C}^4, \text{ linearly spaced between bounds} \\ {}^7\lambda_{j_7} &\in \mathbb{C}^2, \text{ linearly spaced between bounds} \end{aligned}$$

n-D Loewner matrix, barycentric weights and Lagrangian basis:

$$\begin{aligned} \mathbb{L} &\in \mathbb{C}^{1920 \times 1920} \\ \mathbf{c} &\in \mathbb{C}^{1920} \\ \mathbf{w} &\in \mathbb{C}^{1920} \\ \mathbf{c} \cdot \mathbf{w} &\in \mathbb{C}^{1920} \\ \mathbf{Lag}(x_1, x_2, x_3, x_4, x_5, x_6, x_7) &\in \mathbb{C}^{1920} \end{aligned}$$

4.44 Function #44 ($n = 8$ variables, tensor size: 763 MB)

$$\frac{1}{x_1^4 + x_2^2 x_3 + x_4^2 + x_5 + x_6 + x_7 + x_8}$$

4.44.1 Setup and results overview

- Reference: Personal communication, [none]
- Domain: \mathbb{R}
- Tensor size: 763 MB (10^8 points)
- Bounds: $(\frac{1}{10}, 20) \times (\frac{1}{10}, 20)$

#	Alg.	Parameters	Dim.	CPU [s]	RMSE	min err.	max err.
44	A/G/P-V 2025 (A1)	0.0001,2	1.44e+04	183	5.96e-13	8.47e - 22	1.06e-11
	A/G/P-V 2025 (A2)	1e-15,3	1.44e+04	377	1.6e - 13	1.98e-18	3.2e - 12
	MDSPACK v1.1.0	0.5,0.01	2.22e + 03	171	0.00194	1.87e-06	0.00987
	P/P 2025	NaN	NaN	NaN	NaN	NaN	NaN
	B/G 2025	NaN	NaN	NaN	NaN	NaN	NaN
	B/G 2025 (LR)	NaN	NaN	NaN	NaN	NaN	NaN
	TensorFlow	NaN	NaN	NaN	NaN	NaN	NaN

Table 45: Function #44: best model configuration and performances per methods.

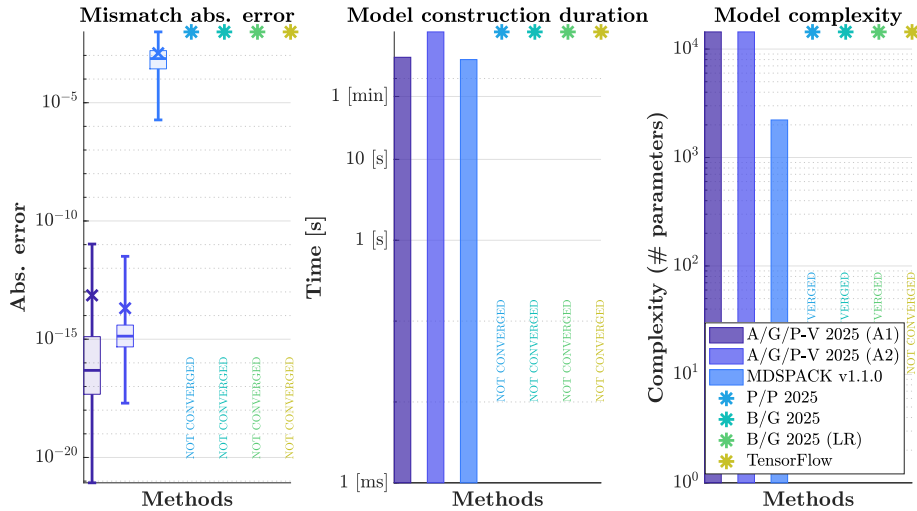


Figure 107: Function #44: graphical view of the best model performances.

$$x_{3..8} = [8.3987; 0.10228; 3.0204; 3.8066; 7.9957; 8.442]$$

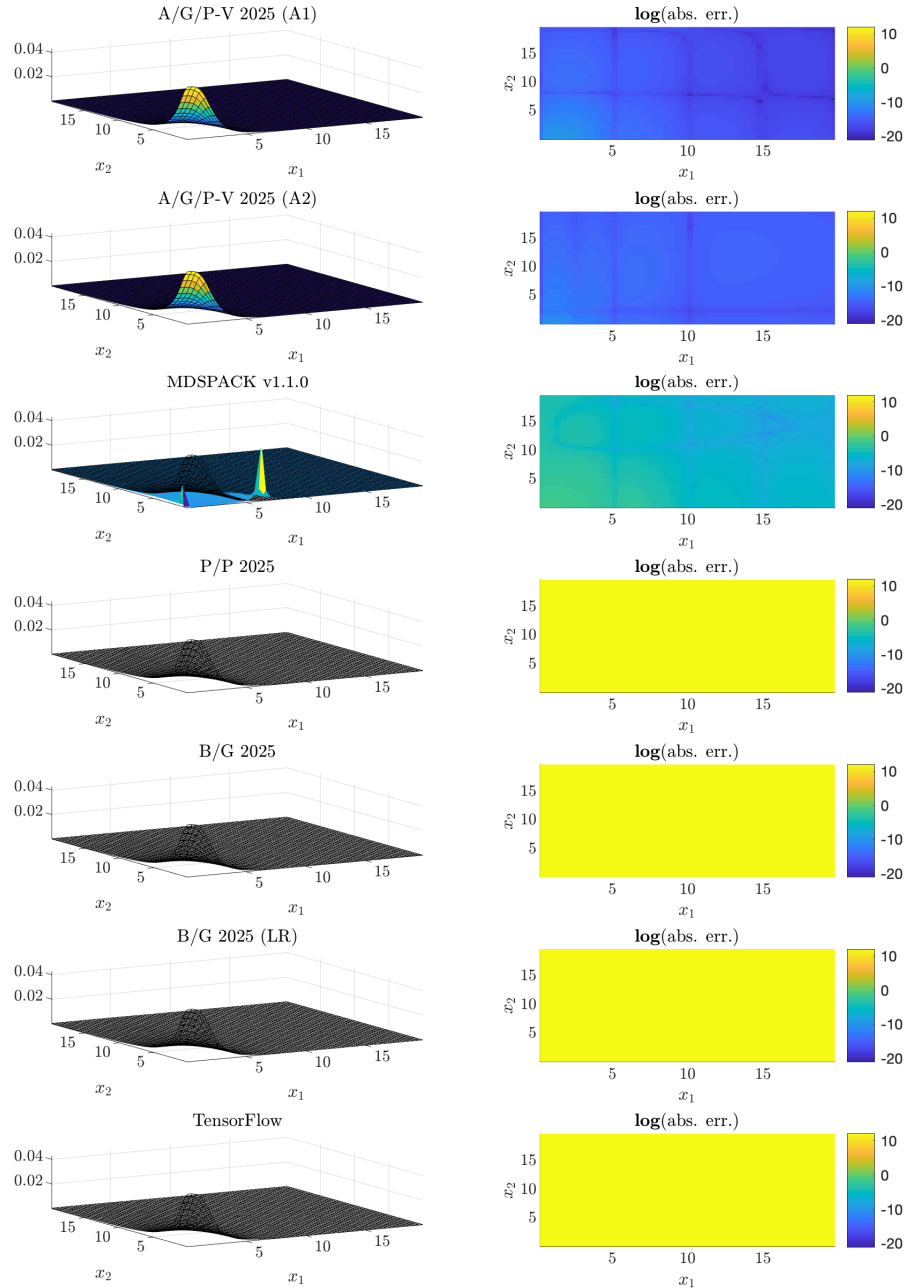


Figure 108: Function #44: left side, evaluation of the original (mesh) vs. approximated (coloured surface) and right side, absolute errors (in log-scale).

4.44.2 mLF detailed informations (M1)

Right interpolation points: $k_l = (5 \ 3 \ 2 \ 3 \ 2 \ 2 \ 2 \ 2)$, where $l = 1, \dots, n$.

$$\begin{aligned} {}^1\lambda_{j_1} &\in \mathbb{C}^5, \text{ linearly spaced between bounds} \\ {}^2\lambda_{j_2} &\in \mathbb{C}^3, \text{ linearly spaced between bounds} \\ {}^3\lambda_{j_3} &\in \mathbb{C}^2, \text{ linearly spaced between bounds} \\ {}^4\lambda_{j_4} &\in \mathbb{C}^3, \text{ linearly spaced between bounds} \\ {}^5\lambda_{j_5} &\in \mathbb{C}^2, \text{ linearly spaced between bounds} \\ {}^6\lambda_{j_6} &\in \mathbb{C}^2, \text{ linearly spaced between bounds} \\ {}^7\lambda_{j_7} &\in \mathbb{C}^2, \text{ linearly spaced between bounds} \\ {}^8\lambda_{j_8} &\in \mathbb{C}^2, \text{ linearly spaced between bounds} \end{aligned}$$

n-D Loewner matrix, barycentric weights and Lagrangian basis:

$$\begin{aligned} \mathbb{L} &\in \mathbb{C}^{1440 \times 1440} \\ \mathbf{c} &\in \mathbb{C}^{1440} \\ \mathbf{w} &\in \mathbb{C}^{1440} \\ \mathbf{c} \cdot \mathbf{w} &\in \mathbb{C}^{1440} \\ \mathbf{Lag}(x_1, x_2, x_3, x_4, x_5, x_6, x_7, x_8) &\in \mathbb{C}^{1440} \end{aligned}$$

4.45 Function #45 ($n = 9$ variables, tensor size: 76.9 MB)

$$\frac{1}{x_1^2 + x_2^2 x_3 + x_4^2 + x_5 + x_6 + x_7 + x_8 + x_9}$$

4.45.1 Setup and results overview

- Reference: Personal communication, [none]
- Domain: \mathbb{R}
- Tensor size: 76.9 MB (6^9 points)
- Bounds: $(1 \ 5) \times (1 \ 5)$

#	Alg.	Parameters	Dim.	CPU [s]	RMSE	min err.	max err.
45	A/G/P-V 2025 (A1)	0.01,1	1.9e + 04	9.81	3.37e - 17	0	1.49e - 16
	A/G/P-V 2025 (A2)	1e-15,1	1.9e+04	20.2	1.66e-16	0	4.94e-16
	MDSPACK v1.1.0	0.01,0.01	1.9e+04	10.2	5.21e-17	0	3.19e-16
	P/P 2025	NaN	NaN	NaN	NaN	NaN	NaN
	B/G 2025	NaN	NaN	NaN	NaN	NaN	NaN
	B/G 2025 (LR)	NaN	NaN	NaN	NaN	NaN	NaN
	TensorFlow	NaN	NaN	NaN	NaN	NaN	NaN

Table 46: Function #45: best model configuration and performances per methods.

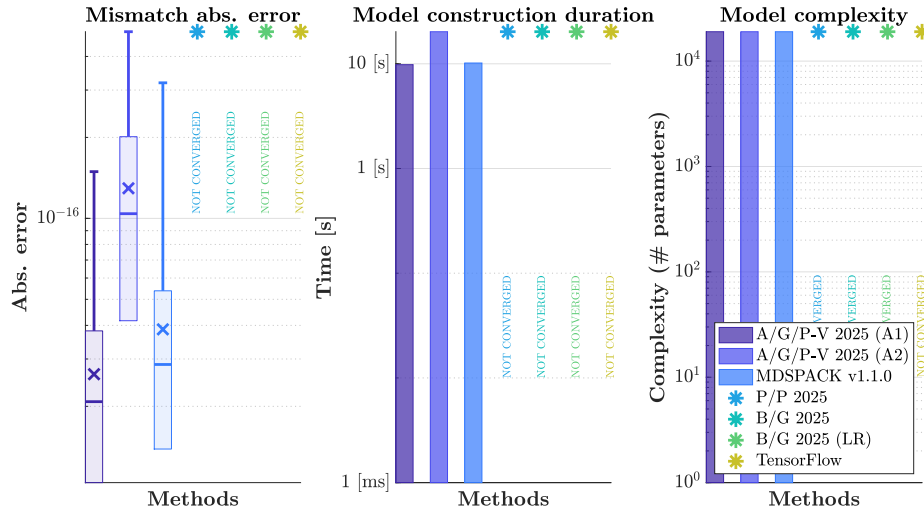


Figure 109: Function #45: graphical view of the best model performances.

$$x_{3..9} = [2.6681; 1.0005; 1.587; 1.745; 2.5871; 2.6768; 1.8178]$$

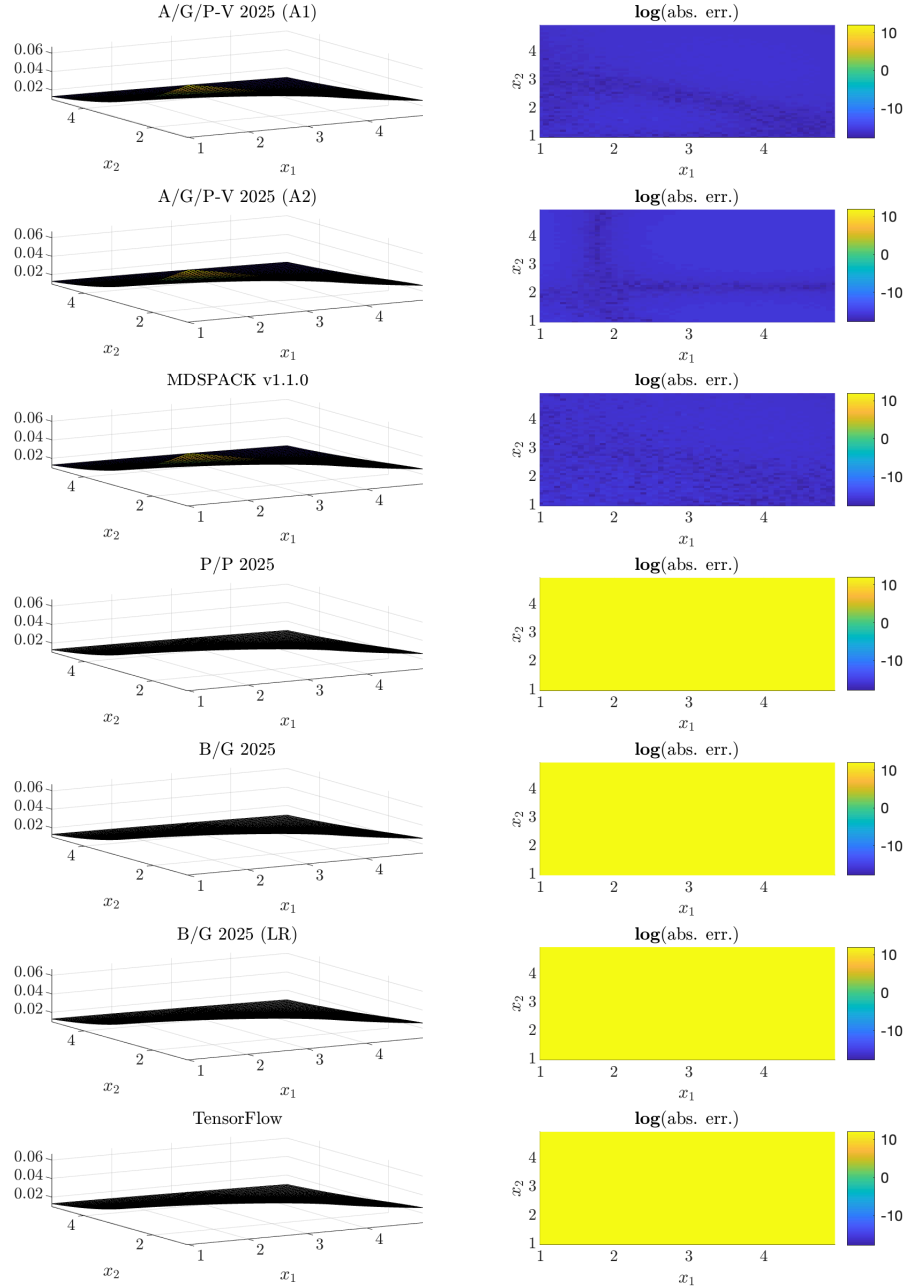


Figure 110: Function #45: left side, evaluation of the original (mesh) vs. approximated (coloured surface) and right side, absolute errors (in log-scale).

4.45.2 mLF detailed informations (M1)

Right interpolation points: $k_l = (3 \ 3 \ 2 \ 3 \ 2 \ 2 \ 2 \ 2 \ 2)$, where $l = 1, \dots, n$.

$$\begin{aligned} {}^1\lambda_{j_1} &\in \mathbb{C}^3, \text{ linearly spaced between bounds} \\ {}^2\lambda_{j_2} &\in \mathbb{C}^3, \text{ linearly spaced between bounds} \\ {}^3\lambda_{j_3} &\in \mathbb{C}^2, \text{ linearly spaced between bounds} \\ {}^4\lambda_{j_4} &\in \mathbb{C}^3, \text{ linearly spaced between bounds} \\ {}^5\lambda_{j_5} &\in \mathbb{C}^2, \text{ linearly spaced between bounds} \\ {}^6\lambda_{j_6} &\in \mathbb{C}^2, \text{ linearly spaced between bounds} \\ {}^7\lambda_{j_7} &\in \mathbb{C}^2, \text{ linearly spaced between bounds} \\ {}^8\lambda_{j_8} &\in \mathbb{C}^2, \text{ linearly spaced between bounds} \\ {}^9\lambda_{j_9} &\in \mathbb{C}^2, \text{ linearly spaced between bounds} \end{aligned}$$

n-D Loewner matrix, barycentric weights and Lagrangian basis:

$$\begin{aligned} \mathbb{L} &\in \mathbb{C}^{1728 \times 1728} \\ \mathbf{c} &\in \mathbb{C}^{1728} \\ \mathbf{w} &\in \mathbb{C}^{1728} \\ \mathbf{c} \cdot \mathbf{w} &\in \mathbb{C}^{1728} \\ \mathbf{Lag}(x_1, x_2, x_3, x_4, x_5, x_6, x_7, x_8, x_9) &\in \mathbb{C}^{1728} \end{aligned}$$

4.46 Function #46 ($n = 10$ variables, tensor size: 461 MB)

$$\frac{1}{x_1 + x_1^2 x_2 x_3 + x_4 + x_5 + x_6 + x_7 x_8 + x_9^2 + x_{10}}$$

4.46.1 Setup and results overview

- Reference: Personal communication, [none]
- Domain: \mathbb{R}
- Tensor size: 461 MB (6^{10} points)
- Bounds: $(1 \ 5) \times (1 \ 5)$

#	Alg.	Parameters	Dim.	CPU [s]	RMSE	min err.	max err.
46	A/G/P-V 2025 (A1)	0.01,2	2.76e + 04	164	6.29e - 17	0	2.6e-16
	A/G/P-V 2025 (A2)	1e-15,3	2.76e+04	327	8.18e-17	0	3.64e-16
	MDSPACK v1.1.0	0.01,0.0001	2.76e+04	137	7.08e-17	0	2.5e - 16
	P/P 2025	NaN	NaN	NaN	NaN	NaN	NaN
	B/G 2025	NaN	NaN	NaN	NaN	NaN	NaN
	B/G 2025 (LR)	NaN	NaN	NaN	NaN	NaN	NaN
	TensorFlow	NaN	NaN	NaN	NaN	NaN	NaN

Table 47: Function #46: best model configuration and performances per methods.

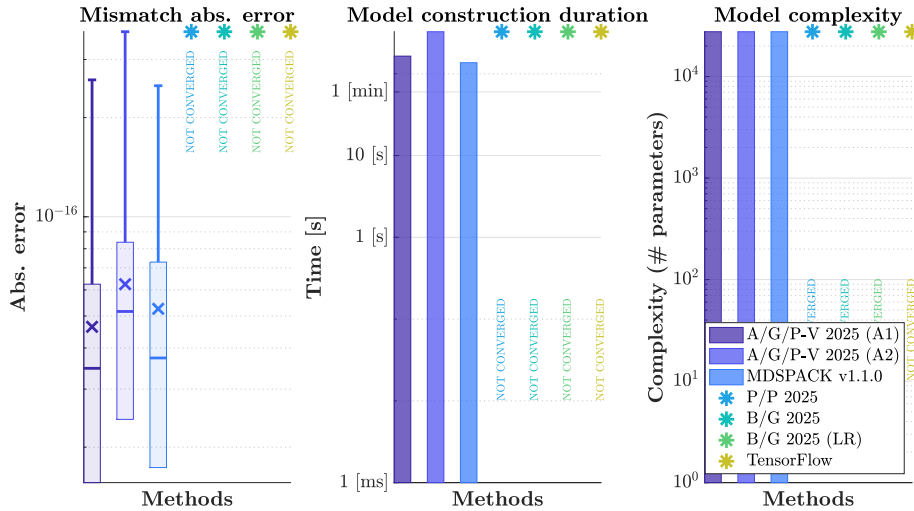


Figure 111: Function #46: graphical view of the best model performances.

$$x_{3\ldots 10} = [2.6681; 1.0005; 1.587; 1.745; 2.5871; 2.6768; 1.8178; 1.1096]$$

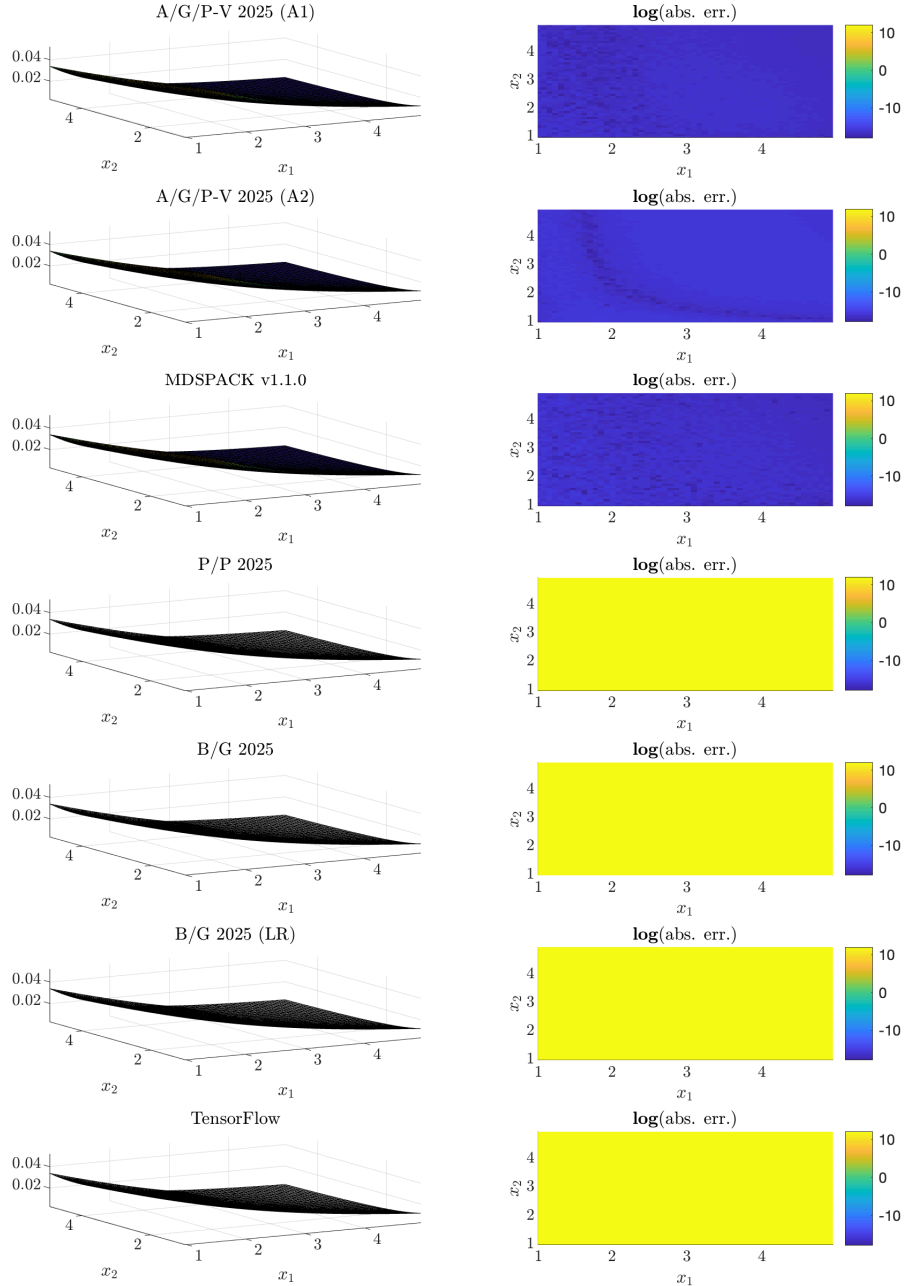


Figure 112: Function #46: left side, evaluation of the original (mesh) vs. approximated (coloured surface) and right side, absolute errors (in log-scale).

4.46.2 mLFI detailed informations (M1)

Right interpolation points: $k_l = (3 \ 2 \ 2 \ 2 \ 2 \ 2 \ 2 \ 2 \ 3 \ 2)$, where $l = 1, \dots, n$.

$$\begin{aligned} {}^1\lambda_{j_1} &\in \mathbb{C}^3, \text{ linearly spaced between bounds} \\ {}^2\lambda_{j_2} &\in \mathbb{C}^2, \text{ linearly spaced between bounds} \\ {}^3\lambda_{j_3} &\in \mathbb{C}^2, \text{ linearly spaced between bounds} \\ {}^4\lambda_{j_4} &\in \mathbb{C}^2, \text{ linearly spaced between bounds} \\ {}^5\lambda_{j_5} &\in \mathbb{C}^2, \text{ linearly spaced between bounds} \\ {}^6\lambda_{j_6} &\in \mathbb{C}^2, \text{ linearly spaced between bounds} \\ {}^7\lambda_{j_7} &\in \mathbb{C}^2, \text{ linearly spaced between bounds} \\ {}^8\lambda_{j_8} &\in \mathbb{C}^2, \text{ linearly spaced between bounds} \\ {}^9\lambda_{j_9} &\in \mathbb{C}^3, \text{ linearly spaced between bounds} \\ {}^{10}\lambda_{j_{10}} &\in \mathbb{C}^2, \text{ linearly spaced between bounds} \end{aligned}$$

n-D Loewner matrix, barycentric weights and Lagrangian basis:

$$\begin{aligned} \mathbb{L} &\in \mathbb{C}^{2304 \times 2304} \\ \mathbf{c} &\in \mathbb{C}^{2304} \\ \mathbf{w} &\in \mathbb{C}^{2304} \\ \mathbf{c} \cdot \mathbf{w} &\in \mathbb{C}^{2304} \\ \mathbf{Lag}(x_1, x_2, x_3, x_4, x_5, x_6, x_7, x_8, x_9, x_{10}) &\in \mathbb{C}^{2304} \end{aligned}$$

5 Discussions and conclusions

5.1 Discussion and generic comments

The following comments can be raised and would benefit further investigations in the future:

- When data are obtained from a **rational function \mathbf{H}** , M1, M2 and M3 are by far the most efficient methods since they are fast, accurate, and recover the exact complexity (without over-fitting). In addition, we demonstrate that whatever the tensor size, the solution is perfectly recovered with model construction time largely acceptable on a standard computer.
- When data are obtained from a **non-rational function \mathbf{H}** , the adaptive interpolation point selection scheme seems a really good candidate, and M2 and M5, M6 reveal to be very efficient methods. M2 benefits from the recursive barycentric values construction and is much more fast and scalable when complexity increases (n , tensor size, etc.). However, M2's current implementation suffers from issues in some configurations.
- The size (dimension and size on the disk) of the original tensor is the main limit to M4, M5, M6 and M7. Indeed, the computation time is largely dictated by the dimension n of the tensor and of its size. This highlights the interest of M1, M2 and M3 where the size vs. time slope is much lower.
- Algorithmic strategies are under investigation to automatize as much as possible the parameter tuning, the order estimation and interpolation point selection. To make the user experience smoother and propose a solution that robustly solves the tensor approximation problem.

5.2 General conclusion

In this note, we reported on different methods allowing to construct a surrogate approximate model directly from tensors. Each method optimizes a specific model structure (rational in barycentric basis, MLP and KAN with different splines). Still each approaches and code share the very same input: **a n -D tensor**. We believe that a complete comparison over a large set of tensors, constructed from different functions (with a large variety of complexity and dimensions), for varying method parametric tuning, is provided, and that metric used are fair to evaluate the efficiency of the methods. Among the 46 cases considered in this study, most of the approaches successfully reached an appropriate and accurate surrogate. However, we believe that the approach proposed in [3] is a serious candidate to deal with very complex real-life tensors. Obviously we advocate our method proposed in [3] (and its implementation in [10]) as it shows a very fast computation time, large flexibility, few tuning parameters while still providing very accurate approximating functions, easily interpretable, scalable to very-large tensors. Future investigations and updates will include more cases and other methods. Improvements of M1, M2 and M3 to meet the practical expectations for non-expert users and reach its full potential will be sought.

Before closing this report, we want to briefly comment on third the parties methods (namely M4, M5, M6 and M7) used in this report: (i) we warmly thank authors for making their code available; (ii) we report on the fact that their use was actually quite simple and enough documented; (iii) we repeat that we may have badly / non-optimally use their code and apologize if so; (iv) we remain open for modifications and comments.

References

- [1] Martín Abadi, Ashish Agarwal, Paul Barham, Eugene Brevdo, Zhifeng Chen, Craig Citro, Greg S. Corrado, Andy Davis, Jeffrey Dean, Matthieu Devin, Sanjay Ghemawat, Ian Goodfellow, Andrew Harp, Geoffrey Irving, Michael Isard, Yangqing Jia, Rafal Jozefowicz, Lukasz Kaiser, Manjunath Kudlur, Josh Levenberg, Dandelion Mané, Rajat Monga, Sherry Moore,

Derek Murray, Chris Olah, Mike Schuster, Jonathon Shlens, Benoit Steiner, Ilya Sutskever, Kunal Talwar, Paul Tucker, Vincent Vanhoucke, Vijay Vasudevan, Fernanda Viégas, Oriol Vinyals, Pete Warden, Martin Wattenberg, Martin Wicke, Yuan Yu, and Xiaoqiang Zheng. TensorFlow: Large-scale machine learning on heterogeneous systems, 2015. Software available from tensorflow.org.

- [2] A. C. Antoulas, A. C. Ionita, and S. Lefteriu. On two-variable rational interpolation. *Linear Algebra and its Applications*, 436(8):2889–2915, 2012. <https://doi.org/10.1016/j.laa.2011.07.017>.
- [3] A.C. Antoulas, I-V. Gosea, and C. Poussot-Vassal. The Loewner framework for parametric systems: Taming the curse of dimensionality. *to appear in SIAM Review*, 2024. <https://arxiv.org/abs/2405.00495>.
- [4] A.P. Austin, M. Krishnamoorthy, S. Leyffer, S. Mrenna, J. Müller, and H. Schulz. Practical algorithms for multivariate rational approximation. *Computational Physics Communications*, 261:107663, 2021. <https://doi.org/10.1016/j.cpc.2020.107663>.
- [5] L. Balicki and S. Gugercin. Multivariate Rational Approximation via Low-Rank Tensors and the p-AAA Algorithm. 2025. <https://arxiv.org/abs/2502.03204>.
- [6] R. Bellman. Dynamic programming. *Science*, 153(3731):34–37, 1966. American Association for the Advancement of Science.
- [7] A. C. Ionita and A. C. Antoulas. Data-Driven Parametrized Model Reduction in the Loewner Framework. *SIAM Journal on Scientific Computing*, 36(3):A984–A1007, 2014. <https://doi.org/10.1137/130914619>.
- [8] Z. Liu, Y. Wang, S. Vaidya, F. Ruehle, J. Halverson, M. Soljačić, T.Y. Hou, and M. Tegmark. KAN: Kolmogorov-Arnold Networks. 2025. <https://arxiv.org/abs/2404.19756>.
- [9] A. J. Mayo and A. C. Antoulas. A framework for the solution of the generalized realization problem. *Linear Algebra and its Applications*, 425(2-3):634–662, 2007. <https://doi.org/10.1016/j.laa.2007.03.008>.
- [10] MOR Digital Systems. MDSPACK (v1.1.0), 2025. Main page (<https://mordigitalsystems.fr>) & Documentation (https://mordigitalsystems.fr/static/mdspack_html/MDSpack-guide.html).
- [11] R. Pintelon and J. Schoukens. *System Identification: A Frequency Domain Approach*. Wiley-IEEE Press, 2012. <https://doi.org/10.1002/9781118287422>.
- [12] M. Poluektov and A. Polar. Construction of the Kolmogorov-Arnold representation using the Newton-Kaczmarz method. 2025. <https://arxiv.org/abs/2305.08194>.